

Development of optical based characterisation and detection methods for quantitative and qualitative assessment of phytoplankton in their natural environment.

CAMPBELL, I.

2000

The author of this thesis retains the right to be identified as such on any occasion in which content from this thesis is referenced or re-used. The licence under which this thesis is distributed applies to the text and any original images only – re-use of any third-party content must still be cleared with the original copyright holder.

**Development of optical based characterisation and
detection methods for quantitative and qualitative
assessment of phytoplankton in their natural environment**

By

Ian Campbell

A thesis submitted in partial fulfilment for the degree of
Doctor of Philosophy

The Robert Gordon University, September 2000



IMAGING SERVICES NORTH

Boston Spa, Wetherby
West Yorkshire, LS23 7BQ
www.bl.uk

BEST COPY AVAILABLE.

VARIABLE PRINT QUALITY

Contents

CONTENTS	I
ABSTRACT.....	IX
ACKNOWLEDGEMENTS.....	X
LIST OF PUBLICATIONS.....	XI
LIST OF FIGURES	XII
GLOSSARY	XIX
CHAPTER 1.....	1
INTRODUCTION	1
1.1 Microscopic Plants and Organisms and the Food Chain.....	1
1.2 Phytoplankton in the Carbon Cycle	2
1.3 Pollution in the Marine Environment.....	2
1.3.1 Hydrocarbon Pollution	2
1.3.2 Shipping Pollution.....	4
1.3.3 Agricultural Pollution.....	4
1.5 Traditional Sampling Techniques	6
1.5.1 Net Sampling for Measuring Phytoplankton	6
1.5.2 Multi-net Sampler	8
1.5.3 Water Bottle Sampling	9
1.5.4 Hose-pipe and Bucket	11
1.6 Summary	11
CHAPTER 2.....	13
REVIEW OF OPTICAL TECHNIQUES USED IN MARINE MONITORING.....	13

2.0 Introduction	13
2.1 Absorption Spectrometry	14
2.2 Laboratory Based Fluorimetry	15
2.2.1 Flow Cell Fluorimeters.....	17
2.3 Submersible Fluorimetry	18
2.3.1 Submersible Single Wavelength Fluorimeters.....	18
2.3.2 Submersible Multi-Wavelength Fluorimeters.....	22
2.3.3 Submersible Primary Productivity Fluorimeters.....	23
2.3.4 Laser Fluorimeters.....	24
2.4 Discussion: Submersible Measurement Systems	25
2.5 Remote Sensing Measurements	27
2.5.1 Lidar (Laser) Monitoring.....	27
2.5.2 Airborne Oceanographic Lidar (AOL)	33
2.5.3 Laser Environmental Airborne Fluorosensor (LEAF)	33
2.5.4 ENEA Frascati Lidar Fluorosensor	34
2.5.5 Oceanographic Lidar System – Federal Institute for Hydrology	35
2.5.6 Discussion: Lidar Technology.....	35
2.5.7 Satellite Monitoring.....	36
2.5.8 Discussion: Satellite Technology	39
2.6 Summary	39
CHAPTER 3.....	43
THEORY AND INSTRUMENTATION TECHNIQUES.....	43
3.0 Introduction	43
3.1 Molecular Orbitals.....	44
3.1.1 Basic Molecular Structure	44
3.2 Absorption.....	48
3.3 Fluorescence and Phosphorescence	51

3.3.1 Fluorescence Characteristics	52
3.4 Photosynthesis	54
3.5 Noise Sources and Signal Enhancement Techniques.....	56
3.5.1 Optical Noise.....	57
3.5.2 Optical Detection	57
3.5.3 Signal Enhancement Techniques.....	58
3.5.4 Signal Averaging.....	59
3.5.5 Boxcar Integration.....	60
3.5.6 Pulse-Height Analysis	61
3.5.7 Lock-in and Phase Sensitive Detection	62
3.6 Summary	63
CHAPTER 4.....	65
PHYTOPLANKTON CULTURING.....	65
4.0 Introduction	65
4.1 Phytoplankton Selection	65
4.2 Base Medium Preparation and Sterilisation.....	66
4.3 Nutrient Preparation	67
4.3.1 Trace Metal Stock Solution.....	67
4.3.2 Vitamin Stock Solution	68
4.4 Phytoplankton Growth and Cell Harvesting	69
4.5 Cell Disposal	72
4.6 Summary	73
CHAPTER 5.....	74
FLUORESCENCE SPECTROSCOPY OF PHYTOPLANKTON.....	74
5.0 Introduction	74
5.1 Standard Fluorescence Equipment.....	74

5.2 Calibration of the LS-50B Spectrofluorimeter	75
5.2.1 Wavelength Calibration.....	75
5.2.2 Intensity Calibration	75
5.3 Fluorescence Spectra of Selected Algae Species	76
5.3.1 Fluorescence Measurements.....	76
5.3.2 <i>Chaetoceros calcitrans</i> Sample	77
5.3.3 <i>Nannochloris atomus</i> Sample.....	79
5.3.4 <i>Nannochloropsis oculata</i> Sample	80
5.3.5 <i>Tetraselmis suecica</i> Sample	81
5.3.6 <i>Scripsiella trochoidea</i> Sample.....	82
5.4 Discussion: Standard Phytoplankton Fluorescence.....	84
5.5 Laser Fluorescence Spectroscopy	85
5.5.1 Design of the Laser Fluorimeter.....	85
5.5.2 Monochromator Control and Data Collection	86
5.5.3 Wavelength calibration of the Monochromator	87
5.5.4 Laser Excitation Spectra of Selected Phytoplankton Samples.....	88
5.6 Fluorescence Saturation Measurements.....	90
5.7 Summary	91

CHAPTER 6.....94

**TIME RESOLVED FLUORESCENCE SPECTROSCOPY OF PHYTOPLANKTON
AND HIGH ENERGY LASER RADIATION EFFECTS ON PHYTOPLANKTON....94**

6.0 Introduction	94
6.1 Time Dependent Fluorescence Emissions	95
6.2 Nanosecond Fluorescence Decay Monitoring.....	95
6.3 Nanosecond Fluorescence Decay Results.....	97
6.3.1 <i>Chaetoceros calcitrans</i> Sample	98
6.3.2 <i>Nannochloris atomus</i> Sample.....	99

6.3.3 <i>Nannochloropsis oculata</i> Sample	100
6.3.4 <i>Tetraselmis suecica</i> Sample	101
6.3.5 <i>Scropsiella trochoidea</i> Sample	102
6.4 Discussion - Nanosecond Fluorescence	103
6.5 Effects of High-Energy Laser Radiation on Algae	105
6.6 Experimental Setup	106
6.7 Results from Laser Radiation Treatment using 355nm	108
6.7.1 <i>Chaetoceros calcitrans</i> Sample	108
6.7.2 <i>Nannochloris atomus</i> Sample	110
6.7.3 <i>Nannochloropsis oculata</i> Sample	111
6.7.4 <i>Tetraselmis suecica</i> Sample	111
6.8 Optical Microscopy of the Planktons Exposed to 355nm Laser Radiation.	112
6.9 Discussion: 355nm Laser Treatment.....	113
6.10 Effects of Three Different Laser Wavelengths on <i>Chaetoceros</i> Fluorescence	114
6.10.1 Chlorophyll-a (PSII) Fluorescence after Exposure to 430nm Laser Radiation .	115
6.10.2 Chlorophyll-a (PSII)Fluorescence after Exposure to 474nm Laser Radiation ..	120
6.10.3 Chlorophyll-a Fluorescence after Exposure to 633nm Laser Radiation.....	124
6.11 Discussion: Multiple Frequency Laser Radiation on <i>Chaetoceros</i>	127
6.12 Summary	130
CHAPTER 7.....	132
LASER MARINE SURFACE FLUOROSENSOR DEVELOPMENT.....	132
7.0 Introduction	132
7.1 Initial Laboratory Experiments.....	132
7.2 Design of the Laser Marine Surface Fluorosensor Mk 1	135
7.2.1 Laser Marine Surface Fluorosensor Mk I Experimental Results	137
Sodium Fluorescein Tests	137
Plankton Tests.....	138

7.3 Discussion: LMSF Mk I system	139
7.4 Design of the Laser Marine Surface Fluorosensor Mk II.....	140
7.4.1 Laser Marine Surface Fluorosensor Mk II Experimental Results	142
Sodium Fluorescein Tests	142
Plankton Tests	144
Hydrocarbon Tests	145
7.5 Discussion: LMSF Mk II System	147
7.6 Design of the Laser Marine Surface Fluorosensor Mk III	148
7.6.1 Experimental Results Using the LMSF Mk III.....	150
Sodium Fluorescein Tests	150
7.6.2 Detector Response to Fluorescence Along the Axes of the Telescope.	153
7.7 Discussion: LMSF Mk III System	154
7.9 Summary	154

CHAPTER 8.....158

LASER MARINE SURFACE FLUOROSENSOR AND LASER FLUORIMETER SEA TRIALS.....158

8.0 Introduction	158
8.1 LMSF Mk I Sea Trials “Lowland <i>Searcher</i> ” June 1996	158
8.1.1 Setup of the Laser Marine Surface Fluorosensor Mk I.....	160
8.1.2 Results.....	161
8.2 Discussion: June 1996 Sea Trial.....	163
8.3 Sea Trials of the Laser Fluorimeter	164
8.3.1 Comparison of Fluorescence Measurements	165
8.3.2 Scapa Flow and Clift Sound Fluorescence Measurements	167
8.4 Discussion: June 1998 Sea Trial.....	169
8.5 LMSF Mk III System Sea Trials “Sovereign <i>Explorer</i> ” Aug/Sept 1998.....	171
8.5.1 Setup of the Laser Marine Surface Fluorosensor Mk III	172

8.5.2 Sea Trial Calibration	174
8.5.3 Hydrocarbon Monitoring.....	177
8.6 Discussion: October 1998 Sea Trials.....	181
8.7 Summary	183
CHAPTER 9.....	184
DIODE-PUMPED LASER MARINE SURFACE FLUOROSENSOR	184
9.0 Introduction	184
9.1 Oil Fluorescence.....	184
9.2 System Setup	185
9.3 Results.....	186
9.3.1 Instrumental	186
9.3.2 Oil Detection.....	188
9.4 Summary	190
CHAPTER 10.....	191
CONCLUSIONS.....	191
10.1 Laser Marine Surface Fluorosensor	191
10.2 Laser Fluorimeter	193
10.3 Time Resolved Fluorescence Spectroscopy.....	194
10.4 High Energy Laser Effects on Phytoplankton.....	195
10.5 Treatment of <i>Chaetoceros</i> using Selected Laser Wavelengths	196
CHAPTER 11.....	199
FUTURE WORK.....	199
Introduction	199
11.1 Laser Marine Surface Fluorosensor System.....	199
11.1.1 Polarisation.....	200
11.1.2 Laser Types	201

11.2 Applications of the LMSF to other environmental monitoring	204
11.2.1 Oil Production Flaring Operations.....	204
11.2.2 Inland Waterway Monitoring	205
11.3 Laser Fluorimeter	206
11.4 Time Dependent Fluorescence Emissions	207
11.5 High Energy Laser Effects on Phytoplankton.....	208
11.6 Raman Scattering.....	209
REFERENCES.....	210
APPENDIX.....	220

Abstract

The marine environment is an extremely complex and varied ecosystem playing a very important role in the world's existence. The oceans are a fruitful source of food and host some of the world's largest mammals. Vegetation in the form of billions of tiny plants and animals called plankton extract carbon dioxide from the atmosphere, which is used in the photosynthesis process to produce carbohydrates, allowing them to grow. This effectively cleans the atmosphere of carbon dioxide and releases oxygen as a by-product of photosynthesis, back into the atmosphere, allowing us to survive.

It is important to monitor the algae which are important indicators of fish stocks and the amount of carbon dioxide being removed from the atmosphere. It is also important to monitor the effects of pollution on the environment and the algae. Today there are a variety of methods for monitoring algae and pollution in the marine environment but most of these have limitations such as cost, portability, effectiveness and sampling resolution. Most of these systems are also designed for monitoring algae and pollution below the sea surface. There are, however, few, low cost, compact and portable measurement systems available for monitoring phytoplankton or pollution on the sea surface.

This project investigates and develops a laser based surface measurement system along with evaluating laser-induced changes within phytoplankton as possible indicators for identifying selected phytoplankton samples. This work is designed to provide a rapid method for characterising and quantifying algae on the sea surface and also provide a method for detecting hydrocarbon pollution around oil production installations.

Acknowledgements

I would like to thank Professor Daniel McStay for the opportunity to study and work under his direction in the Optoelectronics Research Centre at The Robert Gordon University, for his enthusiasm and support during the course of this PhD. I would also like to thank Dr Patricia Pollard for her advice and constructive criticism. I would also like to thank The Robert Gordon University for the partial funding received.

I would like to thank Dr Michael R. Heath of Fishery Research Services (formerly the Scottish Office Environmental and Fisheries department), Marine Laboratory, Aberdeen, for advice relating to the biological aspects of the project. I also wish to thank the establishment for the funding provided for the project. Also at the Marine Laboratory, my external advisor, John Dunn, a constant guide in obtaining samples and helping to organise sea trials. I would also like to thank Dr Eileen Bresnan for her constant supply of phytoplankton during the early stages of the project and the crews of the “FRV *Clupea*”, “Lowland *Searcher*” and especially the “*Toisa Invincible*” for their help, encouragement and support during the research trips. Thanks go to Dr Ron Stagg for the opportunity to participate in one of his research cruises. I would also like to thank Conoco for their interest and financial support in the project during sea trials of the system close to an oil production platform.

Special thanks go to Mr Allan McPherson, our mechanical technician, for his rapid prototyping of designs and his suggestions from a mechanical engineer’s point of view and to Mr Neil Foster, our electronics technician, for his electronics knowledge and design suggestions during the course of the project.

Finally, I would like to thank my family - Mum, Dad, George and Neil - who have supported me in everything I have done and have been a constant source of encouragement, laughter and love.

Kimberly, thank you for being here whilst I was writing up, for dragging me away from writing when I needed a break, for proof reading my thesis, for your constructive comments, for listening and most of all, for being you.

List of Publications

During the course of this work, several research papers (See Appendix 1) have been published and presented at major international and national conferences.

Research Papers

1. A ship-borne system for the detection of surface oil, I.Campbell, D. McStay, Advanced Technologies for Environmental Monitoring and Remediation, 1996, Denver, Colorado, SPIE Vol. 2835, Pg. 214-220
2. Laser Surface Fluorosensor for Monitoring Phytoplankton, I.Campbell, D. McStay, P.M. Pollard, M.R. Heath, J. Dunn, Advances in Fluorescence Sensing Technology III, BIOS '97, 1997, San Jose, California, SPIE Vol. 2980, Pg. 182-186
3. A Ship-borne Laser Surface Fluorosensor for Marine Sensing Applications, I.Campbell, D. McStay, P. Pollard, M.R. Heath, J.Dunn, 1997, IOP, Sensors and their Applications VIII, Glasgow, 1997, Pg. 143-147
4. A novel blue LED based hand-held fluorimeter for detection of terrestrial algae on solid surfaces, E. Brechet, D. McStay, R.D. Wakefield, I.Campbell, Lasers and Materials meet Industry, 1998, Quebec, Canada, SPIE Vol. 3414, Pg. 184-190

List of Figures

Figure 1.1: Schematic showing a chain-forming plankton from <i>Chaetoceros</i> genus.....	1
Figure 1.2: Photograph of the Amoco Cadiz oil spill in 1978	3
Figure 1.3: Schematic showing the different sampling strategies for the Methot net.	7
Figure 1.4: Modern day Methot net deployment.	8
Figure 1.5: Water sampling tubes ready to be mounted on the winch wire	9
Figure 1.6: Carousel water sampling system.....	10
Figure 2.1: Diagram showing the major components of a UV/Vis spectrometer	14
Figure 2.2: Diagram showing the major components of a fluorimeter	16
Figure 2.3: Diagram of a fluorimeter flow-cell	17
Figure 2.4: Diagram illustrating depth profile measurements	19
Figure 2.5: General diagram of submersible fluorimeters.	20
Figure 2.6 : Comparison of the sensitivities of the four main submersible fluorimeters in use today	21
Figure 2.7: Multi-wavelength detection fluorimeter.....	22
Figure 2.8: General components of a lidar system.	28
Figure 2.9: Table showing gate delay times for monitoring different water depths.....	29
Figure 2.10: Photograph of a C-130 “Hercules”(left) and a P-3B “Orion” (right) used to house the Airborne Oceanographic Lidar.....	29
Figure 2.11: Main characteristics of the various lidar systems in use today.....	32
Figure 3.1: Space filled representations of the shape of the atomic orbitals of the first 3 angular quantum numbers, s, p and d.....	45
Figure 3.2: Electron distribution in sigma (σ) and pi (π) molecular orbitals	46
Figure 3.3: Various electronic transitions and associated absorption regions.....	46
Figure 3.4: Diagram showing the electron spin.....	47
direction for different excited states.....	47

Figure 3.5: Simplified energy level diagram showing energy absorption transitions	49
Figure 3.6: Simplified energy level diagram showing non-radiative de-excitation	50
Figure 3.7: Energy level diagram showing absorption, fluorescence and phosphorescence.....	51
Figure 3.8: Diagram showing the approximate time for electron transfers during photosynthesis	56
Figure 3.9: The effect of signal averaging.....	59
Figure 3.10: Diagram of a boxcar integrator	60
Figure 3.11: Diagram of the components to enable lock-in detection	62
Figure 4.1: Phytoplankton species used for experiments.....	66
Figure 4.2: Trace metal stock solution concentrations	68
Figure 4.3: Vitamin stock solution concentrations	68
Figure 4.4 : Photograph of the cooled incubator used for growing phytoplankton.....	69
Figure 4.6: Growth curve for <i>Tetraselmis suecica</i>	71
Figure 4.7: Cell concentration against fluorescence intensity (430nm excitation/680nm emission) for <i>Tetraselmis</i> in the linear growth phase.	71
Figure 5.1: Basic components of the LS-50B bench fluorimeter.....	74
Figure 5.2: Photograph of the Perkin-Elmer LS-50B fluorimeter showing the sample housing.	75
Figure 5.3: Calibration of the LS-50B spectrofluorimeter using sodium fluorescein	76
Figure 5.4: Multi-excitation fluorescence spectrum of <i>Chaetoceros calcitrans</i> diatom	78
Figure 5.5: Fluorescence spectra of <i>Chaetoceros calcitrans</i> - 430nm excitation	78
Figure 5.6 Multi-excitation spectra of <i>Nannochloris atomus</i>	79
Figure 5.7: Multi-excitation spectra of <i>Nannochloropsis Oculata</i>	80
Figure 5.8: Fluorescence Spectra of <i>Nannochloropsis oculata</i> , 450nm excitation	81
Figure 5.9: Multi-excitation fluorescence spectrum of <i>Tetraselmis suecica</i>	82
Figure 5.10: Multi-excitation fluorescence spectrum of <i>Scropsiella trochoidea</i>	83
Figure 5.11: Fluorescence spectra of <i>Scropsiella trochoidea</i> , 400nm excitation.....	83

Figure 5.12: Excitation wavelength producing maximum fluorescence at 680nm for the selected species.....	84
Figure 5.13: Photographs of the laser fluorimeter main components and set-up	86
Figure 5.14: Laser fluorescence spectra of sodium fluorescein showing the excitation wavelength at 488nm with the peak fluorescence emission at 514nm.....	88
Figure 5.15: Laser Fluorescence scan of <i>Chaetoceros</i>	89
Figure 5.16: Laser fluorescence scan of <i>Scripsiella trochoidea</i>	89
Figure 5.17: Fluorescence saturation of <i>Chaetoceros</i> using an argon ion laser.	90
Figure 5.18: Summary of plankton characteristics obtained when using the standard bench fluorimeter.	92
Figure 6.1: Fast fluorescence experimental apparatus setup.....	96
Figure 6.2: Fluorescence decay curves for <i>Chaetoceros</i> over a 5-day period.....	98
Figure 6.3: Fluorescence decay curves for <i>Nannochloris</i> over a 2-day period	99
Figure 6.5: Fluorescence time decay curves for the <i>Tetraselmis</i> sample over a 4-day period. .	101
Figure 6.6: Fluorescence decay curves for <i>Scripsiella</i> over a 3-day period.....	102
Figure 6.7: Table showing the largest differences between fluorescence emission at various times after excitation for each of the species.....	104
Figure 6.8: Table showing the time for the fluorescence to decay to half the original value for each of the plankton's.....	105
Figure 6.9: High-energy laser treatment experiment setup.....	107
Figure 6.10: Phytoplankton laser treatment wavelengths and fluorimeter excitation wavelengths observing fluorescence emissions at 680nm.....	108
Figure 6.11: <i>Chaetoceros</i> laser treatment wavelengths and fluorimeter excitation wavelengths observing fluorescence emissions at 680nm.....	108
Figure 6.12 Effect of 355nm laser radiation on 680nm fluorescence at various excitation wavelengths for <i>Chaetoceros</i>	109

Figure 6.13: Effect of 355nm laser radiation on 680nm fluorescence at various excitation wavelengths for <i>Nannochloris atomus</i>	110
Figure 6.14: Effect of 355nm laser radiation on 680nm fluorescence at various excitation wavelengths for <i>Nannochloropsis oculata</i>	111
Figure 6.15: Effect of 355nm laser radiation on 680nm fluorescence at various excitation wavelengths for <i>Tetraselmis suecica</i>	112
Figure 6.16: Changes in 680nm fluorescence after exposure to 355nm laser radiation.....	113
Figure 6.17: Effects of 430nm radiation on chlorophyll-a fluorescence intensity	116
Figure 6.19a-c: Chlorophyll-a PSII fluorescence peak wavelength for selected excitation wavelengths after 430nm laser treatment	119
Figure 6.20: Effects of 474nm radiation on chlorophyll-a fluorescence intensity	120
Figure 6.22a-c: Chlorophyll-a PSII fluorescence peak wavelength for selected excitation wavelengths after 474nm laser treatment	122
Figure 6.23: Effects of 633nm radiation on chlorophyll-a fluorescence intensity	124
Figure 6.24a-c: Change in the PSII fluorescence peak width at half the maximum for selected excitation wavelengths after 633nm laser treatment.....	125
Figure 6.25a-c: Chlorophyll-a PSII fluorescence peak wavelength for selected excitation wavelengths after 633nm laser treatment	126
Figure 6.26: Chart showing the changes in fluorescence intensity, peak width and peak shift when monitored using selected wavelengths after treatment for three wavelengths of laser radiation.....	128
Figure 6.27: Table showing possible rules which may allow the identification of selected algae	131
Figure 7.1: Initial Laboratory Remote Sensing Experiments.....	133
Figure 7.2: Concentration dependence of sodium fluorescein measured remotely	134
Figure 7.3: Plan (a) and Elevation (b)views of the Laser Marine Surface Fluorosensor Mk I..	136
Figure 7.4: LMSF Mk I response to standard concentrations of sodium fluorescein.....	138

Figure 7.5: Response of the Laser Marine Surface Fluorosensor Mk I to different concentrations of <i>Chaetoceros</i> phytoplankton at a range of 6m.....	139
Figure 7.6: Laser beam and telescope centreline intersections for the LMSF Mk 1	140
Figure 7.7: Diagram showing the changes in the first upgrade of the Laser Marine Surface Fluorosensor	141
Figure 7.8: Photograph showing the telescope incorporated into the upgraded Laser Marine Surface Fluorosensor	142
Figure 7.10: Graph showing the response of the LMSF Mk II to a	144
1×10^{-7} M solution of sodium fluorescein at different ranges	144
Figure 7.11: Response of the LMSF Mk II response to various concentrations of phytoplankton at a fixed range of 15m.....	145
Figure 7.12: Response of the LMSF Mk II to various surface concentrations of oil at a fixed range of 3m.	146
Figure 7.13: Diagram of the Laser Marine Surface Fluorosensor Mk III	148
Figure 7.14: Photograph of the Laser Marine Surface Fluorosensor Mk III.....	150
Figure 7.15: Range response of the LMSF Mk III for a standard solution of sodium fluorescein (10^{-7} M).....	151
Figure 7.16: Response of LMSF Mk III to various concentrations of sodium fluorescein at a distance of 21.5m.....	152
Figure 7.17: Diagram showing two possible telescope-to-the target orientations producing a Gaussian (a) and non-Gaussian (b) light distribution across the primary mirror.	153
Figure 7.18a and 7.18b: Telescope axes fluorescence response	154
Figure 7.20 Diagram showing the reduction in the signal under low (a) and ambient (b) light conditions.....	156
Figure 8.1: Map showing the route of the “ <i>Lowland Searcher</i> ” during sea trials of the Mk I instrument during June 1996 and the location of the “ <i>Sovereign Explorer</i> ” during 1998 Mk III sea trials	159

Figure 8.2: Photograph of the “Lowland <i>Searcher</i> ” showing the location of the Laser Marine Surface Fluorosensor Mk I during sea trials.....	160
Figure 8.3: Trace showing backscattered laser light signal from the sea surface obtained during the sea trials of the LMSF Mk1.....	162
Figure 8.4: Photograph of the Laser Fluorimeter located in the underwater camera room onboard “FRV <i>Clupea</i> ”.....	164
Figure 8.5: Comparison of a traditional flow cell fluorimeter (Marlab Chl-a) against a laser based fluorimeter (Laser Chl-a) monitoring phytoplankton fluorescence at 680nm.....	166
Figure 8.6: Phytoplankton distribution in Scapa Flow shown by chlorophyll-a fluorescence emissions at 680nm.....	167
Figure 8.7: Comparison of the fluorescence data from a 12 hour station in “Clift Sound”, Shetland Isles.....	168
Figure 8.8: Scan of seawater sample using laser fluorimeter.....	169
Figure 8.9: Phytoplankton fluorescence signal changes on leaving “Clift Sound”.....	170
Figure 8.10: Photograph showing the location, marked with a circle, of the LMSF Mk III on board the “ <i>Toisa Invincible</i> ” during sea trials west of the Shetland Isles.....	172
Figure 8.11 : Photograph showing the LMSF Mk III during night operations.....	173
Figure 8.12: Photograph showing the fluorescence spars (marked with green circle) on the wooden deck.....	174
Figure 8.13: Range response of the LMSF Mk III during field operations West of the Shetland Isles.....	175
Figure 8.14: Graph showing signal from backscattered radiation from the water surface.....	176
Figure 8.15: Traces from the fibre optic fluorimeter showing the presence of hydrocarbons in the water surrounding the “ <i>Sovereign Explorer</i> ”.....	178
Figure 8.16: Trace from the surface sensor moving through suspected hydrocarbon contaminated area.....	179

Figure 8.17: Diagram showing the main components which affected the signal obtained (also shown) during the “Sovereign <i>Explorer</i> ” sea trial.....	181
Figure 9.1: Multi-excitation fluorescence spectra of Gulfaks oil	185
Figure 9.2: Photograph showing the EPO 5000 system (left) and during operation (right).....	186
Figure 9.3: Graph showing drift in backscattered crude oil fluorescence signal with average laser power at a range of 12m.	187
Figure 9.4: Range response of the EPO-5000 for a 28 μm^2 sample of crude oil	188
Figure 9.5: Response of the EPO-5000 system to surface oil concentrations at a fixed range of 12m	189
Figure 10.1: Chart showing the changes in fluorescence intensity, peak width and peak shift when monitored using selected wavelengths after treatment for three wavelengths of laser radiation	197
Figure 10.2: Table showing possible rules which may allow the identification of selected algae	198
Figure 11.1: Design for the Laser Marine Surface Fluorosensor Mk IV	202
Figure 11.2a&b : Diagram showing modifications to allow scanning of the laser beam	203
Figure 11.3: Sampling area of the current LMSF and a scanning version of the LMSF	203
Figure 11.4: Illustration of the flaring process on oil production platforms	204

Glossary

Abbreviation	Term	Units
POBMs	Pseudo Oil Based Drilling Mud's	-
SBFs	Synthetic Based Fluids	-
SBMs	Synthetic Based Mud's	-
UV	Ultra-violet	-
Vis	Visible	-
LED	Light Emitting Diode	-
PSI	Photosystem I	-
PSII	Photosystem II	-
PAR	Photosynthetically Active Radiation	-
NASA	National Aeronautics and Space Administration	-
AOL	Airborne Oceanographic Lidar	-
CDOM	Chromophoric Dissolved Organic Matter	-
LIDAR	Light Detection and Ranging	-
CCD	Charge Coupled Device	-
NOAA	National Oceanic and Atmospheric Administration	-
CZCS	Coastal Zone Colour Scanner	-
SeaWiFS	Sea-viewing Wide-field-of-view Sensor	-
Nd:YAG	Neodymium Yttrium Aluminium Garnet	-
Chl-a	Chlorophyll-a	-
HC	Hydrocarbons	-
LEAF	Laser Environmental Airborne Fluorosensor	-
Xe-Cl	Xenon-Chloride	-
LAC	Local Area Coverage	-
GAC	Global Area Coverage	-
UVA	Ultraviolet Band A	-
UVB	Ultraviolet Band B	-
FWHM	Full Width at Half Maximum	-
PTFE	PolyTetraFluoroEthylene	-
ILT	Ion Laser Technologies	-
LMSF	Laser Marine Surface Fluorosensor	-
ϕ	Quantum Efficiency	-
S	Singlet state	-

T	Triplet state	-
P	Polarisation	-
A	Anisotropy	-
I	Intensity	-
D	Electron Donor of PSII	-
Pheo	Pheophytin	-
Q_A	Primary Electron acceptor	-
$h\nu$	Represents a photon	-
P_{680}	Chlorophyll-a reaction centre of PSII	-
P_{680}^*	Excited Chlorophyll-a reaction centre of PSII	-
S/N	Signal to Noise ratio	-
MCA	Multi-Channel Analyser	-
ADC or A/D	Analogue to Digital Converter	-
IFE	Institute of Freshwater Ecology	-
CCAP	Culture Collection of Algae and Protozoa	-
DML	Dunstaffnage Marine Laboratory	-
CW	Continuous Wave	-
OPO	Optical Parametric Oscillator	-
C	Capacitance	F
R	Resistance	Ω
ϵ	Molar absorption co-efficient	$M^{-1}cm^{-1}$
M	Concentration	M
L	Length	m
Hz	Frequency (Hertz)	s^{-1}
E	Energy	J
h	Plank's Constant	J s
ν	Frequency of radiation	s^{-1}
c	Speed of light	ms^{-1}
λ	Wavelength	m
τ	Lifetime	s

Chapter 1

Introduction

The marine environment is an extremely complex and varied ecosystem. The oceans contain some of the smallest plants and animals on earth, as well as mammals weighing in excess of a few tons¹. Not only do the oceans sustain the creatures within them, but they also sustain the land animals and man. In particular, the oceans of the world play a major role in the carbon cycle². Without the oceans, carbon dioxide levels would increase and oxygen levels decrease, eventually resulting in asphyxiation of air-breathing creatures. It is therefore important that science monitors the state of the oceans' complex chemistry and biology.

1.1 Microscopic Plants and Organisms and the Food Chain

Microscopic plants and animals are one of the first links in the marine food chain. These plants and animals are termed *plankton*. There are many different types of plankton

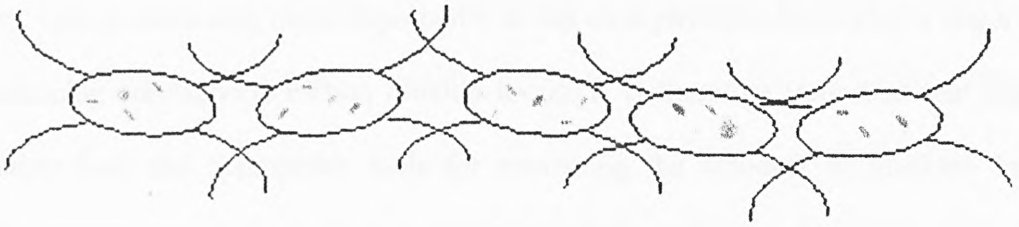


Figure 1.1: Schematic showing a chain-forming plankton from *Chaetoceros* genus

which can be microscopic plant life such as phytoplankton or microscopic animal life, zooplankton³. Shown in figure 1.1 is a schematic of a chain-forming type of phytoplankton. In general, the plant life is consumed by the microscopic animal life which is in turn consumed by fish and so on. By monitoring the plankton at the base of

the food chain marine scientists can give estimates on the amount of fish in the sea⁴ from mathematical models developed from information which has been continually gathered for hundreds of year's. In most maritime countries around the world, fishing is a large industry. It is therefore necessary to monitor fish stocks in order to set fishing quotas and to ensure that the seas are not subject to over-fishing⁵.

1.2 Phytoplankton in the Carbon Cycle

The carbon (Calvin) cycle describes how carbon is produced and used throughout the planet. Burning fossil fuels, decomposing organic material and respirational animals produce carbon dioxide and carbon which circulates in the atmosphere. Carbon dioxide concentrations do not increase to suffocation levels mainly due to a process called *photosynthesis*⁶. During photosynthesis, plants absorb carbon dioxide and produce oxygen which is released back into the atmosphere, allowing humans and animals to live. Photosynthesising plants, which are normally green in colour, contain a molecule, chlorophyll-a⁷, which absorbs the sun's energy, allowing photosynthesis to occur. These plants, such as trees and, more importantly in this case phytoplankton, play a major role in balancing atmospheric carbon dioxide levels. It is therefore important that marine scientists have the appropriate tools for measuring the amounts of plankton in the marine environment over a local area and on a global scale.

1.3 Pollution in the Marine Environment

1.3.1 Hydrocarbon Pollution

Marine pollution has been an ever increasing problem over the past few decades⁸. Greater numbers of ships on the oceans and the development of more oil and gas fields have contributed to the increase in pollution⁹. Both the drilling and transport of oil from

the various production fields around the world has inevitably led to oil spills, such as the Torrey Canyon spill in 1967, the Amoco Cadiz in 1978 which is shown in figure 1.2, the Exxon Valdez¹⁰ in 1989, the Braer in 1993 and Sea Empress in 1996. All these are tankers which ran aground whilst transporting various grades of crude oil.



Figure 1.2: Photograph of the Amoco Cadiz oil spill in 1978

In areas such as the North Sea where oil production is a major industry¹¹, chronic oil pollution is also a major problem. Hydrocarbons from the drilling platforms may be washed over the side of rigs and into the sea. The overall effect is an increase in the amount of hydrocarbons in the marine environment¹². Further pollutants from the drilling process, such as pseudo oil based drilling mud's (POBMs), also known as synthetic based fluids (SBFs), or synthetic based mud's (SBMs) which are used as coolants and lubricants, also find their way into the environment^{13,14}. There may also be hydrocarbon pollution from the flare stack caused by incomplete combustion of the gas/hydrocarbon mixture. Most of these chemicals will interact with the biological processes in the sea and may enter the food chain. Although these hydrocarbons and

chemicals may not be toxic in the lower food chain, accumulation in higher animals, however, may prove to be toxic¹⁵.

1.3.2 Shipping Pollution

Commercial shipping also poses a pollution problem. The accidental discharge of diesel oil and lubrication oil from machinery is not uncommon. Over the past few years, these discharges have been curbed with the introduction of fines for shipping companies^{16,17,18}.

A less obvious biological problem can exist. When a ship which fills its ballast tanks with water, it will almost contain certain types of marine algae native to that area. When the ship arrives at its destination and discharges the ballast water, the algae are introduced into another area¹⁹. Although these algae species may grow at a controlled rate, in their own environment, introduction into a new environment may cause the algae to bloom. Differences in temperature, nutrient conditions, and light levels can all work synergistically to increase cell production. Some algae also produce toxins. If filter feeding shellfish consume these algae, the concentration of toxins in shellfish increases rapidly^{20,21,22}. This in turn produces hazardous problems when humans consume the shellfish and can produce serious physiological effects in humans who consume the shellfish, even death²³.

1.3.3 Agricultural Pollution

Agricultural pollution also contributes to pollution in the marine environment. It is widely known that agricultural operations use fertilisers for ensuring healthy growth and increasing the yield of crops^{24,25}. These fertilisers contain phosphates and nitrates which, along with other trace metals and carbon dioxide, form the basic elements for

plant growth by photosynthesis²⁶. Not all the fertiliser however is absorbed by the crops. It remains on the soil until it rains, when the fertiliser is dissolved and carried into the soil and drains away naturally and in most cases will end up in streams. These streams in turn will flow into ponds or larger rivers which will eventually find their way to the sea. This natural drainage process immediately raises two potential problems. The first of these is the pond or reservoir. These water bodies tend to have very slow movements of water compared to a river for example. Primarily evaporation or other slow processes may govern the water level. No matter the process, the problem still remains, rich, nutrient-filled water from the agricultural land flows into a pond or reservoir where over time, the nutrient level increases making conditions ideal for algae growth²⁷ and potentially leading to algae blooms which can suffocate or poison aquatic life.

The second problem is very similar to the first except that instead of the nutrient rich drainage water being deposited into a pond, it is carried to the sea via larger rivers and deposited in coastal waters. Although the nutrient concentrations may not be as high, there may still be enough to cause an algal bloom. Many coastal locations around the United Kingdom have fish farms which provide an income for local communities. In the event of an algae bloom in one of these such areas, whole farms can be wiped out resulting in millions of pounds in lost revenue and possible ruin for the fish farm owners. In 1996, the salmon fish farming industry was valued at approximately £200 million²⁸. It is therefore important to develop monitoring systems for use in inland, coastal and open waters.

1.4 Ocean Measurements

Many marine creatures function in the absence of sunlight at depths where existence may seem impossible, producing light through biochemical processes. Most of the

plants and animals, however, require the presence of sunlight for healthy growth. The sun, providing energy in the form of heat and light allows plants and animals to grow.

In order to understand more about the oceans and the interactions between the world's climates and the marine environment, work has been ongoing to acquire as much physical, chemical and biological data to produce mathematical models which may predict the effects of various changes in the environment and climates of the world. Scientific inquiry over the past 60 years or so has been directed into determining the smaller picture: how these plants and animals function. A better understanding of the smaller plants and animals of the marine ecosystem (which are at the base of the food chain) would allow better insights into the future of animals further up the food chain, such as fish and mammals. These not only have commercial value, but also some regions of the world still rely on the oceans for their survival.

Much of this information-gathering requires long sea expeditions, often in hazardous conditions to collect water samples, larvae, fish trawls etc, all in an attempt to gain a better insight into the dynamics of the oceans. Today, automated systems collect water samples and more efficient nets are used for collecting plankton and fish.

1.5 Traditional Sampling Techniques

1.5.1 Net Sampling for Measuring Phytoplankton

The net sampling technique is concerned with the collection of fish and fish larvae. If algae was to be collected using this type of system, a very fine mesh would be required. This however would tend to become obstructed very easily. As the net becomes full, the ocean is no longer being filtered and hence the collection of the algae is reduced.

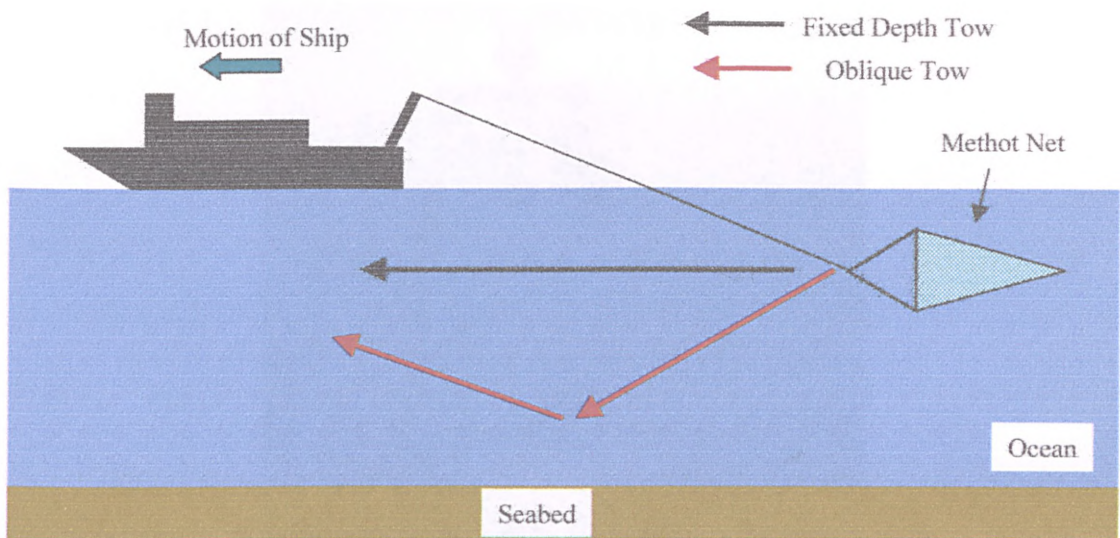


Figure 1.3: Schematic showing the different sampling strategies for the Methot net.

Once the net has been deployed over a certain time in either a fixed depth or oblique tow, it is recovered by the deck personnel and emptied. Shown in figure 1.3 is a representation of the sampling strategies for the Methot net. The net can either be towed at a fixed depth, which is shown by the black arrow, or in an oblique tow, which is represented by the red arrow.

Improvements were made to these nets in subsequent years, improving stability of the nets in the water and producing systems whereby nets could be opened and closed, allowing different sections of the water column to be monitored. These systems are still in use today, as can be seen in figure 1.4, although they have very limited use in phytoplankton monitoring.

The Methot net frames are made of steel which can weigh up to a few tons. On land, with a suitable crane, a frame is relatively safe and easy to move. It becomes much more hazardous when the net and frame are on the stern of a moving ship in rough weather. It can be seen that this technique is labour intensive, requiring a lots of preparation.



Figure 1.4: Modern day Methot net deployment.

1.5.2 Multi-net Sampler

Another system more routinely used for phytoplankton monitoring is the multi-net sampler which does not use the large net system. It is smaller and uses a plastic funnel to direct water through fine nets designed for collecting plankton. Up to 12 nets are mounted on a carousel and can be triggered to change position at various time or depth intervals. Once used, the net is sealed and the next one moved into place. This allows various samples to be obtained at different positions in a tow or at different depths, rather than giving an average over a whole tow as in the large Methot net system. The same type of tow is carried out as with the Methot net and the samples are stored as mentioned previously. This system, although providing more representative information than the Methot net, still requires a lot of preparation time and recovery time making it very labour intensive.

1.5.3 Water Bottle Sampling

Although water bottles were mainly used for water chemistry analysis, phytoplankton has also been collected using various water bottle configurations. One of the earliest systems had a bottle which closed when it reached the sea bed. Later developments saw the introduction of a water bottle with two corks at either end. The system was triggered, usually by a sliding weight, which closed the bottle before being hauled to the sea surface. This allowed monitoring of the water column at different depths whereas earlier systems were limited to the sea floor. More developments saw the introduction of multiple water bottles which were attached to a wire at various intervals. A photograph of these can be seen in figure 1.5. These are lying on the ships deck ready to be attached to the winch wire.

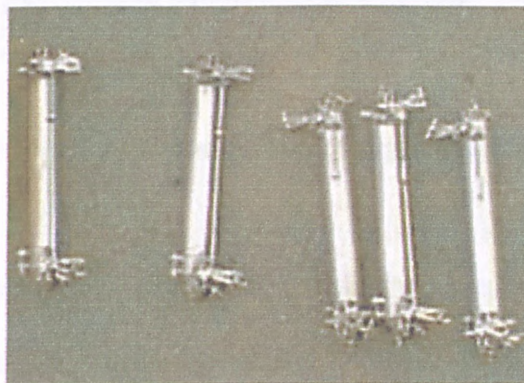


Figure 1.5: Water sampling tubes ready to be mounted on the winch wire

The wire is then lowered over the side of the ship until a certain length has been played out. A sliding weight (messenger) is then attached to the wire and allowed to slide down to the first bottle which triggers it to close much the same as the corks closing on earlier systems. The first messenger also triggers the release of a messenger attached to the first bottle which went on to trigger the second bottle and so on. Once all the bottles have

been closed, the wire is recovered and each of the bottles with their samples. There is however no guarantee that all of the bottles will close. If one of the messengers fail to release, there is no way of knowing this until the wire and bottles are recovered. Today the messenger is often replaced by electronics which sense the depth of the sampling carousel, shown in figure 1.6 , and trigger the bottles to close.

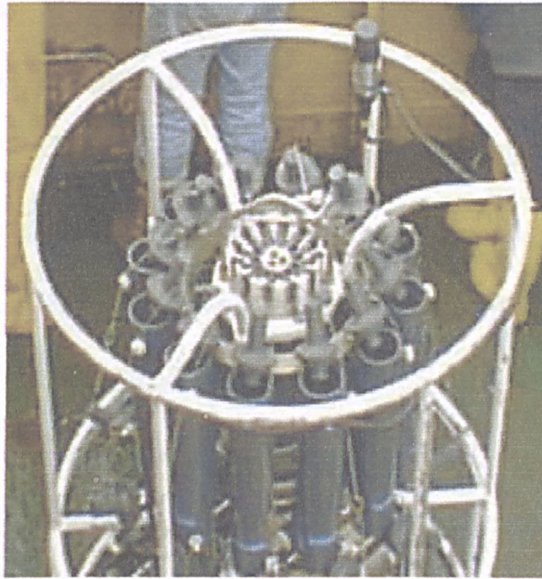


Figure 1.6: Carousel water sampling system

Although probably more accurate and less labour intensive, problems can arise if the battery system is low on power and cannot provide enough voltage to run the electronics or when a total power failure occurs. Time is wasted when the instrument is recovered only to find the water sample bottles empty. This can be very frustrating and calls into question whether the older systems were more reliable. All these systems are designed mainly for monitoring the sea water at depths. When measuring the upper water levels, a different sampling technique is required.

1.5.4 Hose-pipe and Bucket

When measuring water near the surface of the ocean, a pumping system is usually used. Water is pumped onboard the ship and water samples are taken frequently and analysed. The hose-pipe is normally located at a depth of around 6m below the sea surface, which is sufficient to prevent contamination of the water from discharges from the ship itself. If the ship is stationary, another technique using a hose pipe is employed to give an average of the phytoplankton concentration over a specific depth. A wide-bore, weighted hose-pipe is lowered into the sea until the desired depth is reached. The pipe is then sealed at the top, pulled back onboard the ship and emptied into a suitable container for analysis. Measurement and storage of the phytoplankton is carried out as previously described in this chapter.

If measurements at the sea surface are required, there are various methods available. An open bottle or bucket can be used to take a surface water sample. This however is a very crude system. Other sampling instruments can be used at the sea surface to obtain measurements but these have an immediate limitation in that they disturb the water that is being measured. This effectively disrupts the material being measured limiting the systems ability to provide representative and repeatable results.

1.6 Summary

The marine environment is an extremely complex system with a multitude of natural and synthetic variables which affect its condition and the life within it. These synthetic variables are in most cases detrimental to the health of the world's oceans and therefore require policing if damage to the ecosystem is to be curbed. It is only possible to control pollution if you can detect when there is a pollution incident and measure the magnitude of the pollution. It therefore requires measurement and monitoring methods to be

developed.

The past century has seen the development of marine biology with information being collated on various marine parameters from water chemistry and microscopic plant and animal life up to the larger mammals which inhabit the worlds oceans. But the resources used for both funding and monitoring the oceans have been very limited. The systems that have been developed are bulky, mechanical and relatively expensive to manufacture. When deployed, there is a serious risk of loss of the equipment due simply to the conditions in which it operates. The operating conditions also produce a real hazard to the operators. The measurements obtained using these systems are not necessarily representative of a body of water. Data is collected at intervals, which are often kilometres apart. These point-sampling techniques do not provide representative data over the area being monitored. Plumes of pollutants can easily be missed by point-sampling regimes.

Technology, however, has taken a step forward in marine science, allowing more information to be obtained in a safer manner. Advances in optical technology have allowed larger areas of the worlds oceans to be monitored using satellite technology²⁹ or airborne monitoring systems³⁰ that should provide more representative data. It is therefore important to review these optical techniques and to discuss their suitability in marine monitoring programs.

The objectives of this thesis is to investigate the potential of using optical techniques which may produce more information on the phytoplankton or oil on the sea surface and to develop a low cost, portable, optical real time monitoring system which can provide more representative data on the distribution of phytoplankton in areas such as the North Sea.

Chapter 2

Review of Optical Techniques used in Marine

Monitoring

2.0 Introduction

Modern optical analysis in biological monitoring has its foundations back around the early 1800s, when Sir David Brewster observed the passing of a strong beam of the sun's light through an alcohol extract of laurel leaves³¹. It was found that the green fluid produced a red glow when a strong beam of sunlight passed through the solution. The green solution would have contained *chlorophyll*, as it was named by Pelletier and Caventou in 1818³². The term *fluorescence* was not recognised until 1852, when Professor G.G Stokes sought a term to describe his observations. He originally used the phrase "*dispersive reflection*". However, as can be seen from a footnote in his report: "I confess I do not like this term. I am almost inclined to coin a word, and call the appearance *fluorescence*, from fluoro-spar, as the analogous term opalescence is derived from the name of a mineral"³³, he was not convinced. From this, Stokes has been credited as the first to recognise this phenomenon as light emission.

Since the discovery of chlorophyll fluorescence, many experiments have been carried out to determine the processes of photosynthesis in both terrestrial and marine plants. In simple terms, this fluorescence can be used to determine the quantity of chlorophyll-a within a certain plant. Experiments carried out in 1931 by Kautsky and Hirsch at the Chemistry Institute of the University of Heidelberg in Germany reported some of the initial time dependence results of chlorophyll-a fluorescence in a paper entitled "New experiments on carbon dioxide assimilation"³⁴. Chlorophyll-a

fluorescence, if interpreted properly, can also provide information on the identity of various pigments and complexes, their organisation, excitation energy transfers amongst them and various electron transfer reactions within the photosynthesising system.

Progress in optical technology over the past few decades has made it possible to develop instrumentation which would prove beneficial to marine science. Automation in the analysis of samples and the collection of data allows more information to be obtained and requires less intervention by personnel. This reduces the labour requirements and the time required for analysis. As more samples can be processed in a shorter time, more samples can be taken, hence allowing better representation of the parameters being measured.

2.1 Absorption Spectrometry

One of the simplest of optical techniques used for measuring species is absorption spectrometry. Shown in figure 2.1 is a diagram of a typical single beam ultraviolet /visible (UV/Vis) spectrometer.

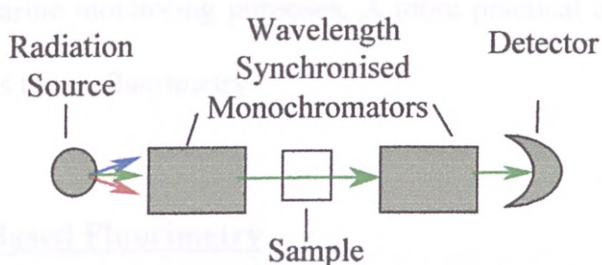


Figure 2.1: Diagram showing the major components of a UV/Vis spectrometer

This consists of an excitation source, excitation monochromator, sample holder, emission monochromator and detector. The monochromators work synchronously allowing the selection of a specific wavelength to be passed through the sample and into the emission monochromator, then onto the detector. The detected signal is that of the initial light intensity from the source reduced by any absorption when passed through the sample. The amount of light absorbed can be used to determine the concentration of the species (quantitative measurement) and the wavelength at which the absorption occurs gives information on the electronic transitions for the species (qualitative measurement). Both pieces of information are important in determining the properties of the species. This technique, however, is not ideal. Absorption spectroscopy has a limited sensitivity compared with other optical techniques, due to the nature of the signal, i.e. A small change on a large background signal is being detected. As the concentration of the species is reduced, the change in the initial light level becomes smaller and more difficult to detect because the signal to noise ratio is decreased. There is also the problem of the geometry of the instrument. In the marine environment, this would require water to be pumped on board the ship for analysis. This method is not ideal for remote marine monitoring purposes. A more practical approach, which has a higher sensitivity, is to use fluorimetry.

2.2 Laboratory Based Fluorimetry

Fluorimetry comes from the term fluorescence, whereby high energy light is imparted into a molecule, raising an electron in a molecule or atom to an excited state. In fluorescence, some energy is lost from the system by non-radiative decay before the remaining energy is lost by radiative decay in the form of a lower energy photon of a specific wavelength depending upon the species. The emitted photon is therefore at a

different wavelength from the excitation radiation. This method of analysis is much more sensitive as the fluorescence signal is being measured on a small background also geometry of the instrumentation is much more flexible. As can be seen in figure 2.2, fluorescence from the sample is emitted in all directions. This is another major advantage of using fluorescence. The components of the system are essentially the same as the UV/Vis spectrometer with the major difference being the geometry of the system and that the monochromators can be scanned independently.

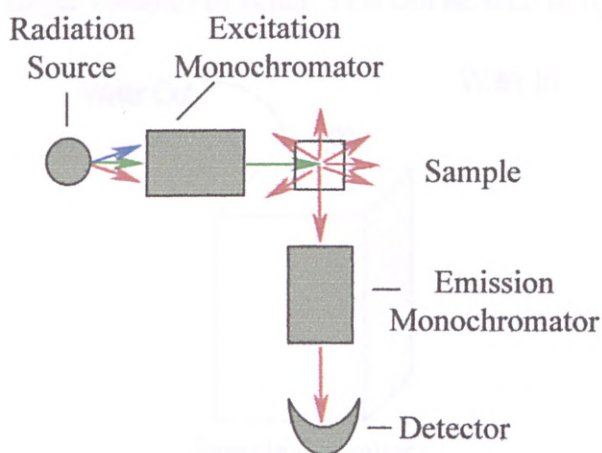


Figure 2.2: Diagram showing the major components of a fluorimeter

The second major advantage of using fluorimetry is the increased sensitivity over absorption spectrometry. This is brought about by the nature of fluorescence. It is an active process which absorbs one wavelength of light and emits a different wavelength. The fluorescence signal can be a very weak signal but as it occurs at a different wavelength than the excitation light, the background for the signal is essentially zero, therefore the signal to noise ratio is much higher than can be achieved with UV/Vis spectrometry. The increase in sensitivity is approximately 10-1000 times more than that of absorption spectrometry.

With the development of laboratory fluorimeters, quantitative and qualitative information can be obtained on algae by monitoring their fluorescence properties. This however still requires water to be taken onboard the ship, a sample to be taken and the fluorescence reading to be recorded. This, although not as labour-intensive as actually counting the algal cells, still requires some work.

2.2.1 Flow Cell Fluorimeters

By using fluorescence cells in which samples can be pumped in and out, it becomes possible to monitor larger volumes of water. This can be seen in figure 2.3.

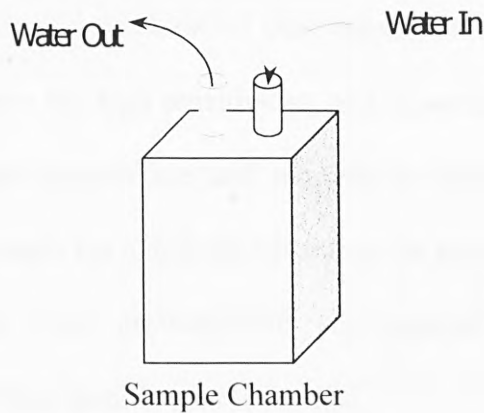


Figure 2.3: Diagram of a fluorimeter flow-cell

The water can be pumped up from under the ship, passed through the fluorimeter and then discharged back into the sea. By using this setup, it is not necessary to take and store water samples to obtain algal cell concentrations in relatively shallow depths up to about 6m below the sea surface. Monitoring the water below this depth is not practical as it would be physically impossible to keep a pipe at a fixed depth with the boat moving. If the ship is stopped, then it may be possible to use a weighted pipe to achieve greater depths. The problem is that the ship has to stop or be travelling very slowly and

hence less area is covered in a fixed time. This is the very problem which was addressed by automating the water sampling. Automation allows more water samples to be taken over a larger area to obtain a better representation of the distribution of phytoplankton within a given water volume, over a given period of time. There is also the problem that the system is not surface specific. It is virtually impossible to take water samples from the sea surface using a discrete sampling or flow cell system

A fluorimeter used routinely today is the Turner Design 10-AU-005-CE field fluorimeter. This can be set up for discrete samples or continuous flow measurements using a 25mm one-piece flow cell. This particular system has a sensitivity of $0.01\mu\text{gL}^{-1}$ for Rhodamine WT, $0.03\mu\text{gL}^{-1}$ of extracted chlorophyll-a and $10\mu\text{gL}^{-1}$ of crude oil in water. Although the system has high sensitivities, and is portable, it is still essentially a bench fluorimeter. Water samples are still required to obtain measurements of the species. Although this system has a definite advantage for monitoring shallow depths, it may be of limited use when measurements are required at depths greater than approximately 6m or surface-specific measurements.

2.3 Submersible Fluorimetry

2.3.1 Submersible Single Wavelength Fluorimeters

To address the problem of monitoring phytoplankton concentration or oil at depths over 6m, similar types of field fluorimeters have been adapted for use under water, usually on towed vehicles. These systems allow many measurements to be obtained in the water. If the research ship is stationary then a depth profile of phytoplankton fluorescence can be obtained, as illustrated in figure 2.4, along with other measurements such as salinity, temperature and depth. These instruments can also be towed along a

certain heading at a fixed depth or on an oblique tow gathering information similar to that seen previously in figure 1.3.

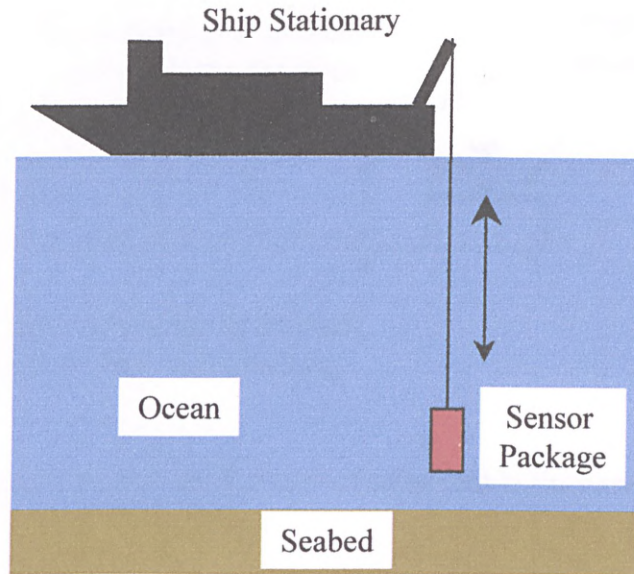


Figure 2.4: Diagram illustrating depth profile measurements

The major advantage over the flow cells systems is that it can be towed at depths where the previous system could not be used. The main fluorimeter instruments used in marine science today and are manufactured by four main companies: Chelsea Instruments in Portsmouth, England; Turner Designs in California, USA; Wetlabs Inc (formerly Seatech Inc) in Oregon, USA; and Seapoint Sensors Inc in New Hampshire, USA. These instruments provide essentially the same information on the plankton present in the ocean.

Traditionally, these submersible fluorimeters are based on a pulsed xenon flash-lamp design although the new *SCUFA* instrument from Turner Designs, launched in May 2000, uses light emitting diodes (LED's) as the excitation source and a photodiode to detect the fluorescence. The basic schematic of the instruments is shown in figure

2.5. The instrument is constructed of a cylindrical pressure housing made of titanium, plastic or stainless steel depending on the operating depth which can be up to 6000m.

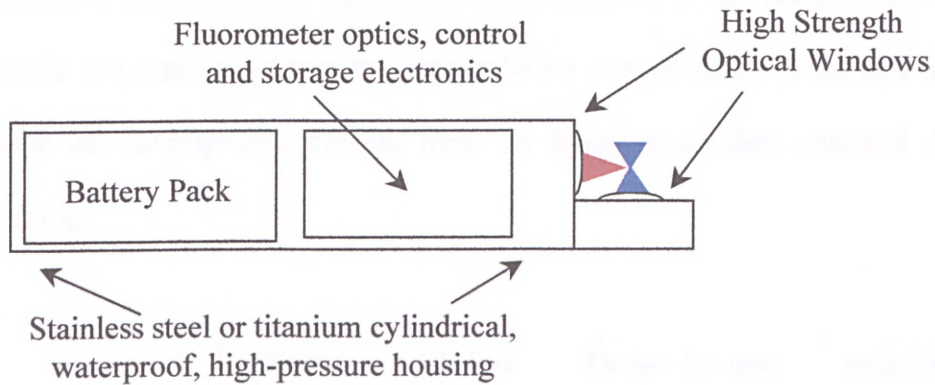


Figure 2.5: General diagram of submersible fluorimeters.

The systems power sources are normally D-cell 1.5 volt batteries or a rechargeable battery pack. These are used to power all the electronics onboard the fluorimeter including the flash-lamp, the electronics controlling the fluorimeter, the data storage memory and controllers and downloading computer link once back on deck. Depending on which species is being observed, the excitation filters and flash-lamp can be changed to give UV or visible radiation. In the case of phytoplankton, a band-pass filter at 430nm is used. The excitation blue light is focused as shown in figure 2.5 to a point which is at the focal point of the lens, at right angles to the excitation lens. If there is any phytoplankton in the vicinity of this light, the plankton may absorb the blue light resulting in a red fluorescence, also shown in figure 2.5. This fluorescence is passed through an optical filter which is fixed at 680nm before passing onto a photomultiplier tube for the hydrocarbon monitoring option or a photodiode for chlorophyll-a and other fluorophor detection. These convert the light signal into a voltage that can be converted into a digital signal and stored in the fluorimeter memory. The instrument is then retrieved and taken onto the ship where the data can be downloaded via RS 232

communications to a computer. The system is normally returned to shore and calibrated once the research trip has been completed. This is done by making up standard suspensions of phytoplankton. The fluorescence intensity is then recorded before part of the sample is treated to obtain the chlorophyll-a concentration. This data is used to determine the chlorophyll-a content from the fluorescence data obtained during the research trip.

	Sea Tech/ Wetlabs <i>Flash lamp fluorimeter</i>	Chelsea Instruments <i>AQUA^{tracka} UV and Mk III</i>	Turner Designs <i>SCUFA submersible fluorimeter</i>	Seapoint <i>Rhodamine and Chlorophyll-a fluorimeters</i>
Rhodamine / μgl^{-1}	0.002	0.01	0.04	0.02
Fluorescein / μgl^{-1}	-	0.01	-	-
Chlorophyll-a / μgl^{-1}	0.015	0.01	0.02	0.02
Oil / μgl^{-1}	-	0.001 Carbazole	-	-

Figure 2.6 : Comparison of the sensitivities of the four main submersible fluorimeters in use today

Obviously these systems provide large amounts of information regarding the populations of phytoplankton in the area being studied. The systems are self-contained requiring only a battery pack for operation. The flashlamp and data collection rates are fully user programmable and the systems can operate under extreme depth and weather conditions. Shown in figure 2.6 is a comparison of the sensitivities of each of the leading submersible fluorimeters. It can be seen from the table that all of the fluorimeters have very similar sensitivities for the most common species which are monitored. In the case of rhodamine, the sensitivities correspond to molar

concentrations of $5 \times 10^{-10} \text{M}$ or higher. Although these systems are able to detect trace quantities of the species in water, the systems do have limitations in that they are essentially point sampling techniques, the whole instrument is submerged, they have a limited data storage capacity, and they are limited to measurements below the sea surface.

2.3.2 Submersible Multi-Wavelength Fluorimeters

Submersible multi-wavelength fluorimeters have recently been developed as an extension of the single wavelength system. The difference in this type of system is in the fluorescence detection. The photomultiplier or photodiode and optical filters are replaced with an optical grating and a linear photodiode array. Use of the grating allows the collected light to be separated into the component wavelengths. This is then imaged onto the linear array, which consists of several small photodiodes side by side. When calibrated, each of these photodiodes corresponds to a narrow wavelength region. By having the array, a complete spectrum can be obtained with the strength of the signal corresponding to the intensity of the fluorescence at a particular wavelength. A diagram of the essential components can be seen in figure 2.7.

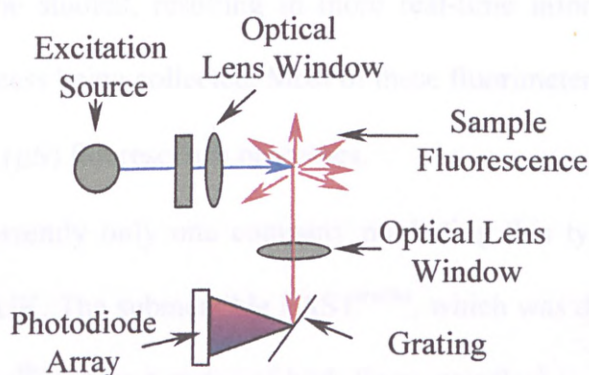


Figure 2.7: Multi-wavelength detection fluorimeter

This system uses a filter wheel on the excitation source, which is rotated constantly at a frequency of 10 Hz. The filters are selected to pass violet, blue, green and blue-green colours from a quartz-tungsten-halogen lamp. By using each of the different wavelength bands, it is possible to differentiate between some classes of phytoplankton from their excitation and emission spectra³⁵. Although this is not a new concept^{36,37}, the advantage in this system is that the excitation filters are changed automatically within the instrument compared to the more traditional single excitation/emission instrument, which requires the instrument to be recovered and the filters changed manually^{38,39}. The system developed by Desiderio et al at the College of Oceanic and Atmospheric Sciences, Oregon State University and WET-labs Inc has been shown to detect chlorophyll-a concentrations down to $0.01\mu\text{g l}^{-1}$. This system has sensitivities comparable to those of single wavelength fluorimeters. This sensitivity is achieved, however, by acquiring 100 spectra, which is a signal average over 10 seconds.

2.3.3 Submersible Primary Productivity Fluorimeters

More recently, the introduction of time-dependent fluorimeters based on pulsed light emitting diode technology has allowed the fluorescence kinetics of marine phytoplankton to be studied, resulting in more real-time information relating to the photosynthesis process being collected. Most of these fluorimeters, however, are used to study relative slow (μS) fluorescence processes.

There is currently only one company marketing this type of system, Chelsea Instruments in the UK. The submersible FAST^{tracka}, which was designed at Brookhaven National Laboratory^{40,41}, uses a series of high-frequency flashes to enable measurement of the absorption cross section of Photosystem II (PS II), the rate of photosynthetic electron transport and the level of photochemical quenching. All these measurements

are taken in real time, in-situ and, by also monitoring the photosynthetically active radiation (PAR), the phytoplankton primary productivity can be estimated. This system has a sensitivity of $0.1\text{-}30\mu\text{g l}^{-1}$ for chlorophyll-a. Although not as sensitive as the other towed fluorimeters, information is obtained on the relative health of the phytoplankton as well as chlorophyll-a concentration.

2.3.4 Laser Fluorimeters

Laser fluorimeters have been developed primarily for calibrating remote sensing systems. When airborne monitoring systems are used, these types of laser fluorimeters are normally used on research ships where water samples are taken and analysed using the same type of laser wavelengths of the airborne systems. This provides a method for calibrating the aircraft signals and improving algorithms for these remote sensing systems.

There are two main systems in use, one by NASA⁴² and the other by ENEA⁴³. The NASA system is fully automated using a flow cell system for the seawater. The system uses a dual wavelength Nd:YAG laser operating at 355nm and 532nm which correspond to the same wavelengths for the Airborne Oceanographic Lidar (AOL) which will be discussed later. This system records chromophoric dissolved organic matter (CDOM) fluorescence, phycoerythrin fluorescence and chlorophyll-a fluorescence along with the water Raman signals for excitations at 355nm and 532nm which is used for normalising the data and compensate for changes in water clarity.

The second system developed by ENEA, Italy, is a similar system to that above using a Nd:YAG which is operated at 266nm and 355nm. The 266nm wavelength is used for exciting organic pollutants and oils whereas the 355nm is used for exciting

CDOM and chlorophyll-a fluorescence. Again the system uses the Raman scatter peak from exciting at both 266nm and 355nm for normalising the data.

2.4 Discussion: Submersible Measurement Systems

It can be seen that all of the techniques discussed require the measurement system to be in contact with the sample. Absorption spectrometry has a limited sensitivity and requires a 180 degree geometry for the system to work. This could be used on a marine ship but may not be sensitive enough and samples would have to be taken onboard to be analysed.

Fluorescence, however, is a more suitable option for marine monitoring. It is more sensitive than absorption spectrometry and a 90 degree or back scattering geometry can be used. There are two options in using this technique. Samples from relatively shallow depths can be pumped onboard the ship for analysis. This limits the working depth to approximately 6m. If greater depths are required then submersible fluorimeters can be used.

The first limitation in all these systems is that they use a pulse of light to excite the phytoplankton. This in effect makes them point sampling techniques which only collect data whilst the excitation light is on. As these systems are normally towed, both the speed of the ship and the frequency of the flashlamp or LED's determine the resolution of data obtained. A high flashlamp rate and slow tow would result in lots of data points which would give high resolution information of the area under study. These systems however, have a limited data storage capacity, which means the system would have to be recovered frequently and re-initialised after the data onboard had been downloaded. This, as expected, takes a lot of time and also uses a large amount of energy in powering the flashlamp, making the system in this configuration very

impractical. The system is normally then operated at an intermediate ship speed of 5 knots and a moderate flashlamp rate of approximately 5 Hz. This allows larger areas of the ocean to be covered, less time in recovering and deploying the instrument and relatively good data. Consideration of this setup, however, does introduce some questions. When towing the system, there are only three possibilities: a fixed depth tow, or an oblique tow or variants on those. In each case, the system is only collecting limited data. At a fixed depth, other depths are not monitored. During an oblique tow different depths are sampled at different times and positions along the route of the ship. In each case, information is being lost. Due to the fact that plankton do not grow uniformly throughout an expanse of water, but rather grow in patches where nutrients are plenty, it is possible that an unrepresentative picture of an expanse of water may be obtained.

Secondly, these systems are designed to operate below the sea surface. Due to the geometry of the instrument, it is virtually impossible to monitor the sea surface using such systems. If this was tried, the vehicle carrying the sensor would disturb the water surface and hence the results would be invalid. The systems are further limited in that deployment of the instruments generally require a winch or crane system. This introduces more personnel and hence labour costs in addition to safety considerations when towing instruments. There may also be a large financial risk involved in carrying out this type of work. These instruments which cost in the region of £30k, are being towed at up to 6000m below the sea surface. It is possible for the instrument to become snagged on the sea bed or the attaching pins to work themselves loose, resulting in the instrument being lost.

Although these systems certainly have their place in marine science especially in monitoring the ocean depths, there is a requirements for monitoring surface waters also.

This problem has been partially addressed by using remote sensing optical techniques as can be seen in section 2.5.

2.5 Remote Sensing Measurements

In this context, remote sensing may be broken into two main areas: laser-based detection methods and satellite imaging systems. The laser-based systems actively induce fluorescence within the species being monitored, whereas the satellite-based systems use solar stimulation to determine the emissions and absorption characteristics of the ocean.

2.5.1 Lidar (Laser) Monitoring

Light detection and ranging (Lidar)⁴⁴ is a broad term which was initially used for distance measurement instruments. Systems using a pulsed laser and a detector could measure the time it took for the laser light to strike a target and return to the detector, thus measuring the distance between the system and the target. However, it is still used in its broadest sense to describe remote sensing systems which use a laser as an excitation source along with a detector to measure an optical property of a material at some distance. Most of these systems also use a smaller laser range-finder alongside the remote sensing instrument.

The invention of lasers in 1960⁴⁵ allowed scientists to exploit the features associated with them. Lasers often provide a high intensity and highly selective wavelength radiation source to be used for measuring physical, chemical and biological properties. These types of systems can be classified as active sensors in that continuous wave or pulsed laser radiation is directed onto the sea surface, normally down the major axis of a telescope. The laser radiation is then absorbed and re-emitted as fluorescence

or scattered by the species being monitored. Some of this radiation is scattered back towards the laser source (backscattered radiation) and is collected by the telescope. The light is then passed through some wavelength selection optics, which could be interference filters or a spectrograph. These allow different components of the returning signal to be separated and passed onto a detector arrangement. These detectors normally take the form of photomultipliers or a charge coupled device (CCD). The outputs from the detectors are then converted into a digital signal then stored and processed on a computer. The general layout of a lidar system can be seen in figure 2.8. A laser range-finder is also included with the system to determine the height of the aircraft above the sea surface alongside the altimeter.

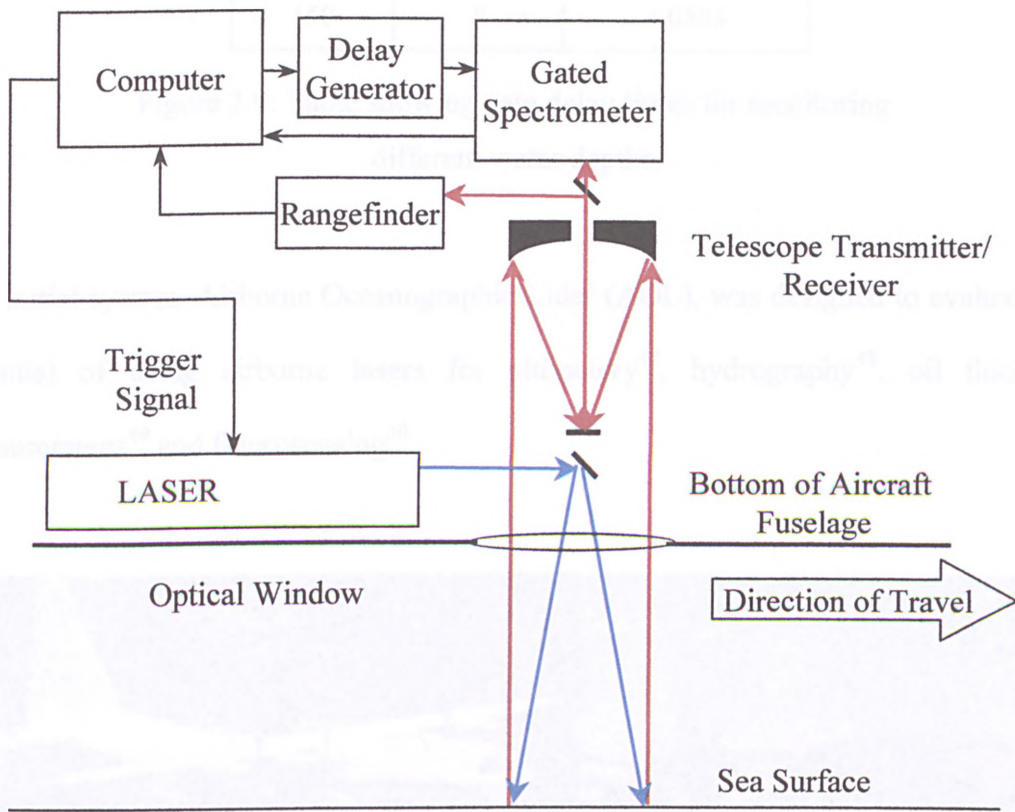


Figure 2.8: General components of a lidar system.

This information can also be used to set the gate delay time on the spectrometer,

allowing different depths of water to be monitored, as can be seen in figure 2.9.

In 1977, one of the first airborne oceanographic Lidar systems was built by the AVCO Everette Corporation under a joint sponsored program with the National Aeronautics Space Administration (NASA) and National Oceanic and Atmospheric Administration (NOAA)⁴⁶.

Aircraft to water distance/m	Depth monitored/m	Gate delay time/ μ s
150	0	1.0000
150	2	1.0133
150	4	1.0267
150	6	1.0400
150	8	1.0533

Figure 2.9: Table showing gate delay times for monitoring different water depths

The initial system, Airborne Oceanographic Lidar (AOL), was designed to evaluate the potential of using airborne lasers for altimetry⁴⁷, hydrography⁴⁸, oil thickness measurements⁴⁹ and fluorosensing⁵⁰.



Figure 2.10: Photograph of a C-130 “Hercules”(left) and a P-3B “Orion” (right) used to house the Airborne Oceanographic Lidar

This system was located in NASA C-130 or P-3B aircraft which were flown at approximately 150m from the sea surface at a speed of approximately 150ms⁻¹. Photographs of the different aircraft are shown in figure 2.10. The size of the aircraft should be noted in comparison with the ground personnel. This gives an indication of the size of the AOL instrument. The instrument also collects solar induced (passive) ocean colour measurements which are used to develop and validate algorithms for satellite monitoring systems such as NASA's Sea-viewing Wide-field-of-view Sensor (SeaWiFS)⁵¹.

There are various other lidar systems in use today. These are of various configurations and are used for monitoring different species such as hydrocarbons^{52,53,54}, chlorophyll-a mapping^{55,56}, chemical species⁵⁷ and more recently phytoplankton productivity^{58,59,60}. The main components of these systems are detailed in figure 2.11. It can be seen that most of the early systems used a pulsed nitrogen laser as the excitation source up until around the middle of the eighties. Since then, the use of excimer lasers has been widespread due to their ability to produce UV radiation which is ideal for exciting hydrocarbons. When monitoring chlorophyll-a and gelbstoff, however, most of these system require the addition of a dye laser. By selecting an appropriate dye, it is possible to generate wavelengths which correspond to absorption maxima of chlorophyll-a. More recently, as crystal technology has progressed, Nd:YAG lasers have become cheaper and more versatile than the nitrogen, excimer or dye lasers. By using the second, third and fourth harmonics, the lasers can reach well into the UV as well as providing emission in the near UV and visible regions. These options make the laser more attractive not only in running costs compared to an excimer laser but also in the physical size of the laser and the relatively clean operation.

There have also been improvements in the detectors used for lidar systems. Early lidars used banks of gated photomultiplier tubes with a range of filters to cover a wide spectral range. With the increased production, stability and sensitivity of charged coupled devices (CCDs) and spectrographs, a single detector and spectrograph can be used to replace the many (up to 64 in some cases) photomultipliers and filters.

Sensor	Country	Year	Laser Type	Wavelength/nm	Energy/mJ	Detector Range/nm	Resolution/nm	Species	Platform
Airborne Oceanographic Lidar (AOL)	USA	1980	Nitrogen	337	1	350-800	11.25	HC & Chl-a	Aircraft
		1983	Nitrogen/Nd:YAG	337/532	1/300	400-800		Chl-a	Aircraft
		1994-	Nd:YAG	335/532	100/300	400-800	12.6	Chl-a	Aircraft
Laser Environmental Airborne Fluorosensor (LEAF)	Canada	1980	Nitrogen	337	1	386-690	20	HC & Chl-a	Aircraft
		1995	Excimer/Dye	308/480	20/1.8	328-668/517-715	5.3/3		Aircraft
Oceanographic Lidar System-Federal Inst for hydrology	Germany	1992	Excimer	308	approx 20	300-800	-		Aircraft/Van
Hydrographic Laser Sensor - University of Oldenburg	Germany	1990	Excimer/Dye	308/450	120/6	344-730	ave 43		Aircraft
National Electricity Generating board (ENEA) - Frascati system	Italy	1991	Excimer	308	150	330-800	0.5	HC	Ship
		1998	Nd:YAG	266/355	7/30(3)	402,450,650,690	approx 10	HC & P/P	Ship
Chekalyuk/Demidov et al-Moscow State University	Russia	1993	Nd:YAG					Chl-a & P/P	Ship/aircraft
KLS-10	Estonia	1991	Excimer	308	200	250-570/500-750	1	HC & Chl-a	ship
Quimm/Al-Bahrani et al	Kuwait	1994	Nd:YAG	266		360-620	20	HC	
			Nd:YAG	355		400-660	20	HC	
			Nitrogen-Dye	428		460-720	20	OFTD	
			Nd:YAG	532		550-810	20	HC	

Key

HC = Hydrocarbons

Chl-a = Chlorophyll-a

P/P = Chlorophyll-a pump and probe

HFTD = Hydrocarbon Fluorescence Time decay

Figure 2.11: Main characteristics of the various lidar systems in use today.

2.5.2 Airborne Oceanographic Lidar (AOL)

The latest version of the AOL instrument uses a single spectra physics DCR2-20, Nd:YAG laser, operating at 20Hz. The laser is frequency-doubled and tripled to produce 532nm and 355nm. These are then directed onto two different spots on the sea surface using beam splitting mirrors. The resulting fluorescence is collected using a 30cm telescope. As the spots on the sea surface are at different positions, the resulting fluorescence is observed at different positions on the spectrometer focal plane. This allows simultaneous processing of both the spectra.

The 532nm, 300mJ radiation is used for stimulating chlorophyll-a and phycoerythrin pigments in plankton⁶¹. The 355nm, 100mJ radiation is used to excite organic carbon molecules. Recording the spectrum from 370nm to 740nm allowed the fluorescence for the two phycoerythrin pigments – phycourobilin at 565nm and phycoerythrobilin at 580nm to be measured along with the fluorescence at 685nm due to chlorophyll-a fluorescence. The water Raman signal from each of the two laser excitations, 404nm for 355nm excitation and 650nm from 532nm excitation, were also recorded to normalise the laser-induced fluorescence signals for surface spatial differences in water attenuation properties⁶².

Oil thickness measurements have been carried out using the suppression of the water Raman peak when using a nitrogen laser. This has been shown to detect oil between 0.05 and 5 micrometers thick on sea water.

2.5.3 Laser Environmental Airborne Fluorosensor (LEAF)

The last upgrade of the LEAF was carried out in 1992. The updated system now boasts 64 channels giving a spectral resolution of approximately 5nm. This system, developed in Canada, is used primarily for monitoring oil spills. A xenon-chloride (Xe-Cl) excimer

laser, operating at 308nm, is used as the excitation source. This laser is capable of operating for 6 hours before the cavity gas requires changing. This is an obvious and immediate drawback. This either requires carrying compressed gases on board an aircraft for extended monitoring programs or the aircraft has to land to have the system re-charged. The danger is further increased by the type of gas used; xenon chloride is very toxic. It is therefore not one of the most desirable systems for routine use. The detector consists of a 203mm, Dahl-Kirkham telescope which is coupled to a spectrometer. The detector consists of a gated 1024-channel intensified diode array with a gate width of less than 20ns. Compared to the AOL system, the laser system is much larger. The detector, however, does boast a greater resolution and is also more compact.

2.5.4 ENEA Frascati Lidar Fluorosensor

This system, developed in Italy by the ENEA Research Centre, is very similar to the Canadian LEAF system. Again, the excitation source consists of a Xe-Cl laser operating at 308nm. The detection system consists of a 200mm Newtonian telescope which is coupled to a 0.32m monochromator. The detector again uses an 1024-channel intensified photodiode array. This system has the highest resolution of all the systems at 0.5nm. This is primarily due to the setup of the monochromator system. This, however, produces a reduced spectral range of the system. One of the advantage of this system, however, is the incorporation of a second detector. Using a streak camera, fluorescence time decay measurements are possible. This has more recently been used for carrying out pump-probe measurements on phytoplankton⁶³. This information not only gives the distribution of the phytoplankton present in an area with the standard chlorophyll-a fluorescence measurement, but by carrying out the pump-probe allows the relative health of the plankton to be determined.

2.5.5 Oceanographic Lidar System – Federal Institute for Hydrology

The instrument description is similar to the previous two instruments and has been used for detecting oil emulsion and chlorophyll-a.⁶⁴ It has been reported to have a detectability of 0.2µg per litre of rhodamine or chlorophyll-a in water. This is one of the only systems which has reported a minimum detection value for their system compared to those above.

2.5.6 Discussion: Lidar Technology

The systems, described and detailed in figure 2.11 all use a variety of configurations to achieve similar goals. Some of the systems are more alike than others because they share the same types of lasers or photodiode array detectors. Almost all of them require mounting on an aircraft or ship with a few able to be fitted into the back of a van. They are generally bulky in size and weigh upwards of 500kg, which may reduce their portability. Another major drawback is the cost of running them. There is the initial investment in the various components and also the high cost of operating the system. It costs thousands of pounds to have these systems installed in aircraft and flown regularly. There is also a problem in the accuracy of their data. Most of the systems shown here give an indication to the presence of chemicals, phytoplankton or hydrocarbons relative to the water Raman signal. There is however very limited references to the minimum detection limits of these species. It is only recently that the large organisations such as NASA and ENEA have seen the requirement for their airborne data to be verified by the use of a laser based fluorimeter. This again adds to the cost of the technique, requiring a ship with the laser fluorimeter to monitor the same water as the airborne system, effectively using two systems to do the same job. It must

therefore be considered if there are any other methods which could carry out the same measurements for less financial investment.

2.5.7 Satellite Monitoring

The advent of satellite technology in the late 1970s allowed scientists access to platforms located miles above the earth's surface. This allowed large areas of both the land and the oceans to be observed. In October 1978, the experimental satellite, Coastal Zone Colour Experiment (CZCS), was launched onboard NIMBUS-7. This was the first instrument devoted to the measurement of ocean colour.

Previous systems flown on spacecraft had been used for monitoring the ocean colour, but these had been optimised for monitoring land. Their spectral bands, spatial resolution and dynamic range reduced the sensitivity for monitoring water colour.

The new system operated on the principle that as more particulate matter was contained in a water body, the colour of the ocean in that area would change. Open waters where there is very little particulate matter scatter visible light in the deep blue spectral range. As particulate matter is increased in that water expanse, the light scattering characteristics are changed and hence so is the water colour. For example, phytoplankton have specific absorption characteristics around the blue and red regions of the electromagnetic spectrum resulting in the water which appears to be greener. Other types of plankton can cause the ocean to appear red or even yellow. Other scattering sources such as inorganic particulate matter have different colours from organic material. By observing these different ocean colours, the CZCS provided a means by which to monitor chlorophyll-a concentration, sediment distribution, gelbstoff concentrations, water temperatures and ocean currents.

Scattered solar energy was measured using six channels: C1:433-453nm

(chlorophyll absorption), C2:510-530nm (chlorophyll correlation), C3:540-560nm (gelbstoff – used to indicate salinity), C4:660-680nm (aerosol absorption), C5:700-800nm (land and cloud detection) and C6:1050-1200nm (for surface temperature). The system was located at an altitude of 955km above the earth's surface, giving a ground resolution of 0.825km. Although the system provided key information for scientists on an almost global scale, there were very real limitations to this technology. The cost of such a system runs into tens of millions of pounds in the development of the technology, the launch of the satellite and the subsequent operation of the sensor. Over the 8 years of operation, the system was, on average, operational for 2 hours per day due to the power requirements of various on-board experiments. As early as 1984, problems were encountered with the sensor. Failure to activate the system and spontaneous shut-downs plagued the mission for its last 2 years, and the system was finally declared non-operational in December of 1986. Although data was obtained during its operational lifetime, there were problems with calibration of the system once in flight. One of the most significant problems arose when the algorithm for atmospheric correction was applied to the data. Ships in the ocean below would carry out the same measurements as the satellite overhead and the two data sets would be correlated. This process was termed "ground truthing", as the ship's data did not suffer from atmospheric effects which would alter the signals being received by the satellite. It was discovered that the satellite data and the ship-based data had discrepancies when the atmospheric algorithm was applied. These had to be corrected to obtain a calibration. It was also noted around this time that the instrument sensitivity was declining with time resulting in modifications to the sensor gain controls. Later analysis in 1994, of the data obtained during the CZCS lifetime revealed that there had been short-term sensitivity fluctuations during the course of the mission.

With this type of calibration, it should be possible to obtain good data, assuming the system was calibrated frequently to account for declines in system performance and varying atmospheric conditions. This method of ground truthing was however very limited and was only carried out during the early stages of the mission. Calibrations in later years were only obtained if and when a ship was in the area during the time the satellite would pass overhead. This problem with the atmosphere, which contributes a major portion of the backscattered solar radiation (80-100%), required the sensor calibration error to be below approximately 1% to allow the determination of the water-leaving irradiance with an absolute accuracy of 10%. This may have been possible in areas where there was a minimum contribution from the atmosphere and ground truthing was possible. For the same technique to be used in an area such as the North Sea, the system would immediately run into problems. The weather conditions and cloud cover would reduce the sensitivity of the system considerably. A further limitation of the CZCS was the resolution. At 0.825km, it could be considered a rather large area to cover. Trends within these areas would have been very difficult to observe and problems or potential problems may have been overlooked. Subsequent analysis of the data obtained during the operational lifetime of the CZCS has shown that good radiometric calibration and sensitivity are required for an ocean colour sensor. In the report by Evans and Gordon⁶⁵, they conclude "...that extensive ground truth data collection is needed to monitor the performance of the sensor and algorithms over time under varying atmospheric and water conditions". Although the Coastal Zone Colour Experiment provided limited information on the ocean colour due to several problems with the system, the lessons learned by the scientists allowed the next generation of satellite sensing system to be developed: NASA's Sea-viewing Wide-field-of-view Sensor (SeaWiFS).

Finally launched in August 1997 after the expected launch in spring of 1995, the SeaWiFS system, located on the SeaStar satellite, was activated in September of the same year. Again, the system uses 8 bands: 402-422nm, 433-453nm, 480-490nm, 500-520nm, 545-565nm, 660-680nm, 745-785nm and 845-885nm. This system, however, uses more wavelengths in the visible region compared to the CZCS to allow more accurate data to be obtained. The system is able to operate in two modes, local area coverage (LAC), giving a ground resolution of 1.2km, and global area coverage (GAC), with a 4km ground resolution. Requiring only two days to cover the world's oceans, the system is a very powerful tool for obtaining ocean colour trend measurements and hence plankton distributions on a global scale.

2.5.8 Discussion: Satellite Technology

Satellite technology does, however, have its limitations. The technique is not a real time system and requires 24 hours for preliminary data processing. Any part of the ocean is only monitored once every 48 hours. The SeaWiFS system is limited to a 1.2km ground resolution which, at best, may not be sufficient for monitoring smaller expanses of water such as lakes and coastal waters. In areas such as the North Sea where there is substantial cloud cover, the sensitivity of the system would also be reduced considerably. The largest disadvantage of satellite technology is the inherent cost involved in making the satellite and also the large cost of getting the satellite into space. Current cost for transport into space is approximately £16k per kilogram.

2.6 Summary

It is possible that the submerged instruments risk being lost during deployment in the sea resulting in a loss of the fluorimeter. They are also point measurement systems with

a limited data storage capacity. When deployed, there is no way of determining if the instrument is recording data until the system is recovered. If this is the case, then the ship may have to repeat the transverse, which would cost more money.

Remote sensing lidar systems are expensive to build, generally require an aircraft for deployment in the field, and they are heavy and bulky. The lasers normally used in these types of systems produce high laser powers in a few nanoseconds, giving peak powers of the order of hundreds of kilowatts which could be dangerous to operators and mariners. These systems measure relative changes in concentrations of a species and are used primarily for mapping relatively large areas of the sea surface and may not be suitable for measuring smaller areas of water or inland waters. For aircraft based systems, it is impossible to take water samples to verify the fluorescence data. There is also the additional cost of operating the aircraft and the operating costs of the lasers themselves which may require additional toxic gases to be stored on the aircraft.

These same types of systems have been used on ships and suffer from many of the same problems as the aircraft based systems. They are expensive, bulky, dangerous and heavy. As the laser beam strikes the sea surface at a relatively shallow angle compared to aircraft systems, the danger to other mariners increases. The high energies associated with the laser beam can be magnified by binocular instrument which are routinely used on marine vessels. The cost of operating a ship is also expensive. These systems are operated on research vessels which are often modified to accommodate the lidar systems. The size, cost and dangers of these system make them unfeasible for routine monitoring.

Satellite technology does provide a great advantage in the monitoring of the oceans in that large areas can be covered in a relatively short time. This allows scientists to observe plankton concentrations on a global scale. The technology, however, does

have very important drawbacks. The most prominent limitation of a satellite based system is the cost. The development, launch and maintenance of a system is very expensive and can run into hundreds of millions of pounds. This technology is limited to government funded organisations such as NASA or large company conglomerates. At present, these systems do not have high enough resolution for monitoring smaller expanses of water such as the north sea and inland waters. They can also suffer from effects such as cloud cover which may considerably reduce the sensitivity of the instrument. In an area such as the North Sea where cloud cover is relatively high compared to the Mediterranean ocean for example, the instrument is not an ideal candidate for marine monitoring purposes. There is also the problem that the instrument data is not obtained in real time. Data processing of the information gathered by the system requires at least forty eight hours.

Clearly there is a need for the development of a integrated measurement scheme which should be able to address some of these problems discussed above.

As part of an integrated measurement scheme, the instrument would require the following properties:

- Relatively cheap to build and operate
- Give real-time data
- Use a low power laser to minimise optical hazards
- Compact and portable for easy deployment in the field
- Capable of remote measurements for inaccessible areas
- Capable of detecting different waterborne pollutants
- Capable of verifying the collected data

By adopting a technology combining the above properties, a measurement scheme may be realised and may be beneficial to a wide range of people. Fish farmers may use the instrument for detecting the presence of an algae bloom allowing them to take remedial action, the oil industry may use the system for detecting accidental oil releases quickly and also for monitoring the efficiency of their flaring operations. Marine science may be able to gather much more representative over an area hence allowing more accurate prediction of the worlds fish stock. This would allow governments to make much better informed decisions when making decisions on fishing policies.

The objectives of the research work in this thesis are :

- Develop a ship-based, real-time phytoplankton monitoring system
- Provide a system to give a better representation of the area under study
- Develop a non-contact sea surface measurement system
- Assess optical techniques which may provide more qualitative information on phytoplankton in their natural environment.
- To carry out a series of sea trials with the systems

In developing such an optical technique it is necessary to review some of the optical processes of light and its interaction with biological and chemical species. It is also important to be familiar with the different types of optical and electrical signal enhancement techniques which may allow small quantities of the species to be detected.

Chapter 3

Theory and Instrumentation Techniques

3.0 Introduction

There are various forms of spectroscopy which can be used to determine physical, chemical and biological species. Luminescence is used to describe a wide variety of photon emission processes such as fluorescence, phosphorescence, chemiluminescence and bioluminescence. Fluorescence and phosphorescence occur when a system absorbs photons and re-emits them at different wavelengths. Chemiluminescence is a process whereby molecules reach an excited state through a chemical reaction. Light is again emitted from the system as the species relaxes to the ground state. Bioluminescence is very similar to chemiluminescence in that a chemical reaction produces the excited molecules when then return to the ground state give out light. The difference between these two excitation methods is that bioluminescence only occurs in living organisms and is brought about by the chemical reaction of luciferase and luciferin such as can be seen in fire-flies.

Only fluorescence and phosphorescence are of concern in this thesis. For these processes to work, light must first be absorbed by the species. Absorption and emission occurs at specific wavelengths characteristic of the species being measured. This gives information on the molecular configurations, electronic transitions and energy levels within the molecule. This information can be used to characterise a particular species, possibly identifying it and certainly determining the quantity of a species present. By measuring the amount of light emitted by fluorescence, it is possible to determine the

quantity of material present. This can be calculated using the modified Beer-Lambert law:-

$$I_f = k\phi I_0 (1 - e^{-\epsilon c l})$$

I_f = Measured fluorescence intensity

k = constant

ϕ = Quantum efficiency of the system

I_0 = Intensity of the incident light

ϵ = molar absorption constant

c = concentration of the species : M

l = path length : m

Once the light has been absorbed by the species, promoting the valence electrons from the ground state to an excited state, the system will try to return to the ground state by releasing energy by non-radiative decay or by emitting a photon. The emission of a photon is known as fluorescence or phosphorescence depending on the time scale of the emission of the light. To understand where the fluorescence originates in the molecule it is necessary to be aware of some molecular theory.

3.1 Molecular Orbitals

3.1.1 Basic Molecular Structure

Atomic orbitals are described by the three quantum numbers n , l and m which arise naturally in the solution of Schrodinger's equation^{66,67}. The principle quantum number, n , determines the overall size of the orbital and may only have positive integer values greater than zero. The greater the number, the higher is the probability of finding an

electron at greater distances from the nucleus. The angular quantum number, determines the shape of the atomic orbital. This too has a restriction in value, being $n-1$ for any given value of n . Traditionally, the first four l values are assigned the letters s , p , d and f . These correspond to sharp, principle, diffuse and fundamental, which spectroscopists use to describe the lines in atomic spectra before wave mechanics. Shown in figure 3.1 are space-filled models of the shape of the atomic orbitals of the first 3 angular quantum numbers.

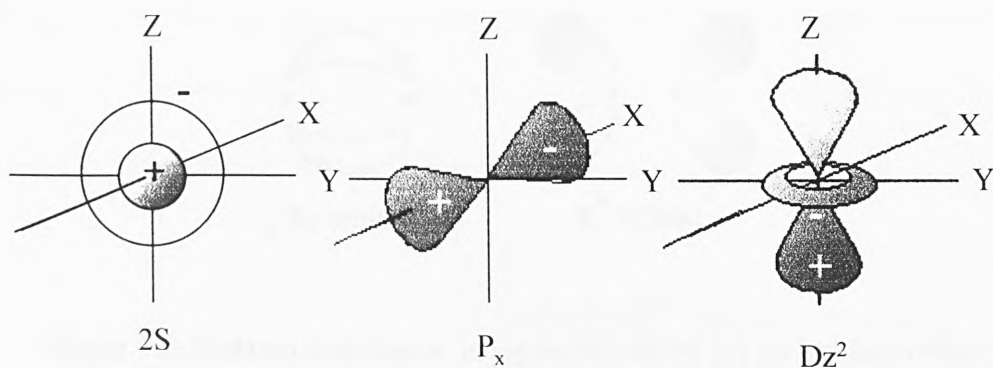


Figure 3.1: Space filled representations of the shape of the atomic orbitals of the first 3 angular quantum numbers, s , p and d

When dealing with molecules which consist of many elements, the electrons within these molecules also reside in orbitals. These are known as molecular orbitals and also are described by wave functions⁶⁸. These molecular orbitals describe the energy levels of the electrons within a molecule and arise from the combination of atomic orbitals. All organic compounds are capable of absorbing electromagnetic radiation because they all contain valence electrons which can be excited to higher energy levels. Organic compounds can have single, double and triple bonds. The molecular orbitals associated with single bonds are designated as sigma (σ) orbitals containing one pair of bonding electrons arising from the overlap of s orbitals, whereas double bonds have a sigma

orbital and a pi (π) orbital which is formed by the parallel overlap of atomic p orbitals. When in the ground state, the electrons occupy the σ and π low energy orbitals. When in an excited state, the electrons are in the corresponding anti-bonding orbitals σ^* and π^* . The electron distribution of these electrons can be seen in figure 3.2.

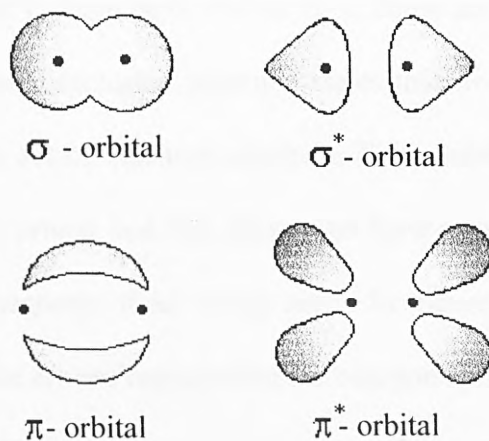


Figure 3.2: Electron distribution in sigma (σ) and pi (π) molecular orbitals

In addition to σ and π orbitals, organic molecules also contain non-bonding electrons, n. Shown in figure 3.3 are various electronic transitions within molecular bonds and the regions where absorption occurs.

Electron Transition	Wavelength Absorption Region/nm
σ to σ^*	<200
π to π^*	200-700
n to σ^*	150-200
n to π^*	200-700

Figure 3.3: Various electronic transitions and associated absorption regions

It can be seen that absorption in the visible region produces π to π^* and n to σ^* transitions and also photons are produced in the visible region when these transitions relax.

The final quantum number, m , is the magnetic quantum number. This number is dependent on the value of l . It can be 0, $+1$ to -1 . These are known as the spin states of the electrons. The Pauli exclusion principle states that no two electrons within an atom can have the same set of quantum numbers. This means that no more than two electrons can fit into an orbital and that they must have opposed spin states $+$ and $-$ resulting in the net magnetic field being zero. In figure 3.4, this can be seen diagrammatically with the arrows representing the electron spin directions.

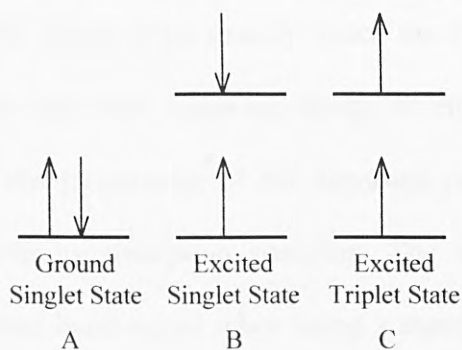


Figure 3.4: Diagram showing the electron spin direction for different excited states

The normal situation of a system is shown in figure 3.4A, with the electrons in the ground state with opposing spins. When an electron is excited to a higher energy level, the electron normally opposes the spin of the electron in the ground state, resulting in an excited singlet state as can be seen in figure 3.4B. If, however, the electron spin in the excited state is the same as that of the electron in the ground state, the system is said to be in an excited triplet state, as in figure 3.4C. These show how the electrons may

behave when they have been promoted to an excited state. In order to be excited, energy must be imparted to the system. This process occurs by absorption.

3.2 Absorption

When light is passed through a liquid or gas, certain frequencies of radiation may be removed by absorption which is dependent upon the bonding within the species. This is a process whereby the energy of a photon can be transferred into a molecule promoting it from the ground state to one or more higher energy levels, or excited states. From section 3.1, it can be seen that molecules have a limited number of discrete energy levels which depend on the bonding within the molecule. For absorption to occur, the photon passing through the sample must exactly match the energy difference between the ground state and any excited state. Since the energy differences for most species are different, by monitoring the frequencies of the absorbed radiation, it is possible to characterise a sample from its absorption spectrum. The absorption spectrum of a molecule gives a very broad band signal when using a standard laboratory absorption spectrometer. What is actually occurring within the molecule is multiple absorption's. The energy associated with an absorption band is made up of three components which are :

$$E_{\text{Total}} = E_{\text{electronic}} + E_{\text{vibrational}} + E_{\text{rotational}}$$

Each of these different energies correspond to different energies which can be absorbed by the molecule. The $E_{\text{electronic}}$ is the energy of the molecule associated with the energy states of its bonding electrons, whereas $E_{\text{vibrational}}$ corresponds to the total energy associated with the inter-atomic vibrations present in the molecule. In most molecules, there are many more vibrational energy levels than electronic levels. The rotational energy component, $E_{\text{rotational}}$, comes from all the rotational motion present in a molecule.

There are even more rotational energy levels than vibrational levels. When a spectrum of a sample is taken, a smooth, broad peak is observed, but it really consists of all these transitions within the molecule.

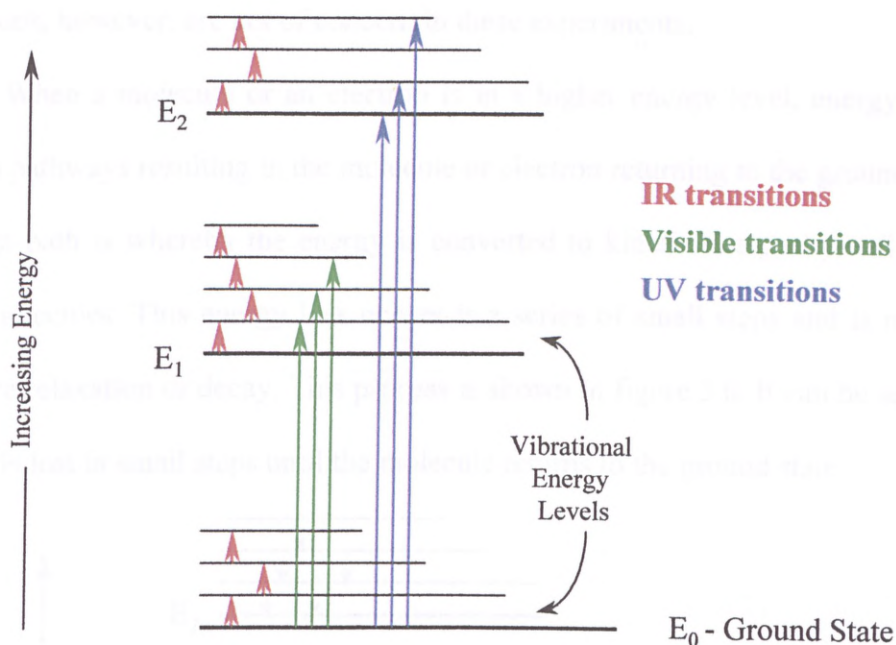


Figure 3.5: Simplified energy level diagram showing energy absorption transitions

Shown in figure 3.5 is a general diagram of some of the electronic and vibrational energy levels. For simplicity, the rotational energy levels are not shown.

In molecular absorption, radiation is absorbed throughout different parts of the electromagnetic spectrum. Radiations absorbed in the ultraviolet and visible regions normally correspond to excitation of a molecule to higher energy levels. A diagram of these transitions can be seen in figure 3.5. It can be seen that visible radiation produces transitions between the ground state and any of the vibrational energy levels of excited state E_1 which is the first electronic state. When ultra-violet light is passed through a sample, any absorption promotes the molecule to higher excited states which may be electronic or vibrational. Near or mid-infra-red radiation causes transitions between

vibrational levels. Radiation is also absorbed at other wavelengths in the electromagnetic spectrum. Transitions between a ground state and an excited rotational state occur when long infra-red or microwave radiation is used on the sample. These transitions, however, are not of concern in these experiments.

When a molecule or an electron is in a higher energy level, energy is lost via various pathways resulting in the molecule or electron returning to the ground state. The simplest path is whereby the energy is converted to kinetic energy by collisions with other molecules. This energy loss occurs in a series of small steps and is named non-radiative relaxation or decay. This process is shown in figure 3.6. It can be seen that the energy is lost in small steps until the molecule returns to the ground state.

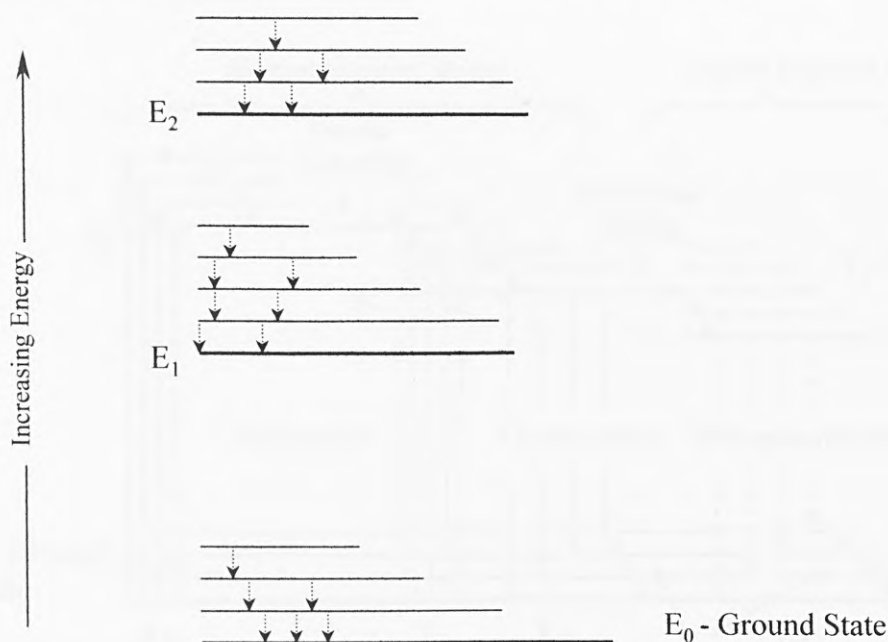


Figure 3.6: Simplified energy level diagram showing non-radiative de-excitation

The electrons within the excited molecule may however return to the ground state by other de-excitation pathways such as Fluorescence or Phosphorescence.

3.3 Fluorescence and Phosphorescence

It has been seen that an electron or molecule can absorb quantised energy which promotes the system to a higher excited energy state. During this time in the excited state, the system may undergo partial de-excitation via non-radiative decay, as described previously. The system may also return to the ground state by releasing the energy in the form of a photon. This light, however, is emitted at a longer wavelength. This process is known as fluorescence. This process generally occurs in a short period of time of around 10^{-9} s. Some systems may stay in an excited state for longer and hence the resulting release of a photon may be of the order of milliseconds to minutes which can be slow fluorescence or phosphorescence.

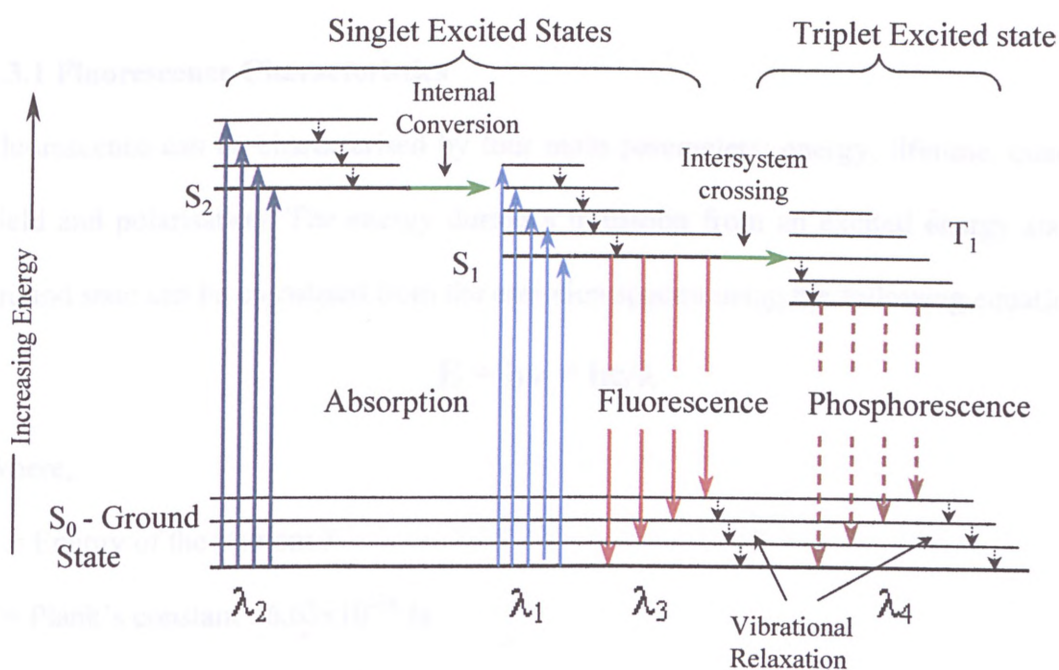


Figure 3.7: Energy level diagram showing absorption, fluorescence and phosphorescence

The phenomenon whereby a photon is emitted from a molecule at a lower energy than the incident photon is named Stokes fluorescence. A simplified energy level diagram showing absorption, fluorescence and phosphorescence can be seen in figure 3.7. S_1 and

S_2 correspond to excited singlet state energy levels whereas S_0 corresponds to the ground state and T_1 corresponds to some excited triplet state. The diagram shows how energy can be absorbed to excite the molecule or electron into higher singlet energy levels. Where a band between S_2 and S_1 overlaps, the energy is converted internally and passed to the S_1 energy level. The molecule may then undergo a series of non-radiative decays before a photon is emitted as fluorescence. Some of this energy in S_1 may cross to the excited triplet state, T_1 . Again, the molecule or electron may undergo some non-radiative de-excitation before a photon is given out. Energy released as a photon from a triplet state to ground state is known as phosphorescence and occurs on a longer time-scale to fluorescence.

3.3.1 Fluorescence Characteristics

Fluorescence can be characterised by four main parameters: energy, lifetime, quantum yield and polarisation. The energy during a transition from an excited energy state to ground state can be calculated from the emission spectra using the following equation:

$$E = h\nu = hc/\lambda$$

Where,

E = Energy of the photon: J

h = Planck's constant : 6.63×10^{-34} Js

ν = Frequency of radiation: s^{-1}

c = Speed of light in a vacuum : 2.99×10^8 ms^{-1}

λ = Wavelength of radiation : m

Fluorescence lifetimes have in general been shown to follow first order exponential decay rate equation^{69,70}. This gives a general expression relating the fluorescence intensity, I, with the fluorescence lifetime, τ , of :

$$I = I_0 e^{-t/\tau}$$

I = The fluorescence intensity at any time, t

I_0 = The maximum fluorescence intensity during excitation

t = The time after the excitation source has been removed

τ = The average lifetime of the excited state.

The quantum yield (Φ) of a system is defined as the number of quanta emitted for every quantum absorbed. This is effectively a measurement of the efficiency of the photo system and can be represented as:

$$\Phi = \text{Number of fluorescence quanta emitted/number of absorbed quanta}$$

If the absorbed photons are not used for photochemical reactions, then the total quantum yield of the system must be unity.

The final property in describing fluorescence is the polarisation of the emitted photon. This can be described by polarisation (P) and anisotropy (A) and is given by the equations:

$$P = I_{//} - I_{\perp} / I_{//} + I_{\perp}$$

$$A = I_{//} - I_{\perp} / I_{//} + 2I_{\perp}$$

$I_{//}$ and I_{\perp} are the fluorescence intensities parallel and perpendicular to the excitation source light.

In biological systems such as phytoplankton which contain chlorophyll-a, absorption of light occurs exciting the chlorophyll-a molecule. This molecule can produce fluorescence which allows it to return to the ground state. There is however another pathway in which the molecule can return to the ground state. The energy can be utilised for biochemical reactions leading to the production of organic molecules. This process is known as photosynthesis.

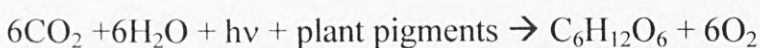
3.4 Photosynthesis

In the photosynthesis process, collections of pigments absorb light. These molecules then transfer the energy to specialised reaction centres, chlorophyll-a molecules, where the primary photochemistry occurs. These collections of pigments are referred to as the photosynthetic unit and contain the light-harvesting system for photosynthesis. There are two light-harvesting pigment systems, known as photosystem I (PSI) and photosystem II (PSII). Of these two light harvesting pathways, PSII is known to be more strongly fluorescent. There are, however, fluorescence emissions which occur at different times during the energy transfer process.

1. $DP_{680} \text{ Pheo } Q_A + hv \rightarrow DP_{680}^* \text{ Pheo } Q_A \rightarrow DP_{680}^+ \text{ Pheo}^- Q_A \rightarrow$
 $D^+ P_{680} \text{ Pheo } Q_A^- \rightarrow DP_{680} \text{ Pheo } Q_A$
2. $D^+ P_{680} \text{ Pheo } Q_A + hv \rightarrow D^+ P_{680}^* \text{ Pheo } Q_A \rightarrow D^+ P_{680}^+ \text{ Pheo}^- Q_A \rightarrow$
 $D^+ P_{680}^* \text{ Pheo } Q_A \rightarrow D^+ P_{680} \text{ Pheo } Q_A + hv_{(680)}$
3. $DP_{680} \text{ Pheo } Q_A^- + hv \rightarrow DP_{680}^* \text{ Pheo } Q_A^- \rightarrow DP_{680}^+ \text{ Pheo}^- Q_A^- \rightarrow$
 $DP_{680}^* \text{ Pheo } Q_A^- \rightarrow DP_{680} \text{ Pheo } Q_A^- + hv_{(680)}$

The above equations show the various possibilities leading to fluorescence emission where $h\nu$ is a photon, D is the electron donor of PSII, Q_A is the secondary electron acceptor, Pheo is pheophytin and P_{680}^* is the excited state of the reaction centre of PSII. When a photon of light is absorbed by the chlorophyll (Eq 1), the reaction centre of PSII (P_{680}) becomes excited (P_{680}^*) resulting in charge separation. The P_{680}^* becomes oxidised with the pheophytin being reduced. The electron is then transferred to the secondary electron acceptor, Q_A . The reaction centre is reduced by the electron donor D, with D itself being oxidised. The electron transfer continues along the photosynthetic chain to PSI where it is used, with other molecules to produce carbohydrates. Fluorescence from PSII arises when a further photon enters the system whilst either the electron donor is still oxidised (Eq 2) or if the secondary electron acceptor is still in a reduced state (Eq 3). As charge separation cannot occur, the excited reaction centre then undergoes de-excitation resulting in a photon of light being emitted as prompt fluorescence ($h\nu_{680}$). The fluorescence is dependent upon the rate of charge recombination between P_{680}^+ and $Pheo^-$ and occurs when Q_A is fully reduced so that electron transfer from $Pheo^-$ is not possible.

Shown above are the steps of the passage of the energy within the photosynthesising pigments when a photon is absorbed by the light harvesting pigments where P680 is the reaction centre *Chl a* of PSII and I is the primary electron acceptor pheophytin. These effectively demonstrate how the energy of the photon is used for photosynthesis which builds the carbohydrates. This can be shown simply using the equation :



It can be seen that the photosynthesis process converts inorganic carbon from dissolved carbon dioxide into organic carbohydrate molecules, with the release of oxygen.

Experiments have also been carried out to measure the time-scales of various de-excitations and electron movements within the photosynthesis chain. An outline of these can be seen in figure 3.8.

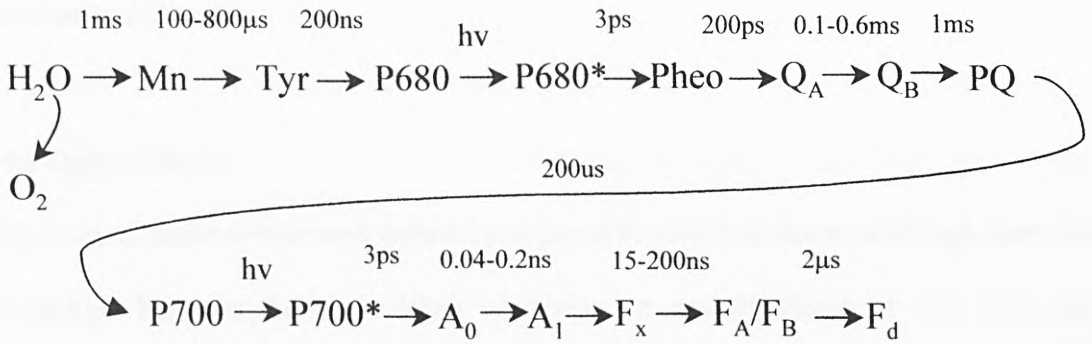


Figure 3.8: Diagram showing the approximate time for electron transfers during photosynthesis

Photosynthesis has been shown to occur in steps. The electron transfers have been measured in the past⁷¹ at different time-scales as can be seen in figure 3.8. In developing instrumentation to monitor the sometimes weak fluorescence from algae and chlorophyll-a it is important to be familiar with techniques for increasing the signal to noise ratio of the instrumentation and be aware of potential noise sources within the instrumentation.

3.5 Noise Sources and Signal Enhancement Techniques

Noise is a common factor in all electronic or optical systems. Measurements of very small or very low concentrations of a specimen are often limited by the noise of the measuring instrument. It is therefore important that care be taken when designing and constructing instruments for measuring small signals whether electrical or optical and that appropriate techniques are used to reduce noise in an instrument to a minimum

level. There are three basic types of noise when dealing with electronic systems: *Fundamental, Random and Interference (Discrete)*. These have been described elsewhere⁷². In optical system noise can be broadly classified in two categories, *Random and Discrete*.

3.5.1 Optical Noise

This form of noise is less well defined compared to electrical noise, although there are similarities between the two. When observing an optical signal of any type, the surrounding light level plays a part in how well the signal can be detected. If all other light was eliminated except for the optical signal being observed, then there would be a very high signal to noise ratio (S/N). In practical terms, however, this is not always possible, and there does exist some background light which reduces the S/N ratio. In the visible spectrum (400-700nm) where these experiments are carried out, the signal will only comprise a very small part of that spectrum; the rest of the visible radiation present can be considered as noise. As with electrical signals, the most effective way of reducing noise and hence increasing the S/N ratio is reducing the bandwidth being observed. This is done quite effectively by using optical filters which selectively allow wavelengths of light to pass and greatly attenuate the intensity of the rest. It is also possible to further increase the signal to noise ratio by making the signal distinct from the background noise. Once appropriate optical filters have been used to limit the optical noise, the optical signal can be converted into an electronics signal for further signal processing. This can be done in a variety of ways.

3.5.2 Optical Detection

There are three main types of detectors available for detecting optical signals:

photodiodes of various forms, photomultiplier tubes and Charge Coupled Device (CCD) arrays. The first of the three detectors, photodiodes, are the easiest and cheapest for converting light into an electrical signal. They come in a variety of sizes, response times and sensitivities. The most sensitive of these are *Avalanche* photodiodes which have quantum efficiencies up to 80%. However, these photodiodes are more sensitive in the infra-red compared to the visible region of the electromagnetic spectrum. The sensing area is normally limited to a few square millimetres and hence they are more commonly used in fibre optic communications.

Photomultipliers provide a larger detector area and are a good choice for a detector. They are sensitive in the visible to near infra-red region making them ideal for monitoring weak fluorescence signals.

CCD arrays are also very useful detectors in that a whole spectrum can be obtained by using a grating to spread the wavelength components of a signal onto multiple, small, light sensitive, silicon chips. These are however are expensive (approximately 30-40 times that of a photomultiplier tube) and would add to the cost of the instrument.

3.5.3 Signal Enhancement Techniques

If the signal has different characteristics compared with the noise in the system, then it can be separated. The major factor which increases the S/N ratio in most cases is narrowing the detection bandwidth, which preserves the signal but reduces the total amount of broadband noise. In using a continuous wave laser such as the Argon ion, operating at 488nm, as the excitation source for sodium fluorescein, there is a constant fluorescence observed at 514nm. If the experiments were carried out in a dark room, then there would be very little background light, leaving mainly the laser light and the fluorescence from the sodium fluorescein. Even if this were the case, it is still very

difficult to obtain very high signal to noise ratios due to interference. With this in mind, various methods of increasing S/N ratios have been developed, most of which, however, depend on a periodic signal. Although this may seem to be a problem, in most measuring instruments, it is possible to force the signal to become periodic if it is not already so. The main signal enhancement techniques include signal averaging, boxcar integration, pulse-height analysis, lock-in detection and phase sensitive detection.

3.5.4 Signal Averaging

Signal averaging is a common method which is used to increase the S/N ratio. In this type of system, sequential samples of the signal are collected and averaged. As noise in most cases is random, the noise in the signal tends to be a minimum value whereas a periodic signal remains at a constant level. It can be seen in figure 3.9 that the initial trace (5 scans) looks like random noise.

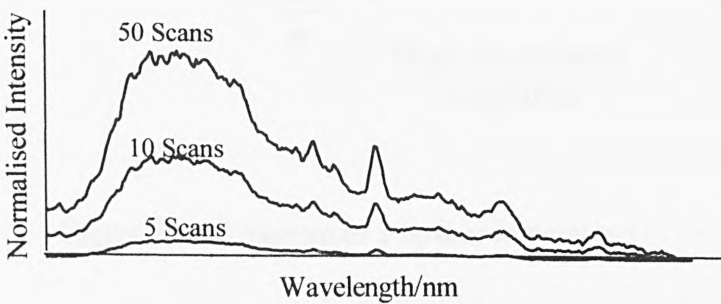


Figure 3.9: The effect of signal averaging

As the number of samples of the signal is increased, however, a recognisable signal is observed (10 scans). As the number of scans is further increased, the fine spectral data can be observed (50 scans). This technique can be useful if the user has time to wait whilst samples are obtained of the signal. If high frequency sampling is used, then this

may be adequate for signal recovery of fast signal events. Slow periodic events, however, require a much longer sampling time and hence this type of signal recovery may not be desirable.

3.5.5 Boxcar Integration

A boxcar integrator is a single channel, analogue, signal-averaging circuit. It is designed for recovering pulsed signals from noise. The system has two possible operating modes: scanning, which is used for detecting waveforms, and single-point, which is used for measuring pulses.

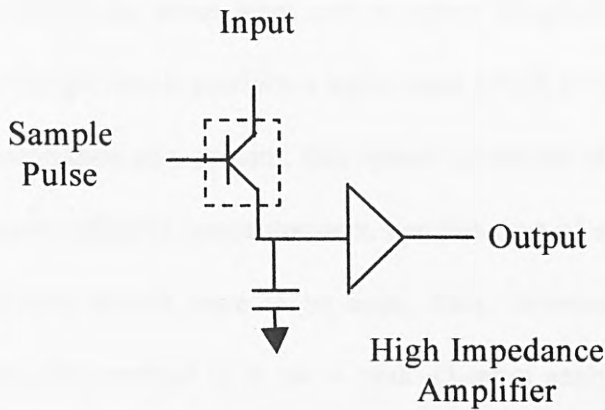


Figure 3.10: Diagram of a boxcar integrator

A basic circuit for a boxcar integrator can be seen in figure 3.10. When used for single pulse measurements, a sampling pulse with a sampling period T switches the sampling gate from a high impedance to a low impedance. If the gate is in a low impedance state, the output signal follows the input. The capacitor C then charges up with time constant RC , where R is the resistance of the gate and the signal source. When the gate is in the holding mode, the capacitor holds the output until the next sample is taken. In all modes of the boxcar integrator, the samples of the waveform containing both noise and the

signal are added together and an average taken for the final value. If n samples are collected and averaged, there will be an enhancement of the signal to noise ratio. Again this system takes a finite time to obtain a signal.

3.5.6 Pulse-Height Analysis

Pulse-height analysis consists of a simple discriminator which can be set above noise level and which gives a logic pulse for every signal that is above the discriminator threshold. If, however, only a small fraction of voltages (pulse heights) are of interest, then a single channel analyser may be used. This system is capable of having two thresholds set, one above the noise level and an upper threshold level. Input signals which fall between the two levels produce a logic pulse which is counted. In the case of monitoring the concentration of a species, this system would be of no use as there is no discrimination between different concentrations. For this type of system to work, many single channel analysers would have to be used. This, however, is impractical and expensive. An alternative method is to use a multi-channel analyser. A multi-channel analyser (MCA), can be considered as a series of SCAs with incrementing narrow windows. It consists of an analogue-to-digital converter (ADC), control logic, memory and display. The multi-channel analyser collects pulses in all voltage ranges at once and displays this information in real time, providing a major improvement over SCA spectrum analysis. By using this type of setup, various concentrations of the species could be measured once the system had been calibrated. This technique however is normally used in experiments where discrete events occur such as radioactivity. For it to be of use in fluorescence measurements, a pulsed laser system capable of producing ultraviolet or blue laser light would have to be employed. Although it would have been possible to obtain such a laser, the cost of purchasing the laser along with a multi-

channel analyser outweighed the necessity for initial studies.

3.5.7 Lock-in and Phase Sensitive Detection

This system is the most useful in the current application. The main advantage is that we have the ability to induce periodicity into the signal at an optical stage before the signal is converted to an electrical signal. This is a major advantage when it comes to signal recovery.

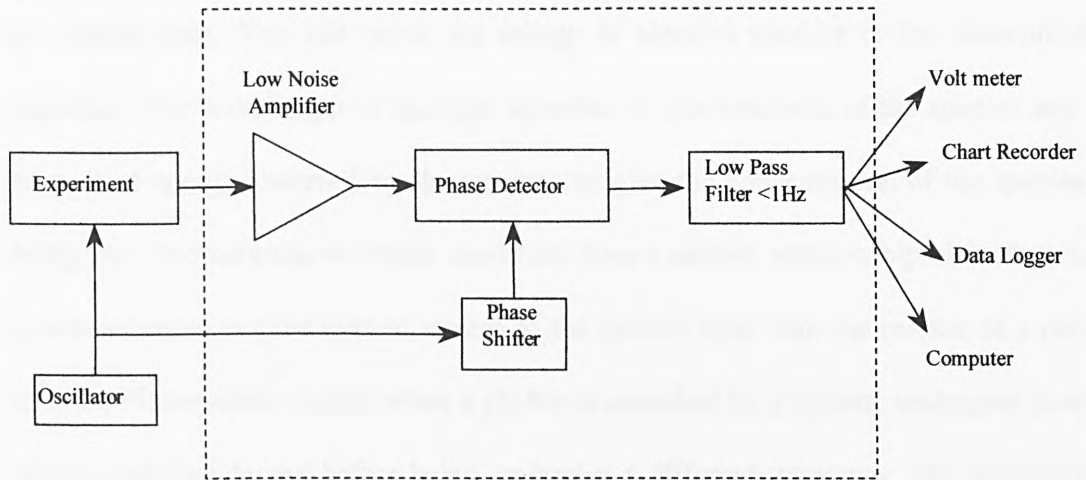


Figure 3.11: Diagram of the components to enable lock-in detection

By modulating the laser light, it is possible to induce that same modulation in the fluorescence emission from the sample, assuming the fluorescence lifetime of the sample is much smaller than the modulating frequency. The laser light can be modulated using a variety of methods, the simplest being an optical chopper.

The laser light is optically chopped and a reference signal is sent to the lock-in amplifier. This is outlined in figure 3.11 as the oscillator. The dashed line box represents the main components within a lock-in amplifier. The optical signal from the experiment is converted via a photodiode or photomultiplier to an electrical signal which can then be amplified and passed to the phase detector. The phase is then

adjusted to give a maximum reading and the low pass filter time constant adjusted to give a good signal to noise ratio. The signal from the lock-in amplifier can then be recorded in a variety of ways: volt meter, chart recorder, data logger or the analogue signal, converted to digital and recorded on a computer.

3.6 Summary

Many physical, chemical and biological systems will absorb energy promoting them to an excited state. This can occur via energy or electron transfer or the absorption of radiation. The wavelength of the light absorbed is characteristic of the species and the amount of energy absorbed by the system can give the concentration of the species by using the fluorescence emission modified Beer-Lambert relationship. Luminescence occurs when an excited system returns to the ground state with the release of a photon of light. Fluorescence occurs when a photon is absorbed by a system, undergoes a series of non-radiative decays before being emitted at a different frequency. The fluorescence photon may also be characteristic of the species being monitored. In the case of chlorophyll-a which is present in most forms phytoplankton, a characteristic peak at 680nm is observed. The energy absorbed by chlorophyll-a is also used in photosynthesis. This process uses light energy to produce carbohydrates allowing the phytoplankton to grow and also releases oxygen back into the atmosphere from the carbon dioxide absorbed by the plankton.

In designing an instrument for monitoring chlorophyll-a fluorescence, it has been shown that there are a number of optical and electronic techniques available for enhancing the signal to noise ratio which is important when monitoring small concentrations of phytoplankton. The most appropriate detector for monitoring the chlorophyll-a fluorescence is a photomultiplier which gives a high sensitivity in the

visible region. This combined with phase sensitive detection, should allow quick and easy detection of the fluorescence from the phytoplankton in real time.

With new methods for measuring phytoplankton parameters being developed in the laboratory, it is necessary to use reference standards. This allows characterisation of the instrument response to different chemical and biological species. Although initial experiments may be carried out using fluorescence dyes or chemicals, there comes a point in the experimental process where samples of the species to be measured must be used to determine the response of the experiment or instrument. In this case samples of phytoplankton must be used.

Chapter 4

Phytoplankton Culturing

4.0 Introduction

When working with organisms such as marine plankton, it is not feasible to collect samples of consistent composition and physiological state from the ocean. This is overcome however by growing samples of selected types of marine algae in the laboratory. During past research trips, numerous different species of phytoplankton and other types of plankton have been collected from various oceans. They were taken back to shore, identified, isolated and stored for future scientific analysis. These are stored in a few laboratories in the United Kingdom, such as Dunstaffnage Marine Laboratory, Oban, which maintains a collection of mainly marine algae and the Institute of Freshwater Ecology (IFE), Windermere Laboratory, Ambleside, which has a collection of freshwater algae and protozoa. The collections are collectively referred to as the Culture Collection of Algae and Protozoa (CCAP).

4.1 Phytoplankton Selection

In this project, phytoplankton phyla were selected from phylum which are common to the North Sea. These strains of phytoplankton were obtained from Dunstaffnage Marine Laboratory (DML). Although some of the taxa obtained from the CCAP were not native to the North Sea, it was thought that they would be very likely to contain pigments common to each of the phylum and hence native North Sea species would contain these pigments also. Each of the species were delivered from CCAP in vials which were transferred to sterile culture flasks upon receipt. The flasks were then placed in an incubator as advised from the Marine Laboratory, Torry, Aberdeen. One from each of

the following taxa were obtained (figure 4.1).

Phylum	Species	CCAP Identification No.
Diatom	<i>Chaetoceros calcitrans</i>	1010/15
Dinoflagellate	<i>Scropsiella trochoidea</i>	1134/5
Prasinophycean Quadriflagellate	<i>Tetraselmis suecica</i>	66/4
Chlorophycean	<i>Nannochloris atomus</i>	251/7
Eustigmatophyte	<i>Nannochloropsis oculata</i>	849/1

Figure 4.1: Phytoplankton species used for experiments

4.2 Base Medium Preparation and Sterilisation

The base medium used for culturing phytoplankton is normally filtered seawater or synthetic seawater, which can be obtained from most pet stores. The water is then usually sterilised and enriched with nutrients to sustain phytoplankton growth whilst in an incubator. The experiments used the latter of the two bases. *Instant Ocean*[®] was purchased from an aquarium shop and made up to the instructions included in the pack. Approximately 10g of the solid was dissolved in 1 litre of distilled water. This was heated until all the solid had been dissolved. Four batches of the base medium were made up and transferred to a dewar. The solution was then gravity filtered using a Whatman 42 filter and collected into a second dewar. Quantities of the base medium were then dispensed as required. The medium was normally transferred in 100ml volumes into 250ml volumetric flask which were then loosely stoppered with non-absorbent cotton wool and covered with aluminium foil. When this had been carried out, the flasks were then autoclaved, four at a time, in a pressure cooker at 15psi for 20 minutes. The flasks were then removed and allowed to cool to room temperature before

being chilled to 12 degrees celcius in the incubator. The flasks and medium were sterilised to ensure there was minimal contamination of the cells once they started growing hence ensuring there were as pure as possible species for analysis.

4.3 Nutrient Preparation

To enable growth of the plankton, nutrients must be added to the flasks containing the plankton cells. The chemicals added to the culture provide the necessary elements to allow healthy growth in the presence of sufficient light. These cells were all grown in f/2 medium⁷³, which was slightly modified for two of the species. F/2 growth medium consisted of the base solution (Instant Ocean[®]) with quantities of KNO₃ and NaH₂PO₄.2H₂O added along with some trace metals and vitamins. All the reagents were made up as concentrated stock solutions, sterilised and stored in a refrigerator.

Both the KNO₃ and NaH₂PO₄.2H₂O stock solutions were made up to 0.5M. When the growth medium was being prepared, 1.5ml of the KNO₃ and 80.7µl of the NaH₂PO₄.2H₂O was transferred into the flask along with 1ml of each of the trace metal and vitamin solutions.

The potassium nitrate and sodium hydrogen phosphate provide the necessary nitrates and phosphates for growth. When growing diatoms, the growth medium was supplemented with 0.3ml of 0.47M Na₂SiO₃.5H₂O per litre of growth medium. This provided the necessary silica for the hard shell which surrounds the algae.

4.3.1 Trace Metal Stock Solution

To obtain the trace metal stock solution, the following chemicals were dissolved in 1 litre of the Instant Ocean[®] solution as can be seen in Figure 4.2. Once this solution had been made and all the chemicals dissolved, it was then refrigerated until required.

Compound	Concentration/M	Compound	Concentration/M
EDTANa ₂	11.2x10 ⁻³	FeCl ₃ .6H ₂ O	11.65x10 ⁻⁶
CuSO ₄ .5H ₂ O	40x10 ⁻⁶	ZnSO ₄ .7H ₂ O	76.5x10 ⁻⁶
CoCl ₂ .6H ₂ O	42x10 ⁻⁶	MnCl ₂ .4H ₂ O	0.9x10 ⁻³
Na ₂ MoO ₄ .2H ₂ O	24.8x10 ⁻⁶		

Figure 4.2: Trace metal stock solution concentrations

4.3.2 Vitamin Stock Solution

To obtain the vitamin stock solution, the following chemicals were obtained from Sigma, Cyanocobalamin, Thiamine HCL and Biotin. These were again dissolved in a litre of Instant Ocean[®] solution as can be seen in figure 4.3.

Vitamin	Concentration/M
Cyanocobalamin	3.7x10 ⁻⁶
Thiamine HCl	0.3mx10 ⁻⁶
Biotin	20.5x10 ⁻⁶

Figure 4.3: Vitamin stock solution concentrations

Once all the stock solution had been added to the growth medium and had been made up to 1 litre, the pH of the solution was adjusted to 8.0 using 1M NaOH or HCl. The solution was then poured into conical flasks. The flasks were loosely stoppered using non-absorbent cotton wool which was kept in place using aluminium foil over the top of the flask. The flasks were then sterilised and allowed to cool on the benchtop. Before being used for new cultures, the flasks were transferred from the benchtop to the incubator and left overnight for the temperature of the flask to reach incubator temperature. This reduced the thermal shock which cells may experience when they are used to inoculate new growth medium.

4.4 Phytoplankton Growth and Cell Harvesting

Once each of the new solutions had been inoculated with the cells from each species, the flasks were placed in an incubator which can be seen in figure 4.4. This maintained constant light levels (4.96 Wm^{-2}) and a temperature of 10 degrees Celsius. This provided the necessary conditions for each of the species to grow.



Figure 4.4 : Photograph of the cooled incubator used for growing phytoplankton

Each day, a sample of the species used for analysis was harvested from the flasks using sterile, disposable pipettes which minimised contamination of the stock cultures. This procedure was done using aseptic techniques and the sample placed in a fluorescence cell. To this, 1ml of ethanol was added to the solution to kill the cells. This was an important step especially in the case of the flagellate species which are very motile. Killing them in this manner, causes the cell movement to cease making the cells easier

to count using a haemocytometer. This is effectively a calibrated counting chamber which holds a fixed volume which can be seen in figure 4.5.

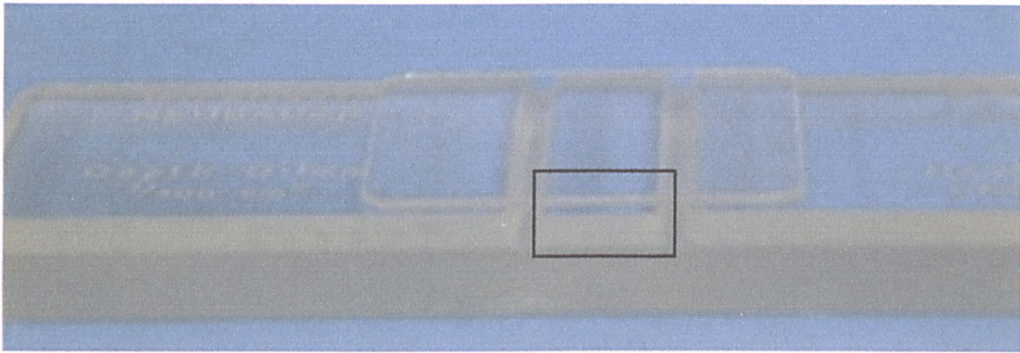


Figure 4.5: Photograph of a haemocytometer with the sample volume region marked with the black rectangle

The chamber is filled with the algae suspension and the cells are then counted under a microscope. The stock suspension of algae was diluted using instant ocean solution before being placed into the counting chamber. If there are too many cells in the chamber counting becomes difficult. Approximately 6 cells per location gives a reasonable count and is easy to observe. Up to 10 replicate counts of the samples are taken to allow a good average concentration of the cells to be obtained.

Simultaneous fluorescence measurements were also carried out alongside the cell counts using a hand-held fluorimeter. This allowed a calibration curve to be obtained, making it easier to obtain a rough cell concentration of the same species at a later date. The growth curve for *Tetraselmis suecica* is shown in figure 4.6. It can be seen that there is a lag phase of approximately 5 days before the cells start growing. The cells are then in this growth phase for 9 days before reaching a stationary phase. During the course of the growth of this species, fluorescence measurements were also taken.

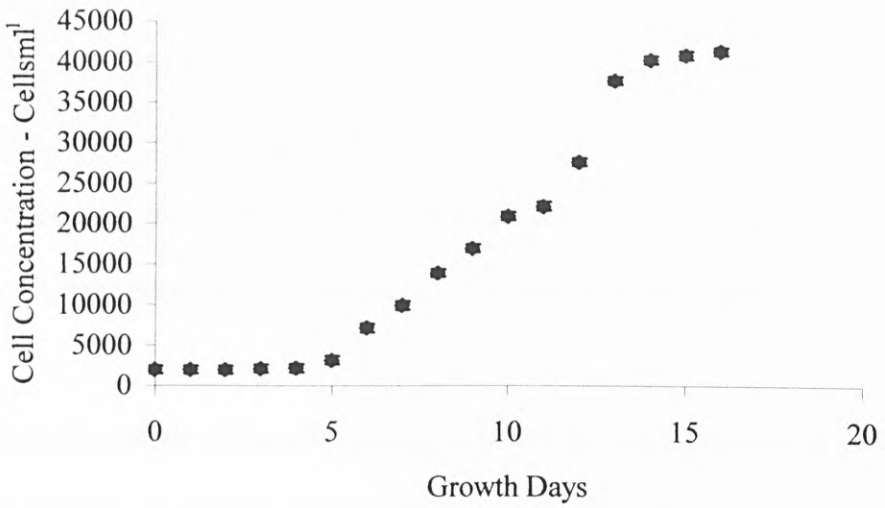


Figure 4.6: Growth curve for *Tetraselmis suecica*

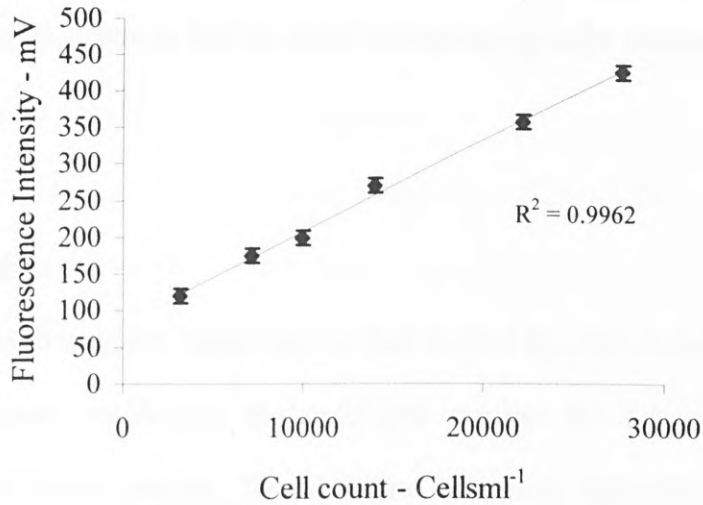


Figure 4.7: Cell concentration against fluorescence intensity (430nm excitation/680nm emission) for *Tetraselmis* in the linear growth phase.

Figure 4.7 shows the comparison between the fluorescence measurements and the cell

count. It can be seen that there is a good correlation between the cell count and the fluorescence measurement during the linear phase of the growth curve. The growth phase shown in figure 4.7 is taken from days 5-12. The graph shows a correlation of 0.9962 between the cell count and the fluorescence reading showing that fluorescence can be used to determine cell concentration when the cells have adequate nutrients for growth.

Due to the nature of the culturing process and the work involved in counting the cells for a number of species simultaneously, cells were harvested on a day-after-inoculation basis. If cells in the growth phase were required, then they were harvested on day 9, after the initial inoculation. When stationary phase cells were required for analysis, they were harvested on day 16, after the inoculation. Although this is not an ideal method for determining the cell state, care was taken to keep all the growth parameters identical, ensuring that the cells were growing under similar conditions after each inoculation.

4.5 Cell Disposal

Once cells had been used for experiment or had reached the end of their growth stages, it became necessary to destroy the cells and sterilise the equipment to prevent contamination of future samples. To ensure the cells were ruptured and killed, some ethanol was added to the cultures before they were placed in an autoclave. This had the immediate effect of killing the cells as shown before in the cell counting stage. The cells were then sterilised for 20 minutes at 15 psi before being disposed to the drain.

4.6 Summary

Selected algae was grown in the laboratory using standard methods. These algae were used to characterise the response of the instrument being developed to real biological samples. Although some of the algae used were not native to the North Sea, they were part of the same phyla as those found in the North Sea. These samples were used as they were readily available from Dunstaffnage Marine Laboratory.

Some species prove easier to culture than others with *Scropsiella* being the most difficult. This was due to the nature of the algae. Certain species are known to be “hardy”, they can grow under varied nutrient and light conditions whereas other species tend to be more sensitive to the local growth environment.

Harvesting of the cells were done on a “day after inoculation” basis which is not the ideal situation, but given the amount of work required in monitoring the cell growth daily to determine the algae growth phase and carrying out experiments on multi-species, this was the seen as a reasonable balance.

Once the cells started growing it was possible to harvest them and characterise their optical properties. This is important when designing an optical system for monitoring phytoplankton.

Chapter 5

Fluorescence Spectroscopy of Phytoplankton

5.0 Introduction

Once the phytoplankton cultures began growing, it became possible to harvest some cells in order to characterise their fluorescence spectra. This was important, as later in the project, this spectra would be used to select a laser excitation source and detection filters for designing a system for the remote monitoring of phytoplankton species.

5.1 Standard Fluorescence Equipment

The fluorescence measurements were carried out using a standard laboratory bench fluorimeter (Perkin-Elmer LS-50B spectrofluorimeter). Essentially this comprises an excitation source, wavelength selective optics, sample holder, collection optics and a detector as can be seen in figure 5.1. This system allowed various excitation and emission wavelengths to be used for characterising the phytoplankton samples, as the instrument being fully computer controlled, allowing independent movement of both the monochromators and synchronous scanning of the monochromators along with computerised collection of the data.

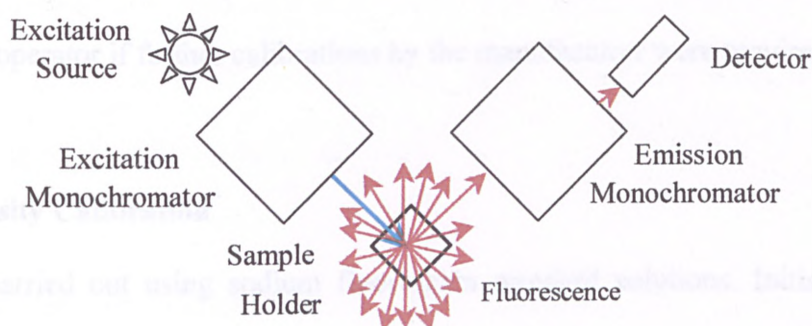


Figure 5.1: Basic components of the LS-50B bench fluorimeter

Shown in figure 5.2 is a photograph of the instrument with the sample chamber housing open. The control computer is located just out of the picture to the left.

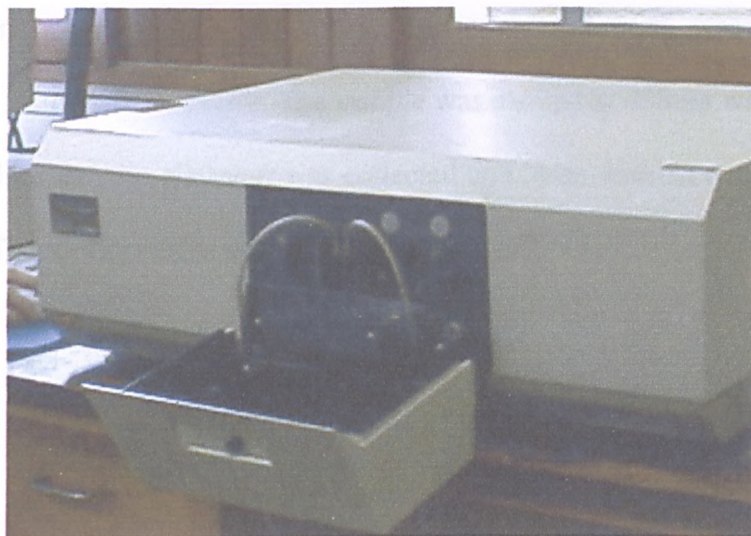


Figure 5.2: Photograph of the Perkin-Elmer LS-50B fluorimeter showing the sample housing

5.2 Calibration of the LS-50B Spectrofluorimeter

5.2.1 Wavelength Calibration

Wavelength calibration was carried out using a distilled water sample. A calibration program, supplied as part of the operating software, used the Raman scatter peak from a pure water sample to determine the wavelength calibration. The signal from the sample was compared with a set of pre-stored values within the instrument. The software then alerted the operator if further calibrations by the manufacturer were required.

5.2.2 Intensity Calibration

This was carried out using sodium fluorescein standard solutions. Initially, a multi-excitation spectra for a $1 \times 10^{-5} \text{M}$ sodium fluorescein was obtained using the fluorimeter. The slits on the instrument were adjusted until this concentration gave a maximum

reading on the fluorimeter without saturating the detector. From this information, the maximum absorption for the fluorescein was found to be approximately 490nm with the peak emission centred at 515nm. Various standard solutions were then used to determine the instrument response. The sample was excited at 488nm with an excitation slit width of 5nm and the emission was collected at 514nm with an emission slit width of also 5nm. The results of this can be seen in figure 5.3

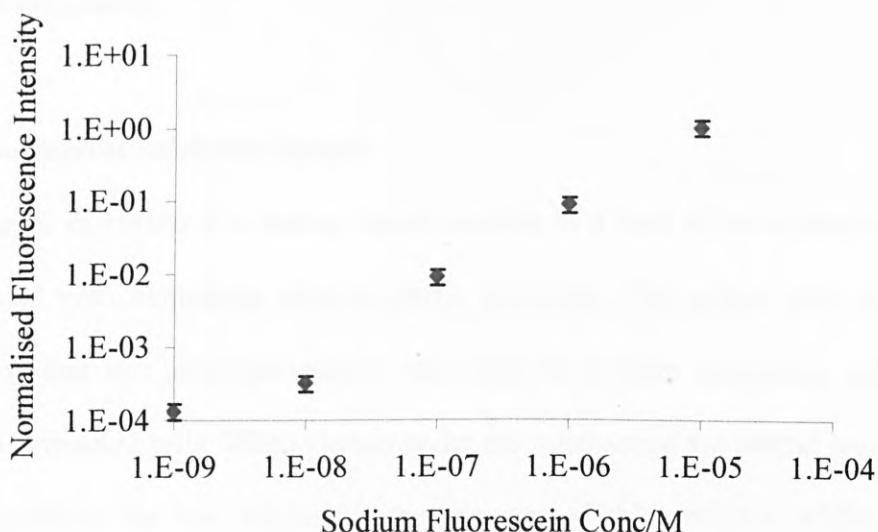


Figure 5.3: Calibration of the LS-50B spectrofluorimeter using sodium fluorescein

As can be seen above, the data gives a straight line when plotted on log/log scales with an R^2 value of 0.98 over the range of $10^{-5} - 10^{-9}$ M sodium fluorescein. The system was shown to be relatively stable over the range of concentrations being used, with five orders of magnitude linearity being achieved.

5.3 Fluorescence Spectra of Selected Algae Species

5.3.1 Fluorescence Measurements

The fluorescence spectra were obtained by taking a 4.5ml sample from the stock

solution which was then pipetted into a quartz cuvette using a sterile pipette. The sample was placed into the fluorimeter sample holder and the fluorescence scan initiated. Each sample was scanned using excitation wavelengths between 400-600nm in 10nm intervals, collecting the emission spectra from 20nm above the excitation wavelength to 800nm. In this way, a multi-excitation/emission spectrum was produced for each sample. The data were then imported into Microsoft *Excel* and the data arranged graphically.

5.3.2 *Chaetoceros calcitrans* Sample

Chaetoceros calcitrans is a diatom which consists of a hard silica structure with silica spines, and cells containing photosynthetic pigments. The spines tend to interlock, suggesting that this particular species may exist in a chain orientation rather than a group of individual cells. When viewed under the microscope the central area of the cell appears green to the eye, suggesting the presence of chlorophyll-a, whilst the spikes appear as diffraction's of light between the silica spines and the growth medium. Under growth conditions, the culture appears to be yellow in colour although under the microscope it appears green, which suggests other pigments within the cell structure.

The fluorescence spectrum measured for the cultured *Chaetoceros calcitrans* sample culture is given in figure 5.4. The multi-excitation fluorescence spectra for *Chaetoceros* shows the typical fluorescence characteristics of most diatoms, with the main fluorescence peak observed at 680nm due to the chlorophyll-a molecule and a very small sideband at 730nm, due to the PSI of the chlorophyll-a molecule. As with most diatoms, there is very little other fluorescence observed below 680 nm. Although these plankton species do contain other accessory pigments, they are either present in too small a quantity to produce measurable fluorescence or the pigments in their local

environment are not fluorescent.

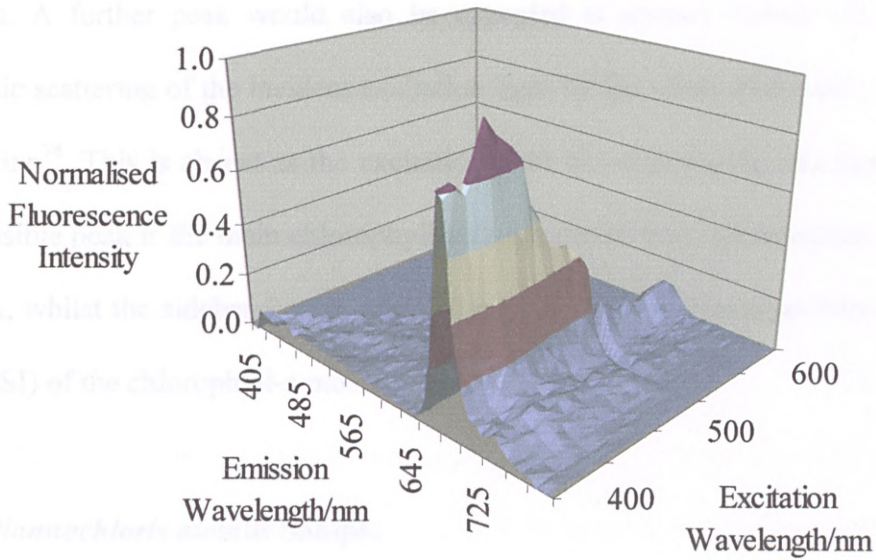


Figure 5.4: Multi-excitation fluorescence spectrum of *Chaetoceros calcitrans* diatom

Shown in figure 5.5 is the emission spectra for excitation at 440nm, the maximum absorption of the chlorophyll-a within the *Chaetoceros* sample.

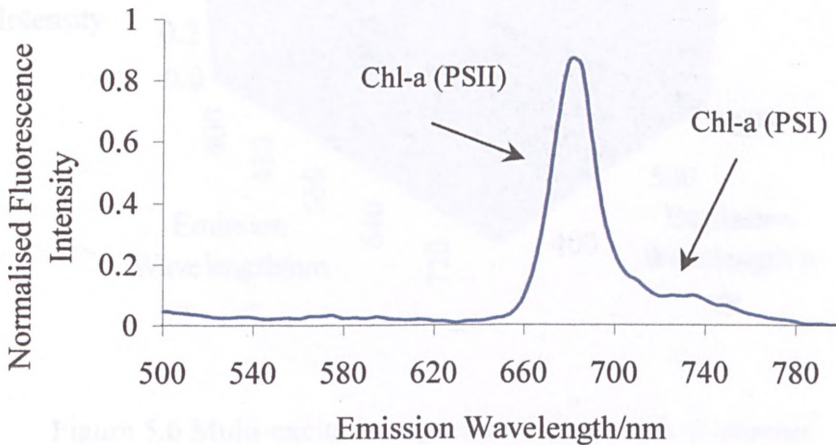


Figure 5.5: Fluorescence spectra of *Chaetoceros calcitrans* - 430nm excitation

There is one peak observed in this spectra at 680nm with a sideband at approximately 730nm. A further peak would also be expected at around 520nm which is due to inelastic scattering of the incident excitation light by the water molecules, water Raman scattering⁷⁴. This is absent as the excitation light was low during this experiment. The first visible peak is the main chlorophyll-a fluorescence from photosystem two (PSII) at 680nm, whilst the sideband at around 730nm is due to fluorescence from photosystem one (PSI) of the chlorophyll-a molecule.

5.3.3 *Nannochloris atomus* Sample

Nannochloris atomus is a small, marine algae species. It comes from the trebouxiophyceae class. This was physically the smallest species which was grown and analysed. The multi-excitation fluorescence spectrum is shown in figure 5.6.

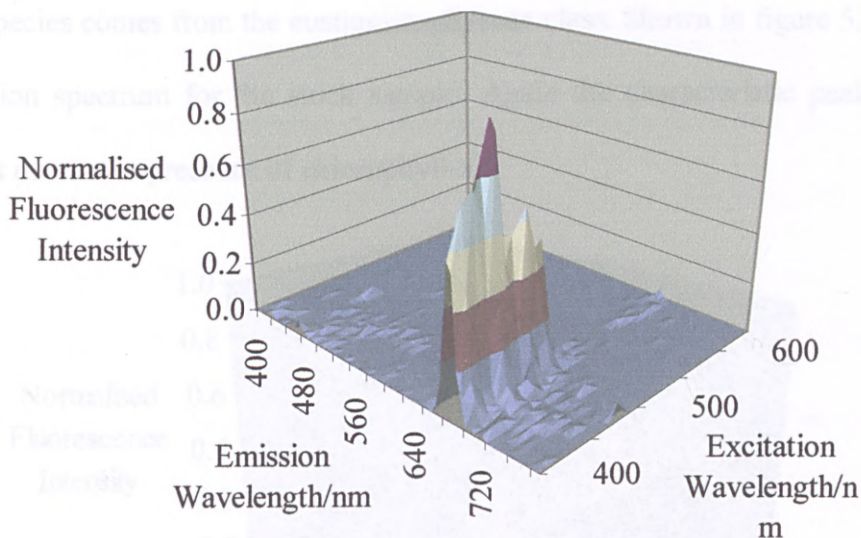


Figure 5.6 Multi-excitation spectra of *Nannochloris atomus*

It can be seen that there is a very distinct peak at 680nm due to chlorophyll-a fluorescence. There appears to be very little fluorescence at any other wavelengths.

There is some weak fluorescence at around 730nm due to PSI of the chlorophyll-a molecule. It can be seen that there is very little fluorescence below 680nm in the region where fluorescence from accessory pigments would be expected. This may suggest that there may be fewer accessory pigments or less efficient fluorescence pigments. Fluorescence does still occur at 680nm suggesting that light is being absorbed and passed to the chlorophyll-a molecule either directly or via an accessory pigment pathway⁷⁵. The intensity of the fluorescence when exciting at lower wavelengths however is reduced compared to *Chaetoceros*. It increases gradually until approximately 460nm. It can also be seen that no or very little fluorescence at 680nm is observed when exciting between 520nm and 600nm.

5.3.4 *Nannochloropsis oculata* Sample

This species comes from the eustigmatophyceae class. Shown in figure 5.7 is the multi-excitation spectrum for the stock sample. Again the characteristic peak at 680nm is present due to the presence of chlorophyll-a.

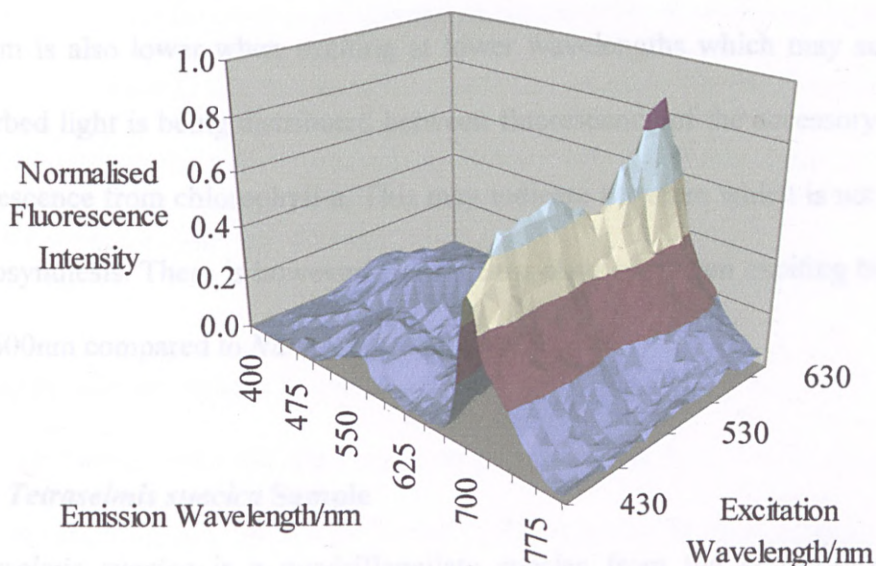


Figure 5.7: Multi-excitation spectra of *Nannochloropsis Oculata*

The 680nm peaks however are much broader than previous samples.

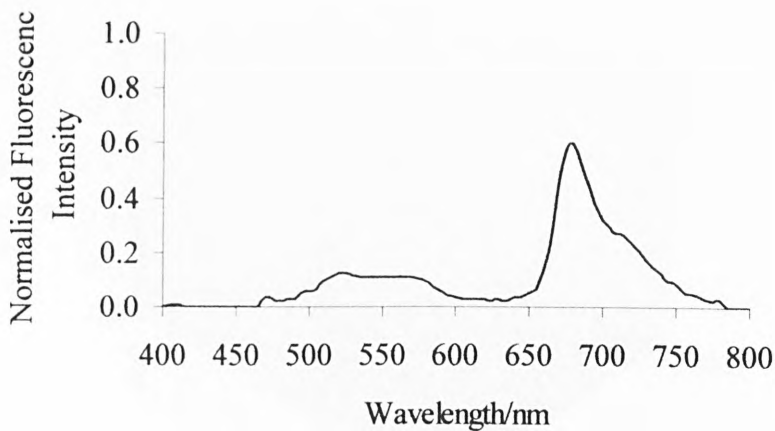


Figure 5.8: Fluorescence Spectra of *Nannochloropsis oculata*, 450nm excitation

It should be noted that this is primarily due to a fluorescence contribution from PSI at 730nm which shows a higher fluorescence output compared to the other species monitored in this way. There is a large fluorescence below 650nm as can be seen in figure 5.8, suggesting that there is other fluorescent material within the plankton. This is most likely due to accessory pigments which are able to fluoresce. The fluorescence at 680nm is also lower when exciting at lower wavelengths which may suggest that the absorbed light is being distributed between fluorescence of the accessory pigments and fluorescence from chlorophyll-a. This may indicate a system which is not so efficient at photosynthesis. There is however fluorescence observed when exciting between 520nm and 600nm compared to *Nannochloris atomus*.

5.3.5 *Tetraselmis suecica* Sample

Tetraselmis suecica is a quadriflagellate species from the prasinophyceae phylum, which by using its flagellates is able to move. This species grows with an almost bright

green culture due to the high chlorophyll-a content..

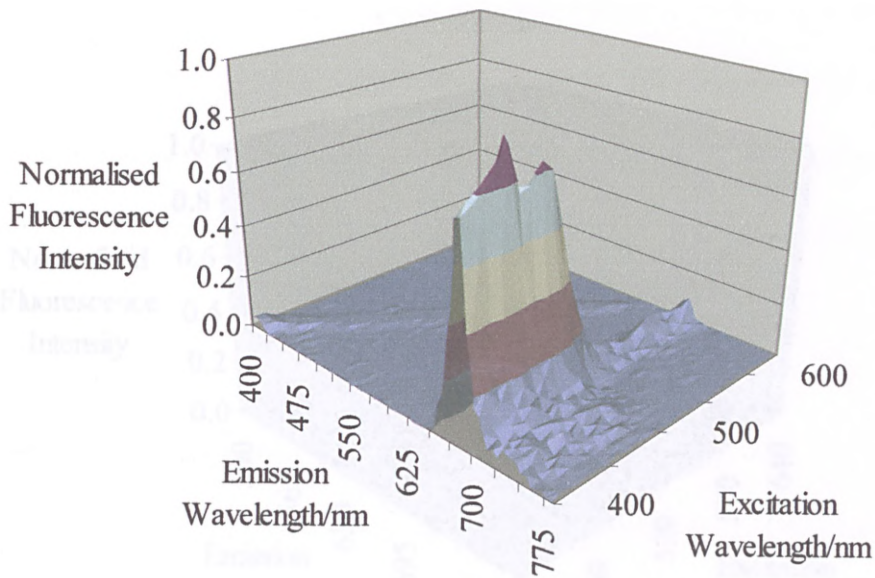


Figure 5.9: Multi-excitation fluorescence spectrum of *Tetraselmis suecica*

In the same way as previously outlined, a multi-excitation spectrum of the sample was taken using the same equipment. The fluorescence from this species can be seen in figure 5.9. The same characteristic peak at 680nm is observed due to the chlorophyll-a within the cells. Again there is an absence of fluorescence at wavelengths below 630nm. This is most probably due to the same reasons as outlined for the *Chaetoceros* and the *Nannochloris* samples. This species also shows a reduced fluorescence at 680nm when exciting between 520nm and 600nm.

5.3.6 *Scropsiella trochoidea* Sample

Scropsiella comes from the dinoflagellate phylum. This is a motile species with one flagellate which allows the cell to “swim”. This is probably one of the most spectrally interesting of the cells grown as this species is known to contain fluorescent accessory pigments. However, the cells were the most difficult to grow and frequently died during

can be seen more clearly in figure 5.11. There is a measurable fluorescence in this region of the spectrum which is almost the same intensity as the fluorescence observed from the PS1 chlorophyll-a transition at 730nm. The fluorescence in this region, however, is not as strong as that observed with the *Nannochloropsis oculata* sample. There is again some fluorescence obtained at 680nm when exciting between 520nm and 600nm.

5.4 Discussion: Standard Phytoplankton Fluorescence

The measured spectra show that all of the species will produce chlorophyll-a fluorescence at 680nm when excited by light below 650nm. The maximum fluorescence obtained, however, occurs at slightly different wavelengths for each of the species except *Nannochloropsis*. Figure 5.12 shows the excitation wavelength which produced the maximum fluorescence at 680nm.

Species	Excitation wavelength/nm
<i>Chaetoceros calcitrans</i>	440
<i>Nannochloris atomus</i>	440
<i>Nannochloropsis oculata</i>	630
<i>Tetraselmis suecica</i>	450
<i>Scropsiella trochoidea</i>	450

Figure 5.12: Excitation wavelength producing maximum fluorescence at 680nm for the selected species

Two of the species, *Nannochloropsis Oculata* and *Scropsiella trochoidea* also show additional fluorescence emissions around 540nm. This is probably due to fluorescence from accessory pigments. The other samples will most likely contain accessory

pigments which do not fluoresce under these conditions but still absorb short wavelength light which can be used for photosynthesis.

5.5 Laser Fluorescence Spectroscopy

In developing a free path, laser excitation instrument for monitoring phytoplankton it is necessary to determine the response of the phytoplankton to laser radiation, it was necessary to use a fluorimeter with a laser as the excitation source. As the plankton samples absorb in both the ultraviolet and visible regions of the electromagnetic spectrum, the effects of visible and ultraviolet laser radiation on the fluorescence of the samples can be investigated.

5.5.1 Design of the Laser Fluorimeter

In order to obtain fluorescence spectra using continuous wave (CW) laser radiation, a system had to be designed and constructed. The system took the form of a standard fluorimeter with an excitation source, wavelength selective optics, sample holder, collection optics, wavelength selective element and a detector. An argon ion laser was used as the excitation source. This provided a range of discrete wavelengths in the visible region, the main transitions being at 457, 488 and 514nm. Although phytoplankton fluorescence is best excited at 430nm, figures 5.4-5.9 show that there is still a high fluorescence yield when excited at 457nm and 488nm. Although the 457nm emission line is closest to the maximum absorption of the chlorophyll-a molecule, the most efficient transition and hence the highest power output was obtained from the 488nm laser line. These wavelengths could be absorbed by the chlorophyll-a and also by sodium fluorescein, which was used as a standard.

the culturing stage, making them very difficult to work with.

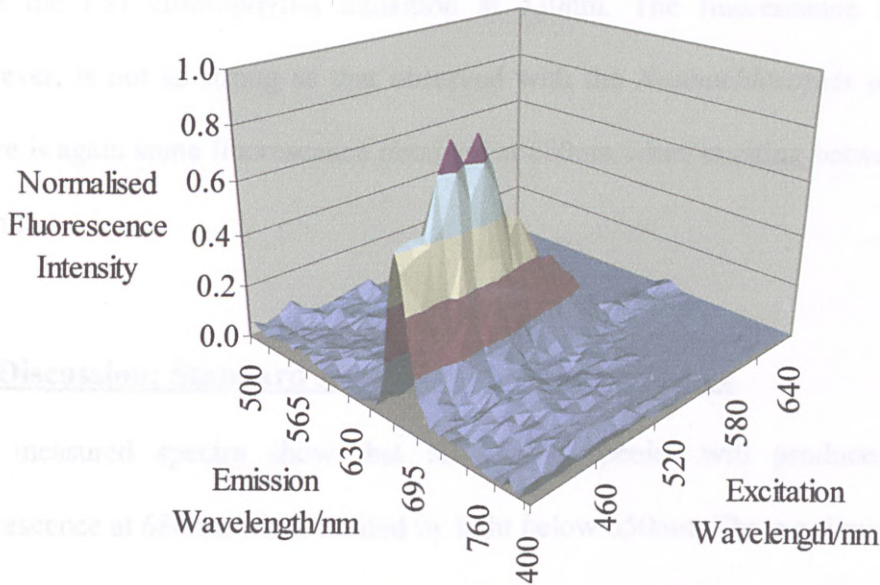


Figure 5.10: Multi-excitation fluorescence spectrum of *Scripsiella trochoidea*

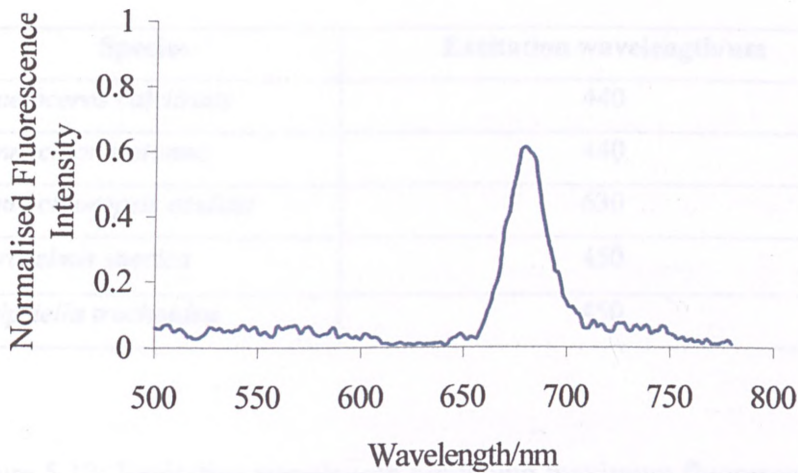


Figure 5.11: Fluorescence spectra of *Scripsiella trochoidea*, 400nm excitation.

As can be seen in figure 5.10, the peak at 680nm is again present due to the chlorophyll-a content of the algae. What is not so obvious is the broad, weak fluorescence observed around 550nm. This is characteristic fluorescence observed in many dinoflagellates and



Figure 5.13: Photographs of the laser fluorimeter main components and set-up

The laser light was modulated using an optical chopper which allowed phase sensitive detection of the fluorescence signal. Laser light was then directed onto a quartz cuvette containing a phytoplankton sample as can be seen in figure 5.13. The fluorescence from the sample was collected using optics and directed onto the input slit of a monochromator. A photomultiplier was used as the detector and was connected to the exit port of the monochromator. The photomultiplier was then connected to the lock-in amplifier which allowed phase-sensitive detection of the fluorescence signal. The output amplitude voltage from the lock-in amplifier was converted to a digital signal using an analogue to digital converter (Picolog) then stored on a computer using custom-written software.

5.5.2 Monochromator Control and Data Collection

To simplify collection of laser spectra, the control of the monochromator and collection

of the data from the picolog A/D converter was done using a computer. By controlling the parallel ports on a standard personal computer using software written with Turbo Pascal, the selection of the start and finish wavelengths, the scan step and the scan speed of the monochromator was possible. Control of the analogue to digital converter was also incorporated within the program, allowing data intensity values to be collected relating to the signal fluorescence. Whilst a fluorescence scan was in progress, the fluorescence spectra is displayed on the screen, allowing the user to see graphically any fluorescence present in the sample. Once a scan was complete, the data is stored on the hard drive of the computer along with software-generated wavelength values corresponding to the monochromator wavelengths. The saved data could then be read directly into software such as *Excel* for easy plotting and manipulation.

5.5.3 Wavelength calibration of the Monochromator

Before any experiments could be carried out using the laser fluorimeter, it was necessary to calibrate the wavelength scale of the monochromator. This was done using a standard solution of sodium fluorescein. The system was set up to scan in steps of 0.1nm starting at 470nm to 630nm with data points being collected for each step. These were then plotted in *Excel* as shown in figure 5.14. As can be seen from the scan, the laser excitation peak can be observed at 488nm along with a broad fluorescence peak at approximately 514nm corresponding to the maximum fluorescence emission peak of sodium fluorescein at standard temperature and pressure. Although the fluorescence spectrum here is shown to stop at 630nm, the monochromator is capable of scanning out to beyond 700nm, allowing the monitoring of the main chlorophyll-a fluorescence peak at 680nm.

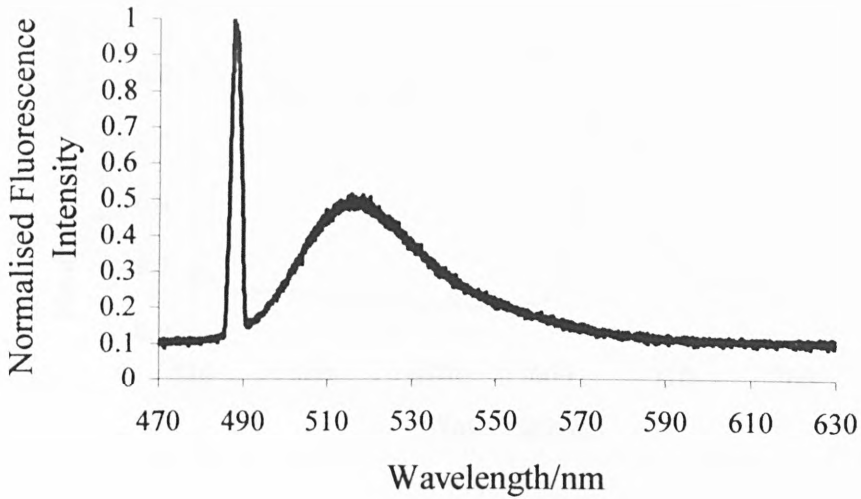


Figure 5.14: Laser fluorescence spectra of sodium fluorescein showing the excitation wavelength at 488nm with the peak fluorescence emission at 514nm

5.5.4 Laser Excitation Spectra of Selected Phytoplankton Samples

Once the monochromator had been calibrated using sodium fluorescein, it was possible to record fixed excitation fluorescence spectra of various phytoplankton samples. A cuvette containing each sample was placed in the path of the laser beam. The monochromator was then scanned from 510-760nm which covers most of the visible spectrum above the laser excitation wavelength. In the first instance, a sample of the diatom *Chaetoceros* was scanned using the 488nm excitation wavelength. This can be seen in figure 5.15. The main feature on the spectrum is a peak centred at 685nm which corresponds to the fluorescence emission of chlorophyll-a. There is a weak, broad sideband which is centred on 730nm. This is due to fluorescence from PSI of the chlorophyll-a molecule.

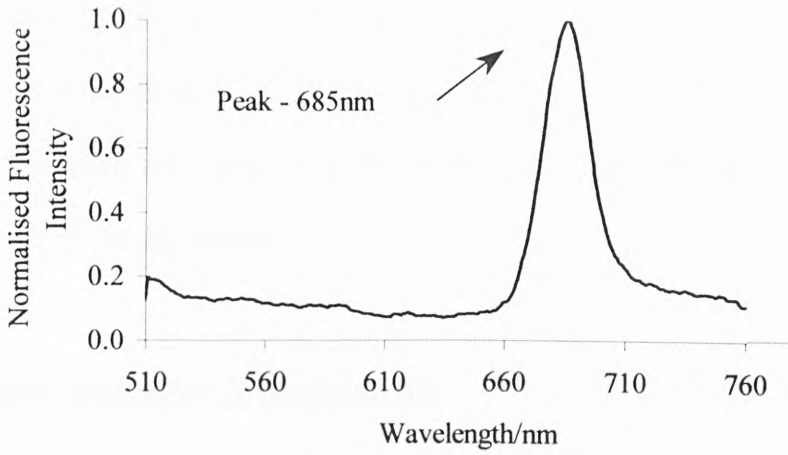


Figure 5.15: Laser Fluorescence scan of *Chaetoceros*

Further laser fluorescence scans were carried out on *Scropsiella trochoidea*, which is from the dinoflagellate phylum. The same procedure was used on these as for the previous sample of phytoplankton.

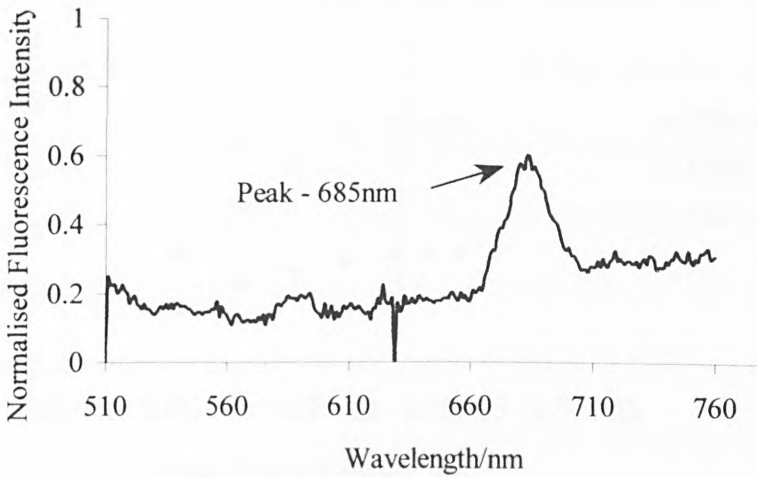


Figure 5.16: Laser fluorescence scan of *Scropsiella trochoidea*

The laser induced spectra for this species is shown in figure 5.16. The main peak observed again at around 685nm is due to the primary chlorophyll-a fluorescence from photosystem II (PSII). It can be seen that these two species show one distinct peak due

to the chlorophyll-a fluorescence. A sideband at 730nm due to fluorescence from PSI is also present. This however is small compared to the fluorescence from PSII at room temperature⁷⁶. The small zero spike at around 630nm was due to the laser beam being blocked during the fluorescence scan.

5.6 Fluorescence Saturation Measurements

Saturation measurements were carried out to determine the maximum fluorescence which could be obtained from the phytoplankton for the laser energy being imparted into the sample. This was done for the *Chaetoceros* sample and each of the other samples were assumed to give a similar response during the exponential growth phase. Shown in figure 5.17 is the fluorescence saturation point with respect to laser power.

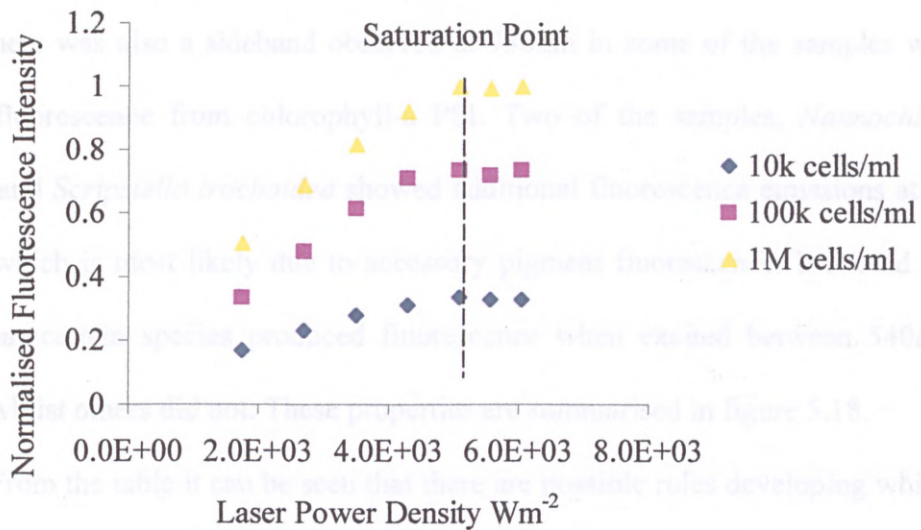


Figure 5.17: Fluorescence saturation of *Chaetoceros* using an argon ion laser.

It can be seen from the graph below that as the laser power density is increased to up to 5 kilowatts per square meter (kWm⁻²), there is a steady increase in the fluorescence emission. For a 2mm beam diameter, a power of 16mW is required at 488nm to obtain

fluorescence saturation of the *Chaetoceros* sample. Beyond this point however, there is no increase in the fluorescence output from the sample and using a higher laser power to induce fluorescence would be a waste of energy as there would be no gain in the detected signal. The experiments were, however, carried out using this power density plus an additional 10% excess laser power (5.05 kWm^{-2}) to ensure the maximum fluorescence was obtained from the samples. As can be seen from the graph, this is sufficient enough power to maximise the fluorescence emission.

5.7 Summary

The fluorescence properties of selected types of phytoplankton have been measured using a standard laboratory fluorimeter. Each of the samples produced fluorescence at around 680nm which corresponds to the chlorophyll-a photosystem II (PSII) emission peak. There was also a sideband observed at 730nm in some of the samples which is due to fluorescence from chlorophyll-a PSI. Two of the samples, *Nannochloropsis oculata* and *Scropsiella trochoidea* showed additional fluorescence emissions at around 550nm which is most likely due to accessory pigment fluorescence. It should also be noted that certain species produced fluorescence when excited between 540nm and 600nm whilst others did not. These properties are summarised in figure 5.18.

From the table it can be seen that there are possible rules developing which may allow the identification of these species by using multi-excitation fluorescence spectra.

Species	Excitation wavelength/nm	Presence of 680nm fluorescence when excited at 550nm	Presence of 540nm fluorescence
<i>Chaetoceros calcitrans</i>	440	Weak	No
<i>Nannochloris atomus</i>	440	No	No
<i>Nannochloropsis oculata</i>	630	Strong	Strong
<i>Tetraselmis suecica</i>	450	Weak	No
<i>Scropsiella trochoidea</i>	450	Weak	Weak

Figure 5.18: Summary of plankton characteristics obtained when using the standard bench fluorimeter.

In the simplest case it should be possible to distinguish *Nannochloropsis Oculata* and *Nannochloris atomus* from the other species and also from each other by exciting at three wavelengths 430nm, 550nm and 600nm and observing fluorescence at 540nm and 680nm.

The information obtained from the standard fluorescence spectra were used to design and construct a laser-based fluorimeter which could be used to determine the suitability of a laser for exciting phytoplankton. The laser excitation source, due to the inherent properties of laser beams, can be used to excite the phytoplankton remotely compared to the lamp excitation source used in more traditional fluorimeters. Two species, *Chaetoceros* and *Scropsiella* were used as representative samples for the selected algae. An argon ion laser operating at 488nm was used as the excitation source.

Software was written to control the monochromator and to log the fluorescence data obtained from the photomultiplier on a computer. The monochromator wavelengths were calibrated using sodium fluorescein and the argon ion emission peak. The fluorescence from the phytoplankton was collected above 510nm. The laser induced spectra showed the characteristic 680nm fluorescence peak from both the samples. What was less obvious from the spectra was a peak which is normally observed at around 720nm due to fluorescence from photosystem 1. At room temperature this peak is weak. There is however an intensity shift as the temperature is reduced considerably⁷⁷. Many other algae also exhibit additional fluorescence bands in the region below 680nm which are due to additional pigments within the plankton cells⁷⁸.

Experiments were also carried out to determine the laser power required to produce the maximum fluorescence from *Chaetoceros*. The laser power was gradually increased until a steady fluorescence signal was obtained from the sample. This was found to be around 16mW for a beam diameter of 2mm giving a power density of 5kWm^{-2} . Increasing the power density beyond this did not provide more fluorescence from the sample and hence energy is being wasted. It was assumed that the fluorescence from the other algae would produce a similar effect to the *Chaetoceros* whilst in the exponential growth phase

Measuring chlorophyll-a fluorescence in the marine environment will give an indication to the presence of phytoplankton. If, however, measurement of the growth state of the plankton is required, the fluorescence measurement must be slightly modified. This technique is called Pump-probe spectroscopy. This requires the use of a pulsed light source or laser for remote measurements and time dependent electronics. It is therefore necessary to determine the response of the plankton to pulsed laser light for remote sensing.

Chapter 6

Time Resolved Fluorescence Spectroscopy of Phytoplankton and High Energy Laser Radiation Effects on Phytoplankton

6.0 Introduction

Standard fluorescence measurements are normally carried out using a continuous beam of excitation light or a long pulse of light typically on a micro-second time scale. This normally results in a constant fluorescence from the species being observed. If, however, the excitation source uses a pulse of light, the resulting fluorescence will normally be a pulse of light. In remote sensing, normally a higher laser power is required to induce fluorescence in the phytoplankton. It is therefore necessary to investigate the effects of high power laser energy on phytoplankton.

Fluorescence in algae is caused when the reaction centre of the chlorophyll-a, which is used for the photosynthesis, is closed (reduced), i.e., cannot accept further electrons. The incident photon of light is absorbed by the molecule and undergoes a series of non-radiative de-excitations until the excess energy is given out as fluorescence and/or phosphorescence. This de-excitation process takes a finite time to occur and is dependent upon a number of factors within the algal cell. By monitoring this fluorescence decay, it may be possible to obtain more information about the algae.

6.1 Time Dependent Fluorescence Emissions

The main pigment in phytoplankton samples is the chlorophyll-a molecule. Previous experiments on the isolated chlorophyll-a molecule have shown that the fluorescence de-excitation of the molecule occurs in different stages with each stage occurring in specific times ranging from picoseconds to milliseconds⁷⁹. These fluorescence characteristics are divided into two classes, fast fluorescence and slow fluorescence. Fast fluorescence has been termed any fluorescence which occurs faster than microseconds, with slow fluorescence being any fluorescence which is longer than this threshold.

Fluorescence from chlorophyll-a has been shown to occur in various time frames from femtosecond to millisecond fluorescence. The latter has been used in instrumentation and is being incorporated into real-time monitoring equipment. Work on femtosecond fluorescence however has concentrated mainly on extracted chlorophyll-a samples in the laboratory due to the high cost and fragile nature of the lasers used. There are however fluorescence processes which occur in the nanosecond timescale which have been studied much less and with nanosecond lasers being relatively cheap, reliable and rugged construction there are possibilities in incorporating these lasers into practical monitoring systems.

6.2 Nanosecond Fluorescence Decay Monitoring

To monitor the fast, transient fluorescence events within the phytoplankton, different instrumentation compared to a traditional fluorimeter is required. The system utilised in the experiments used a short pulse Nd:YAG laser and Optical Parametric Oscillator, which were used to produce fluorescence within the phytoplankton cell. The fluorescence decay was then measured using a gated detector system which records the

fluorescence emission at user programmable intervals after the laser pulse. The system can be seen in figure 6.1. There are essentially two main parts to this instrumentation, fast optical components and fast electronics. The optical components use a frequency tripled Nd:YAG laser producing 140mJ in 4.5ns pulses at 355nm to pump an optical parametric oscillator (OPO).

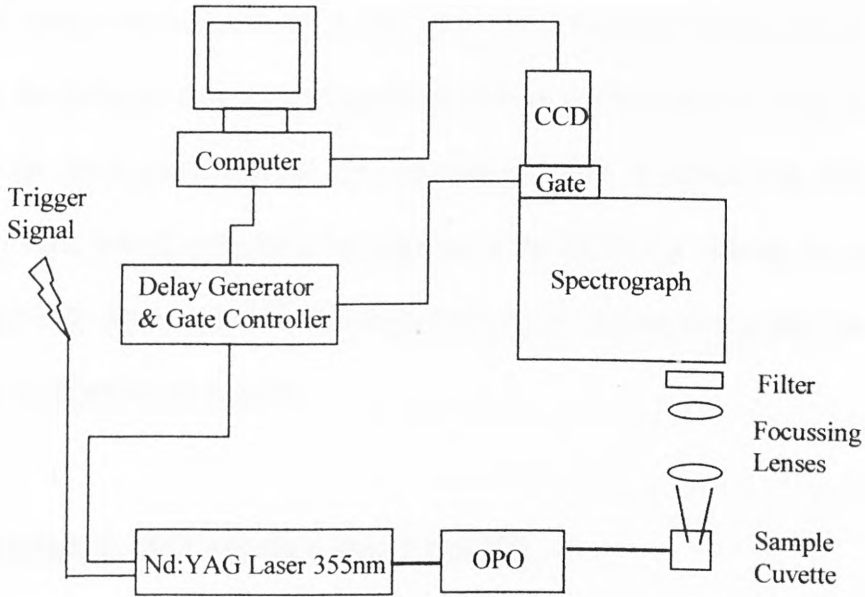


Figure 6.1: Fast fluorescence experimental apparatus setup

The OPO gives the advantage of being able to produce multiple wavelengths from a single laser from 400nm to 2.5 μ m. For these experiments the OPO was set to 430nm which corresponds to the maximum absorption peak for the chlorophyll-a molecule. With the pump laser operating at full power, this gave a pulse energy of 15mJ at 430nm. As the system was operated at 10Hz, the average power was approximately 150mW, giving an average power density of 5.31kWm⁻². This power density is comparable to the level required to produce a maximum fluorescence emission from the phytoplankton as was seen in chapter 5, figure 5.13, when a *Chaetoceros* sample was exposed to 488nm CW laser radiation.

The fluorescence from the sample was collected using focusing lenses and directed through a cut-on interference filter onto the entrance slit of a spectrograph. The filter served to remove most of the laser light. A CCD was connected to the exit slit of the spectrograph, allowing full spectral information to be obtained in real time and displayed on a computer. The other essential part of the experiment was the electronics, which consisted of a time delay generator, an optical gate and the CCD. The laser was triggered using a remote control. At the same time, the laser trigger signal was used to initialise the delay generator, which controlled both the optical gate width and the delay between the laser pulse and the “on” time of the gate. A signal was also sent to the computer card, which controlled the reading of the CCD. By altering the gate delay, it was possible to observe the fluorescence intensity at various times after the laser pulse had been incident on the sample.

6.3 Nanosecond Fluorescence Decay Results

Before any experiments were done on the algae, a cell count was taken to ensure that similar concentrations were being observed at the same time. This was done using the standard method detailed in Chapter 4. The samples were then diluted to 2000 cells per ml using Instant Ocean[®] solution to obtain approximately the same cell concentration to within 10 cells per ml. Once this had been achieved, the cells were used for experiments. Those samples which were not being used, were stored in the incubator until required. Each day, fresh cells from the incubator were harvested. These were diluted to obtain the same cell count as on day 1. The error bars are not shown on the graphs for clarity reasons. There is an average error of +/- 0.05 in the signal intensities.

6.3.1 *Chaetoceros calcitrans* Sample

The first experiments using the above setup were carried out using the *Chaetoceros* species. A sample of the culture was transferred into a quartz cuvette using a sterile pipette. The cuvette was then placed in the sample holder and the gate time delay set to correspond to instant fluorescence from the sample once it had been illuminated by the laser. A total of 50 laser shots were taken at each of the different gate time delays to achieve a good average. Once this had been carried out at the first time delay, the signal delay generator was re-programmed to a longer time delay to observe slower fluorescence emissions. The results for the *Chaetoceros* sample can be seen in figure 6.2. It can be seen that the fluorescence from the *Chaetoceros* sample follows an exponential decay which results in small fluorescence emissions after 15ns. One interesting curve is that for day 1. Note that at 2ns and 5ns, there appears to be slight peaks in the fluorescence emissions after the initial laser pulse with the same trend being observed on days 2 and 3 although to a lesser extent.

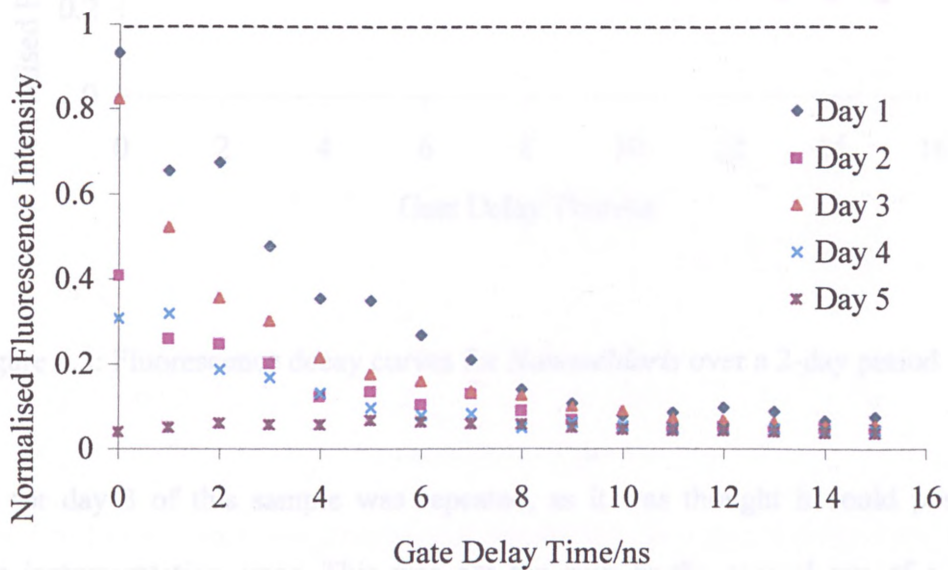


Figure 6.2: Fluorescence decay curves for *Chaetoceros* over a 5-day period

As the days progress, however, the initial fluorescence intensity from the sample shows a large decrease, which suggests the sample has moved from the growth phase into the stationary phase.

6.3.2 *Nannochloris atomus* Sample

Shown in figure 6.3 are the fluorescence decay curves for the *Nannochloris* sample. The curve for day 2 shows a typical exponential decay again, with the fluorescence level reaching a steady state after 15ns. The curve for day 3, however, shows a unique trend compared to all of the other samples. There are small peaks observed at 3, 8 and 11ns.

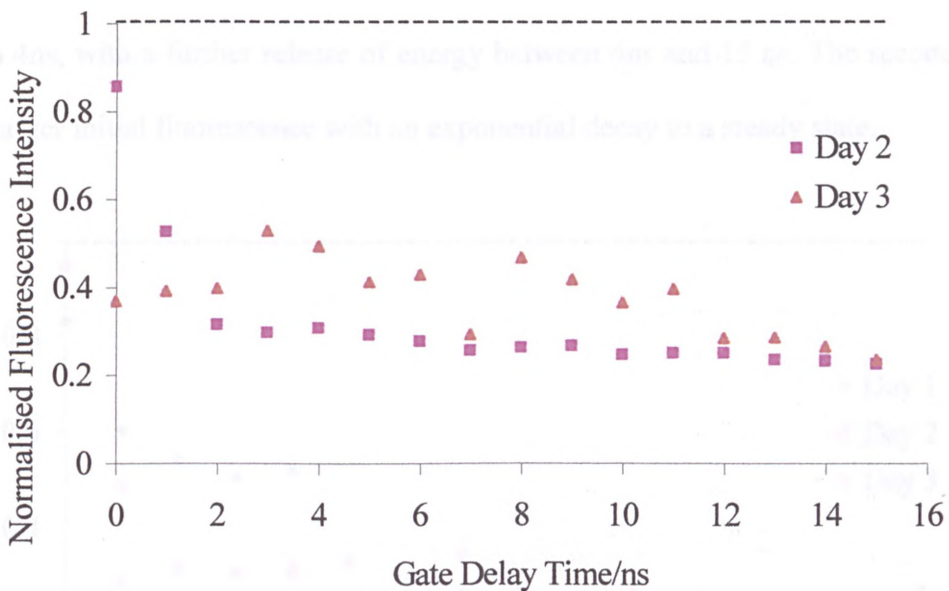


Figure 6.3: Fluorescence decay curves for *Nannochloris* over a 2-day period

The plot for day 3 of this sample was repeated, as it was thought it could possibly reflect an instrumentation error. This was not the case as the second run of a fresh sample produced very similar results. It was, therefore, thought that the sample was no

longer viable and further experimentation with this sample culture was suspended until a sub-culture could be taken.

6.3.3 *Nannochloropsis oculata* Sample

This species was one of the first samples to be used with the system along with the *Chaetoceros* sample. It was chosen at random from all the cultures to test against the *Chaetoceros* sample, which had been used the most during the course of previous experiments.

Day 1 of the experiments shows an interesting fluorescence decay curve, as if the fluorescence decay appears to occur in two distinct steps. The first emission occurs from 0 to 4ns, with a further release of energy between 4ns and 15 ns. The second day shows a larger initial fluorescence with an exponential decay to a steady state.

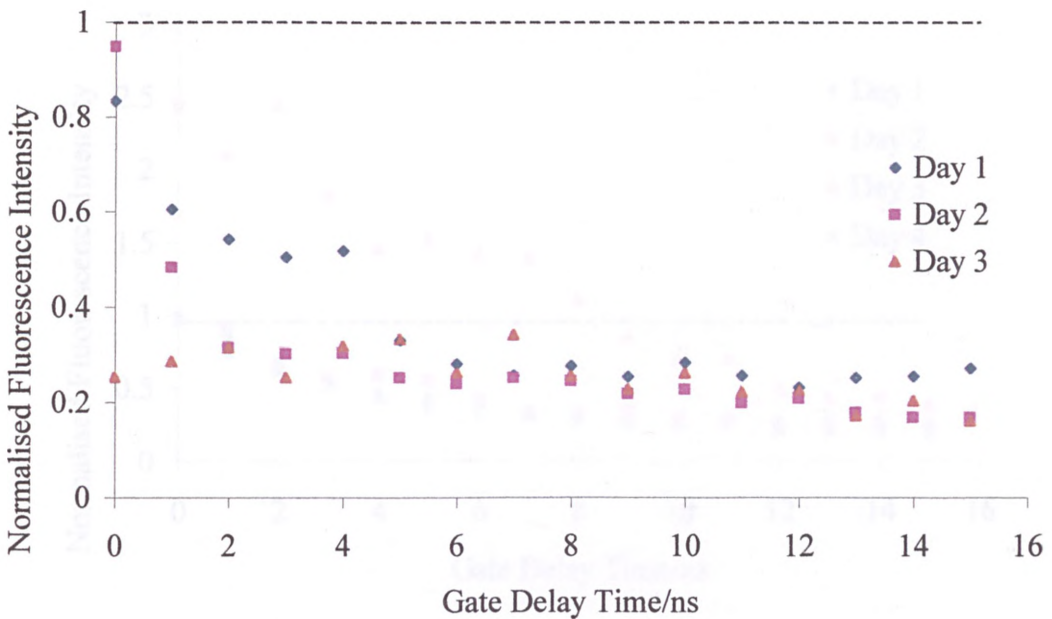


Figure 6.4: Fluorescence decay curves for *Nannochloropsis* over a 3-day period.

There does appear to be a slight peak at 4ns, which is similar to that of day 1, although not as pronounced. The sample tested during day 3 shows that the fluorescence signal has dropped to an almost steady state.

6.3.4 *Tetraselmis suecica* Sample

Shown in figure 6.5 are the fluorescence decay curves for the quadriflagellate, *Tetraselmis*. The data obtained for this species shows a very similar trend for the fluorescence emission on three of the days. It can be seen, however, that on day 3, there is a marked difference in the plot. Although the initial intensity of the fluorescence recorded is less than in days 1 and 2, there is a steady increase in the fluorescence emission, peaking at around 2 nanoseconds after the pulse from the laser.

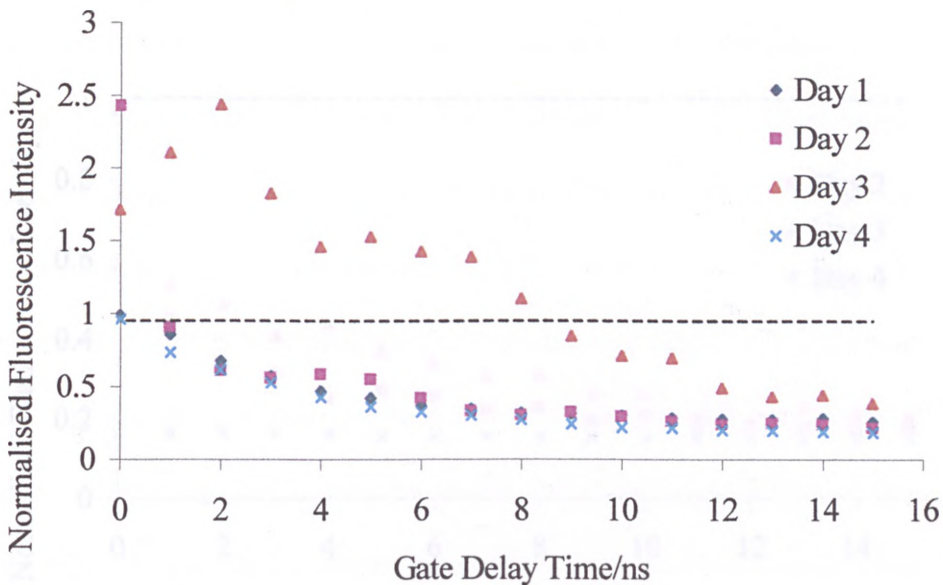


Figure 6.5: Fluorescence time decay curves for the *Tetraselmis* sample over a 4-day period.

There is also a plateau in the signal fluorescence between 5 and 7ns after the initial radiation has been imparted into the sample. The graph also shows that on the other days, there seems to be a slight plateau formed in the signal between 3 and 5ns, although the effect is not easily seen.

6.3.5 *Scropsiella trochoidea* Sample

The final species observed using the fast fluorescence experiment was the dinoflagellate, *Scropsiella*. The sample was treated in the same way as was previously described. Shown in figure 6.6 is the fluorescence decay curves over a 3-day period. The first day of experiments was carried out primarily with the *Chaetoceros* and *Nannochloropsis* samples to determine the response of the system and to ensure the detection electronics and optics were working properly, hence, there is no data on the first day for the *Scropsiella* sample.

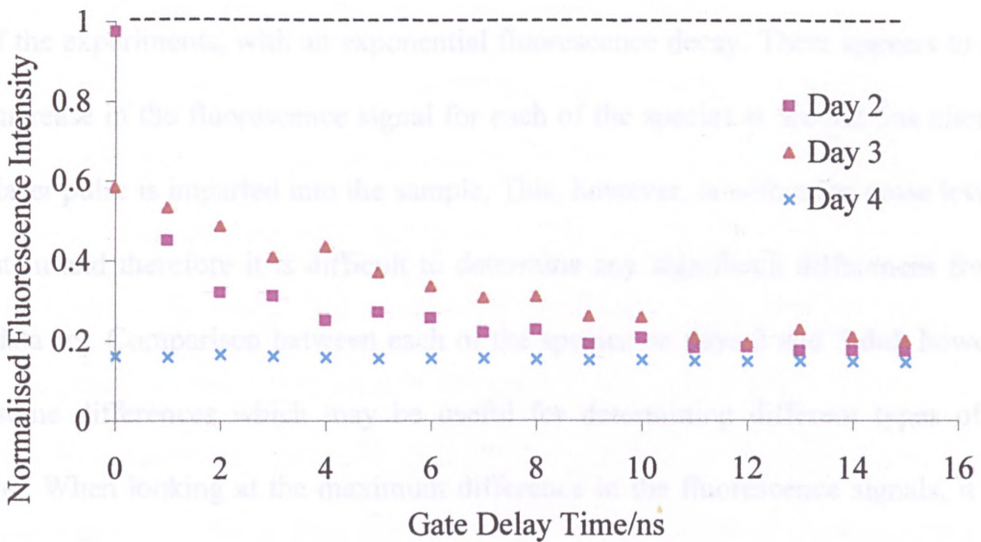


Figure 6.6: Fluorescence decay curves for *Scropsiella* over a 3-day period

As can be seen in figure 6.6, the fluorescence decay curve for day 2 shows a steep exponential decay from the initial fluorescence value as the gate delay time is increased, suggesting that the sample gives very prompt fluorescence whilst in that state. As the experiment progresses to day 3, it can be seen that the initial fluorescence value has dropped to about 60% of the previous day's initial fluorescence. The fluorescence decay is also much slower on the third day, whilst on the final day (day 4) the fluorescence emission from the *Scropsiella* sample is continuous at 20% of the initial fluorescence value on day 2. Again, these graphs tend to suggest that the sample has moved from the exponential phase on day 2 into the stationary phase on day 4. This would account for the decrease in the initial fluorescence intensity, as the initial cell concentration has been maintained.

6.4 Discussion - Nanosecond Fluorescence

All of the above samples have shown similar fluorescence characteristics in the first few days of the experiments, with an exponential fluorescence decay. There appears to be a small increase in the fluorescence signal for each of the species at around 5ns after the initial laser pulse is imparted into the sample. This, however, is within the noise level of the system and therefore it is difficult to determine any significant differences from a small data set. Comparison between each of the species on days 2 and 3 did, however, show some differences which may be useful for determining different types of the plankton. When looking at the maximum difference in the fluorescence signals, it was noted that they occurred at different areas in the time domain. This can be seen in figure 6.7.

	<i>Day 2</i>					<i>Day 3</i>				
	Chaet	Tetra	Nano. O	Nano. A	Scrip	Chaet	Tetra	Nano. O	Nano. A	Scrip
1-13 ns	■									
1-14 ns						■				
1-15 ns		■	■	■	■					
2-15 ns							■			
3-15 ns									■	
7-15 ns								■	■	
1-12 ns										■

Figure 6.7: Table showing the largest differences between fluorescence emission at various times after excitation for each of the species

For all of the algae, each black cell represents a change in fluorescence greater than 40% between each of the fluorescence detector gate delay times stated. On day 2, the differences between each of the selected algae is limited to *Chaetoceros* and the other selected samples. On day 3, however, it can be seen that all the algae have different times when their fluorescence levels are at a maximum. The signals for *Chaetoceros*, *Tetraselmis* and *Nannochloris* are all very similar, making it difficult to tell the difference between them. There are, however, more noticeable differences with the *Nannochloropsis* and *Scripsiella* samples compared to the other plankton. By looking at these changes over two days, it can be seen that the nutrient level in each of the culturing flasks is reducing. This could most likely lead to stress within each of the algae. The data from day 3 may suggest that each of the algae respond differently under stress, resulting in differences in the fluorescence emission in the time domain. When compared with day 2, where there are more nutrients, the differences in the fluorescence emissions are very small. These possible differences in planktons under nutrient limitation alone are not definitive in determining the identity of a species. The data may,

however, be used with other measurements to give an indication, by a process of elimination of the likelihood of a specific species being present.

	Day 2 – Approx. $t_{1/2}$ /ns	Day 3 – Approx. $t_{1/2}$ /ns
<i>Chaetoceros calcitrans</i>	3	1.5
<i>Nannochloris atomus</i>	0.7	>15
<i>Nannochloropsis oculata</i>	1.2	>15
<i>Tetraselmis suecica</i>	0.7	9
<i>Scropsiella trochoidea</i>	0.7	8.5

Figure 6.8: Table showing the time for the fluorescence to decay to half the original value for each of the plankton's

The fluorescence decay from each of the algae could also be another indicator of the species. As there was a limited data set, it was decided that curve fitting of the fluorescence decay data was not advisable. A rough estimate of the time for the fluorescence to decay to half its original value ($t_{1/2}$) from each of the curves on days 2 and 3 was measured and is summarised in figure 6.8. Again, it can be seen that there is little difference between the samples except for the *Chaetoceros* on day 2. On day 3, however, there are large differences between the times to reach $t_{1/2}$. This information may further support fluorescence differences in each of the species as they reach nutrient limitation.

6.5 Effects of High-Energy Laser Radiation on Algae

The previous section showed the effects on the time-dependent fluorescence emissions as different types of phytoplankton went from the exponential growth phase into the nutrient-limited, stationary phase. The experiments were carried out using 430nm radiation with an average power density of 5.31kWm^{-2} , which produced a maximum

fluorescence from the chlorophyll-a within the cells, but did not cause disruption of the cells when observed using an optical microscope after irradiation.

It was also decided to observe the effect of high power pulsed laser radiation on the slow fluorescence characteristics of the various planktons. Ideally, the same wavelength at 430nm would have been the most suitable, giving continuity to the study, but as the Optical Parametric Oscillator was operating at close to the maximum power output at 430nm, it was decided to use the 3rd harmonic of the Nd:YAG. This was closest to the 430nm absorption of the chlorophyll-a molecule and also allowed high powers to be delivered to the samples. The effects of 430nm, 474nm and 633nm laser radiation up to a maximum of 5.31kWm^{-2} on the fluorescence characteristics of *Chaetoceros* were also investigated using the OPO. The samples were excited at 430nm and 630nm, which correspond to absorption maxima of the chlorophyll-a molecule. The samples were also excited at 474nm which does not correspond to an absorption peak of the chlorophyll-a molecule. This area, however, has been shown to contain “accessory pigments” in some species. The *Sciphsiella* sample was not used due to difficulties in culturing the plankton.

6.6 Experimental Setup

The experiment was carried out in three distinct steps: an initial fluorescence reading, laser treatment of the sample and further fluorescence readings. The last two steps were repeated as the sample was exposed to further quantities of laser radiation.

The initial fluorescence reading was obtained using a Perkin-Elmer fluorimeter (LS-501B). Each of the different samples were harvested from cultures which were in the exponential growth phase. They were then, in turn, placed in quartz cuvettes and placed in a standard fluorimeter. The fluorescence reading at 680nm was taken as the

initial fluorescence value for each of the samples. This wavelength was chosen because of the maximum fluorescence emission from the chlorophyll-a molecule.

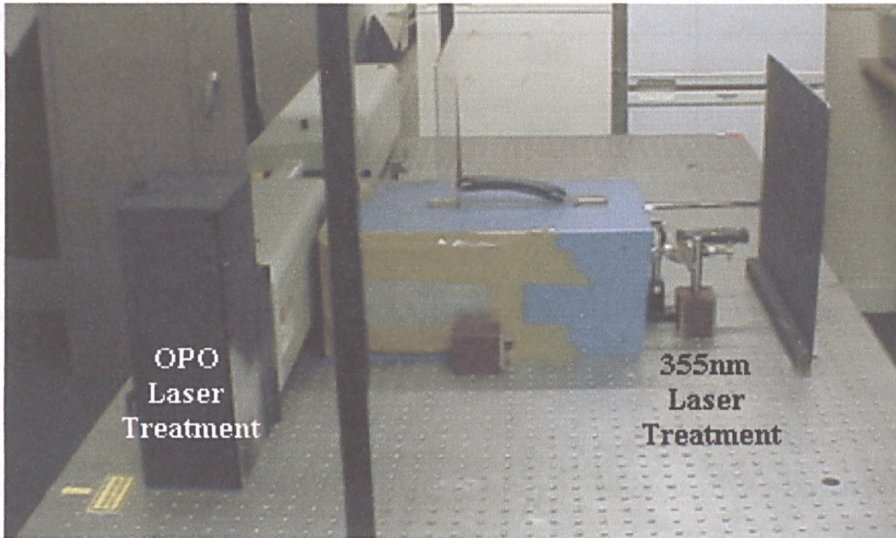


Figure 6.9: High-energy laser treatment experiment setup

Once this value had been obtained, the sample cuvettes were placed on a magnetic stirrer in turn, in the path of the high-power laser beam as outlined in figure 6.10.

The laser was then started on full power, giving a power density of 49.5kWm^{-2} , and the sample exposed to between 40-50 single shots at 5ns each for a fixed wavelength. Each bank of shots took approximately 60 seconds to complete. The total energy for the for each treatment was calculated and plotted against the fluorimeter fluorescence reading.

After each bank of shots, a further fluorescence reading was taken on the fluorimeter. This procedure was repeated until no further change was observed in the fluorescence signal from each of the different species. This process showed the responses of the different species of phytoplankton to single-frequency, high-energy laser light.

Sample	Laser treatment wavelength/nm	Fluorimeter excitation wavelength/nm	Fluorimeter excitation wavelength/nm
<i>Chaetoceros calcitrans</i> .	355	430	633
<i>Nannochloris atomus</i>	355	430	633
<i>Nannochloropsis oculata</i>	355	430	633
<i>Tetraselmis suecica</i>	355	430	633

Figure 6.10: Phytoplankton laser treatment wavelengths and fluorimeter excitation wavelengths observing fluorescence emissions at 680nm

To probe other possible pigments within the phytoplankton, this whole process was repeated for the *Chaetoceros* sample, using a further three different laser wavelengths as outlined in figure 6.11 and detailed in section 6.8.

Laser treatment wavelength/nm	Fluorimeter excitation wavelength/nm	Fluorimeter excitation wavelength/nm	Fluorimeter excitation wavelength/nm
430	430	474	633
474	430	474	633
633	430	474	633

Figure 6.11: *Chaetoceros* laser treatment wavelengths and fluorimeter excitation wavelengths observing fluorescence emissions at 680nm

6.7 Results from Laser Radiation Treatment using 355nm

6.7.1 *Chaetoceros calcitrans* Sample

This was the first sample used in these series of experiments. The initial fluorescence reading, at 680nm, was taken and the sample then placed in the 355nm treatment

sample holder shown in figure 6.9. The sample was then exposed to 30 laser shots whilst being stirred using a magnetic stirrer.

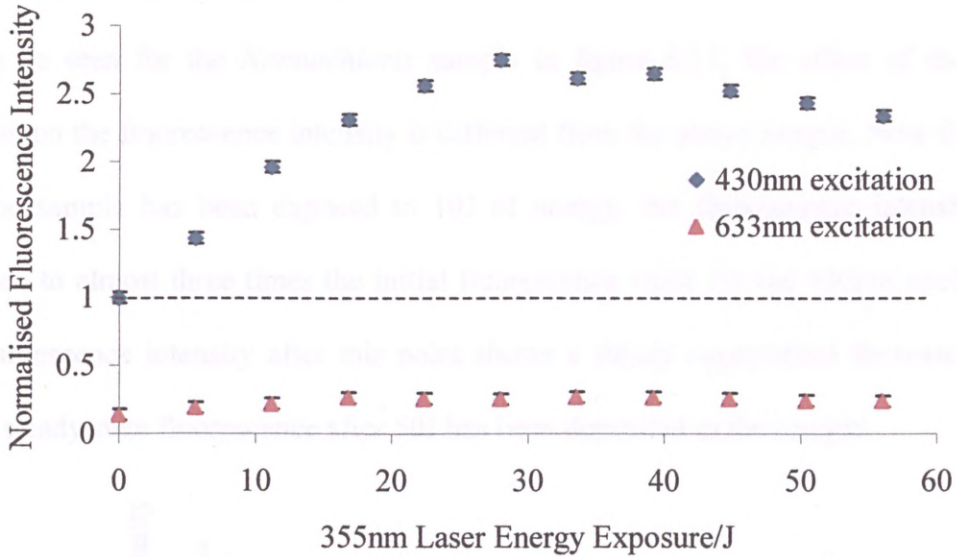


Figure 6.12 Effect of 355nm laser radiation on 680nm fluorescence at various excitation wavelengths for *Chaetoceros*

The sample was then placed back into the fluorimeter and another fluorescence reading was taken. This process was repeated giving the results shown in figure 6.12. The normalised fluorescence intensity for 430nm and 633nm excitation is shown on the y axis whilst the x axis shows the laser energy which the sample was exposed to. This was calculated from the average energy per pulse multiplied by the number of shots. The plot shows that the fluorescence from the 430nm excitation tends to increase to a maximum after approximately 30J of laser energy has been deposited in the phytoplankton sample. This corresponds to a 250% increase in the initial fluorescence intensity. The fluorescence level then shows a steady decrease back to a level which is twice the initial fluorescence level. The 633nm excitation shows a slight increase to an almost steady state fluorescence level when the sample was exposed to approximately

55J of energy which corresponds to approximately 60 minutes experiment time.

6.7.2 *Nannochloris atomus* Sample

As can be seen for the *Nannochloris* sample in figure 6.13, the effect of the laser radiation on the fluorescence intensity is different from the above sample. Note that just after the sample has been exposed to 10J of energy, the fluorescence intensity has increased to almost three times the initial fluorescence value for the 430nm excitation. The fluorescence intensity after this point shows a steady exponential decrease to an almost steady state fluorescence after 50J has been deposited in the sample.

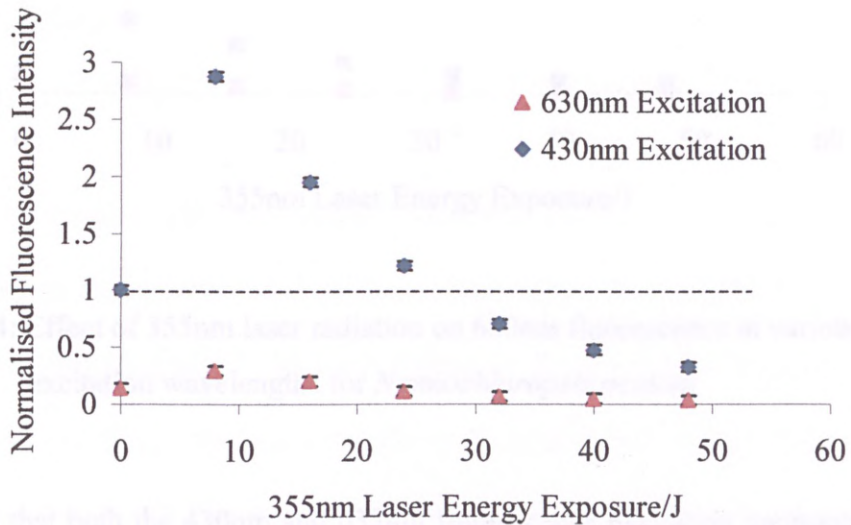


Figure 6.13: Effect of 355nm laser radiation on 680nm fluorescence at various excitation wavelengths for *Nannochloris atomus*

The fluorescence emission when exciting using the 633nm radiation also shows an increase in the signal after exposure to 9J of energy. The increase in the fluorescence, however, is not as large as for the 430nm excitation. Again, the fluorescence level is steady after approximately 50J of laser treatment.

6.7.3 *Nannochloropsis oculata* Sample

Experiment on this sample has shown yet another difference in the fluorescence signal after exposure to 355nm laser radiation. As can be seen in figure 6.14, the fluorescence decreases exponentially as more laser energy is deposited into the sample.

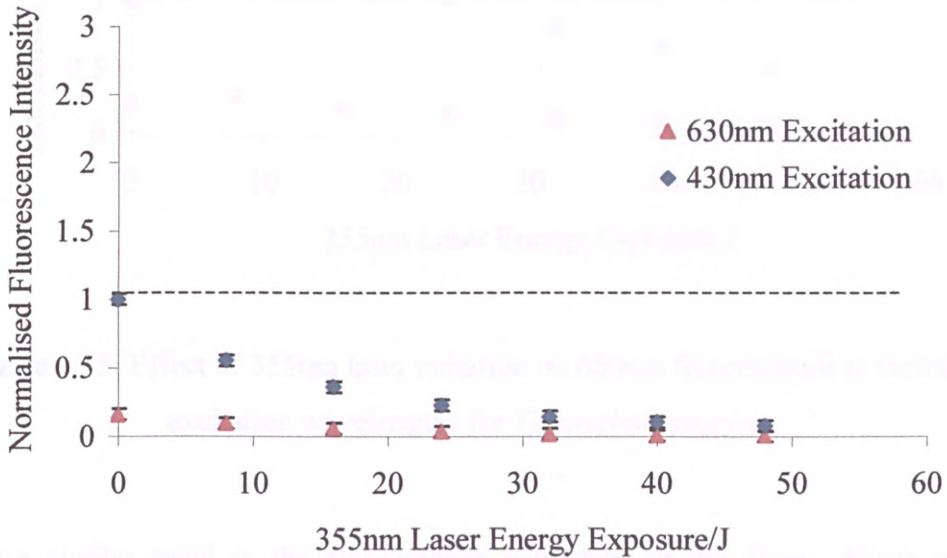


Figure 6.14: Effect of 355nm laser radiation on 680nm fluorescence at various excitation wavelengths for *Nannochloropsis oculata*

The data shows that both the 430nm and 633nm fluorescence excitation measurements follow the same trend, reaching a steady state fluorescence after 50J has been deposited into the sample.

6.7.4 *Tetraselmis suecica* Sample

The final sample in these comparisons of the effects of 355nm laser radiation on the fluorescence properties of phytoplankton is the quadriflagellate *Tetraselmis*. The plot in figure 6.15 shows an increase in the fluorescence signal by 60% after approximately 9J of laser energy has been deposited into the sample.

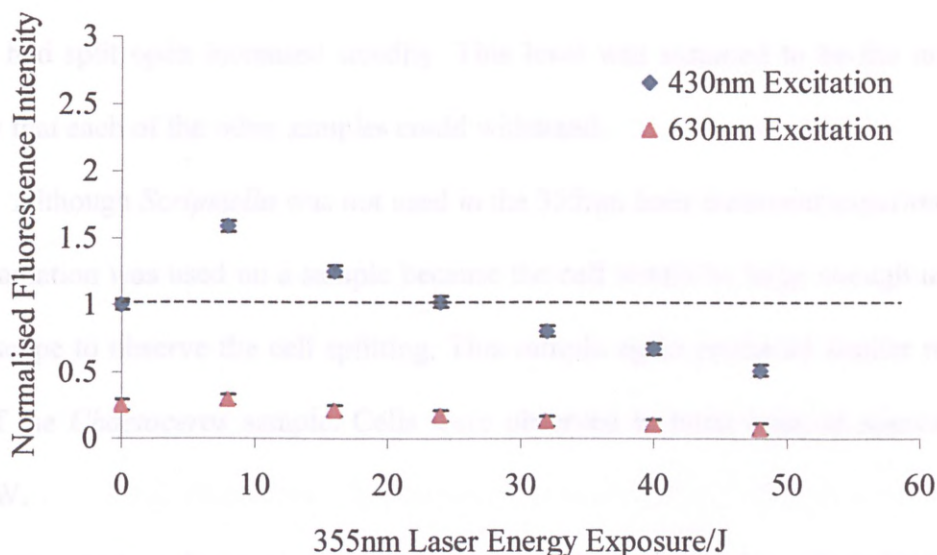


Figure 6.15: Effect of 355nm laser radiation on 680nm fluorescence at various excitation wavelengths for *Tetraselmis suecica*

This is a similar trend to the fluorescence behaviour of the *Nannochloris* sample, although the increase in fluorescence is much smaller compared to the 190% increase in the *Nannochloris* sample after 8J. As more energy is deposited into the sample, the fluorescence level gradually decreases to almost a steady state after 49J. As with previous samples, both excitations follow the same trends in the fluorescence levels.

6.8 Optical Microscopy of the Planktons Exposed to 355nm Laser Radiation.

The effects of 355nm laser radiation on treated samples was also monitored using an optical microscope. Each of the samples was exposed to greater laser power levels and the effects on the cell were then observed using an optical microscope. The microscope was set up to give 40x magnification. Of the four samples exposed to high energy UV laser radiation, only *Chaetoceros* was large enough to observe the cell wall before and after treatment. It was found that up to approximately 150mW average power, there was

no visible effects on the plankton cell. Above this value however, the number of cells which had split open increased steadily. This level was assumed to be the maximum energy that each of the other samples could withstand.

Although *Scropsiella* was not used in the 355nm laser treatment experiments, the laser radiation was used on a sample because the cell would be large enough under the microscope to observe the cell splitting. This sample again produced similar results to that of the *Chaetoceros* sample. Cells were observed to burst open at approximately 160mW.

The 355nm laser treatment experiments would therefore most likely cause disruption of the algae cells as the laser power was 1.4W when the laser was operating at full power.

6.9 Discussion: 355nm Laser Treatment

These graphs show quite large differences between each of the species examined. This can be seen in figure 6.16. These fluorescence readings are taken when the sample is excited in the fluorimeter using 430nm radiation. It can be seen that by monitoring the peak fluorescence level relative to the amount of laser energy which has been imparted into the sample, it is possible to determine three of the four species.

	Energy Exposure to peak/J	% Change in fluorescence	
		Initial Fluorescence to Peak	Peak to Lowest Fluorescence
<i>Chaetoceros</i>	32	176	-8
<i>Nannochloropsis</i>	0	0	-92
<i>Nannochloris</i>	8	89	-188
<i>Tetraselmis</i>	8	59	-68

Figure 6.16: Changes in 680nm fluorescence after exposure to 355nm laser radiation

This information alone does not allow distinction between *Nannochloris* and *Tetraselmis*. When the changes in the fluorescence signals are observed between the initial fluorescence and the peak (column 1) and the peak to the lowest fluorescence (column 2), however, it can be seen that there are noticeable differences between each of the algae. This method provides another possible effect within different algae which could be used to determine the species of a plankton in conjunction with other methods.

Some of the effects observed in the above experiments have been observed previously by other researchers. Experiments by Gerber et al⁸⁰ have shown that when algae are exposed to UV light from strong sunlight, a decrease in the fluorescence at 680nm is observed along with a loss in photosynthetic oxygen production. The fluorescence data are not discussed further “as the steady state signal fluorescence is difficult to interpret due to the number of complex processes involved” whilst the loss in photosynthetic oxygen production is attributed to photoinhibition or photodamage. It should be noted however that the experiments by Gerber et al were carried out using broadband light with multiple UVA, UVB and visible wavelengths present. This differs from the experiments here in that a single UVA wavelength at high power was used to treat the algae samples. The results presented here are most likely due to laser induced modification of the cell which may account for the differences in the fluorescence emissions observed which may also be characteristic of the algae cells.

6.10 Effects of Three Different Laser Wavelengths on *Chaetoceros* Fluorescence

The next step in the investigation was to monitor the effects of different wavelengths of light on the fluorescence emissions of a single species. The information obtained in

section 6.8 was used to ensure that the radiation did not burst the cells open. The laser power for these experiments was limited to 150mW.

These multi-wavelength experiments were carried out using the OPO to probe the effects of three wavelengths at 430nm, 474nm and 633nm. The absorption at 430nm and 633nm corresponds to the absorption maximum for chlorophyll-a, thus direct changes in the chlorophyll-a fluorescence system could be monitored. Absorption at 474nm corresponds to a region where chlorophyll-a absorption is at a minimum. This wavelength, however, does occur in a region, around 500nm, where accessory pigments have a high absorption. By using this wavelength, it should be possible to probe the effects of the laser radiation on this indirect pathway. For each of the laser wavelengths, fluorescence intensity changes, peak width changes (Full Width at Half Maximum – FWHM) and chlorophyll-a peak emission wavelengths were recorded.

6.10.1 Chlorophyll-a (PSII) Fluorescence after Exposure to 430nm Laser Radiation

Shown in figure 6.17 is the change in the fluorescence intensity centred at 680nm for excitation at three selected wavelengths after the sample was exposed to 430nm laser radiation. Once the sample had been exposed to 40 laser shots, the fluorescence reading at the maximum emission centred on 680nm was recorded whilst exciting at 430nm, 474nm and 633nm using a bench fluorimeter. As can be seen in figure 6.19, the peak fluorescence intensity from the chlorophyll-a shows a small change as the laser energy exposure increases. For this reason, the fluorescence intensities recorded in figure 6.17 were recorded at the peak emission and not at 680nm. This shows the variations in the peak fluorescence intensity independent of the actual fluorescence wavelength, although the peaks still correspond to PSII of the chlorophyll-a molecule.

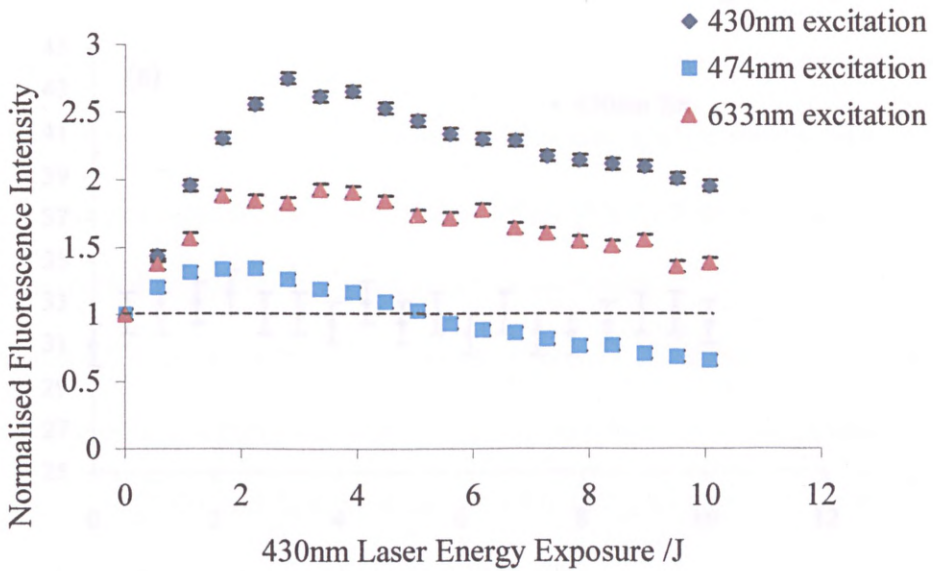


Figure 6.17: Effects of 430nm radiation on chlorophyll-a fluorescence intensity

It can be seen that as the energy exposure increases, the fluorescence intensity increases steadily when the sample was exposed up to approximately 3J when the sample was excited using 430nm or 633nm in the fluorimeter. After this point, the fluorescence intensity decreases steadily. The largest change in the fluorescence signal from the initial value to peak occurs when the fluorescence intensity was recorded using 430nm excitation light. Shown in figures 6.18a-c are the changes in the fluorescence peak width after treatment with 430nm laser radiation. When exciting the sample in the fluorimeter using 430nm radiation, the fluorescence peak width was constant at approximately 32nm with a small variation of 4nm. When the fluorescence peak width was observed whilst exciting at 474nm, there is a steady increase in the peak width from 31nm to 40nm giving a change of approximately 9nm.

Figure 6.18a-c: Changes in the PSII fluorescence peak width at half the maximum for selected excitation wavelengths after 430nm laser treatment

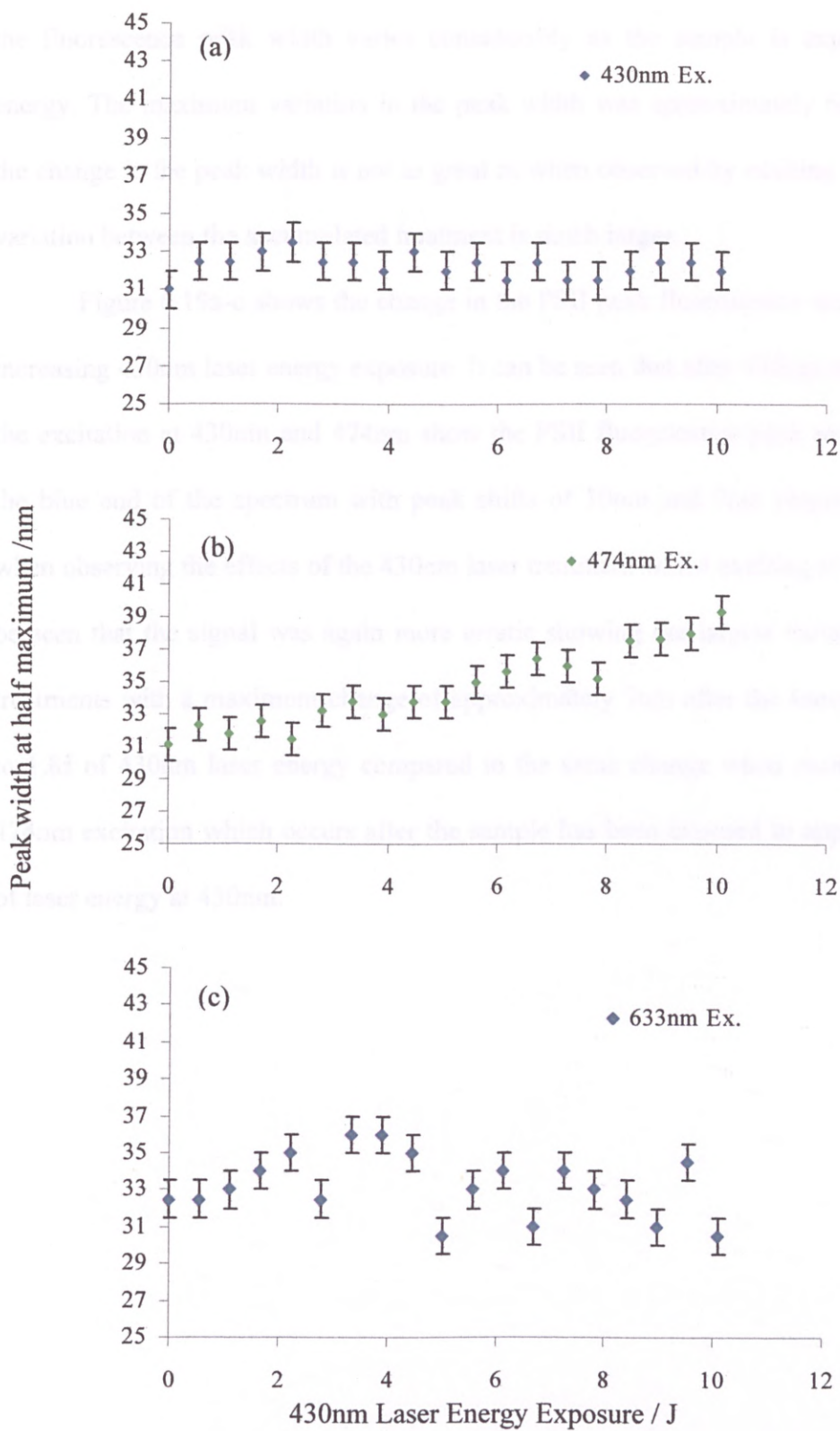
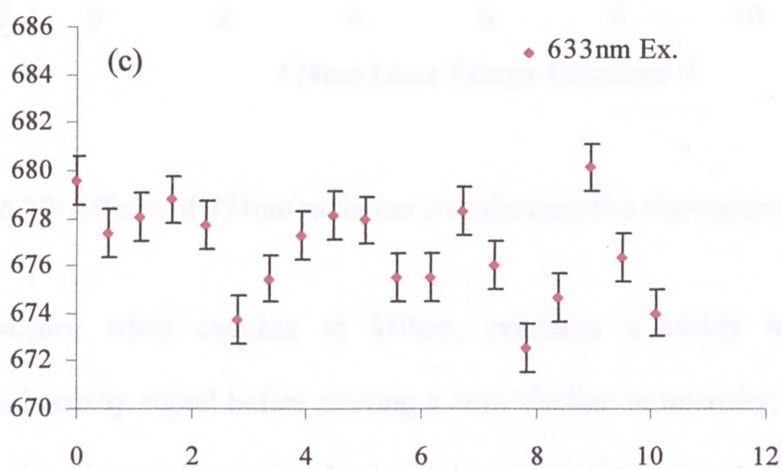
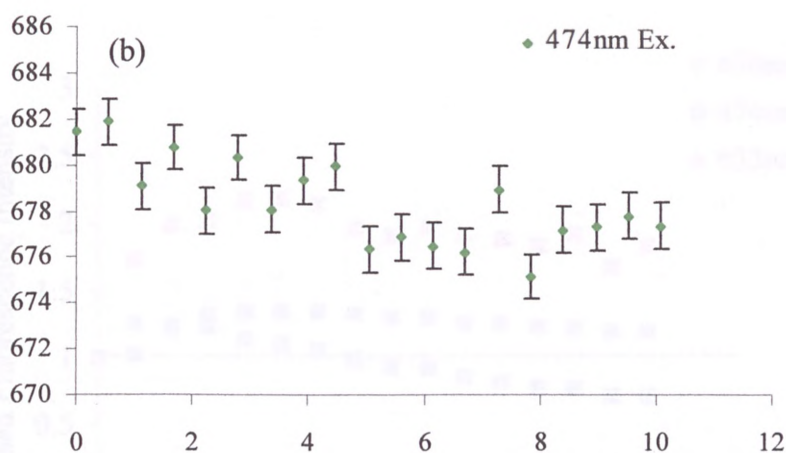
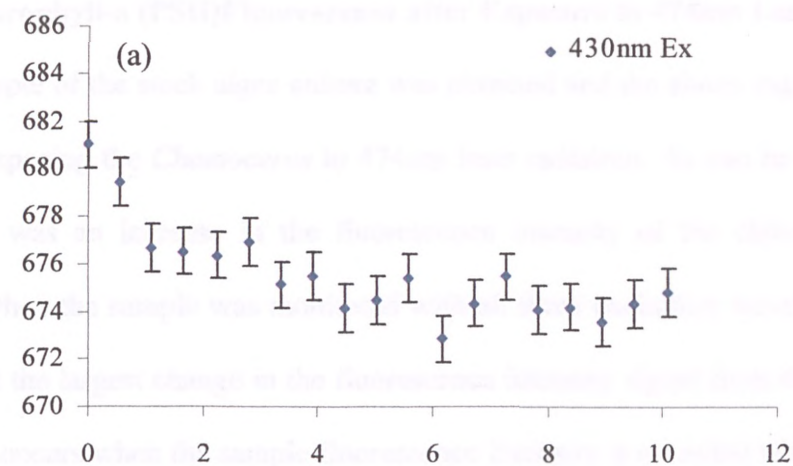


Figure 6.18a-c: Changes in the PSII fluorescence peak width at half the maximum for selected excitation wavelengths after 430nm laser treatment

As the fluorescence is monitored using 633nm excitation radiation, it can be seen that the fluorescence peak width varies considerably as the sample is exposed to laser energy. The maximum variation in the peak width was approximately 6nm. Although the change in the peak width is not as great as when observed by exciting at 474nm, the variation between the accumulated treatment is much larger.

Figure 6.19a-c shows the change in the PSII peak fluorescence wavelength with increasing 430nm laser energy exposure. It can be seen that after 430nm treatment, both the excitation at 430nm and 474nm show the PSII fluorescence peak moving towards the blue end of the spectrum with peak shifts of 10nm and 7nm respectively. Again when observing the effects of the 430nm laser treatment whilst exciting at 633nm, it can be seen that the signal was again more erratic showing the largest variations between treatments with a maximum change of approximately 7nm after the sample is exposed to 1.8J of 430nm laser energy compared to the same change when monitored via the 474nm excitation which occurs after the sample has been exposed to approximately 8J of laser energy at 430nm.

Chlorophyll-a peak emission wavelength / nm



430nm Laser Energy Exposure / J

Figure 6.19a-c: Chlorophyll-a PSII fluorescence peak wavelength for selected excitation wavelengths after 430nm laser treatment

6.10.2 Chlorophyll-a (PSII) Fluorescence after Exposure to 474nm Laser Radiation

A fresh sample of the stock algae culture was obtained and the above experiments were repeated, exposing the *Chaetoceros* to 474nm laser radiation. As can be seen in figure 6.20, there was an increase in the fluorescence intensity of the chlorophyll-a after treatment when the sample was monitored with all three excitation wavelengths. It can be seen that the largest change in the fluorescence intensity signal from the initial value to the peak occurs when the sample fluorescence intensity is recorded whilst exciting at 633nm.

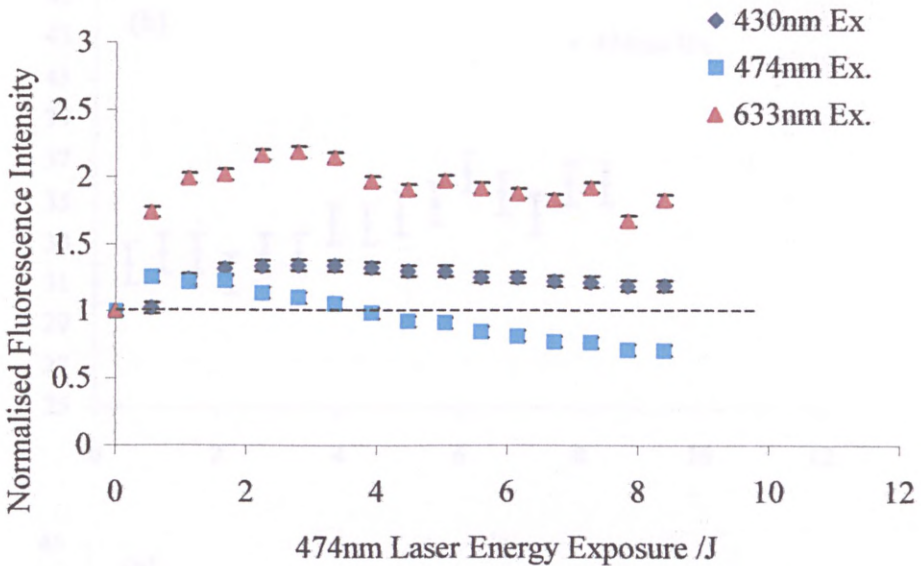


Figure 6.20: Effects of 474nm radiation on chlorophyll-a fluorescence intensity

The fluorescence when exciting at 430nm, produces a steady increase in the fluorescence intensity signal before starting a slow decline in intensity. When exciting at 474nm, the fluorescence signal shows an immediate, small increase in the fluorescence intensity which gradually reduces as the sample was exposed to more 474nm laser energy.

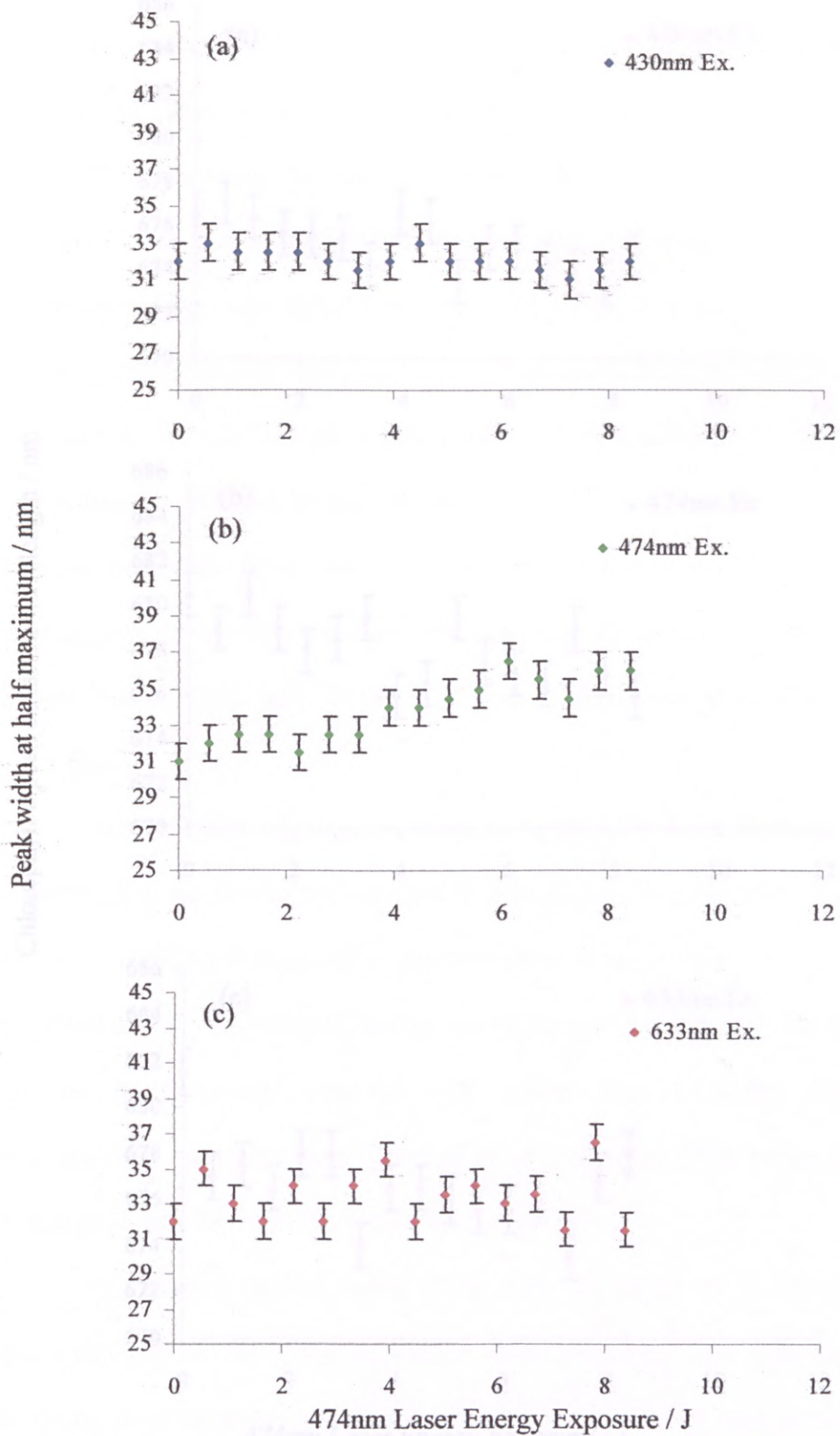


Figure 6.21a-c: Change in the PSII fluorescence peak width at half the maximum for selected excitation wavelengths after 474nm laser treatment

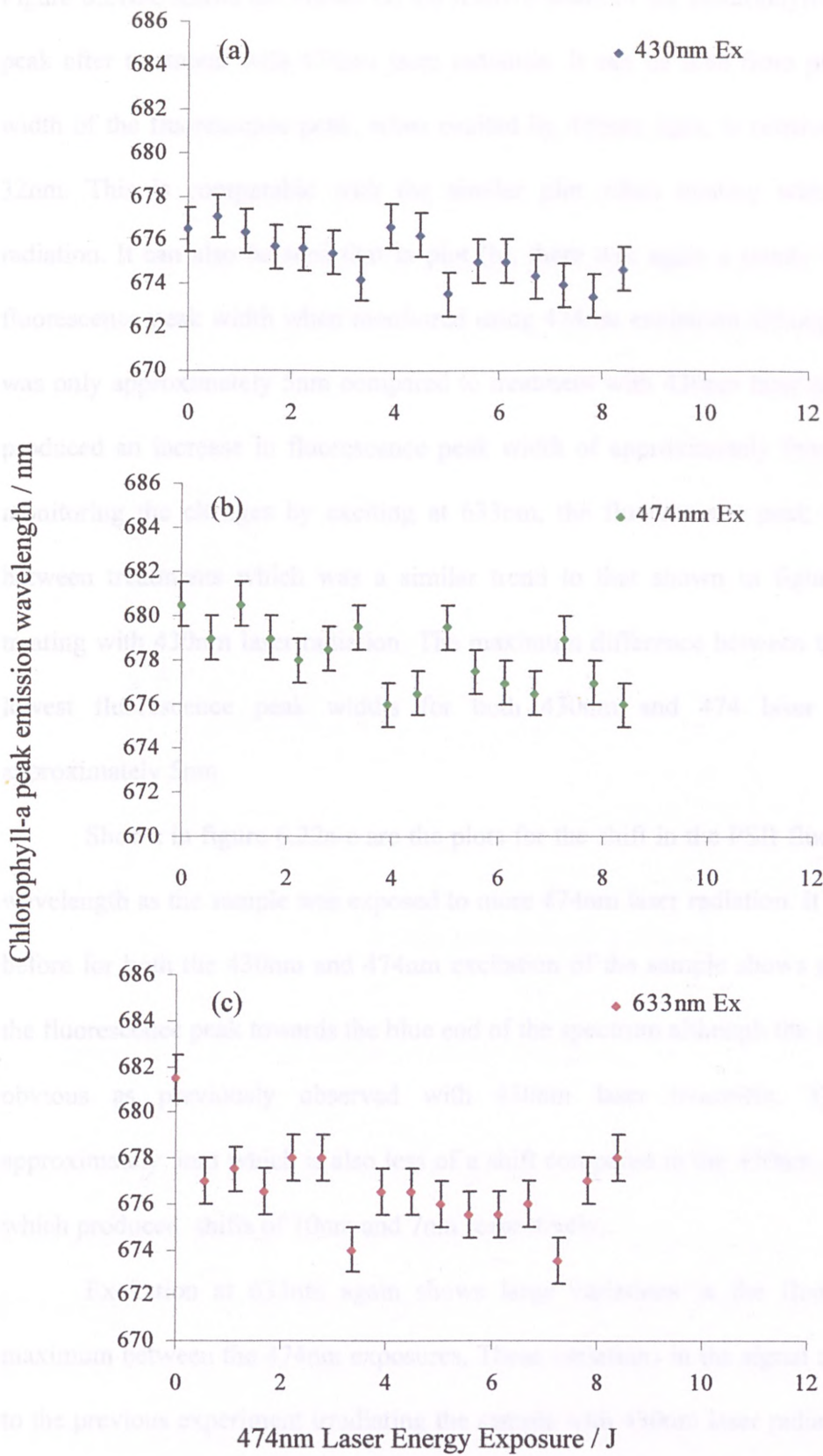


Figure 6.22a-c: Chlorophyll-a PSII fluorescence peak wavelength for selected excitation wavelengths after 474nm laser treatment

Figure 6.21a-c shows the effects on the relative width of the chlorophyll-a fluorescence peak after treatment with 474nm laser radiation. It can be seen from plot (a) that the width of the fluorescence peak, when excited by 430nm light, is relatively constant at 32nm. This is comparable with the similar plot when treating with 430nm laser radiation. It can also be seen that in plot (b), there was again a steady increase in the fluorescence peak width when monitored using 474nm excitation although the increase was only approximately 5nm compared to treatment with 430nm laser radiation which produced an increase in fluorescence peak width of approximately 9nm. Again when monitoring the changes by exciting at 633nm, the fluorescence peak width changes between treatments which was a similar trend to that shown in figure 6.18c when treating with 430nm laser radiation. The maximum difference between the highest and lowest fluorescence peak widths for both 430nm and 474 laser treatments is approximately 5nm

Shown in figure 6.22a-c are the plots for the shift in the PSII fluorescence peak wavelength as the sample was exposed to more 474nm laser radiation. It can be seen as before for both the 430nm and 474nm excitation of the sample shows a movement of the fluorescence peak towards the blue end of the spectrum although the shift was not as obvious as previously observed with 430nm laser treatment. The shift was approximately 5nm which is also less of a shift compared to the 430nm laser treatment which produced shifts of 10nm and 7nm respectively.

Excitation at 633nm again shows large variations in the fluorescence peak maximum between the 474nm exposures. These variations in the signal are comparable to the previous experiment irradiating the sample with 430nm laser radiation producing a maximum difference of 7nm.

6.10.3 Chlorophyll-a Fluorescence after Exposure to 633nm Laser Radiation

The final experiments were carried out on a fresh sample of *Chaetoceros*, this time exposing the sample to 633nm laser radiation from the optical parametric oscillator. As with the previous treatment wavelengths, the pump laser energy was adjusted to obtain 15mJ (150mW) output at 633nm. In the same way, this sample was treated as described earlier and various properties of the fluorescence emission from the sample were recorded.

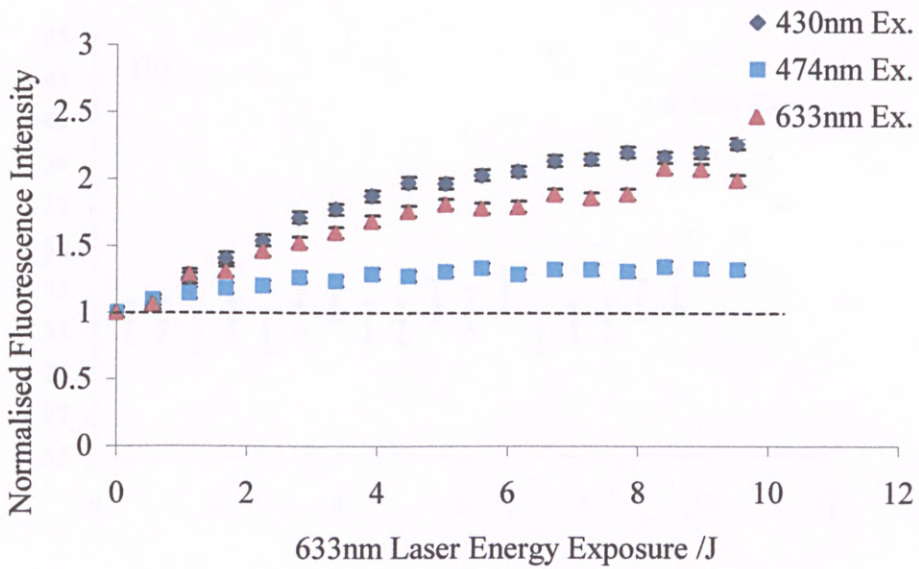


Figure 6.23: Effects of 633nm radiation on chlorophyll-a fluorescence intensity

In figure 6.23, there is a change in the behaviour of the fluorescence emission observed. When exciting at each of the three wavelengths, all of the fluorescence emissions show the fluorescence intensity level increasing to a steady state as the energy deposited in the sample increases. This was in contrast to the previous laser treatments, where the fluorescence intensity level was seen to increase, then decrease to a steady state. The change in the fluorescence intensity signal is approximately equal in both the 430nm and 633nm excitations of the 633nm laser treated sample.

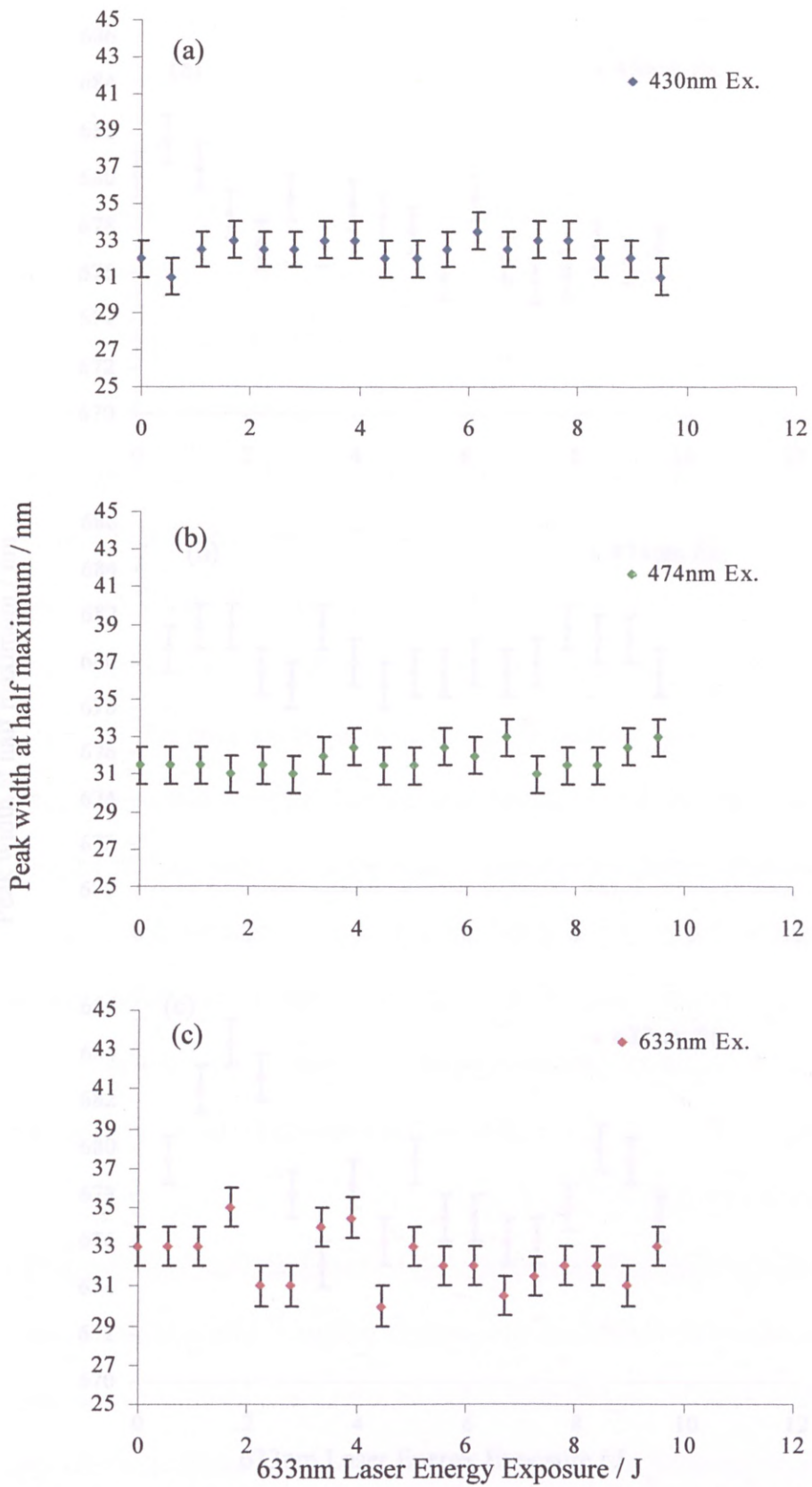


Figure 6.24a-c: Change in the PSII fluorescence peak width at half the maximum for selected excitation wavelengths after 633nm laser treatment

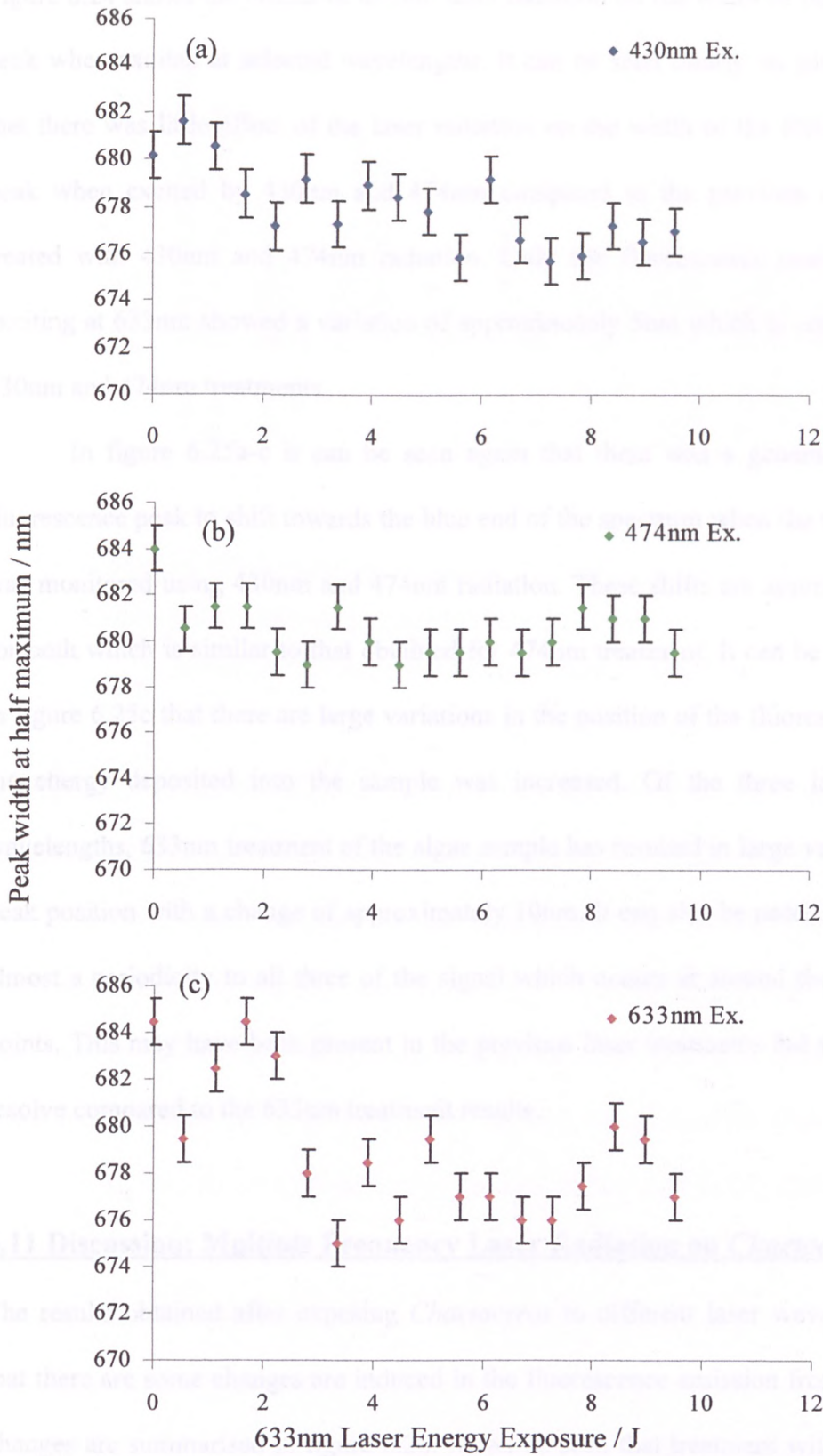


Figure 6.25a-c: Chlorophyll-a PSII fluorescence peak wavelength for selected excitation wavelengths after 633nm laser treatment

Figure 6.24 shows the effects of 633nm laser radiation on the width of the fluorescence peak when excited at selected wavelengths. It can be seen clearly on plots (a) and (b) that there was little effect of the laser radiation on the width of the PSII fluorescence peak when excited by 430nm and 474nm compared to the previous changes when treated with 430nm and 474nm radiation. Only the fluorescence peak width when exciting at 633nm showed a variation of approximately 5nm which is comparable with 430nm and 474nm treatments.

In figure 6.25a-c it can be seen again that there was a general trend in the fluorescence peak to shift towards the blue end of the spectrum when the treated sample was monitored using 430nm and 474nm radiation. These shifts are approximately 5nm for both which is similar to that obtained for 474nm treatment. It can be seen however in figure 6.25c that there are large variations in the position of the fluorescence peak as the energy deposited into the sample was increased. Of the three laser treatment wavelengths, 633nm treatment of the algae sample has resulted in large variations in the peak position with a change of approximately 10nm. It can also be noted that there was almost a periodicity to all three of the signal which occurs at around the same energy points. This may have been present in the previous laser treatments but too difficult to resolve compared to the 633nm treatment results.

6.11 Discussion: Multiple Frequency Laser Radiation on *Chaetoceros*

The results obtained after exposing *Chaetoceros* to different laser wavelengths show that there are some changes are induced in the fluorescence emission from PSII. These changes are summarised in figure 6.26. It can be seen that treatment with both 430nm and 633nm laser radiation produced the greatest effect on the fluorescence intensity signal when the sample fluorescence is measured by exciting at 430nm.

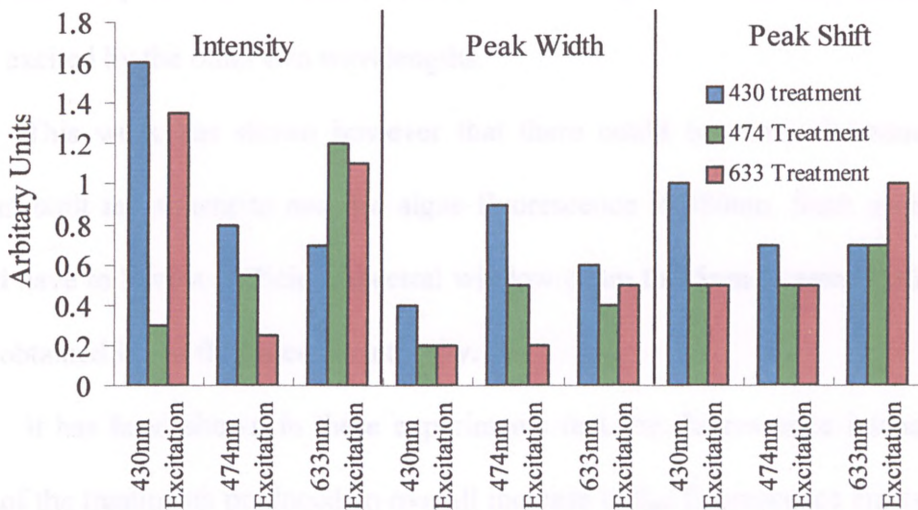


Figure 6.26: Chart showing the changes in fluorescence intensity, peak width and peak shift when monitored using selected wavelengths after treatment for three wavelengths of laser radiation

Large changes in the fluorescence intensity were also observed when the sample was treated with 474nm and 633nm radiation and measured by exciting at 633nm.

The information obtained on the fluorescence peak widths show the largest differences when the sample was treated with 430nm and 474nm whilst being monitored by exciting at 474nm. Compared to this result, treatment with 633nm laser radiation only produced a large effect in the fluorescence peak width when measured by exciting at 633nm. It can be seen that in monitoring the shift in the PSII fluorescence peak, the 430nm treatment produced almost similar results in that a shift of 7-10nm was observed when exciting at all three wavelengths with excitation at 430nm producing the largest fluorescence peak shift of 10nm. Treatment with 474nm produces similar results when exciting with 4430nm and 474nm but produces a slightly greater effect when exciting at 633nm. The largest difference between the fluorescence peak shifts occurs when the 633nm excited fluorescence when the sample is treated with 633nm laser

radiation. The peak shift is approximately 10nm compared to the 5nm shifts observed when excited by the other two wavelengths.

This work has shown however that there could be errors introduced into a custom built instrument to monitor algae fluorescence at 680nm. Such an instrument, would have to have a sufficient spectral window of up to 15nm to ensure true readings were obtained in the fluorescence intensity.

It has been shown in these experiments that the fluorescence intensities, after most of the treatments produced an overall increase in the fluorescence emission before decreasing which is contradictory to most papers reporting chlorophyll fluorescence behaviour when exposed to UV radiation⁸¹. There was also shifts in the PSII fluorescence peaks which has been previously reported but not discussed.

The previous investigations have in general focused on the interaction of algae with conventional light sources. Using Gerber et al as an example, their algae samples were exposed to solar radiation, which gave multiple wavelengths for their treatments from 280nm-700nm at various irradiances integrated over a 4 hour period. If an average value for their UVA exposure between 315nm and 400nm was taken (480kJm^{-2}) and this figure divided to get the average irradiance for 1 second, a value of approximately 34Jm^{-2} is obtained compared to the visible and UV wavelengths used for these experiments with irradiances of 760Jm^{-2} for a single wavelength being delivered in 4.5nS. Gerber et al did not consider the shift in the PSII fluorescence peak nor the changes in the fluorescence peak widths which may provide information on the mechanisms within the algae cell.

Although the changes seen in the fluorescence intensities after laser treatment generally increased before decreasing there are possible explanations for this effect. This could be due to the chlorophyll-a reaction centres becoming closed or modified

and hence unable to accept electrons which results in the energy being given out as fluorescence. This is the exact process in which fluorescence originates from chlorophyll-a within an algal cell⁸². This is similar to the pump-probe method, whereby the reaction centres are closed temporarily using a bright flash of light followed by a weak light to measure the maximum fluorescence. By using higher energy laser radiation this effect may be more permanent.

The blue shift in the PSII fluorescence peak after laser treatment 680nm has been seen before in previous work when the algae was been exposed to UVA and UVB radiation resulting from light and heat denaturation of chlorophyll-a⁸³ or changes in the pigment composition⁸⁴.

6.12 Summary

The information provided from the experiments has shown that there are differences between the algae species when they are treated using the above techniques. It can be seen that by compiling this information along with the spectral information obtained in Chapter 5, it is possible to identify the key parameters which may be used to separate the different types of algae. This is shown in figure 6.27. From the table, it is possible to identify which type of algae are present in the different samples by a process of elimination. The samples that have the closest characteristics are *Tetraselmis* and *Nannochloris*. There is the possibility that these two algae may not be correctly identified by running the above tests alone. The work does, however, demonstrate that by subjecting each of the samples to four tests, it may be possible to identify a single species.

Possible Rules	Chaet. C	Nano. A	Nano. O	Tetra. S	Scrip. T
Biggest fluorescence change in time domain/ns	1-13	3-15	7-15	2-15	1-12
Approx. time to half 680nm initial fluorescence intensity/ns	1.5	>15	>15	9	8.5
Peak in 680nm fluorescence after 355nm treatment/J	32	8	0	8	-
Initial to Peak fluorescence % change	176	89	0	59	-
Peak to End fluorescence % change	-8	-188	-92	-68	-
Fluorescence observed below 600nm	N	N	Y	N	Y

Figure 6.27: Table showing possible rules which may allow the identification of selected algae

If the tests are run simultaneously, it may be possible to determine a single species within approximately one minute if the tests were automated giving scientists a rapid tool for determining if there are toxic algae present in an area. The biggest advantage of all of the above measurements is that they can be carried out remotely using laser radiation and a detector with a spectrograph.

This particular data is generally observed in algae which are under nutrient limited conditions. The differences between the species under normal growth conditions, however, may not be as large, making identification more difficult. The results also suggest that the system may be able to discriminate between different phyla which may be nutrient depleted in the stationary phase and those which are nutrient replete in the exponential phase. This could be used to tell if the algae are healthy and growing or dormant.

Chapter 7

Laser Marine Surface Fluorosensor Development

7.0 Introduction

The development of this sensor was undertaken to allow remote measurements to be obtained in the marine environment which would otherwise be hazardous or difficult to obtain. It may also have the potential of collecting information continuously over the area of water being monitored, rather than point measurements being taken, as is so often the case in traditional measurement instrumentation. By utilising the spectral information obtained from traditional laboratory instrumentation such as absorption and fluorescence, it was possible to optimise the design of a remote sensing laser based system.

7.1 Initial Laboratory Experiments

Chapter 5 presented results which demonstrated that sodium fluorescein has a maximum absorption around 490nm with a fluorescence emission at 514nm. When using laser technology, it was determined that an argon ion laser operating at 488nm would be the best excitation source for sodium fluorescein. The experimental data in Chapter 5 showed that the argon ion laser was also suitable for exciting the algae, producing a fluorescence emission from chlorophyll-a.

Initial experiments in the laboratory were carried out using a water-cooled argon ion laser. The laser power was set at 300mW and the output was filtered using a narrow band interference filter centred on 488nm (1 nm FWHM Ealing 35-8366) to remove any spontaneous emissions from the output and give a narrow band emission. It was then directed, using front-silvered mirrors, to the edge of an optical table before being

expanded to give a laser spot size of 100mm at a range of 3m, which gives an excitation area of $7.85 \times 10^{-3} \text{m}^2$. A sample of sodium fluorescein was then placed on the floor at the far end of the laboratory approximately 3m from the edge of the optical table, in the path of the laser beam. The fluorescein samples were placed in a 350x200x30mm foil-lined tray. By using the foil, any fluorescence from the tray was eliminated. This size of tray was chosen to ensure that all of the laser beam would strike the sample.

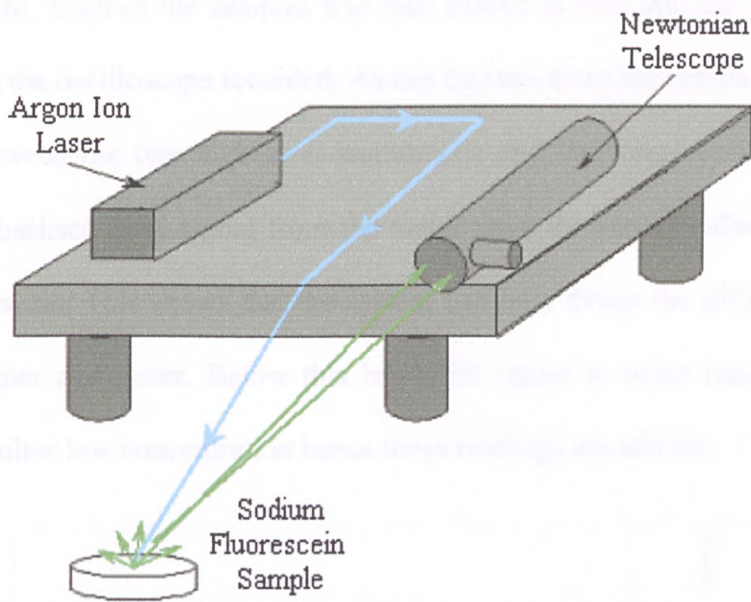


Figure 7.1: Initial Laboratory Remote Sensing Experiments

A Newtonian-type telescope was used to collect the backscattered fluorescence. This was positioned adjacent to the point where the laser beam left the optical table and was directed towards the fluorescein samples, as can be seen in figure 7.1. With the laser off, the telescope was aligned by eye to get the sample in the centre of the eyepiece image. Once this had been done the laser was switched on. Once the system had been roughly aligned and an image of the sample fluorescence observed at the telescope eyepiece on a piece of white card, a photomultiplier with an optical filter to select the fluorescein

fluorescence (Ealing 35-35-65, 514nm 8nm FWHM) was put at the eyepiece to act as a detector (Thorn Electron Tubes Ltd 9804B). Due to the sensitivity of photomultipliers to ambient visible light, the laboratory lights were turned off before the photomultiplier was switched on. This action should also reduced the amount of background light. The output from the photomultiplier was connected to an oscilloscope and the telescope further adjusted to maximise the fluorescence signal.

Varying concentrations of sodium fluorescein were then made up in the range from 10^{-1} - 10^{-6} M. Each of the samples was then placed in turn into the laser beam and the voltage on the oscilloscope recorded. As can be seen from the results in figure 7.2, a difference between the two highest concentrations and the lower concentrations was evident. The backscattered signal from the water gave the same reading as 10^{-3} M of sodium fluorescein. This shows that the system can only detect the difference between 10^{-2} M or higher and water. Below this level, the signal to noise ratio was not high enough to monitor low concentration hence these readings are similar.

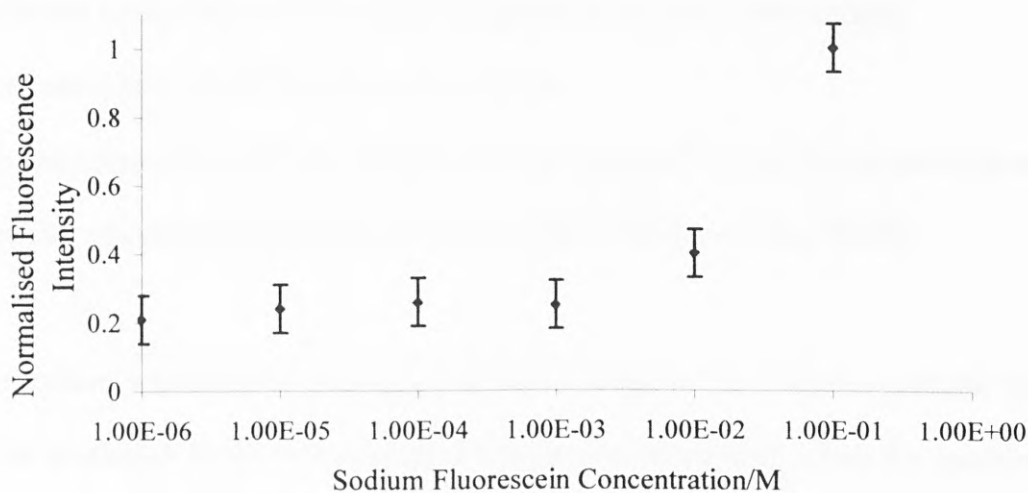


Figure 7.2: Concentration dependence of sodium fluorescein measured remotely

Although the system has been shown to be viable, the signal to noise ratio is not

adequate for monitoring low concentrations of fluorescein. This system is shown to have a detection limit of 2.29×10^{-2} M. This was calculated using the average of the 4 lowest concentration and water signals plus 3 standard deviations. This is a very high concentration for this sample which can clearly be seen by eye. To obtain lower concentration measurements, the signal processing and optical system needed to be improved.

7.2 Design of the Laser Marine Surface Fluorosensor Mk 1

The initial tests have demonstrated the potential of the fluorosensor for monitoring sodium fluorescein remotely in the laboratory. For practical use, however, the system needs to be more compact, portable and sensitive. The following specifications were used as a guide in developing the instrument.

Operating Range : 12-25m (Calculations have shown that between 12 and 25m is sufficient for operation of the system on typical North Sea research ships)

Detection Limit : 1×10^{-8} M sodium fluorescein

Physical size and weight : As compact and light as possible with the current equipment

Detector : Standard visible photomultiplier (Thorn Electron Tubes 9804B)

The system was therefore redesigned as shown in figure 7.3 to allow a portable system to be developed. In the first stage of developing the instrument, a base for mounting of the optical components was selected. For this, a 5-ply wooden base plate was selected for ease of construction. Although perhaps not the most rigid of base plates, the plywood base allowed easy alteration and modifications to the instrument setup during initial experiments. This also reduced the prototyping time as most of the work could be

carried out without the assistance of engineering equipment. The first stage was to substitute the water-cooled argon ion laser for a portable air-cooled argon ion laser. This allowed the excitation source to be run from a 13Amp/ 240Volt supply rather than the 3-phase 40Amp/215Volt water-cooled argon laser. The system was constructed using the new optical design that was developed for the instrument as can be seen in figures 7.3 a & b.

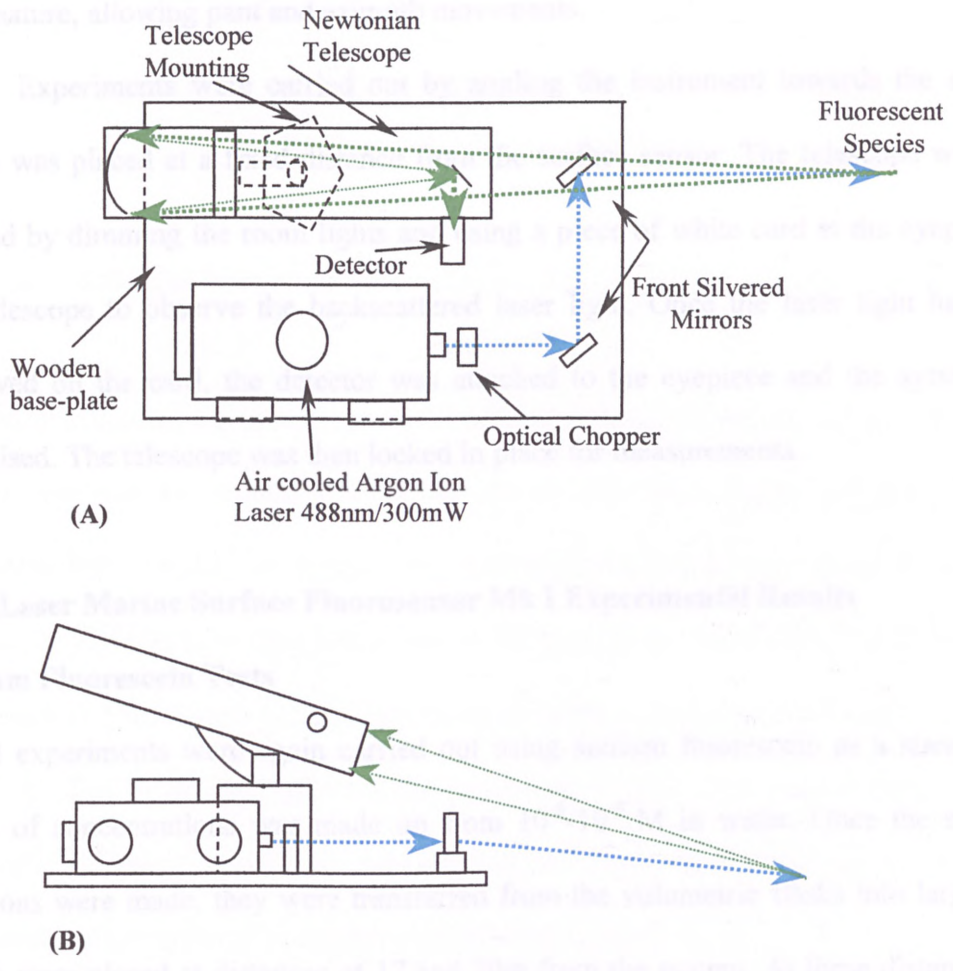


Figure 7.3: Plan (a) and Elevation (b) views of the Laser Marine Surface Fluorosensor Mk I

Once the positions had been determined, the base was marked out and cut. Each of the

components were secured to the base in turn using angled aluminium where necessary to provide locating guides. Aluminium was used to keep the overall weight of the system as low as possible.

As the system was to be deployed on marine research vessels in the North Sea, it required an enclosure to protect the laser and the optics. With this in mind, a cover for the instrument was made from reverse engineered aluminium boxes, ensuring adequate ventilation for the enclosed argon ion laser. The telescope system was then mounted on an armature, allowing pan and azimuth movements.

Experiments were carried out by angling the instrument towards the sample, which was placed at a fixed distance from the surface sensor. The telescope was then aligned by dimming the room lights and using a piece of white card at the eyepiece of the telescope to observe the backscattered laser light. Once the laser light had been observed on the card, the detector was attached to the eyepiece and the system was optimised. The telescope was then locked in place for measurements.

7.2.1 Laser Marine Surface Fluorosensor Mk I Experimental Results

Sodium Fluorescein Tests

Initial experiments were again carried out using sodium fluorescein as a standard. A range of concentrations was made up from 10^{-6} - 10^{-9} M in water. Once the standard solutions were made, they were transferred from the volumetric flasks into large trays which were placed at distances of 17 and 20m from the system. At these distances, the laser spot size was adjusted until a diameter of 100mm was obtained. The samples were then placed into the laser beam at each of the two ranges in turn and the system was allowed to settle. The photomultiplier voltage, lock-in amplifier gain and time constant were kept the same for all the samples. The returning signal was then recorded by

computer.

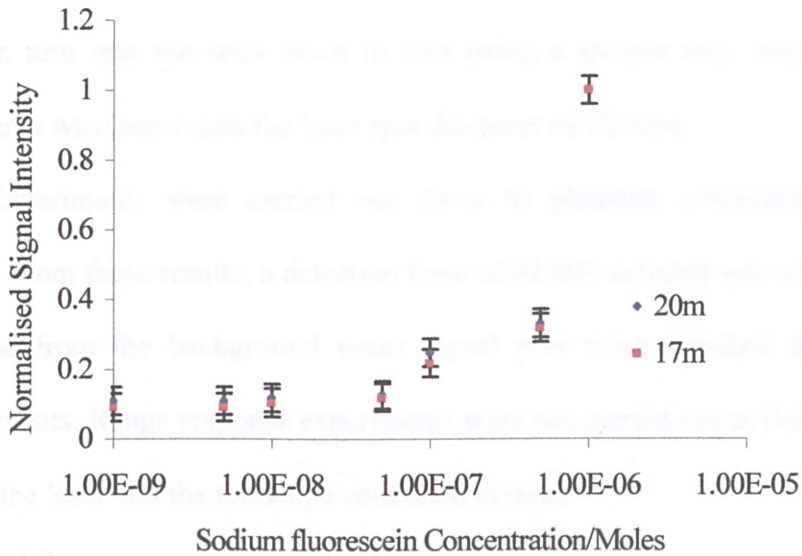


Figure 7.4: LMSF Mk I response to standard concentrations of sodium fluorescein

The performance of the system to sodium fluorescein was measured at two ranges the first at 20m and the second at 17m. As can be seen from figure 7.4, there is good agreement between the two ranges. The data is plotted on a log scale to show all the data points. By fitting an exponential line to the data, an R^2 value of 0.94 is obtained for the system at both ranges for concentrations of sodium fluorescein between 1×10^{-9} M – 1×10^{-6} M. The detection limits for the system at 17 and 20m were 2.5×10^{-7} M and 2.39×10^{-7} M respectively. This was calculated using the average of the 4 lowest concentration and water signals plus 3 standard deviations

Plankton Tests

Initial plankton tests were carried out using stationary phase *Chaetoceros* cells which were obtained from the Marine Laboratory. The stock culture was counted to obtain a cell concentration. The stock was then diluted in regular steps using Instant Ocean[®]

solution. Shown in figure 7.5 is the system response to a range of concentrations of algae, which were placed at a fixed distance of 6m. Each of the different solutions was placed in turn into the laser beam in turn using a sample tray, ensuring the sample surface area was larger than the laser spot diameter of 100mm.

Experiments were carried out down to plankton concentrations of 90,000 cells/ml. From these results, a detection limit of 42,000 cells/ml was obtained. This was calculated from the background water signal plus three standard deviations of the measurements. Range response experiments were not carried out at this stage due to the setup of the laser and the telescope collection system.

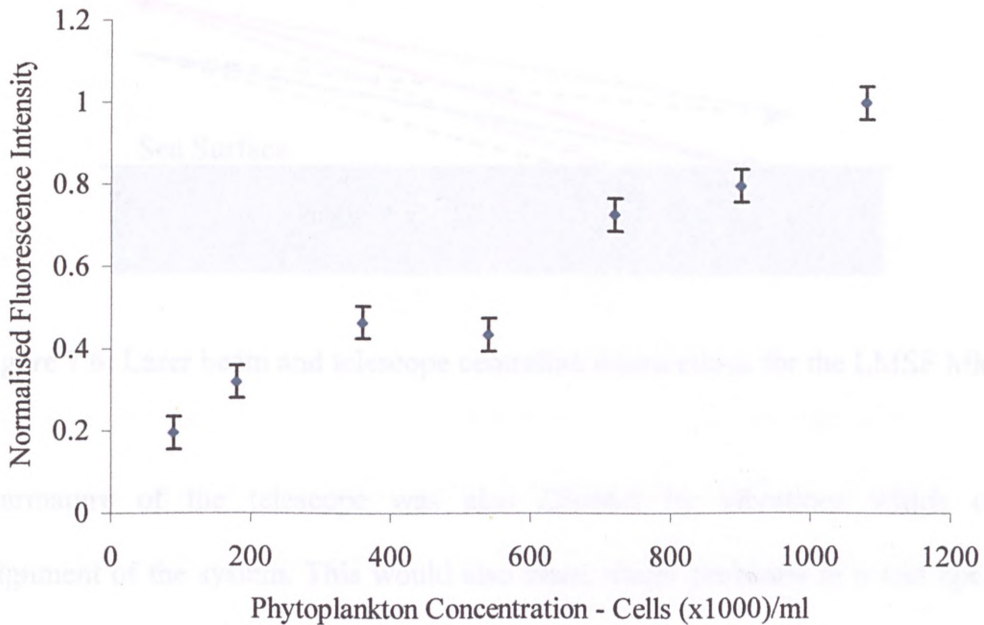


Figure 7.5: Response of the Laser Marine Surface Fluorosensor Mk I to different concentrations of *Chaetoceros* phytoplankton at a range of 6m.

7.3 Discussion: LMSF Mk I system

Although the system performed well during the initial laboratory tests, some difficulties were encountered in the laboratory. Due to the nature of the telescope mounting, every time the position of the test sample was moved, a complete alignment of the system had

to be carried out. As can be seen in figure 7.6, by having the telescope mounted on an armature, the centreline of the telescope and the laser beam intersection is fixed for a given sensor to sample distance. If that distance changes, as may be the case on a moving ship, the intersection point would vary and the intersection point would either be above or below the sea surface. To maintain the laser striking the surface and the telescope monitoring that area, the angle between the laser beam and telescope centreline needed to be adjusted.

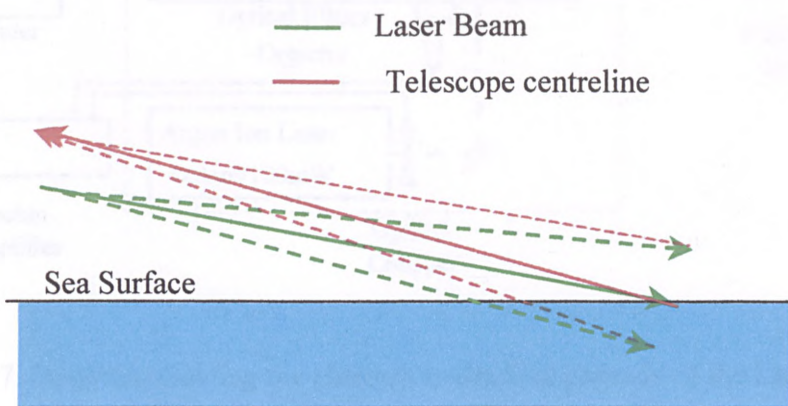


Figure 7.6: Laser beam and telescope centreline intersections for the LMSF Mk 1

The armature of the telescope was also affected by vibrations which caused misalignment of the system. This would also cause major problems in a real operating environment.

7.4 Design of the Laser Marine Surface Fluorosensor Mk II

By changing the system configuration and firing the laser beam down the longitudinal axis of the telescope, this problem was resolved. This was done by removing the telescope mounting armature and fixing the telescope onto the base of the system. Mirrors were used to steer the beam down the telescope centreline. By mounting the

telescope in this manner, the telescope was more stable whilst taking measurements. As can be seen in figure 7.7, changing the alignment of the laser to lie along the long axis of the telescope also removed the requirement for telescope alignment should the sensor to target distance change. By using this setup, vibrations experienced by the instrument should not cause mis-alignment so easily.

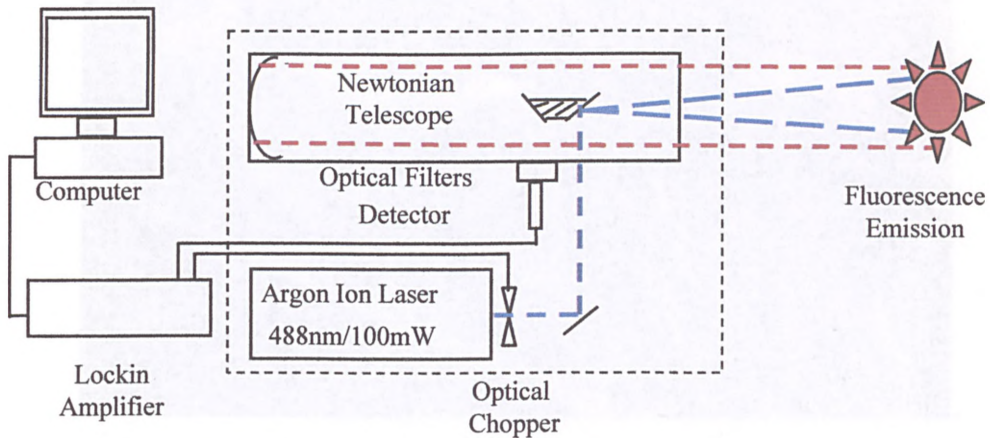


Figure 7.7: Diagram showing the changes in the first upgrade of the Laser Marine Surface Fluorosensor

To enhance the portability of the instrument, the high voltage supply for the photomultiplier and the complete optical chopper unit was incorporated into the enclosure along with the telescope. The cover was connected to earth to reduce pick-up interference on the photomultiplier signal line and also to stop the build-up of static electricity by the movement of air from the laser cooling fans. A further change was in the detector. Until now, a standard photomultiplier (Thorn Electron Tubes 9804B) was used to detect sodium fluorescein. The spectral response of the photomultiplier was, however, not suitable for detecting chlorophyll-a fluorescence which, is emitted at around 680nm. The detector was upgraded to a red sensitive photomultiplier (Thorn Electron Tubes, 9113B). This detector had a spectral response which reached out to 850nm. The manufacturer recommended voltage divider network for the

photomultiplier was used along with a negative voltage power supply. Both the high voltage and signal lines used screened coaxial cable to minimise noise in the detected signal.

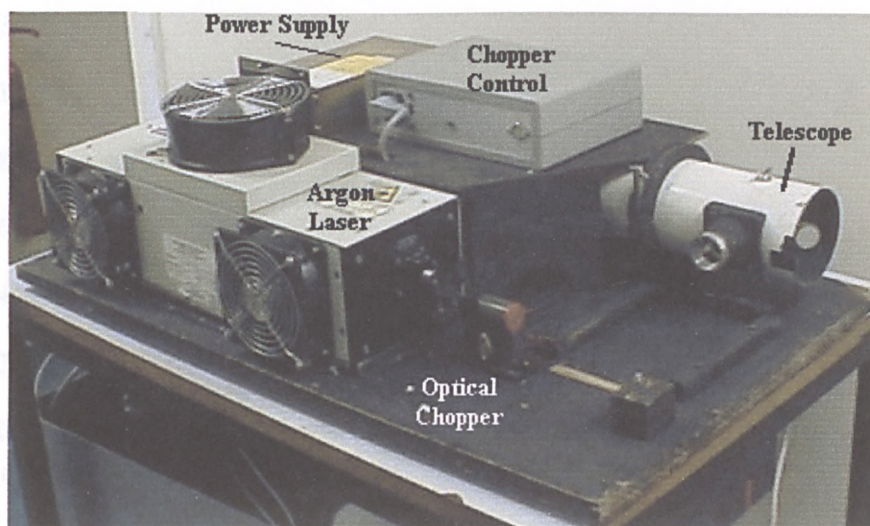


Figure 7.8: Photograph showing the telescope incorporated into the upgraded Laser Marine Surface Fluorosensor

These were soldered into a PTFE base designed for the particular photomultiplier tube then the whole assembly fixed into the custom made housing the casing of which was kept at ground. A photograph of the upgraded system is shown in figure 7.8. Note the grey box on top of the telescope which is the chopper controller, located alongside a stabilised 240vac-12vdc power supply which was used to run the photomultiplier high voltage electronics. Also shown is the ILT-5500 argon ion laser used as the excitation source for this system and the Newtonian telescope located on the instrument base.

7.4.1 Laser Marine Surface Fluorosensor Mk II Experimental Results

Sodium Fluorescein Tests

As with the first system, sodium fluorescein was again used as a standard for calibrating

the upgraded instrument. Initial experiments were carried out to determine the response of the system for different concentrations of sodium fluorescein at a fixed distance from the sensor.

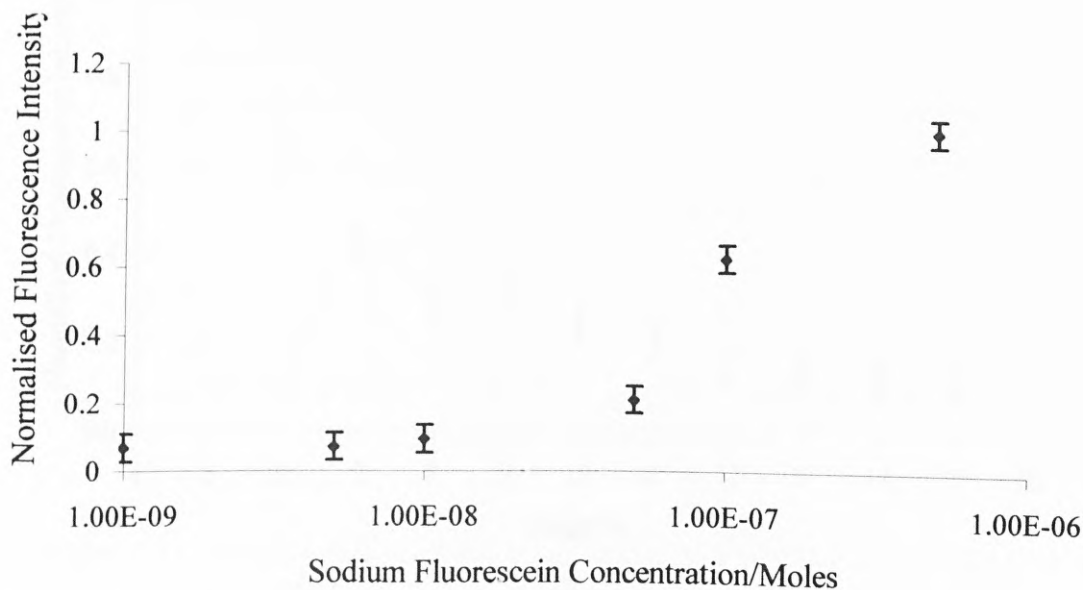


Figure 7.9: Graph showing response of the LMSF Mk II to a range of concentrations of sodium fluorescein at a fixed distance of 15m.

As can be seen in figure 7.9, the system was capable of detecting concentrations down to 1×10^{-9} M sodium fluorescein at a range of 15m. Not shown on the graph is the relative value for water. This was found experimentally as 0.03, which is approximately half the relative intensity for the weakest solution (1×10^{-9} M) of sodium fluorescein.

The detection limit for this version of the system for sodium fluorescein was found to be 2.8×10^{-8} M. This was calculated using the average of the three lowest concentration and water signals plus 3 standard deviations

Further experiments were also carried out to determine the response of the instrument at different ranges. Distances were marked out on the floor from the position of the sensor. A sample of sodium fluorescein was then made up to a concentration of

10^{-7} M and placed in a tray. The tray was placed at each of the positions in turn and the sensor was optimised before a reading was taken.

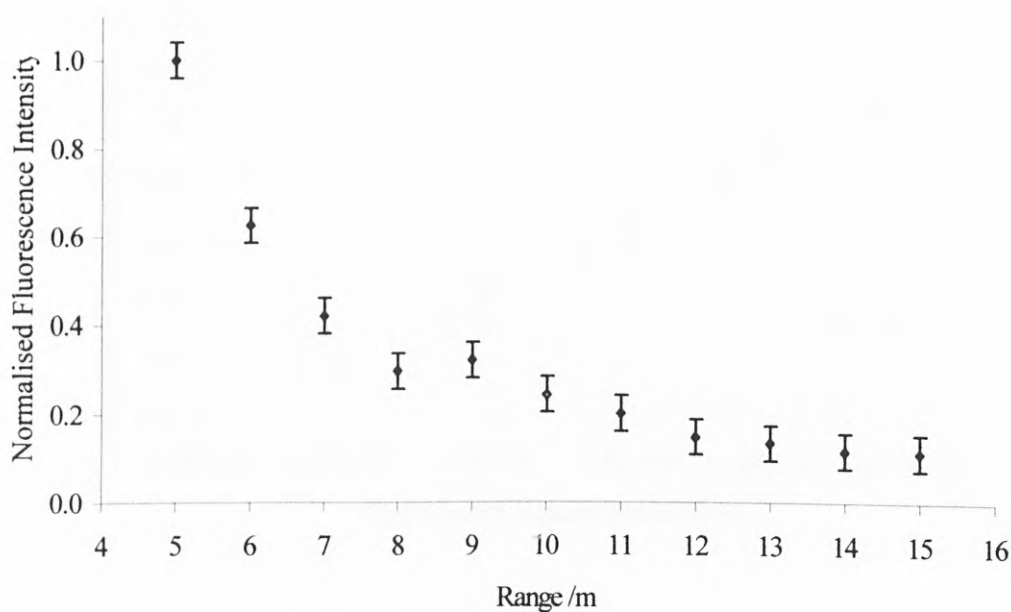


Figure 7.10: Graph showing the response of the LMSF Mk II to a 1×10^{-7} M solution of sodium fluorescein at different ranges

The results of this experiment can be seen in figure 7.10. The graph shows that the system is capable of detecting over distances ranging from 5-15m for the 10^{-7} M sodium fluorescein solution.

Plankton Tests

Changing the optical filters on the photomultiplier allowed only chlorophyll-a fluorescence to be detected. Two band pass filters (Comar 680IL25 - 680nm 10nm FWHM) were used to select the fluorescence which is centred around 680nm.

Stock samples of *Chaetoceros* were again counted before a range of concentrations were made up using Instant Ocean[®] solution. As before, each of the samples was placed into a tray which was in the path of the laser beam and fluorescence

measurements were taken.

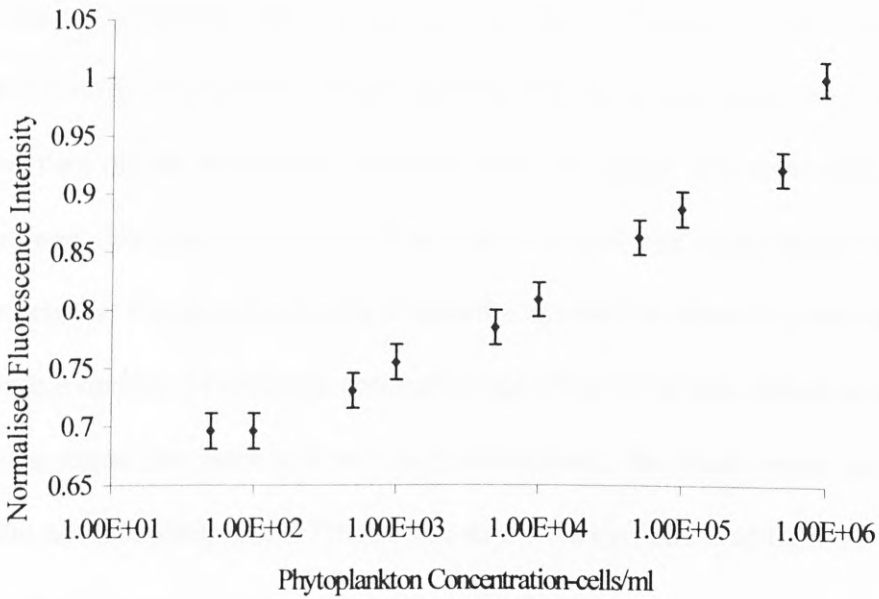


Figure 7.11: Response of the LMSF Mk II response to various concentrations of phytoplankton at a fixed range of 15m.

As can be seen in figure 7.11, the system is capable of detecting down to 100 cells/ml at a range of 15m. These results show a 400-fold improvement over the detection limit of the LMSF Mk I system, which can be seen in figure 7.5.

Hydrocarbon Tests

As the system was designed to be multifunctional in monitoring a number of waterborne species, experiments were also carried out using hydrocarbons. Different concentrations of crude, Gulfaks oil, at a fixed distance of 3m, were used to determine the response of the system to hydrocarbons. It was thought that as an argon ion laser was being used as the excitation source, the fluorescence from the oil would be weaker than if an ultraviolet laser source was used, and hence the range of operation would be reduced. A surface sample of oil at a concentration of $14\mu\text{m}^{-2}$ was used as the bottom range of

concentrations. Although μm^{-2} is not a standard unit for representing oil concentrations in water, these experiments were carried out with the oil floating on the water surface and hence it is difficult to give a volume concentration as is more commonly used. This sample was then placed at different distances from the sensor and measurements were taken. This was also repeated using a clean water sample. The range where the largest difference between the two signals was obtained was used for observing the response of the system to a number of different concentrations of oil. This was found to be around 3m using the argon ion laser system. Once determined, the blank water sample was placed at 3m and a reading taken. This served as the background reading from the water sample. Surface oil concentrations were then obtained by dispensing $2\mu\text{l}$ quantities of oil from an analytical syringe (SGE $5\mu\text{l}$ analytical syringe) onto a water surface measuring $0.46\text{m} \times 0.30\text{m}$.

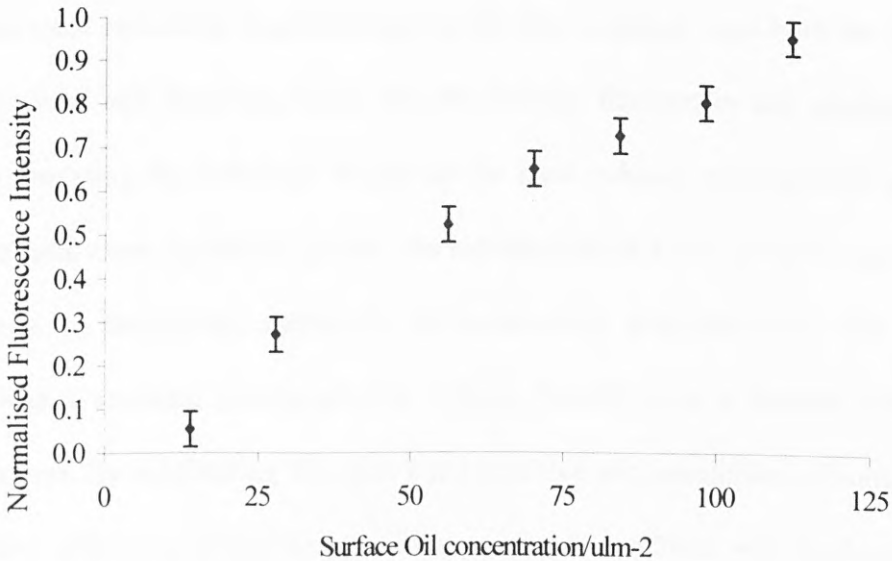


Figure 7.12: Response of the LMSF Mk II to various surface concentrations of oil at a fixed range of 3m.

The surface tension of the oil allowed a droplet to be formed on the needle tip which was then touched on the surface of the water, depositing a thin layer. Once the oil had spread out, the system was allowed to settle and a measurement was taken. This was repeated until a range of measurements had been obtained. The surface oil concentration was then calculated using the known surface area of the tank. It can be seen in figure 7.12 that the system is capable of detecting down to at least $14\mu\text{m}^{-2}$ of oil on a water surface at a range of 3m giving a detection limit of $9.6\mu\text{m}^{-2}$ for Gulfaks oil. This was calculated using the average of the water signals plus 3 standard deviations

7.5 Discussion: LMSF Mk II System

The improved design of the LMSF Mk II instrument has better mechanical properties and has been shown to produce an improvement on a number of measurement aspects. One of the most noticeable improvements in the data collected were both the increased operating range and detection limits for the sodium fluorescein and phytoplankton. Although mounting the telescope firmly on the base reduced misalignment problems and hence gave more repeatable results, the introduction of a new detector accounts for the increase in sensitivity, especially for monitoring phytoplankton. The original detector was a standard photomultiplier (Thorn 9804B) with a limited wavelength response range. By substituting this with a red sensitive photomultiplier (Thorn 9113B), the quantum efficiency of the detector at approximately 680nm was increased by 16 times.

The system was also shown to detect oil on a water surface. The range of the system was limited however, due to the inefficiency in exciting the oil using a 100mm spot size beyond 3m. By reducing the spot size and hence increasing the power density, it should be possible to induce a measurable fluorescence at increased ranges with the

argon laser.

7.6 Design of the Laser Marine Surface Fluorosensor Mk III

Although there was an improvement in the Mk II instrument, the overall size of the sensor was determined by the length of the Newtonian telescope used and the size of the laser used. By changing the telescope configuration and the size of the laser, it was possible to reduce the overall size of the instrument, making it more compact and portable. The major changes were in the telescope and the laser system used. The original 100mm diameter Newtonian telescope was replaced by a 300mm Cassegrain-type telescope. Originally the system was constructed for use with a diode pumped laser (Continuum EPO-5000) which produced 355nm laser radiation. Due to the heavy use of the diode pumped Nd:YAG by other laser users within the laboratory, an alternative laser source was required for the Mk III system. A smaller argon ion laser (Omnichrome 532 AP, 60mW) was incorporated into the system as a replacement for the EPO-5000 laser.

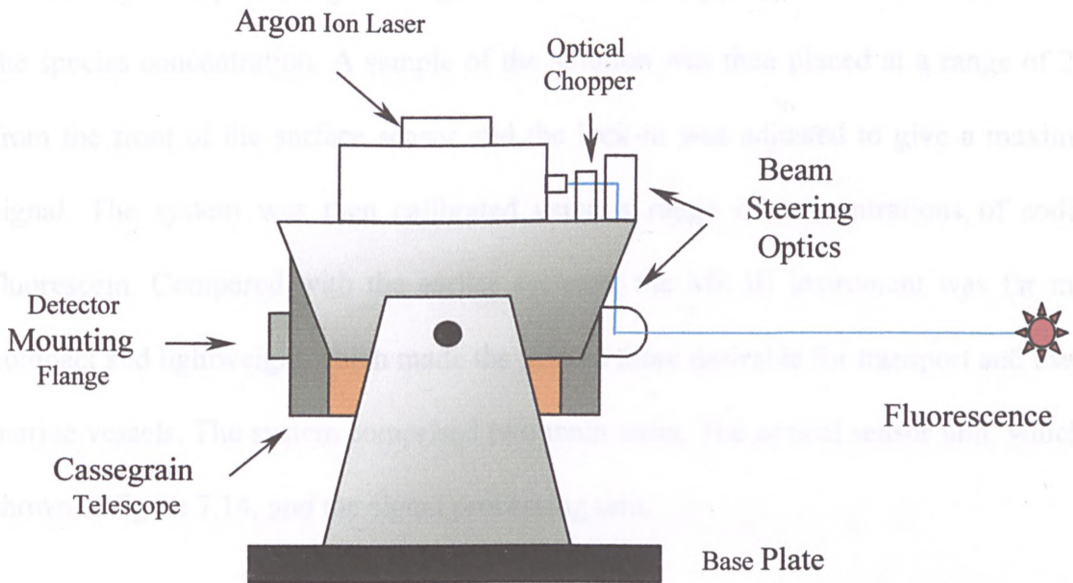


Figure 7.13: Diagram of the Laser Marine Surface Fluorosensor Mk III

This was used for all further experiments using the new version of the Laser Marine Surface Fluorosensor. The Cassegrain telescope was mounted in a jig which allowed movement in azimuth. The laser was mounted on the same jig, on top of the telescopes can be seen in figure 7.13. Adjustable mirrors were used to steer the laser beam down onto the centre line of the telescope. A custom-made optical housing, containing another adjustable mirror was fixed onto the centre of the telescope. The laser was then switched on at low power and directed to a target 21m from the front of the telescope. The position of the laser spot was observed from the back of the telescope with an eyepiece. A piece of white card was used to display the image of the laser light being collected by the telescope. Adjustments were made to both steering mirrors to position the laser spot in roughly the centre of the telescope image. Once roughly aligned, a photomultiplier tube was attached to the eyepiece port of the telescope and further adjustments were made to the mirrors to maximise the backscattered laser light signal. The filters for selecting sodium fluorescein fluorescence were then introduced into the detector. The output from the photomultiplier was again treated in the same way as the previous system, producing a voltage on the lock-in amplifier which could be related to the species concentration. A sample of the solution was then placed at a range of 20m from the front of the surface sensor and the lock-in was adjusted to give a maximum signal. The system was then calibrated using a range of concentrations of sodium fluorescein. Compared with the earlier systems, the Mk III instrument was far more compact and lightweight which made the system more desirable for transport and use on marine vessels. The system comprised two main units. The optical sensor unit, which is shown in figure 7.14, and the signal processing unit.

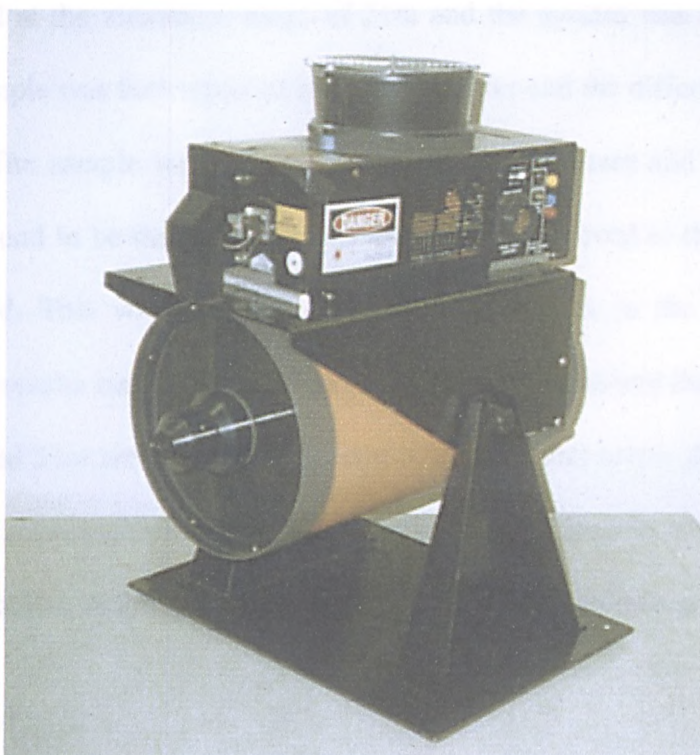


Figure 7.14: Photograph of the Laser Marine Surface Fluorosensor Mk III

The compact size and separate optical and electronic units allow easier placement on vessels which are designed to make the most of available space.

7.6.1 Experimental Results Using the LMSF Mk III

Sodium Fluorescein Tests

Initial experiments were carried out to determine the range response of the instrument. In this system, the laser beam was not expanded to 100mm as a lower power laser was being used. It was decided to leave the laser beam non-diverged to maximise the operating range for monitoring sodium fluorescein at 1×10^{-9} M. A spot size of 5mm was obtained at 20m from the sensor, giving an excitation area of 1.96×10^{-5} m².

The system was initialised and target distances were measured out and marked on the ground in 3m intervals from 3-21m. A 1×10^{-7} M sample of sodium fluorescein

was then placed at the maximum range of 21m and the system was optimised on the sample. The sample was then replaced by distilled water and the difference between the signals noted. The sample was then placed back into the beam and the signal noted again; it was found to be the same. The sample was then moved to the 18m mark and the signal noted. This was repeated until all the distances in the range had been completed. The results can be seen in figure 7.15. It should be noted that only the results between 12m and 21m are shown. This is due to the fact that below the 12m mark, the signal from the photomultiplier caused an overload in the lock-in amplifier. This was not seen as a problem as the system was designed to be operated at a greater distance.

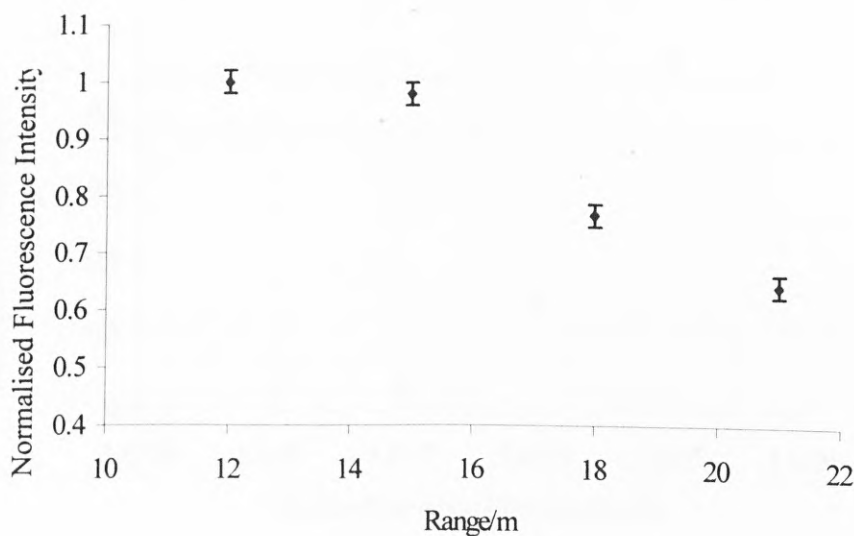


Figure 7.15: Range response of the LMSF Mk III for a standard solution of sodium fluorescein (10^{-7} M)

Further experiments were then carried out to determine the response of the system to various concentrations of sodium fluorescein at a fixed range of 21.5m.

Standard samples in the range of 1×10^{-9} – 1×10^{-5} M were placed at 21.5m approximately 0.20m apart. The system was switched on, directed towards the most

concentrated sample and optimised to produce a maximum signal from the lock-in amplifier without causing an overload condition. Once this had been achieved, the lock-in was connected to a computer to collect the fluorescence data. For each sample, the sensor was allowed to settle before the measurements were taken. As the system was run continuously and measurements were taken every second, a robust average of the signal can be obtained in a very short time. The results of this experiment could be seen in figures 7.16. The results are plotted on a logarithmic scale to show each of the measurement points. A linear relationship was observed for concentration dependence against fluorescence intensity.

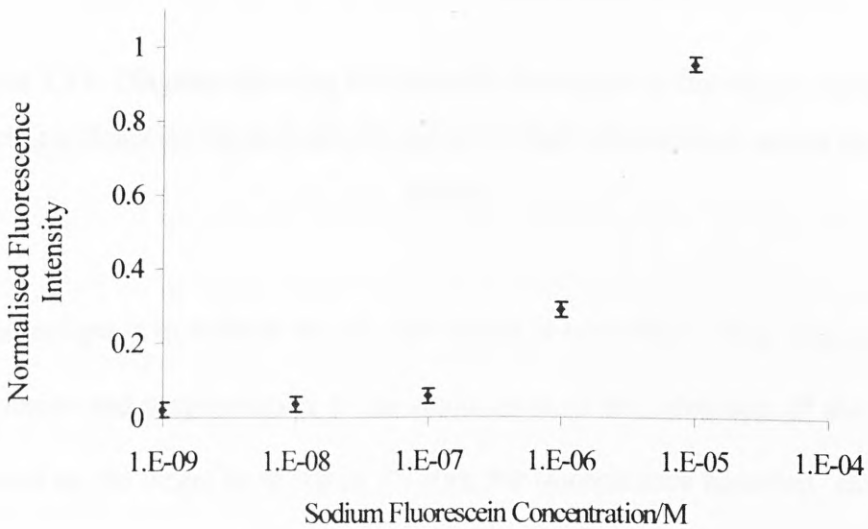


Figure 7.16: Response of LMSF Mk III to various concentrations of sodium fluorescein at a distance of 21.5m

From the data it was possible to determine the detection limit of the system. This was found to be 2.19×10^{-7} M at a range of 21.5m. This was calculated using the average of the 3 lowest concentration and water signals plus 3 standard deviations.

7.6.2 Detector Response to Fluorescence Along the Axes of the Telescope.

A small laser spot was used to excite a fluorescent targets placed at regular interval on the laboratory floor at a fixed distance as can be seen in figure 7.17.

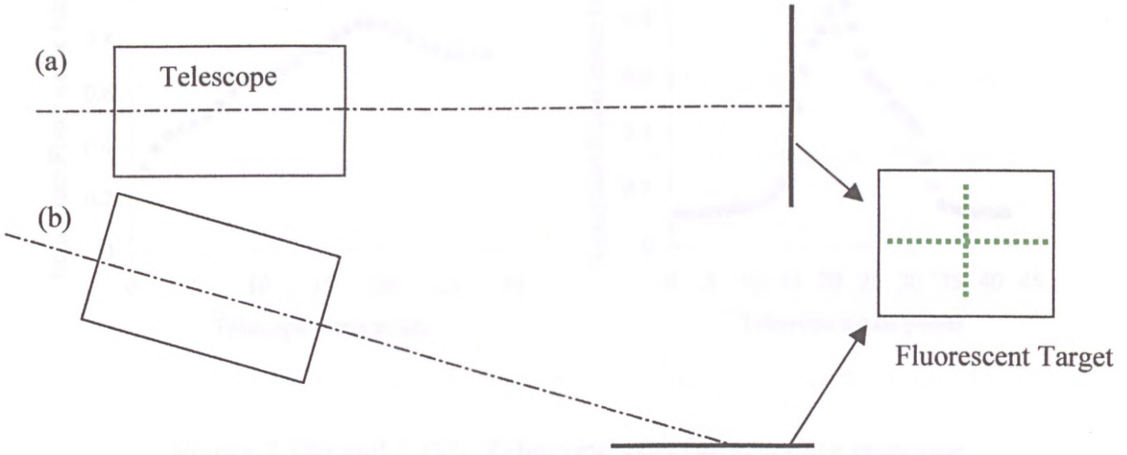


Figure 7.17: Diagram showing two possible telescope-to-the target orientations producing a Gaussian (a) and non-Gaussian (b) light distribution across the primary mirror.

When a telescope is in normal use (a), the object is normally a large distance from the primary mirror and perpendicular to the major axes of the telescope. If the laser beam was scanned on the target as in figure 7.17(a), the fluorescence recorded should follow a normal Gaussian distribution in both the x and y axes. The case for the laser marine surface fluorosensor however is different as can be seen in figure 7.17(b). This produces a distorted distribution in the fluorescence signal on the primary mirror which as can be seen in figures 7.18a and 7.18b, does not use the whole mirror to collect the backscattered fluorescence. This reduces the collected signal and hence the efficiency of the system. By carrying out this experiment it has shown that collection efficiency of the system can be improved by increasing the width of the laser beam in the x-axes by

100% before it strikes the sea surface. This would maximise the amount of fluorescence on the collection area of the telescope, thus improving the signal.

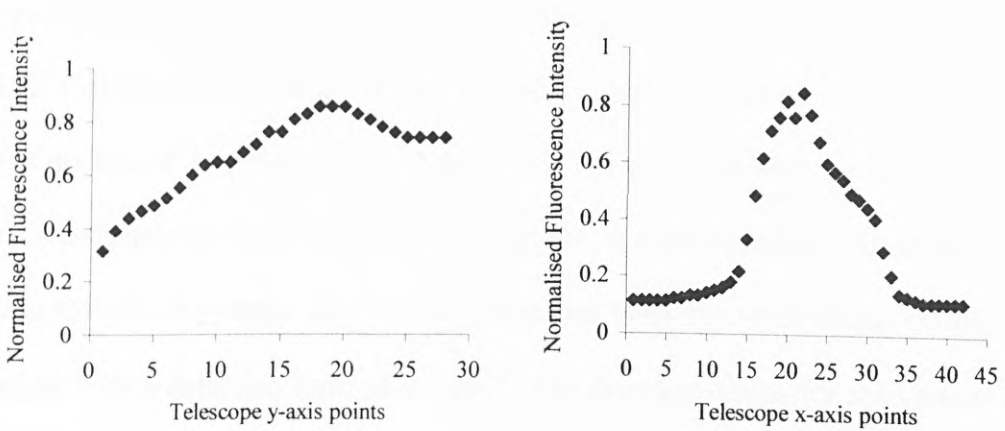


Figure 7.18a and 7.18b: Telescope axes fluorescence response

7.7 Discussion: LMSF Mk III System

The design aims of the system were achieved resulting in a compact sensor system. Initial laboratory trials were carried out using sodium fluorescein at ranges of up to 21m. Measurements beyond this range were not possible due to the limits of the available facilities. The system was shown to detect down to 1×10^{-9} M solutions of fluorescein at this range. The detection limit was found to be 2.19×10^{-7} M. The system range was increased to 21.5m compared to the Mk II version of the system. The detection limit however was reduced by an order back to similar levels shown with the Mk I system. Due to time limitations, experiments using phytoplankton and oil were not carried out in the laboratory.

7.9 Summary

The development of a laser-based marine surface sensor has been described. A concept has been taken from initial laboratory experiments to the development of a system

capable of operating under controlled conditions in the laboratory. By altering and improving the design of the instrument, the detection limits of the system have been improved. For sodium fluorescein, the detection limit has been improved from 2.8×10^{-7} M @ 15m to 2.19×10^{-7} M @ 21.5m. The Mk II version of the instrument was shown to have the lowest detection limit of 2.8×10^{-8} M. The detection limit for the phytoplankton has been improved from 42,000 cells/ml @ 6m to approximately 500 cells/ml @ 15m using the Mk II system. The Mk II system has been shown to detect oil on a water surface with a detection limit of $9.6 \mu\text{m}^{-2}$. The detection limits for the various species are summarised in figure 7.19 below with the range the measurements took place at shown in parenthesis.

	Sodium Fluorescein /M	Phytoplankton /Cellsml ⁻¹	Surface Oil / μm^{-2}
Mk I system	2.39×10^{-7} (20m)	42000 (6m)	-
Mk II system	2.8×10^{-8} (15m)	100 (15m)	9.6 (3m)
Mk III system	2.19×10^{-7} (20)	-	-
EPO-5000 system	-	-	1 (12m)

Figure 7.19: Summary of the detection limits for the different versions of the surface sensor system

These results suggest that the Mk II version of the system was the best instrument. It should however be noted that the Mk III version of the instrument was not optimised as it was constructed purely for a sea trial on board the *Toisa Invincible*.

The changes in the instrument design have however progressively reduced the overall size of the instrument from 1.5m x 0.5m x 0.3m to 0.5m x 0.4m x 0.6m making

it very portable. There has also been a reduction in the possible manufacturing costs by reducing the size of the laser being used. Although the detection limits are not as low as the conventional instruments, these measurements can be carried out on the sea surface where other instruments have difficulty.

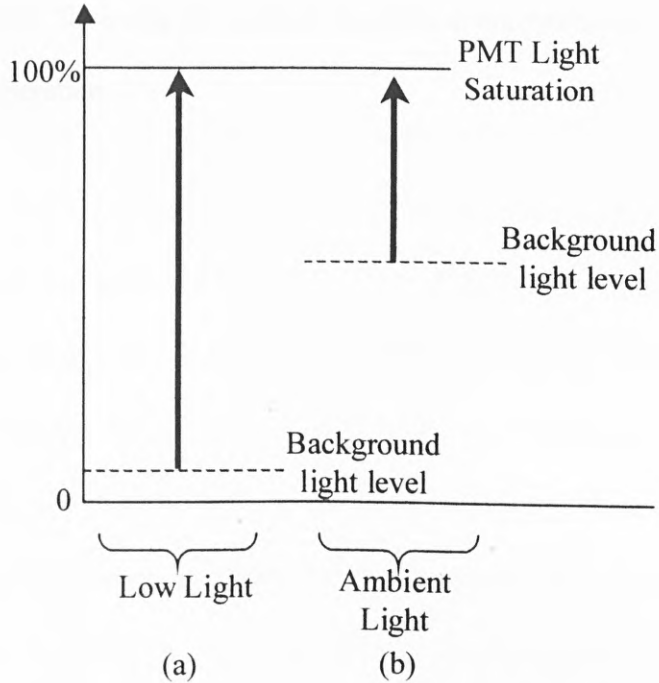


Figure 7.20 Diagram showing the reduction in the signal under low (a) and ambient (b) light conditions

One problem that has been encountered during use of all the instruments, is the decrease of the signal to noise ratio under ambient light conditions. This is due to the increase in the background light level at on the photomultiplier. An illustration of this can be seen in figure 7.20. Under low light conditions, the background light level is very low allowing a small signal to be detected. This gives a high signal to noise ratio as can be seen in figure 7.20a. If the background light level however is increased by working under ambient laboratory lighting, the background light level in the photomultiplier increases thus reducing the signal which can be detected and hence

reducing the signal to noise ratio as can be seen in figure 7.20b. This limits the minimum concentration of pollutant that can be measured. The signal from a low concentration gets “lost” in the background noise. This is the most restrictive factor of the instrument. All the experiments above have been carried out during the evening under low light conditions. By using the current operational configuration, the system is restricted to low light operation.

Chapter 8

Laser Marine Surface Fluorosensor and Laser Fluorimeter Sea Trials

8.0 Introduction

In order to assess the practicality of the Laser Marine Surface Fluorosensor and to determine its response in real conditions two major sea trials were carried out during the project using two different versions of the LMSF. The first sea trial was carried out onboard the charter vessel “Lowland Search”, which was mobilised by the Scottish Office Agriculture, Environmental and Fisheries Department (SOAEFD) Marine Laboratory, Aberdeen (now Fishery Research Services, Marine Laboratory, Aberdeen) to study hydrocarbons in the North Sea in June 1996. The second trip was on board the oil rig supply boat “*Toisa Invincible*” during normal operations west of the Shetland Isles in October 1998 whilst on station around the “*Sovereign Explorer*”, semi-submersible, oil installation. This trip was commissioned by Conoco to study hydrocarbons in this area. In addition to these another trip was undertaken in June 1998 in which the laser fluorimeter was tested alongside traditional flow cell fluorimeters on the Fishery Research Vessel (FRV) “*Clupea*”. This sea trial was for monitoring phytoplankton in Scapa Flow in the Orkney Islands and some Voes in the Shetland Islands.

8.1 LMSF Mk I Sea Trials “Lowland Searcher” June 1996

This sea trial of the Mk I version of the Laser Marine Surface Fluorosensor was carried out over a 10-day period in June 1996. A team from the Marine Laboratory in Aberdeen

was involved in taking water samples for hydrocarbon analysis and plankton trawls for assessing the impact of hydrocarbons on fish larvae. The trip started out north west of the Shetland Isles moving in an easterly direction toward the coast of Norway. The actual route of the ship over the ten days is shown in figure 8.1. This route takes the ship through most of the major oil fields in North Sea, allowing a coarse distribution of the hydrocarbon concentrations to be produced. As can be seen from the map, there were only 33 stations monitored in an area of approximately 65,000 square miles. Although this in itself provides invaluable data, it can be seen that the data set was very limited.

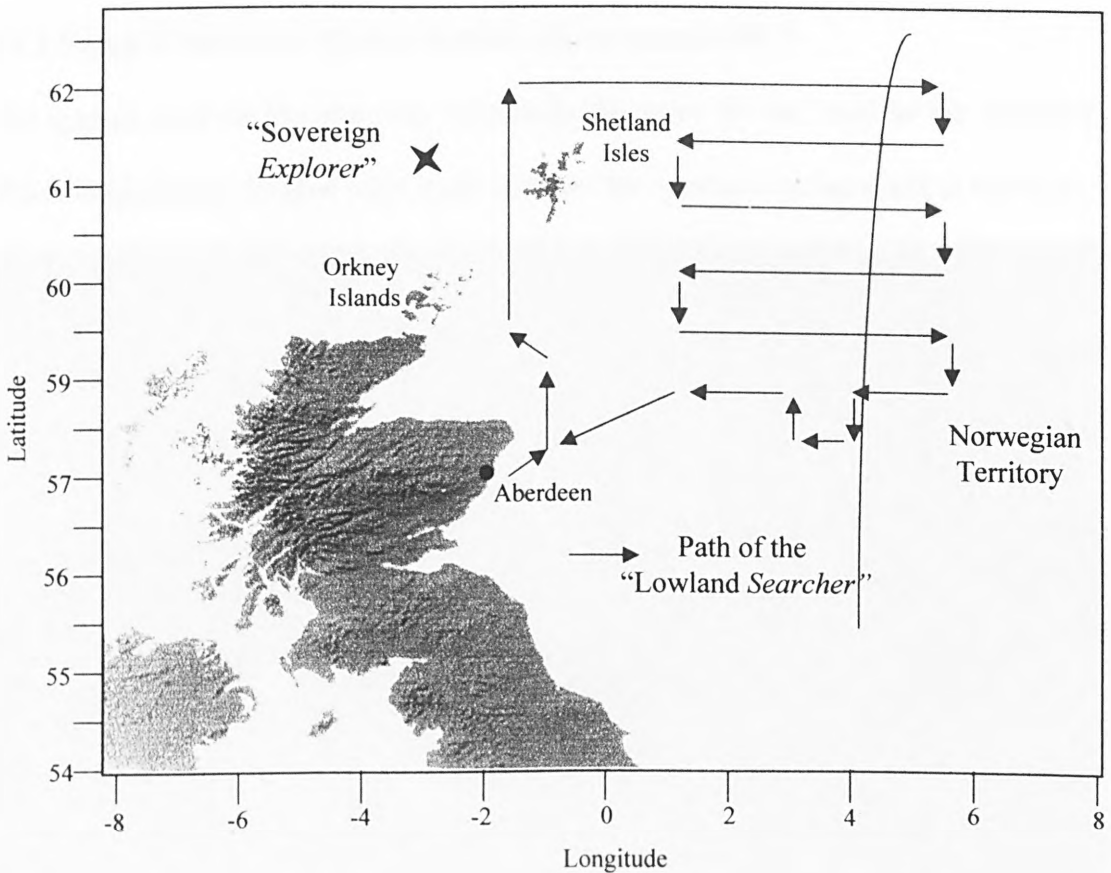


Figure 8.1: Map showing the route of the “Lowland Searcher” during sea trials of the Mk I instrument during June 1996 and the location of the “Sovereign Explorer” during 1998 Mk III sea trials

To obtain an accurate picture of the distribution of hydrocarbons, many more samples would be require monitoring. In practical terms however, this would require ships to spend more time at sea, and the cost would become prohibitively expensive. This is one of the main reasons for the development of the Laser Marine Surface Fluorosensor, which may be able to take measurements continuously along the path of the research vessel thus allowing a higher resolution map of the distribution of hydrocarbons to be obtained. This first sea trial was used to try out a laboratory version of the system for performing this task.

8.1.1 Setup of the Laser Marine Surface Fluorosensor Mk I

The system used on the ship was essentially the same as that used in the laboratory. Minor engineering changes were made to allow the system to be mounted in the ship.

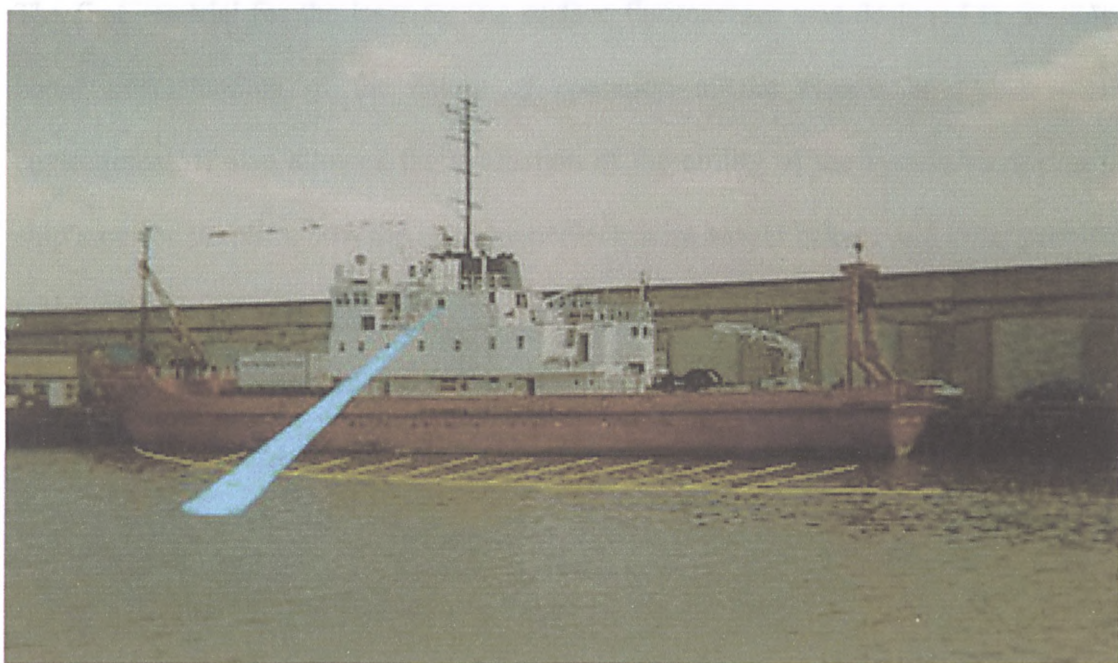


Figure 8.2: Photograph of the “*Lowland Searcher*” showing the location of the Laser Marine Surface Fluorosensor Mk I during sea trials.

The LMSF was set-up just behind the bridge of the ship in an unused radio room located approximately 4m above the sea surface. With the range of the system taken as 7m which is 50% of the operating range for detecting fluorescein, the distance of the laser spot from the side of the ship was calculated to be 5.7m. Due to the size, design and speed of the ship, this distance was adequate for clearing the bow wave and hence sampling undisturbed water. The position of the sensor in relation to the research vessel can be seen in figure 8.2. An additional overlaying illustration in figure 8.2 shows the approximate path of the laser beam along with the crosshatched area relating to the position of the ships bow wave whilst in motion. With the laser aimed out past the bow wave, the sensor could measure undisturbed water.

8.1.2 Results

The first sea trial for the laser marine surface fluorosensor was designed to provide a better understanding of the nature of operation of the system in a real marine environment. It also allowed the evaluation of the ability of the system to run on the ship's power supplies, how the instrument electronics would behave and other problems which could arise in a working environment.

The first of the challenges encountered on the ship was the positioning of the system within the ship's superstructure. Although an old radio room had been allocated for the trip, the ability to "fire" the laser from this room required minor engineering work to be carried out. The system had to be elevated and angled to allow the laser beam to be fired through a window out onto the sea surface beyond the ship's bow wave. This, however, was overcome by building a frame for the system and securing it fast within the radio room. Once this had been carried out, the system could be mounted in the frame to enable measurements to be taken. Once mounted, the laser part of the

sensor was activated to determine if the ships power supply could handle the start-up current surge. This was not found to be a problem. It was, however, noted that the laser power level was varying with time and it was therefore allowed to settle before any further parts of the sensor were switched on. Once the laser had warmed up, the detection system was activated. With the laser beam on the surface and the detection filters set to the laser wavelength, detection of the backscattered laser light was relatively easy. The lock-in amplifier was set to an integration time of 3 seconds which would normally allow a relatively stable signal to be obtained in the laboratory. The backscattered light from the sea surface was detected but was found to vary with time. Although this was expected when working on a moving ship on the sea surface, the changes in the backscattered were very large. The variation in the signal was equivalent to a change in fluorescence from over 4 orders of magnitude of fluorescein in under two minutes. This change in the backscattered intensity was also very periodic as can be seen in figure 8.3.

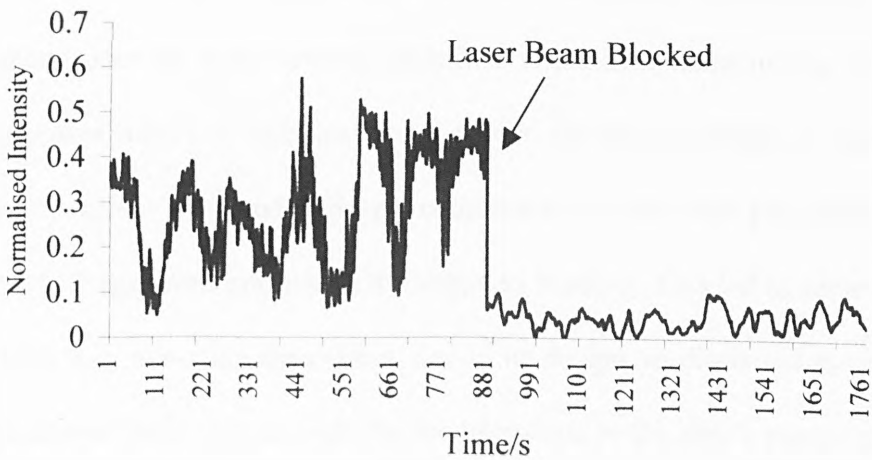


Figure 8.3: Trace showing backscattered laser light signal from the sea surface obtained during the sea trials of the LMSF Mk1

It was also noted that the laser cooling fans were experiencing a change in sound consistent with a reduction in power to the laser. At this point it was thought that the ship's power may be varying enough to cause disruption of the laser marine surface fluorosensor. Figure 8.3 is the trace obtained from monitoring the backscattered laser radiation from the sea surface and also with the laser beam blocked. For up to 900 seconds, the laser beam was directed onto the sea surface. After this time, the laser beam was blocked. When the laser beam was on the sea surface, there was a large variation in the signal, even with a 3 second integration time on the lock-in amplifier. When the laser beam was blocked at 897 seconds, the signal intensity decreased as would be expected. There was still some noise in the signal, which should be almost a flat line. This suggests that the optical section of the instrument was introducing large variations in the signal.

8.2 Discussion: June 1996 Sea Trial

The variations observed in the signal could be due to a number of influences. The three main possible causes are wave motion, variations in the laser intensity due to variation in the ship's power supply or electrical noise. Due to the sea conditions at the time, it is thought that the effect was produced by a combination of the three possibilities. There was a relatively large swell into which the ship was heading. This led to some rolling of the ship which may mis-align the system, due to its design, as discussed in section 7.3. The sea conditions could also account for the variations in the ship's power supply due to the varying load on the engines.

With all these problems, it was impossible to detect any surface species. What has been shown, however, is that the laser light hitting the sea surface was detected using the telescope arrangement and the lock in amplifier detection electronics.

Although the trip did not provide any information on hydrocarbon contamination on the sea surface, it did provide a vast amount of experience and information concerning the engineering of the system, the interaction of the electronics and the ships power supplies, and the deployment of such a system in a real working environment.

8.3 Sea Trials of the Laser Fluorimeter

During a sea trial in June 1998, a portable version of the laser fluorimeter, detailed in chapter 5.5 was tested onboard the fishery research vessel “FRV Clupea”. The research trip was carried out in the waters in and around the Orkney and Shetland Islands. This trip forms part of Fishery Research Services, Toxic Algal Monitoring program.

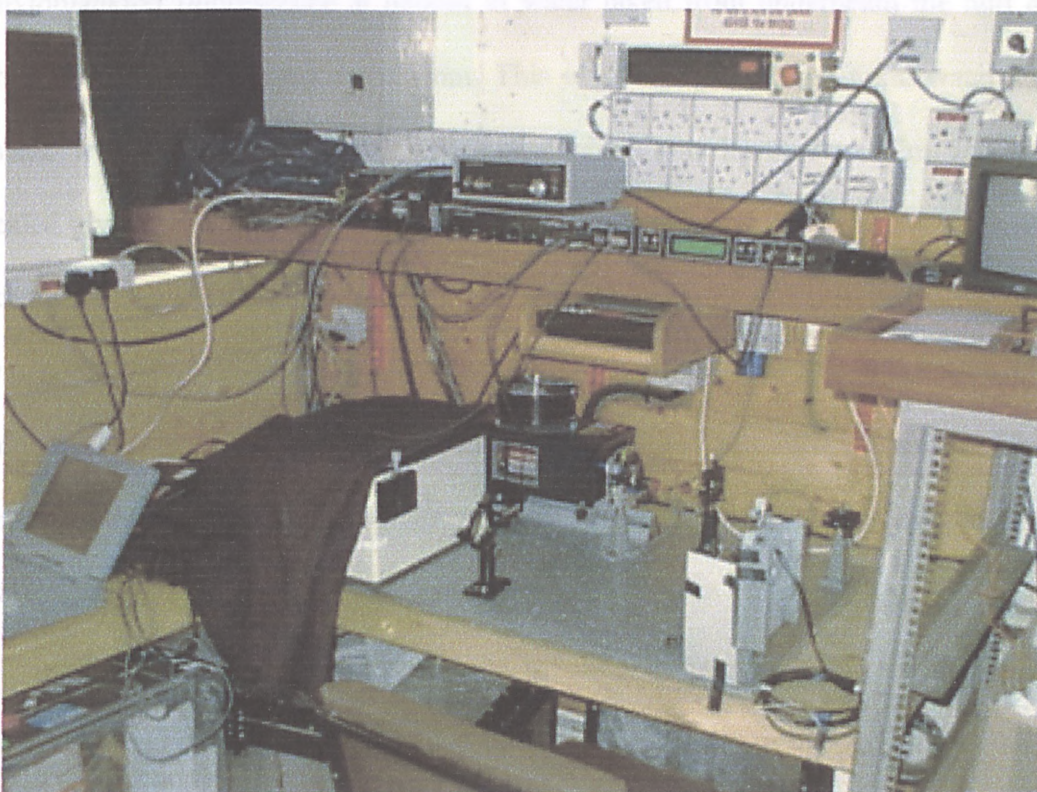


Figure 8.4: Photograph of the Laser Fluorimeter located in the underwater camera room onboard “FRV Clupea”

This was seen as an opportunity to test the laser fluorimeter system against standard

fluorescence measurements being carried out by the Marine Laboratory. The system used was identical to the bench-top system shown in figure 5.11 with the only difference being that the components were mounted on a lightweight aluminium optical table as can be seen in figure 8.4. During operation of the laser fluorimeter, this room was kept in the dark using blackout blinds which helped reduce the background light levels and hence increase the signal to noise ratio.

8.3.1 Comparison of Fluorescence Measurements

The Marine Laboratory carried out two main measurements which could be related back to the laser fluorimeter. A standard flow cell fluorimeter was used to monitor phytoplankton fluorescence at 680nm in water taken from underneath the hull of the ship at a depth of approximately 6m. This is known as the non-toxic water supply. Water was also collected from a hose-pipe which was lowered to 12m. It was then sealed giving an average fluorescence of the first 12 m of water. The laser fluorimeter scanned a water sample from the non-toxic water supply and a sample taken from the water surface for measuring phytoplankton fluorescence. The advantage of using the laser fluorimeter is that a number of wavelengths can be scanned relatively quickly. The more traditional techniques being used have a fixed emission wavelength filter at 680nm. With the traditional techniques, it is impossible to give an indication of the type of phytoplankton present. It could be a diatom, flagellate, microflagellate, dinoflagellate, blue-green algae etc. The only way of determine the type of algae at present, is to look at a sample under a microscope. With the laser fluorimeter, it may be possible to give an early indication of the type of plankton by differences in the fluorescence spectrum. During this trip there were two main types of plankton expected, diatoms in the open waters and flagellates in inshore waters. The fluorescence spectra of

these two species was expected to be different with the flagellates having more fluorescent accessory pigments below 680nm compared to the diatoms which have in general very low fluorescence activity below 680nm.

Shown in figure 8.5 is a comparison of the standard fluorescence measurements taken using the flow cell system on board the boat compared with the relative laser chlorophyll-a signal which was corrected to the water Raman scattering peak intensity. As can be seen in the plot, there is a good comparison between the flow cell measurements and those of the laser fluorimeter.

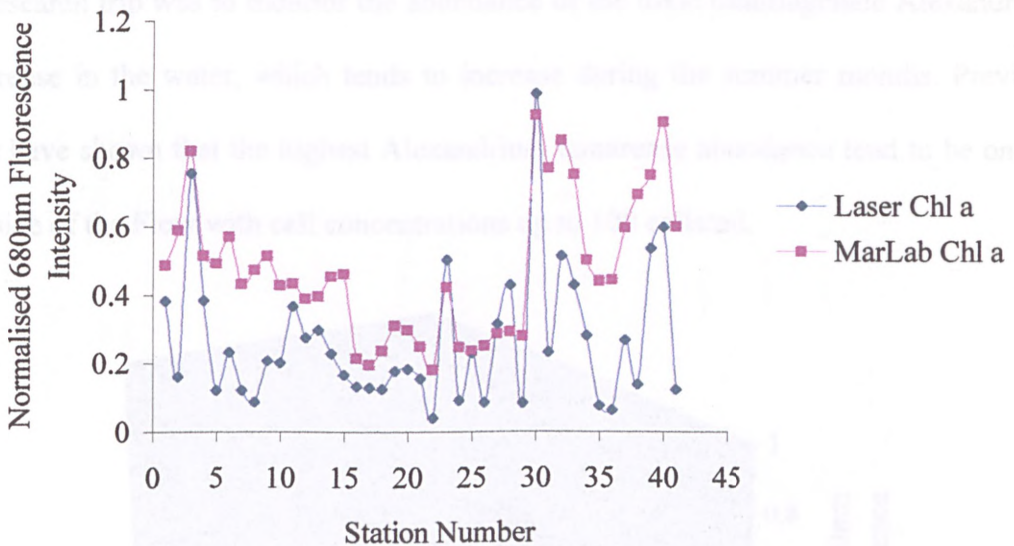


Figure 8.5: Comparison of a traditional flow cell fluorimeter (Marlab Chl-a) against a laser based fluorimeter (Laser Chl-a) monitoring phytoplankton fluorescence at 680nm.

Although the measurements are not exactly the same between the two systems, the trends in the signals are very much alike as can be seen from the lines drawn in figure 8.5 for illustrative purposes. These particular measurements were taken from a depth of 6m below the hull of the ship at fixed points on a sampling plan organised by Fishery Research Services.

The data Water from that depth was pumped onboard the ship and passed into the flow-cell of the fluorimeter before being discharged back into the sea on a continual process. The slight discrepancies may be due to the flow-cell fluorimeter monitoring a band of wavelengths around 680nm and the laser fluorimeter signal was taken as the peak reading at 680nm, hence on average, the laser fluorimeter showed a decreased signal.

8.3.2 Scapa Flow and Clift Sound Fluorescence Measurements

An important part of the cruise was into Scapa Flow in the Orkney Islands. This part of the research trip was to monitor the abundance of the toxic dinoflagellate *Alexandrium tamarensis* in the water, which tends to increase during the summer months. Previous years have shown that the highest *Alexandrium tamarensis* abundance tend to be on the east side of the Flow with cell concentrations up to 100 cells/ml.

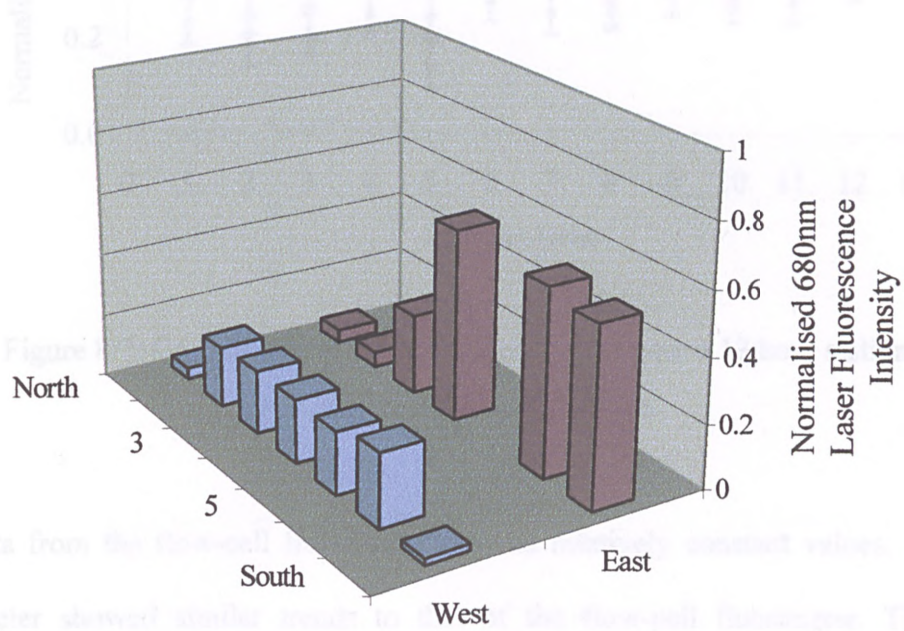


Figure 8.6: Phytoplankton distribution in Scapa Flow shown by chlorophyll-a fluorescence emissions at 680nm

The ship was taken north up the east side of the Flow before moving west then south down the west side of Scapa Flow. As expected, higher concentrations of phytoplankton (all species) were observed on the east side as can be seen in figure 8.6. The ship was then taken into “Clift Sound” in the Shetland Islands where it was anchored over a 12-hour period. Water samples were taken hourly over the sampling period and the results recorded. Shown in figure 8.7 are the fluorescence measurements taken over the 12 hour period.

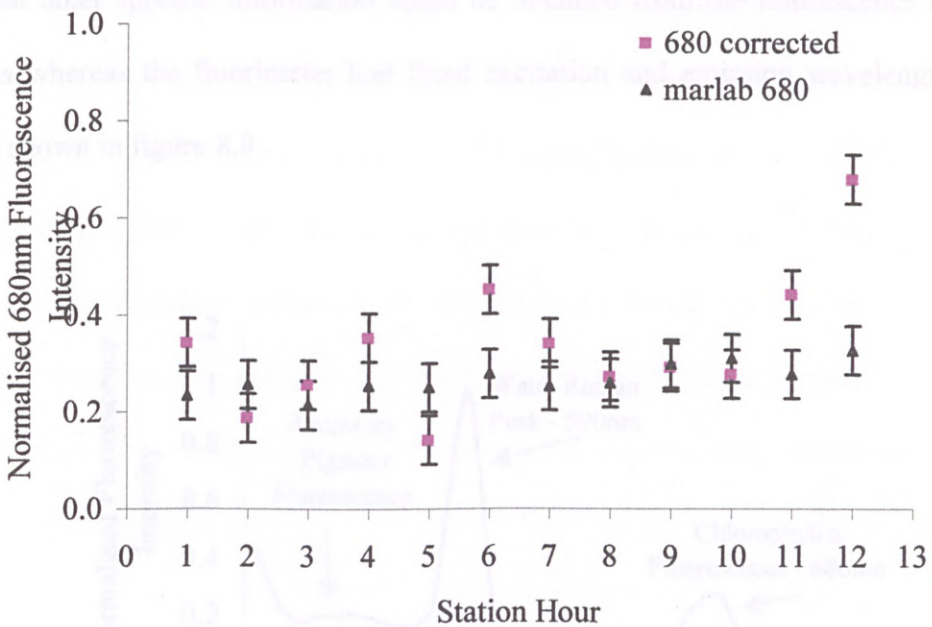


Figure 8.7: Comparison of the fluorescence data from a 12 hour station in “Clift Sound”, Shetland Isles.

The data from the flow-cell fluorimeter showed relatively constant values. The laser fluorimeter showed similar trends to that of the flow-cell fluorimeter. These data however are more volatile and is most likely due to the nature of the measurement. The flow-cell measures the fluorescence as an integration of the fluorescence peak whereas the laser fluorimeter reading is taken as the peak fluorescence value. It is also possible that the water sample being measured in both instruments was slightly different as the

marine laboratory value was from a flow cell measurement system whereas the laser fluorimeter used a discrete water sample taken from the exit of the flow cell. In general however, it can be seen that both sets of data tend to follow the same trends with most of the measurements within the errors of the instruments.

8.4 Discussion: June 1998 Sea Trial

One major advantage of the laser based system compared to the flow cell fluorimeter was that other spectral information could be obtained from the fluorescence scanning process whereas the fluorimeter had fixed excitation and emission wavelengths. This can be shown in figure 8.8 .

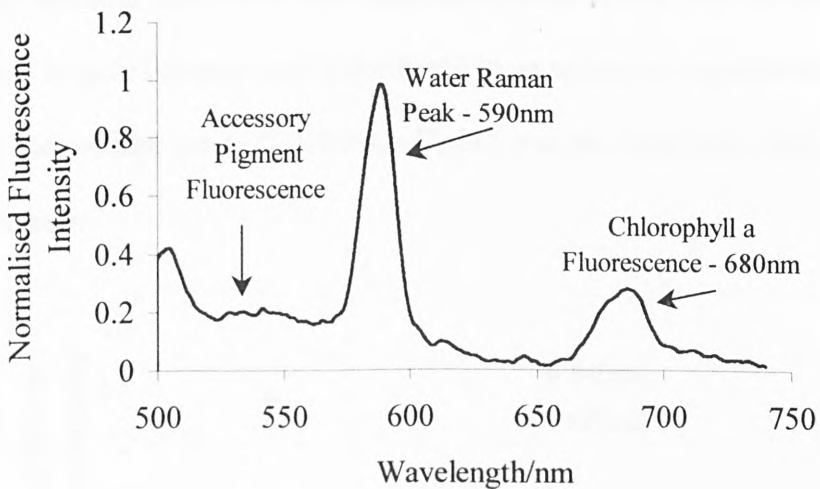


Figure 8.8: Scan of seawater sample using laser fluorimeter

The first and important feature of the spectra is the signal obtained from the water Raman scattering at 590nm. The intensity of this peak is almost constant and is therefore a good reference point for comparing spectra. During the course of this sea trip, all the data from the chlorophyll-a and accessory pigments were normalised to the

water Raman peak. The second important piece of information that can be obtained from the spectra above is, of course, the chlorophyll-a fluorescence intensity at 680nm. This is the peak used when comparing to the flow cell fluorimeter. This intensity at 680nm is the only information obtained by the flow cell system. It can be seen that the laser fluorimeter also gives a second piece of information which can, in effect, be used as an internal standard for monitoring sea water. The last piece of information obtained using the laser fluorimeter is the fluorescence observed below 590nm. In this particular scan there is a clear increase in the fluorescence signal at around 540nm which is due to accessory pigments within the phytoplankton being monitored. Microscopic analysis of water samples showed that its main types of phytoplankton present at this particular sampling station were the dinoflagellates *Alexandrium* spp and *Pseudonitschia* spp and *Dinophysis* spp. Spectral analysis of dinoflagellate species shows that the fluorescence at around 540nm is quite common and is attributed to an accessory pigment in the cell.

During the passage out of “Clift Sound”, full spectral data were collected using the laser fluorimeter.

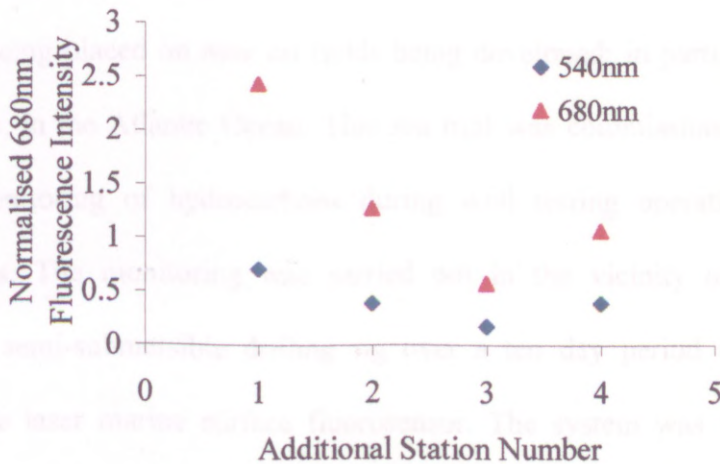


Figure 8.9: Phytoplankton fluorescence signal changes on leaving “Clift Sound”

In figure 8.9, both the 680nm fluorescence and the 540nm fluorescence from the dinoflagellates are shown. It can be seen from the plot that the accessory pigment fluorescence at 540nm follows the same trend as the chlorophyll-a at 680nm, suggesting that this particular band may also be of use in determining the phytoplankton concentration of dinoflagellates. This has been shown in the past⁸⁵. Although this band does not necessarily appear in all plankton's such as diatoms, it may however be used to indicate the type of algae present in the area being monitored when both the fluorescence bands are monitored.

8.5 LMSF Mk III System Sea Trials “Sovereign Explorer” Aug/Sept 1998

Although the laser marine surface fluorosensor was initially developed for monitoring phytoplankton on the sea surface, interest was expressed in the system by oil companies as a potential tool for monitoring hydrocarbons on the sea surface around oil installations. As more legislation is passed protecting the environment against pollution, oil companies are increasingly required to take steps to address the problems associated with oil production. Although oil production in the North Sea produces pollution, emphasis is being placed on new oil fields being developed; in particular, west of the Shetland Isles, in the Atlantic Ocean. This sea trial was commissioned by Conoco, to carry out monitoring of hydrocarbons during well testing operations west of the Shetland Isles. The monitoring was carried out in the vicinity of the “Sovereign Explorer”, a semi-submersible drilling rig over a ten day period using the Mk III version of the laser marine surface fluorosensor. The system was used onboard the supply ship “Toisa *Invincible*.”

8.5.1 Setup of the Laser Marine Surface Fluorosensor Mk III

Compared to previous versions of the LMSF, the Mk III system is much more compact and portable. This was a major advantage as it was being deployed from a supply ship rather than a designated marine research vessel. The priority at the beginning of the trip was to establish whether the ship had a “clean” electrical supply. The chief engineer was consulted and some minor electrical tests were carried out. This was not seen as a problem, primarily as the ship was relatively new and had the latest in electrical circuitry for powering various navigation and positioning systems within the ship. During normal operations, the ship’s powers supply produced no visible transients.

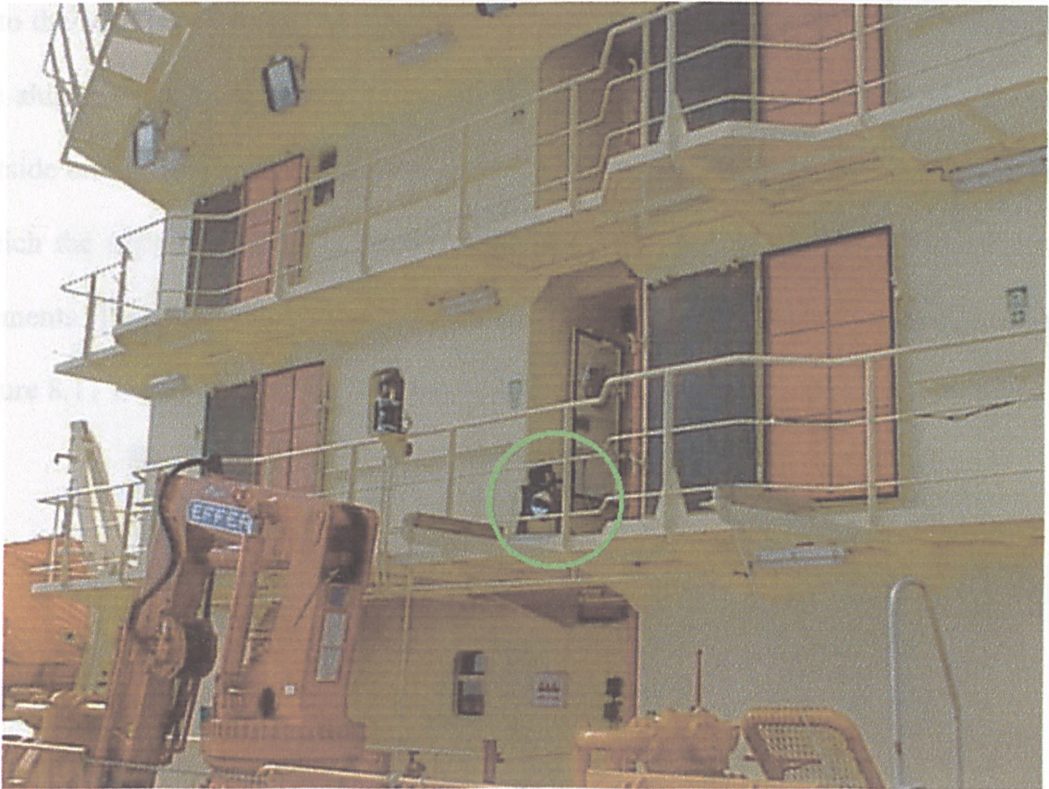


Figure 8.10: Photograph showing the location, marked with a circle, of the LMSF Mk III on board the “*Toisa Invincible*” during sea trials west of the Shetland Isles

When the ship came in for manoeuvring next to the oil installation, bow and stern thrusters were started; this was the only time when a surge in the electrical supply was

observed. Due to the layout of the ship, there was no permanent space for the sensor to be mounted. When the system was non-operational, it was in storage. However, the compact size and portability of the system enabled it to be set-up in approximately 15 minutes. For this particular trip, the system was set-up on a walkway at the rear of the ship, some two levels off the deck. The laser beam was aimed off the side of the ship into undisturbed water. The location can be seen in figure 8.10. The green circle in the photograph marks the sensor. The photograph also illustrates the relatively small size of the sensor in comparison to the ship itself. The sensor was placed on the gantry at a position which gave the laser and the telescope a clear line of sight, through the railings onto the sea. The main electronics for the system were kept inside the superstructure of the ship, ensuring they were protected from moisture. The only pieces of equipment outside on the gantry were the laser and the photomultiplier. Due to the short notice at which the trip was organised, it was impossible to create a cover for these essential elements. This limited the conditions in which the sensor could be deployed. Shown in figure 8.11 is a photograph of the system in operation during some of the night trials.



Figure 8.11 : Photograph showing the LMSF Mk III during night operations.

Although the sensor had been calibrated in the laboratory before being taken for sea trials, it had to be disassembled for transport to the ship then re assembled once on board. It was noted that the ship was painted with a fluorescent orange colour part which showed some fluorescence when excited at 488nm. This was very useful for carrying out a quick check to see if the sensor was responding.

8.5.2 Sea Trial Calibration

Before any measurements were taken on the sea surface, the sensor was directed onto the fluorescent paint on the ship. The aft of the ship had a wooden covered deck which was sectioned using metal beams running across the ship. This can be seen clearly in figure 8.12.



Figure 8.12: Photograph showing the fluorescence spars (marked with green circle) on the wooden deck

From the photograph, it can be seen that there are 5 spars shown which are 3m apart, giving fluorescent targets at regular intervals up to 15m away from the surface sensor. As the ship was unloaded, more spars became visible, giving fluorescent targets up to 21m. This range was more than adequate for testing the system response taking measurements on the sea surface. The system was switched on and allowed to “warm up” for approximately five minutes. It was then aligned so the laser beam was pointing down the stern of the ship onto the wooden deck. This was used as the zero for the measurements, assuming that there was no significantly fluorescent material on the deck. Once the system had settled and a stable signal could be obtained, the laser was directed onto the furthest fluorescent spar and the signal monitored. If there was no difference in the signals, the lock-in amplifier gain was changed and the process was repeated.

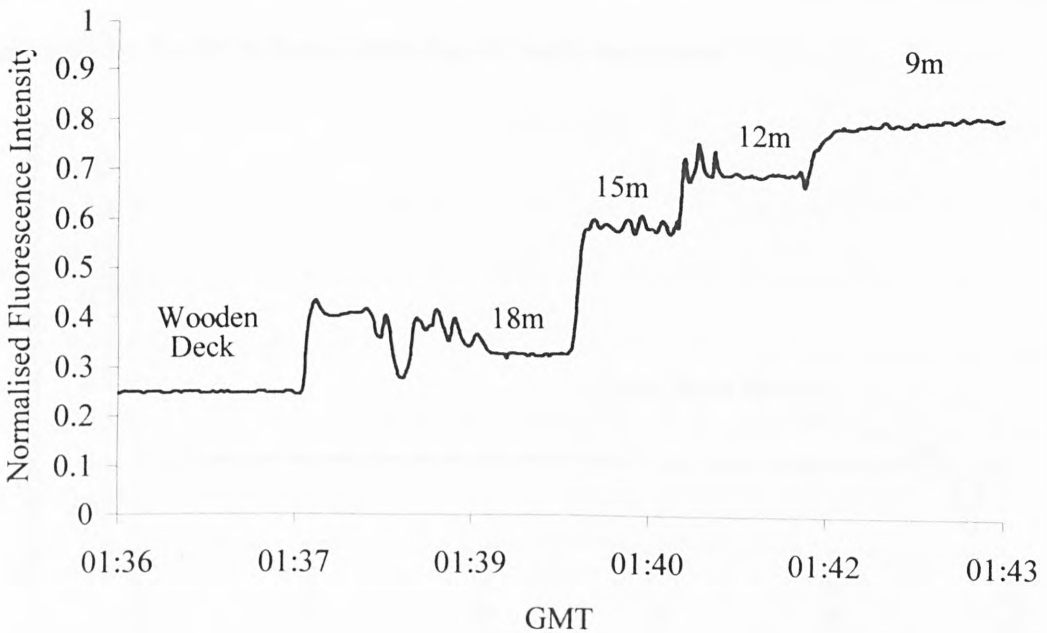


Figure 8.13: Range response of the LMSF Mk III during field operations West of the Shetland Isles

Once a difference had been observed between the wooden deck and the furthest spar, the laser was directed on to the next closest spar and a signal recorded until the nearest one had been reached. The results of this can be seen in figure 8.13. From figure 8.13, it can be seen that there was a clear distinction between the wooden deck and the fluorescent spars located at a range of distances from the sensor. It can also be seen how quickly results could be obtained for the calibration, with a total time of 7 minutes. Once this had been carried out, the sensor was directed onto the sea surface to begin monitoring for fluorescent material. Initially, the sensor was deployed and directed onto the sea surface where it was thought there would be few hydrocarbons, to allow a background reading to be taken. The result of this can be seen in figure 8.14. It can be seen that backscatter from the sea surface is a relatively small, steady signal. The graph also shows the effect of block-ing the laser beam before it goes into the water. Note how the signal drops almost to zero. It can be seen that the water does give some signal which may be due to inelastic scattering of water molecules.

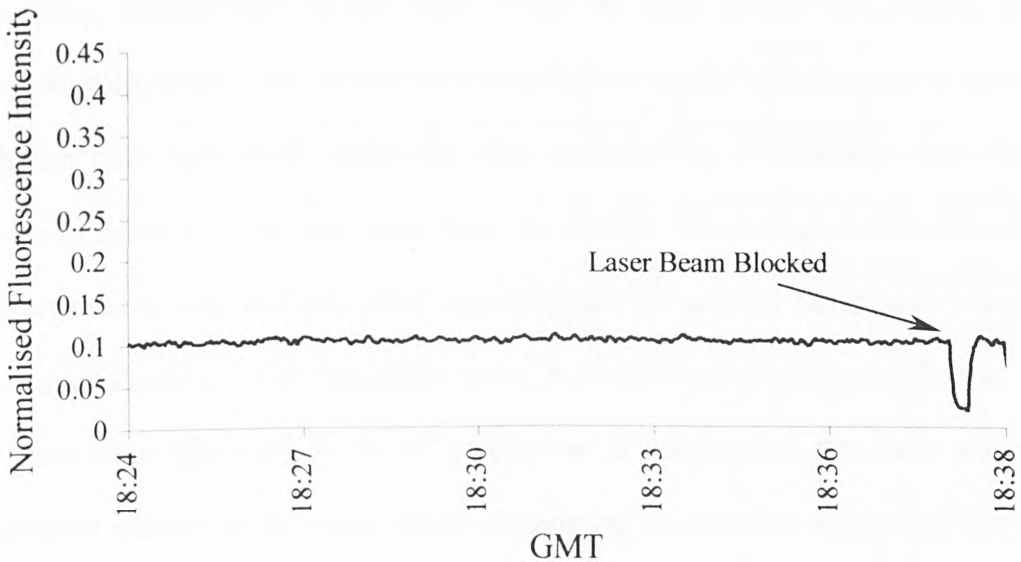


Figure 8.14: Graph showing signal from backscattered radiation from the water surface

Once a background signal had been obtained, it was possible to use the system for hydrocarbon monitoring purposes.

8.5.3 Hydrocarbon Monitoring

Before moving into the area for monitoring, two main factors were taken into account to determine the possible location of hydrocarbons. One of the main parameters which would determine the higher concentrations of surface hydrocarbons was the wind direction during flaring operations. Due to technical difficulties, no flaring occurred during the trip. The second dominant factor affecting the distribution of hydrocarbons around the platform was the direction of the tide in relation to the installation and position of the ship. This information was obtained from sea charts located on the bridge of the ship.

During the trip a fibre optic system which has been described elsewhere⁸⁶ was used for monitoring hydrocarbons in the water whilst the ship was in the vicinity of the “Sovereign Explorer”. The system used blue light to excite hydrocarbons in the water with one fibre optic cable whilst the other collected the fluorescence from the oil. Shown in figure 8.15 are two traces from the system. The background on this system was constant at zero and was taken approximately 10 nautical miles (n.m.) from the “Sovereign Explorer”. The first of the traces, A, was obtained approximately 10m from the “Sovereign Explorer” on the 5th of October. It can be seen that there was some fluorescent material in the water which, considering the location of the ship, was most likely due to hydrocarbons.

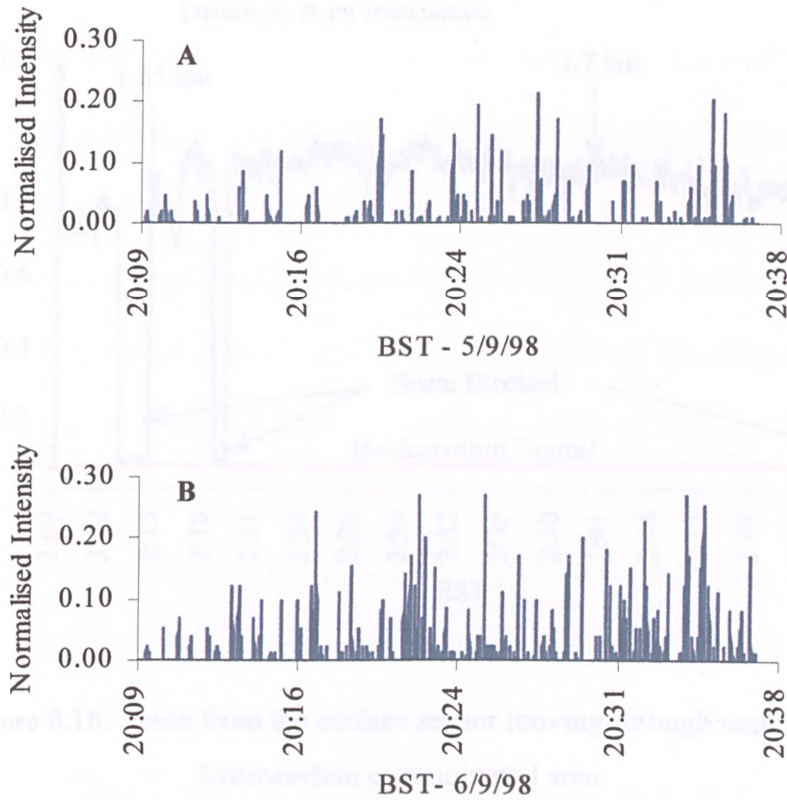


Figure 8.15: Traces from the fibre optic fluorimeter showing the presence of hydrocarbons in the water surrounding the “Sovereign Explorer”

The second trace (B) shows the data obtained on the 6th of October, again 10m from the “Sovereign Explorer”. It can be seen that there was an increase in the number of fluorescent events recorded during the same time. This indicates that there was an increase in the amount of hydrocarbons in the water surrounding the oil installation. The data confirmed that there were hydrocarbons present in the vicinity of the installation.

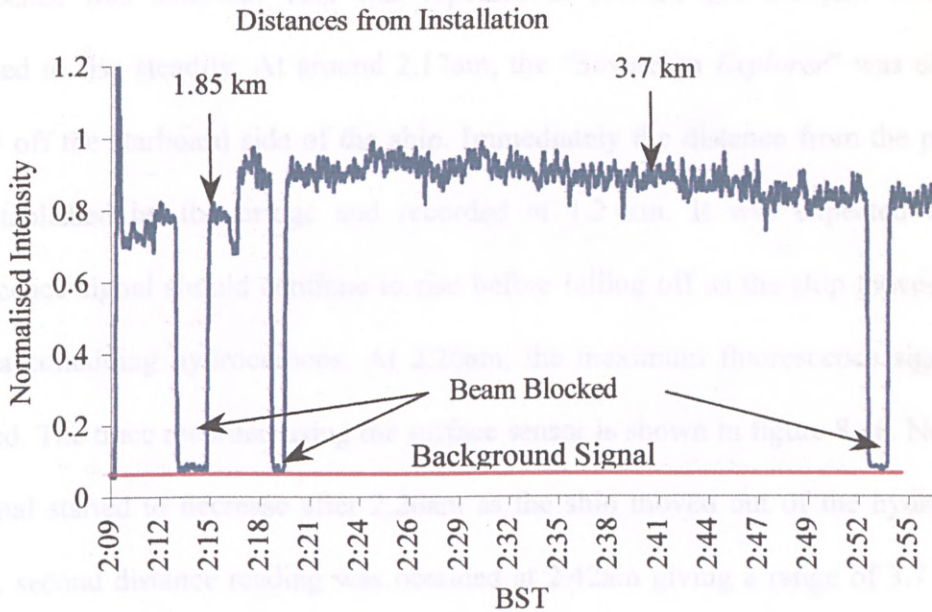


Figure 8.16: Trace from the surface sensor moving through suspected hydrocarbon contaminated area

On the 6th of October 1998, the “*Toisa Invincible*” was on close standby which meant that the ship was within 2-4 km of the “*Sovereign Explorer*”. Supply ships are kept at about 10 km whilst they are not working. It was fortunate that the weather was favourable compared to the previous few days, which allowed the surface sensor to be set up and tested. The sensor underwent some testing from about 11pm onwards and was eventually directed onto the sea surface off the starboard side of the ship. The instrument gain and time constant were adjusted to give a reasonable signal from the water, approximately 50% of full scale deflection. This took place at approximately 2.10am. The sensor was left running to determine if there was any change in fluorescence. By 2.12am, there was an appreciable increase in the signal and the beam was blocked to determine if the electronics were still working and detecting from the sea surface. At 2.15am, the beam was allowed back onto the water surface and again

fluorescence was detected. This was repeated at 2.19am and 2.53am. The signal continued to rise steadily. At around 2.17am, the “Sovereign *Explorer*” was observed directly off the starboard side of the ship. Immediately the distance from the platform was established by the bridge and recorded at 1.2 km. It was expected that the fluorescence signal should continue to rise before falling off as the ship moved out of the area containing hydrocarbons. At 2.26am, the maximum fluorescence signal was recorded. The trace recorded using the surface sensor is shown in figure 8.16. Note how the signal started to decrease after 2.26am as the ship moved out of the hydrocarbon area. A second distance reading was obtained at 2.42am giving a range of 3.7 km. As can be seen from figure 8.16, there is quite a large offset in the fluorescence signal possibly due to the water Raman scatter. In figure 8.17, the offset has been removed and the data treated using a 90 point average, which is equivalent to 90 seconds. In this graph, the data points from the times when the laser beam was blocked have also been removed to make it easier to observe the trend in the fluorescence signal. It can be seen from the graph that, as the ship moved from relatively clean water into the area suspected of containing hydrocarbons, the fluorescence signal from the sea surface increased 300% from the background signal at the maximum.

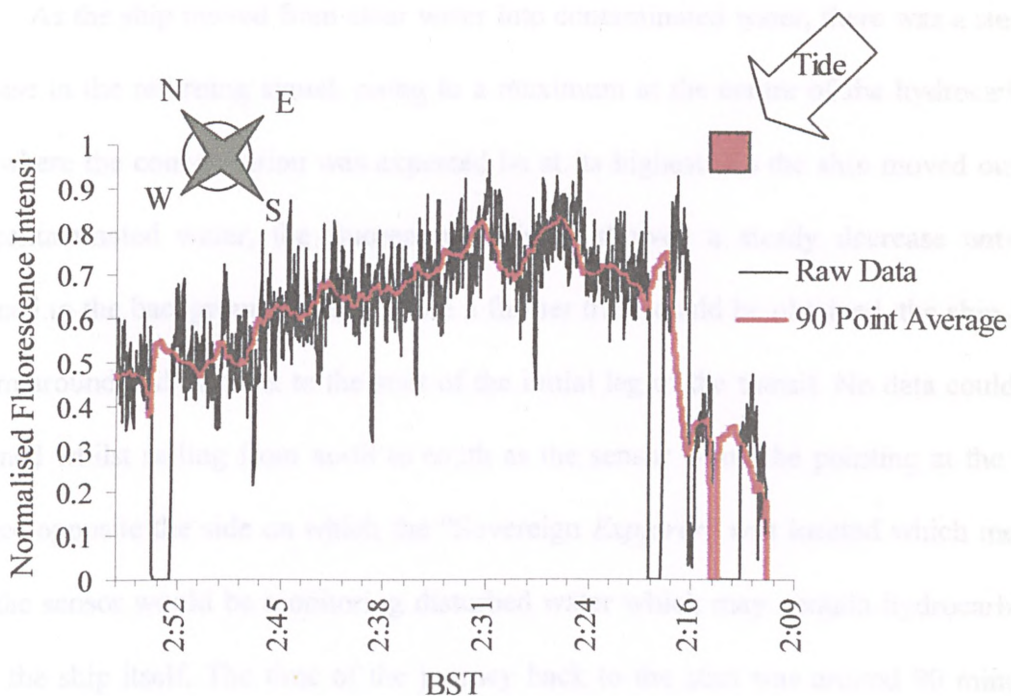


Figure 8.17: Diagram showing the main components which affected the signal obtained (also shown) during the “Sovereign Explorer” sea trial

Figure 8.17 gives a graphical representation of the relative positions of the oil installation and the direction of the supply vessel superimposed on the actual data obtained. It can be seen that the most obvious area for detecting hydrocarbons would be in an area where the tide had carried them along.

8.6 Discussion: October 1998 Sea Trials

From the position of the installation and knowledge of the tidal directions at that particular time of the year from sea charts on board the *Toisa Invincible*, it was estimated that any hydrocarbons present would be located roughly in the area shown. It therefore follows that by transversing across that area (shown by the arrow), it may be possible to obtain a change in the fluorescence backscatter from the sea surface which, due to the nature of the area would almost certainly be due to hydrocarbons.

As the ship moved from clear water into contaminated water, there was a steady increase in the returning signal, rising to a maximum at the centre of the hydrocarbon area where the concentration was expected to be at its highest. As the ship moved out of the contaminated water, the fluorescence signal showed a steady decrease until it returned to the background level. Before a further trace could be obtained, the ship had to turn around and go back to the start of the initial leg of the transit. No data could be obtained whilst sailing from north to south as the sensor would be pointing at the sea surface opposite the side on which the “Sovereign *Explorer*” was located which meant that the sensor would be monitoring disturbed water which may contain hydrocarbons from the ship itself. The time of the journey back to the start was around 90 minutes which was an acceptable time to wait for collecting more data. In a real system, the location of the sensor would be in such a location that measurements off either side or the front of the ship would be possible allowing monitoring whichever way the ship was sailing. As a prototype system, the location of the system was limited in that it required constant attention in case of adverse weather arising or hazardous encounters with personnel.

After 3.15am in the morning as the ship turned on its southerly journey, weather conditions changed requiring the sensor to be switched off and moved indoors to protect the laser and detector. The bad weather continued over the next few days causing no more sensor trials. The well testing which had been scheduled was suspended due to technical difficulties on the installation and the system was returned to the shore.

8.7 Summary

This chapter has documented the testing of the Mk I and Mk III laser marine surface sensors outwith the confines of the laboratory. By using prototype instruments in the field, it is possible to gain knowledge which is essential in directing further developments of the instruments. As can be seen in this chapter, the initial sea trial of the Mk I system did not produce any “real data”, but rather provided valuable information allowing improvement of the design of the system to cope with the conditions which were experienced in the North Sea environment. From this information, modifications to the system were made in the laboratory. Some further laboratory testing was carried out before the system was re-deployed in a working environment. The Mk III system produced valuable hydrocarbon data, in this case for Conoco, who commissioned the trip. Real time data relating to hydrocarbons on the sea surface were successfully obtained using the system in a real working environment. Although the trials were halted due to bad weather, the system was shown to perform well when required to do so.

Chapter 9

Diode-pumped Laser Marine Surface Fluorosensor

9.0 Introduction

Until now all experiments on the Laser Marine Surface Fluorosensor were carried out using an Argon ion laser operating at 488nm. Although this laser is the best for exciting sodium fluorescein, the absorption bands for phytoplankton and oil lie at shorter wavelengths. The optimum excitation for the chlorophyll-a in phytoplankton is around 430nm whilst oil has high absorbances in the ultraviolet region (<400nm) of the electromagnetic spectrum. The EPO-5000 is a diode pumped Nd:YAG laser system with the option of having second and third harmonics installed which produce 532nm and 355nm respectively. In the case of monitoring oil, the third harmonic is ideally suited as an excitation source. There is also the advantage of using this system in that the overall size of the Laser Marine Surface Fluorosensor could be reduced considerably. A further advantage is in the diode technology. The YAG rod is located in the laser head of the instrument whilst the diodes are located in the power supply unit. The diode energy is transferred to the YAG rod via an umbilical cable containing a fibre optic bundle along with relatively low power cables to control the second and third harmonic ovens. Compared to the argon ion laser which has a high voltage umbilical cord between the power supply and laser head, the EPO-5000 is a much safer design for use in the marine environment where the system is designed to operate.

9.1 Oil Fluorescence

Oil absorbs over a wide range of wavelengths with the highest absorption being in the

ultra-violet (UV) region. This can be seen in figure 9.1. This multi-excitation fluorescence spectra of a Gulfaks sample, taken from the *Braer* oil disaster in 1993, shows a large fluorescence between 300nm and 650nm with the maximum emission occurring at 450nm.

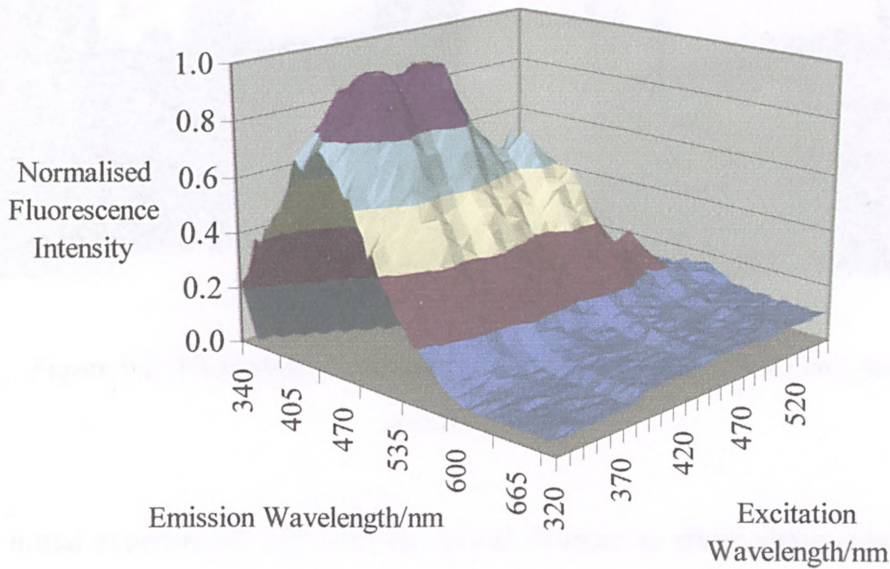


Figure 9.1: Multi-excitation fluorescence spectra of Gulfaks oil

By using UV radiation at 355nm, there is a 300% increase in fluorescence compared to the fluorescence obtained when exciting at 488nm. By exciting in the UV, the sensitivity of the instrument should increase

9.2 System Setup

The diode pumped version of the LMSF Mk II was essentially the same as described in chapter 7.4, the only main change being in the laser source. A photograph of the system can be seen in figure 9.2. The photograph on the right also shows the power supply for the laser. It can be seen that both the laser head and the power supply are small

compared to the argon ion system.



Figure 9.2: Photograph showing the EPO 5000 system (left) and during operation (right)

The initial experiments still used an optical chopper to allow phase sensitive detection of the fluorescence signal. It was thought that by operating the diode pumped laser at the maximum repetition rate, and using a relatively slow chopping speed, the detection electronics should be able to lock on to the returning fluorescence signal.

9.3 Results

9.3.1 Instrumental

Initial experiments were carried out with the EPO- 5000 running at 5000Hz along with the optical chopper which was set at 130Hz. It was noted that the phase of the lock-in amplifier drifted with time and that false readings were observed for the same concentration of sodium fluorescein. This was also noted when increasing the power of the system when monitoring a fixed concentration of crude oil at a fixed range as can be seen in figure 9.3. When the power was increased, there was a steady drift out of phase

when the lock-in was set at the original phase. The second trace shows the detected fluorescence signal when the lock-in phase was readjusted to maintain the maximum signal reading. It can be seen that the value obtained for the uncorrected lock-in phase signal was lower than the actual fluorescence of the phase corrected signal. In an attempt to overcome this drift in the signal phase, the optical chopper was removed from the system and the reference for the lock-in was taken from an output BNC connector on the laser power supply. The lock-in amplifier was, however, unable to lock into the signal. When the signal was observed on an oscilloscope it was noted that the output was a sharp spike which related to the operating frequency of the EPO- 5000. The lock-in amplifier however required a sine or square wave function to be able to lock in properly. It was found out that the laser could be triggered externally using a function generator.

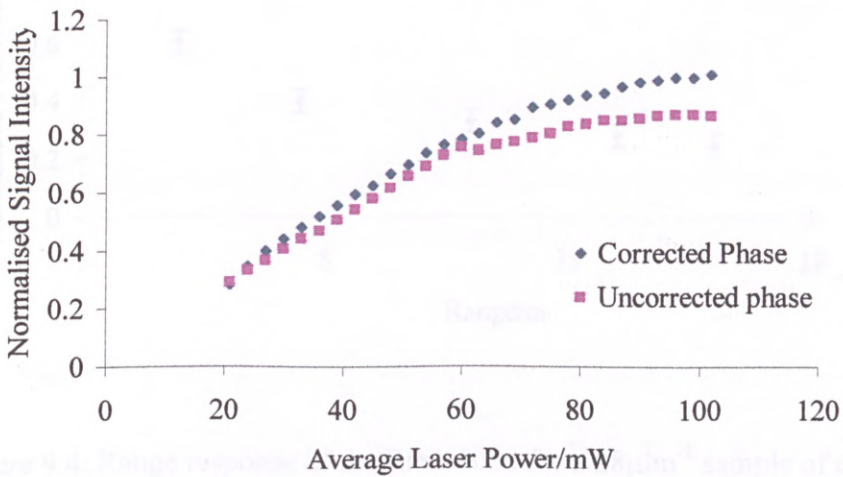


Figure 9.3: Graph showing drift in backscattered crude oil fluorescence signal with average laser power at a range of 12m.

A square wave output from a function generator was used to trigger the laser and also to provide the reference signal for the lock-in amplifier. Once this had been set-up it was

noted that the system was more stable allowing experiments to be carried out.

9.3.2 Oil Detection

As the EPO-5000 operating at 355nm is an ideal source for inducing fluorescence in oil, experiments were concentrated on oil detection and monitoring. Initial experiments were carried out to determine the range response of the instrument. A 0.5 μ l sample of Gulfaks oil was floated in a glass petrie dish which was filled with water. This gave a very thick layer of oil of 28 μ m² for the laser energy to hit and hence minimise any fluorescence interference from other materials such as the glass petrie dish or the laboratory floor. A series of distances from the sensor were marked out and the samples was placed in turn at different ranges.

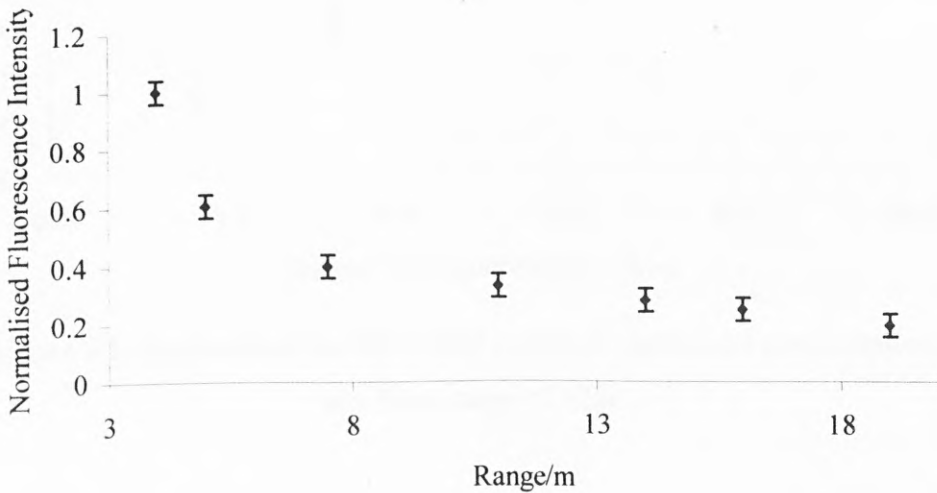


Figure 9.4: Range response of the EPO-5000 for a 28 μ m² sample of crude oil

The sensor was then directed at the sample and the system allowed to settle before a measurement was taken. All the settings on the laser, photomultiplier and the lock-in amplifier remained constant throughout these measurements. As can be seen in figure

9.4, the system was capable of detecting a thick layer of oil in the range from 4-19m. If a higher resolution was required at the longer ranges, then the lock-in amplifier gain could have been increased. To be able to determine a signal at shorter distances without producing an overload condition on the lock-in amplifier, the gain had to be reduced and optimised to allow all the distances shown above to be plotted on the same graph. Further experiments were carried out using different concentrations of oil on the surface of a larger flat container which was kept at a fixed range of 12m from the surface sensor.

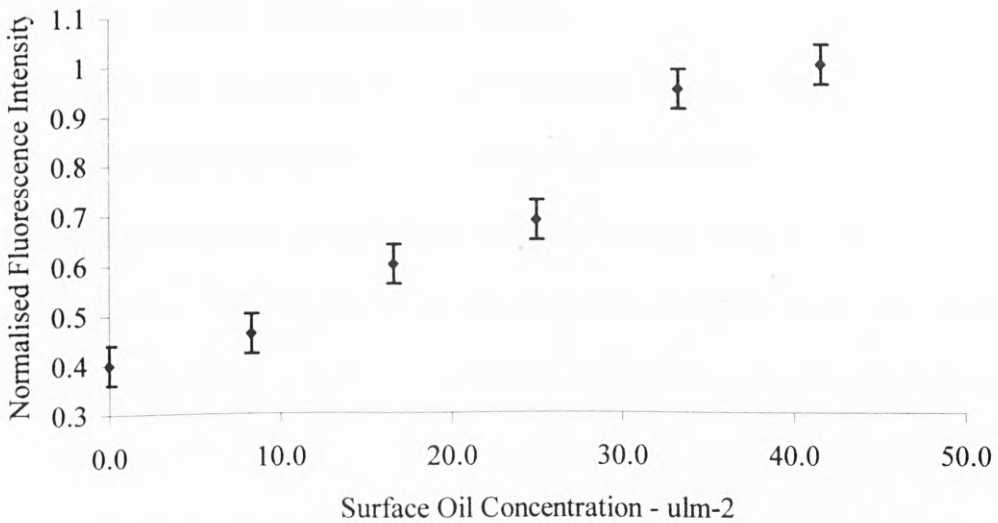


Figure 9.5: Response of the EPO-5000 system to surface oil concentrations at a fixed range of 12m

As can be seen in figure 9.5, the EPO-5000 based system was capable of detecting oil down to $8\mu\text{lm}^{-2}$ at a range of 12m with a detection limit of $1\mu\text{lm}^{-2}$. When comparing with the argon ion laser based system, which was capable of detecting down to $20\mu\text{lm}^{-2}$ at a range of 3m with a detection limit of $9.6\mu\text{lm}^{-2}$, it can be seen that by using an ultraviolet laser for inducing fluorescence in oil, the sensitivity of the system has been considerably increased for the detection of Gulfaks oil on a water surface.

9.4 Summary

The feasibility of using diode pumped laser technology and an excitation source in the Laser Marine Surface Fluorosensor has been shown. The laser system as part of the Mk II version of the system has shown a 900% increase in the detection limit and the range of the instrument has been increased from 3m to 12m. By coupling the diode pumped UV laser to the Mk III system, with the larger telescope, it is expected that the range and sensitivity of the system would be further enhanced.

Chapter 10

Conclusions

A low cost, portable Laser Marine Surface Fluorosensor monitoring system for detecting phytoplankton and hydrocarbons on the sea surface has been developed and tested in both the laboratory and during a series of sea trials in the North Sea.

10.1 Laser Marine Surface Fluorosensor

Experiments have demonstrated that amplitude modulated, low power, argon ion laser light can be used to remotely induce a periodic fluorescence in algae and hydrocarbons which can be collected using a telescope and detected using interference filters and a photomultiplier. The fluorescence signal was recovered from the light at the photomultiplier using a lock-in amplifier which gives a signal proportional to the concentration of a species.

The Mk III version of the system was used under low light conditions (less than 6mWm^{-2}) to achieve a detection limit of $2.19 \times 10^{-7}\text{M}$ for sodium fluorescein at a range of 21m in the laboratory. This system has also been used successfully to detect hydrocarbons in the marine environment under similar conditions.

The Mk II version of the system was used under low light conditions (less than 6mWm^{-2}) to achieve a detection limit of $2.8 \times 10^{-8}\text{M}$ for sodium fluorescein at a range of 15m, a detection limit of 500 cells/ml for phytoplankton at a range of 15m, and a detection limit of $9.6\mu\text{lm}^{-2}$ for hydrocarbons (Gulfaks) at a range of 3m using the argon ion laser excitation source in the laboratory.

The use of a diode pumped, frequency tripled Nd:YAG laser as the excitation source was also investigated for detecting hydrocarbons. This not only gave UV radiation at 355nm which is more efficient at exciting hydrocarbon, but it also demonstrated the possibility of making the overall system smaller and more practical in a working environment. This variant of the LMSF Mk II gave an improved detection limit for hydrocarbons (Gulfaks) of $1\mu\text{m}^{-2}$ at a range of 12m in the laboratory whilst operating under low light conditions ($< 6\text{mWm}^{-2}$).

The detection limits for hydrocarbons were obtained in the laboratory, however, it is difficult to give an actual concentration in the real marine environment due to the changes in the fluorescence properties of the hydrocarbons as they are weathered.

At present the system can be used to give an indication as to the presence of hydrocarbons which is true of all fluorescence based monitoring systems. If, however, the system was to be mounted on an oil production installation as a hydrocarbon monitor, it should be possible to give quantitative data as it is reasonable that the hydrocarbons being released into the environment are fresh and not weathered to any extent. This was tested in the second of two sea trials. The initial sea trial using the LMSF Mk I allowed evaluation of the conditions under which a system would have to be able to operate. The second trip using the LMSF Mk III system was used for monitoring the presence of hydrocarbons around a test-well drilling platform west of the Shetland Isles. The system was shown to detect fluorescent material in the vicinity of an oil production platform which was most likely due to the presence of hydrocarbon on the sea surface.

Current legislation limits the amount of oil in produced water to 40ppm. At present there is no legislation specifically covering oil which has been deposited onto the sea surface. As a rough indication of the effectiveness of the surface sensor for

detecting oil, if all of the maximum limit was present on the sea surface, a concentration of 40mlm^{-2} would be observed. As the diode pumped system is capable of detecting down to $1\mu\text{lm}^{-2}$, only 1/40,000 of the total oil distributed in a 1 litre volume would have to be present on the sea surface to be detected.

10.2 Laser Fluorimeter

The laser fluorimeter developed as part of the project was found to be a useful tool for calibrating the laser marine surface fluorosensor. It was also useful in monitoring the fluorescence of other pigments within the algae in real time. Unlike traditional flow-cell or submerged fluorimeters which have fixed excitation and emission bands, the laser fluorimeter can scan the fluorescence emission spectra of a sample.

In using the laser fluorimeter, it has been demonstrated that phytoplankton samples containing only diatoms have very little fluorescence below 680nm. Some species such as dinoflagellates, may have additional fluorescent pigments at around 540nm. By monitoring both these areas of the fluorescence spectrum it should be possible able to give an indication of the type of phytoplankton present in the water.

A sea trial was carried out in June 1998 using the laser fluorimeter alongside a traditional flow-cell bench fluorimeter. It has been shown that in open waters a higher percentage of diatoms is likely to be present whereas in more stratified waters, such as sea lochs, flagellate species would contribute more to the fluorescence signal. It was found that when the ship was in open waters, there was very little fluorescence below 680nm. By using this information alongside the Laser Marine Surface Fluorosensor, it could be used to validate the surface sensor fluorescence measurements and provide additional fluorescence data on the area being monitored.

10.3 Time Resolved Fluorescence Spectroscopy

This research work and that of others⁸⁷ has shown that the de-excitation process within algae takes a finite time. The time for de-excitation and hence fluorescence to occur may be related to the physical and chemical state of a particular algae. As very fast (picosecond^{88,89} / femtosecond⁹⁰) and slow (millisecond⁹¹) fluorescence in algae have been well documented, experiments were restricted to a nanosecond time scale fluorescence. There has been limited experiments carried out monitoring terrestrial algae monitoring carried out using nanosecond excitations⁹² although the response of this algae may be different to marine algae.

The selected species in these experiments all showed similar exponential fluorescence decay characteristics during the first few days of experiments when excited using pulsed 430nm laser light from an optical parametric oscillator. Small peaks were observed in the time spectra but were within the noise level of the constructed system and therefore could not be used to differentiate between the species absolutely. As the samples progressed into the stationary growth phase, the maximum variations in the fluorescence occurred at different times for the species. Initially, it was only possible to observe a difference between *Chaetoceros* and the others. When the samples were examined the following day, however, it was possible to determine each of the species individually. The fluorescence signals for *Chaetoceros*, *Tetraselmis* and *Nannochloris* are all very similar, making it difficult to differentiate between them.

By monitoring the time for the fluorescence levels to reduce to half their original intensity, it was again possible to determine differences between species on day three of the experiments. By using these pieces of information along with other standard spectral information, it has been shown that it is possible to differentiate between some of the selected species when they are under nutrient limited conditions. The system has also

shown that it may also be possible to monitor the nutritional state of the algae being monitored.

10.4 High Energy Laser Effects on Phytoplankton

During pump-probe measurements, high intensity pulsed lasers were used to saturate the reaction centres in chlorophyll a, hence maximising fluorescence⁹³. This allows the fluorescence kinetics of the plankton to be studied. It is therefore important to observe the effects of high intensity pulsed laser radiation on phytoplankton.

Initial experiments were carried out using 355nm laser radiation on selected species of phytoplankton. Their fluorescence emissions were recorded after exposure to 355nm radiation. Experiments demonstrated that each of the species examined produced different results. The peak fluorescence emissions occurred after different treatment times in most of the samples. It may be possible, using this information to distinguish between *Chaetoceros calcitrans*, *Nannochloropsis oculata* and *Nannochloris atomus* and *Tetraselmis suecica*. The only samples that could not be distinguished were the *Nannochloris* and *Tetraselmis* samples. This work demonstrated that it is possible to differentiate between selected algae species under these experimental conditions.

As the algae was being exposed to high energy laser radiation, it was foreseen that the algae cells may be ruptured whilst being irradiated. This was tested by using an optical microscope to observe the cells before and after laser treatment. Damage to the cell walls was observed to have occurred in all of the species, suggesting that the differences between each of the selected algae samples may be due to leaching of component molecules from within the cells.

As there was damage observed using high energy 355nm laser radiation, subsequent experiments were modified to use lower pulse energy radiation at selected

wavelengths (430nm, 474nm and 633nm) for the *Chaetoceros* sample. The average power was kept below 150mW for these experiments.

10.5 Treatment of *Chaetoceros* using Selected Laser Wavelengths

These experiments provided more results which may be characteristic of the algae examined. These could be used as a further refinement technique for characterising algae in a measurement system which, along with other spectral methods could provide an insight into the composition and health of algae. Experiments in this case were limited to a single species which showed differences in the chlorophyll-a fluorescence peak after treatment with selected wavelengths of laser radiation which are summarised below in figure 10.1. It can be seen that treatment with 430nm shows an overall decrease in the fluorescence intensity as the excitation wavelength is increased. This trend is also seen in the fluorescence peak shift towards the blue end of the spectrum where the shift in the fluorescence is less with increasing excitation wavelength. When the sample is treated with 474nm radiation, it can be seen that the fluorescence intensity increases as the excitation wavelength is increased. This is also reflected in the peak shift in that as the excitation wavelength is increased, the fluorescence peak shift is greater. Treatment of the sample using 633nm laser radiation shows a different effect on the fluorescence intensity. The sample tends to produce high fluorescence when excited with short wavelength (430nm) and long wavelength (633nm) radiation whilst excitation at 474nm produces the lowest fluorescence.

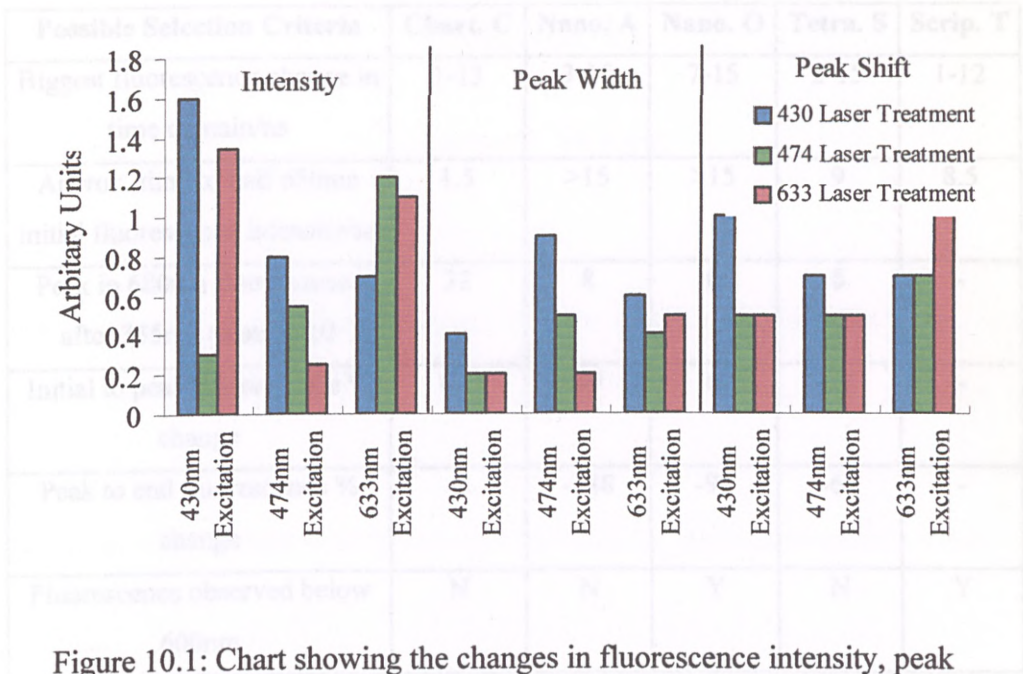


Figure 10.1: Chart showing the changes in fluorescence intensity, peak width and peak shift when monitored using selected wavelengths after treatment for three wavelengths of laser radiation

The fluorescence peak width measurements show similar trends for treatment and excitation at the shorter wavelengths but again the trend for 633nm treatment differs from the others.

These experiments have shown that by exposing algae to selected wavelengths of light, it may be possible to observe differences in the fluorescence behaviour for various species. It has also shown that there could be errors introduced into a custom built instrument to monitor algae fluorescence at 680nm. Such an instrument, would have to have a sufficient spectral window of up to 15nm to ensure true readings were obtained in the fluorescence intensity due to the shifts in the fluorescence peak.

Each of these sets of experiments using medium to high power laser radiation have produced effects within the selected phytoplankton species which may be useful in identifying the samples.

Possible Selection Criteria	Chaet. C	Nano. A	Nano. O	Tetra. S	Scrip. T
Biggest fluorescence change in time domain/ns	1-13	3-15	7-15	2-15	1-12
Approx. time to half 680nm initial fluorescence intensity/ns	1.5	>15	>15	9	8.5
Peak in 680nm fluorescence after 355nm treatment/J	32	8	0	8	-
Initial to peak fluorescence % change	176	89	0	59	-
Peak to end fluorescence % change	-8	-188	-92	-68	-
Fluorescence observed below 600nm	N	N	Y	N	Y

Figure 10.2: Table showing possible rules which may allow the identification of selected algae

The possible criteria for identifying each of the species is given in figure 10.2. If the tests were automated and run simultaneously, it may be possible to determine a single species within approximately one minute. The biggest advantage of all of the above measurements is that they can be carried out remotely using laser radiation and a detector with a spectrograph. These particular data are generally observed in algae which are under nutrient limited conditions. The differences between the species under normal growth conditions, however, may not be as large, making identification more difficult.

Chapter 11

Future Work

Introduction

The work carried out during the course of the project demonstrated the successful development and application of some potentially useful instruments, the main system being the Laser Marine Surface Fluorosensor. At present, this instrument does have some limitations. A number of improvements could be made to overcome these.

11.1 Laser Marine Surface Fluorosensor System

The surface fluorosensor system has been shown to be suitable to quantify algae in the marine environment. As the system is capable of operating continuously, it is possible to gather more information on the algae distribution in the sea, therefore giving a better representation of the quantity of algae in the sea. This increase in the amount of information which can be collected will allow a better understanding of the role of algae in the marine environment and will also allow better mathematical models to be developed to predict future trends in the marine ecosystem.

The system can also be used as a monitoring tool for use with more complex optical techniques e.g. Raman scattering, which could give further refined information on the algae in the marine environment.

Although the system has a high signal to noise ratio when operating under low light conditions, the system does have a reduced signal to noise ratio when operating under ambient light conditions. There are however a number of improvements which could be made to the sensor to increase the sensitivity of the system and also make the system more practical for operating in the marine environment. These include, using

polarisation to discriminate between the signal, laser and background light. By choosing more compact, hermetically sealed lasers, increasing the size of the telescope thus increasing collection efficiency of the signal and by scanning the laser beam to cover a larger area hence giving more representative results.

11.1.1 Polarisation

Polarisation can be used to improve the signal to noise ratio as most of the background light should have little or no natural polarisation. The laser beam can be forced to a specific polarisation which is known.

If the laser beam has a plane polarisation in the vertical plane (V) and a polarisation filter is used which allows this radiation to pass through, then only V-polarised radiation will be used to excite the species. To reduce the amount of laser light reaching the detector, a polarisation filter which only passes plane polarised light in the horizontal plane (H) can be used. Any backscattered laser light which is still at the initial V-polarisation can be filtered. It is also possible that some light striking the sea surface may also become polarised and although this will mostly be random, some of the light will be V-polarised. The use of a polarisation filter can then be used to reduce some of the collected laser light and some of the background light being scattered off the sea surface. This should lead to a decrease in noise by up to two orders of magnitude.

One problem which could arise is that the polarisation of the sunlight off the sea surface could be polarised in the same plane as the signal and therefore a reduction in the signal to noise ratio would be observed. This is an area which requires more experimentation.

11.1.2 Laser Types

At present the system utilises an air cooled argon ion laser. This has a limited applicability in the marine environment. The main limitations of argon ion lasers are that they are generally bulky and are fragile. These are not the ideal characteristics required when operating in a real marine environment where the space on ships is limited and conditions can be harsh.

Modern lasers however, such as diode-pumped systems are an ideal solution to the limitations of argon ion lasers. Diode-pumped lasers can be hermetically sealed eliminating the problem of moisture in the components. The laser head can be pumped remotely using fibre optics allowing the critical electronics to be housed in a safe environment. They also have the ease and flexibility of producing multiple wavelengths with relatively high powers compared to argon ion lasers.

It is also easy to produce the second and third harmonics of a diode pumped Nd:YAG laser, giving light in the visible and ultraviolet regions of the spectrum which cannot be easily done with an argon ion laser. The UV option will allow more efficient excitation of hydrocarbons as the emission at 355nm is closer to the absorption bands of hydrocarbon molecules. This could extend the range or the sensitivity of the system for monitoring hydrocarbons. The visible option at 532nm could be used for exciting phytoplankton. Although the UV light would excite phytoplankton also, it could be possible to determine the presence of hydrocarbons and phytoplankton more accurately by observing the fluorescence ratios at different parts of the spectrum.

By using a pulsed UV laser and gated spectrograph & detector, the system could not only be used to collect more spectral information but it could be used during higher ambient light conditions i.e. $> 6\text{mWm}^{-2}$. Although the laser may add to the cost of the

overall system, it could be operated 24 hours a day and not limited to dusk until dawn operation.

A diagram of a potential future version of the laser marine surface fluorosensor is shown in figure 11.1. It can be seen that by using the diode pumped Nd:YAG laser, the system is more compact and portable than the current version using the argon ion laser.

The system could also adopt a larger telescope which would increase the overall size of the system but there may be a greater gain in the backscattered light collected from the sea surface which would give a larger signal. This should make it easier to apply signal enhancement techniques to the signal thus increasing the signal to noise ratio. The laser spot size and geometry could also be controlled to utilise more area of the primary mirror of the telescope which was investigated in section 7.6.2.

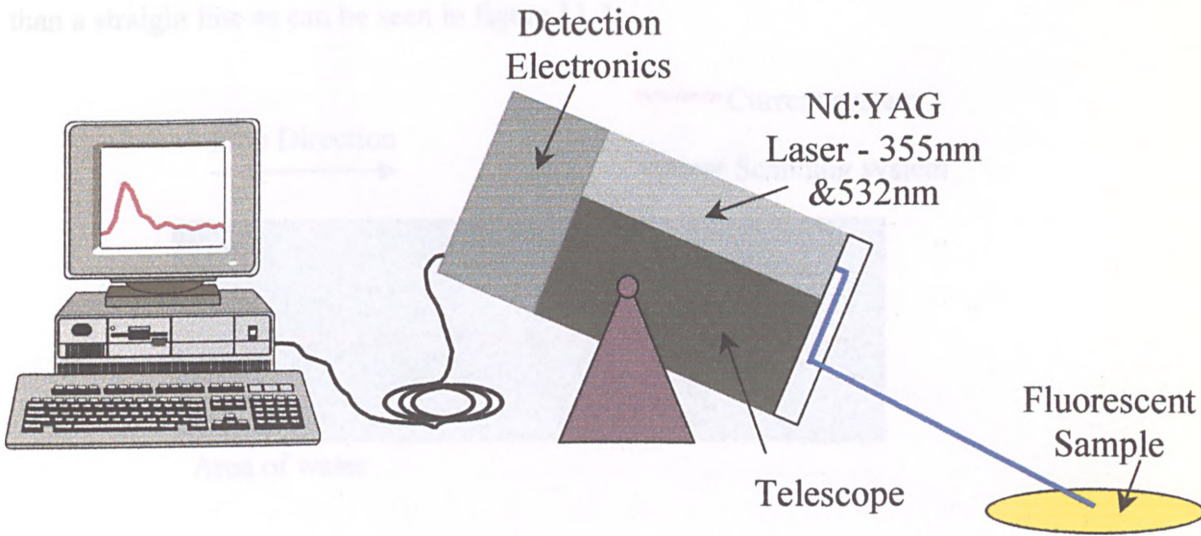


Figure 11.1: Design for the Laser Marine Surface Fluorosensor Mk IV

As can be seen in figure 11.1, the current system is generally fixed and monitors a line of water as the ship moves. It would also be possible to scan the laser beam. This could

be done by using an angled, rotating mirror or lens on the front of the telescope as can be seen in figure 11.2a and b.

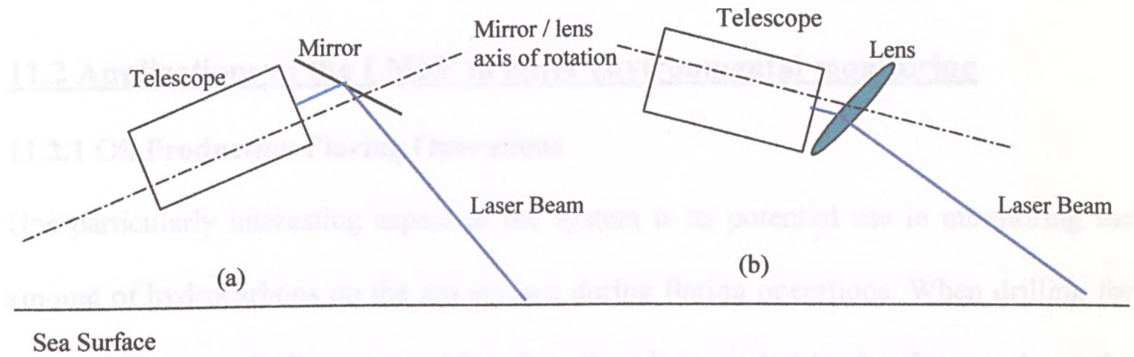


Figure 11.2a&b : Diagram showing modifications to allow scanning of the laser beam

This would produce the effect of scanning the laser beam across the sea surface whilst at the same time the telescope would always be monitoring where the laser beam is directed. By using this method, the system would monitor a saw-tooth pattern rather than a straight line as can be seen in figure 11.3.

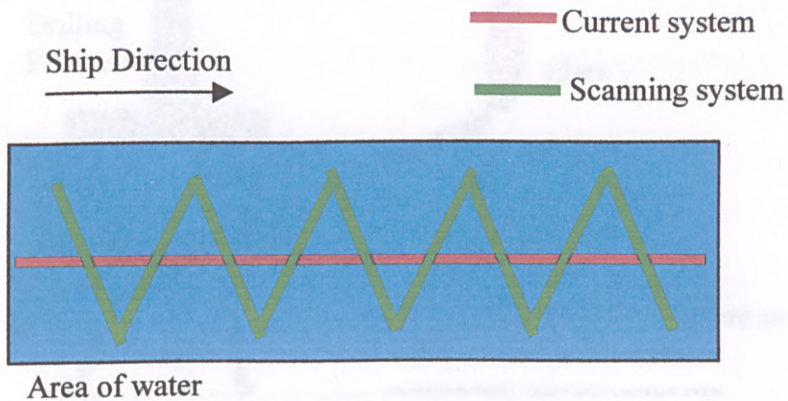


Figure 11.3: Sampling area of the current LMSF and a scanning version of the LMSF

It can be seen that by scanning the laser beam over the surface of the sea, a larger expanse of water could be covered. This is approximately 300% more than monitoring a

single line on the sea surface. This would provide more information on the distribution of algae or hydrocarbons on the sea surface.

11.2 Applications of the LMSF to other environmental monitoring

11.2.1 Oil Production Flaring Operations

One particularly interesting aspect of the system is its potential use in monitoring the amount of hydrocarbons on the sea surface during flaring operations. When drilling for oil, excess gas and oil vapour within the oil well is vented to the flare-stack on the platform where it is set alight to burn off the gas. During these operations, the flare temperature is adjusted to burn gas and oil vapour efficiently from the well. If, however, the flame temperature is too low, incomplete combustion occurs, resulting in the hydrocarbon being deposited as a thin layer onto the sea surface as can be seen in figure 11.4.

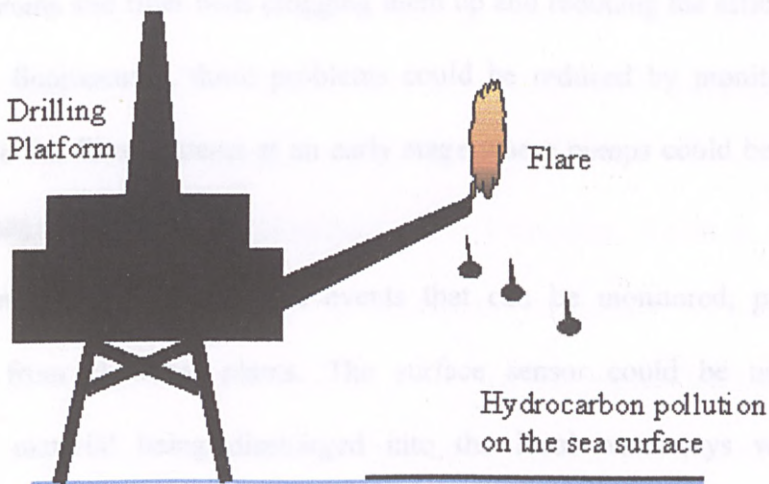


Figure 11.4: Illustration of the flaring process on oil production platforms

This poses a pollution problem for the companies who can incur fines. The Laser Marine Surface Fluorosensor however could be used as an early warning system to alert

controllers to variations in the oil being deposited onto the sea surface allowing remedial action to be taken promptly. It could also be interfaced with the flame control system to automatically adjust the flame temperature to produce more efficient combustion and hence reduce the pollution.

11.2.2 Inland Waterway Monitoring

The system could also be used for monitoring algae in inland waters such as rivers and reservoirs. It could also be adapted for dye tracer studies, monitoring the movement of dye on the surface over an expanse of water and for monitoring pollutants discharged from factories into rivers.

Many factories and water treatment plants use water from rivers and reservoirs in everyday operations such as cooling systems or cleaning it for human consumption. There can be problems however with large quantities of algae being pulled into the filtering systems and filter beds clogging them up and reducing the efficiency. By using the surface fluorosensor, these problems could be reduced by monitoring the water entering into the filter systems at an early stage where pumps could be stopped before serious damage can occur.

There is also the opposite events that can be monitored, particularly with discharges from chemical plants. The surface sensor could be used to monitor fluorescent material being discharged into the local waterways which could be pollutants. The system could also be further modified to monitor non-fluorescence material using other optical techniques.

It is also possible to use dye tracers which mimic the properties of water pollutants, to monitor the distribution of the pollution in a body of water and hence

allow mathematical models to be built to predict future trends in the water pollution of an area.

11.3 Laser Fluorimeter

Although this system was initially intended to determine if an argon ion laser could be used to excite phytoplankton, it has been successfully used as a multi-spectral tool for monitoring real water samples during sea trials. It could also be used as a method for verifying the fluorescence information being collected by the Laser Marine Surface Fluorosensor if they were operated simultaneously during research trips. This system has been shown to provide additional information on accessory pigment fluorescence, which occurs at wavelengths shorter than the chlorophyll-a primary emission peak at 680nm. This information may serve as a rapid indicator for the presence of different types of phytoplankton. The system could be upgraded using a spectrograph and CCD or diode array detector to replace the scanning monochromator and photomultiplier. This would allow almost instantaneous spectra to be obtained and also a better average signal compared to a single monochromator scan.

During the course of the project it was found that NASA is also developing similar instrumentation for calibrating the airborne oceanographic lidar (AOL)⁹⁴. The Shipboard Laser Fluorimeter is based on a doubled and tripled Nd:YAG design which mimics the AOL. The 355nm radiation is used to measure the chromophoric dissolved organic matter (CDOM) whilst the 532nm is used to induce fluorescence in phytoplankton. Again, the Raman peaks from each of these excitations are used to normalise the data, which is then correlated with the AOL. This forms part of the ground truthing instrumentation for calibrating the AOL. The development of shipboard laser fluorimeter shows the requirement for a ground truthing system for most remote

sensing techniques during the early stages of development. This allows the user to gain confidence in the accuracy of the remote sensing data. Although this was not the primary aim of the Laser Fluorimeter in this project, the system can be used to calibrate the Laser Marine Surface Fluorosensor data.

11.4 Time Dependent Fluorescence Emissions

It was demonstrated that there may be effects occurring within the fluorescence decay spectra for the selected species examined which may be characteristic of the species themselves.

The results were obtained using a laser with a pulse width of 4.5ns. To enable higher resolution work to be carried out, at least a 500ps pulse would be required to gain a higher resolution of the fluorescence decay characteristics of each of the selected species in the nanosecond timescale. It has also been reported that fluorescence events up to 600ns occur in terrestrial algae⁹⁵. These may also be reflected in marine algae and therefore more experiments are required.

It would also be advantageous to carry out these experiments on the cultures at different times during their growth cycles. Experiments here were mainly limited to the end of the exponential growth phase and the stationary phase. Further experiments should be carried out in the mid-exponential phase to determine any fluorescence differences in different species. The results shown here suggested that the difference in the fluorescence behaviour occurred as the samples entered the stationary phase.

In this project, use was made of an optical parametric oscillator (OPO) to allow different wavelengths to be probed within the phytoplankton. By using short pulse width (500ps) OPO technology and more wavelengths, it may be possible to further

probe the fluorescence mechanisms within the plankton cells. This work in itself is a large task but it may provide another method for distinguishing different algae species.

It is also reported by Tyystjarvi et al⁹⁶ that the fluorescence induction curves (Kautsky curve) are a “barcode” in plant leaves. By using neural network techniques they have a 95% recognition accuracy. This technique may also be applicable to marine algae where differences in the fluorescence behaviour of certain classes of algae have been reported also⁹⁷.

11.5 High Energy Laser Effects on Phytoplankton

It was observed that radiation above 10mW (average power) using the Nd:YAG laser caused damage to the phytoplankton cells and produced changes in the fluorescence signal of each of the selected species.

The *Chaetoceros* species was exposed to three different wavelengths of laser radiation at approximately 15mW. Although the cells were observed to be intact, there were still changes in the fluorescence emissions from this species. It may be useful to carry out further work treating the other species under similar conditions. This again may reveal differences in the fluorescence signals which may, along with other spectral techniques, provide a method for identifying different species.

By using selected wavelengths, it may be possible to destroy certain excitation pathways within the selected algae which are characteristic of certain species. Experiments on healthy mid-exponential growth phase plankton and stationary phase plankton cells should also be carried out and a comparison of the results from the different phases may provide information about possible mechanisms which reduce the photosynthetic activity of the cells.

11.6 Raman Scattering

The Laser Marine Surface Fluorosensor system may have a wider application if it were modified to observe Raman scatter rather than fluorescence. Raman scattering is based on the inelastic scattering of photons by bonds in a molecule. These interactions result in a shift in the wavelength of the incident light which is characteristic of the molecule being observed. This in effect produces a fingerprint of the molecule being observed. By monitoring these signals with the Laser Marine Surface Fluorosensor, a large number of pollutants in the marine environment may be measured simultaneously and remotely. For example, a Raman scattering based system could be used for monitoring pollutants downstream from factories located on or near rivers. This could be integrated into a spectral database which would allow instantaneous identification of pollutants and their concentration. Also, as the system monitors water remotely, it could be advantageous when factor owners refuse access to monitor the effluent from discharge pipes from the factory.

There is also an advantage in using Raman scattering for monitoring hydrocarbon. Due to the nature of the effect, the bonds within the hydrocarbon molecule are detected (C-H, C-C, C=C). Even as oil is weathered in the marine environment, these molecules will still be present at low concentrations as the hydrocarbons degrade into their constituent elements. As could be seen earlier, this produces a large effect on the fluorescence of the hydrocarbons making it difficult to quantify them. By using Raman scattering however, this should be less of a problem.

The main disadvantage of using Raman scattering however is the low signal intensity which is observed compared to a fluorescence signal. This can be overcome however by using sensitive CCD detectors and choice of excitation wavelength.

References

1. Introduction to Marine Biology, 1974, McConnaughey B.H., 2nd Ed, Mosby
2. Photosynthesis, 1987, Hall D.O, Rao K.K, 4th Ed, Whitstable Litho Ltd, ISBN 071312945x
3. Introduction to Marine Biology, "The Phytoplankton", 1974, McConnaughey B.H., 2nd Ed, pp 59-73, Mosby
4. Seasonal variation in the consumption of food by fish in the North Sea and implications for food web dynamics, 1997, Greenstreet SPR, Bryant AD, Broekhuizen N, Hall SJ, Heath MR, ICES JOURNAL OF MARINE SCIENCE, Vol.54, No.2, pp.243-266
5. Fish, fact and fantasy: A long view, 1998, Beverton R, REVIEWS IN FISH BIOLOGY AND FISHERIES, Vol.8, No.3, pp.229-249
6. Photosynthesis : metabolism, control and physiology, 1987, Lawdor D.W., Longman Scientific and Technical, ISBN 0582446333
7. Photosynthesis, 1987, Hall D.O, Rao K.K, 4th Ed, Whitstable Litho Ltd, ISBN 071312945x
8. The measurement and sensing of water quality: a review, 1990, Briggs R, Grattan K.T.V, Trans Inst MC, Vol. 12, No 2, Pp 65-84
9. The effects of oil-exploration and production in the Northern North Sea 1. The levels of hydrocarbons in water and sediments in selected areas: 1978-1981, 1985, Massie LC, Ward AP, Davies JM, Mackie PR, MARINE ENVIRONMENTAL RESEARCH, Vol.15, No.3, pg.165-213
10. The fate of the oil spilled from the Exxon Valdez, 1994, Wolfe D.A., ENVIRONMENTAL SCIENCE AND TECHNOLOGY, Vol. 28, No 13, Pp 561-567
11. Britain's North Sea oil and gas production: A critical review, 1996, Odell PR, ENERGY EXPLORATION & EXPLOITATION, Vol.14, No.1, pg.3-11

-
12. Hydrocarbon concentrations in the northern North Sea and effects on fish larvae, 1996, Stagg RM, McIntosh A, SCIENCE OF THE TOTAL ENVIRONMENT, Vol.186, No.3, pg.189- 201
 13. Chemical Aspects of North Sea Pollution, 1992, Hardwick D.C., ANALYTICAL PROCEEDINGS, Vol. 29, Pp 440-441
 14. Pollution and Contaminants, 1993, Goldberg E.D., WATER SCIENCE TECHNOLOGY, Vol. 28, No 8-9, Pp 13-18
 15. The physical and Biological Impact of Processed Oil Drill Cuttings, 1993, Minton R.C. et al, SOCIETY OF PETROLEUM ENGINEERS, Vol. 26570, Pp 113-121
 16. Changes in legislation on pollution control and waste management, 1991, Orpwood JL, JOURNAL OF THE OIL & COLOUR CHEMISTS ASSOCIATION, Vol.74, No.1, pg.11-16
 17. Fine for UK tanker disaster sparks landmark case, 08 Mar 2000, London (UK), REUTERS PRESS DIGESTS
 18. Royal Caribbean to pay Alaska \$3.5 million in dumping case, 15 Jan 2000 (USA), Dobbyn P, ANCHORAGE DAILY NEWS(ALASKA)
 19. Transport of toxic dinoflagellates via ships' ballast water: bioeconomic risk assessment and efficacy of possible ballast water management strategies, 1998, Hallegraeff, GM, MARINE ECOLOGY –PROGRESS SERIES, Vol. 168, pp 297-309
 20. Harmful algal blooms: An emerging public health problem with possible links to human stress on the environment, 1999, Morris JG, ANNUAL REVIEW OF ENERGY AND THE ENVIRONMENT, Vol. 24, pp 367-390
 21. SOAEFD Toxic Algal Monitoring Report, 1996, Kelly M, MacDonald E, Marine Laboratory Aberdeen,

-
22. Harmful Marine Phytoplankton and Shellfish Toxicity, 1994, Tester PA, ANNALS OF THE NEW YORK ACADEMY OF SCIENCES, pp 69-76
23. Emerging harmful algal blooms and human health: Pfiesteria and related organisms, 1999, Fleming LE, Easom J, Baden D, Rowan A, Levin B, TOXICOLOGICAL PATHOLOGY, Vol. 27, No 5, pp 573-581
24. Fertilizers and the environment, 1999, Ayoub AT, NUTRIENT CYCLING IN AGROECOSYSTEMS, Vol. 55, No 2, pp 117-121
25. Non-point pollution of surface waters with phosphorus and nitrogen, 1998, Carpenter SR, Caraco NF, Correll DL, Howarth RW, Sharpley AN, Smith VH, ECOLOGICAL APPLICATIONS, Vol. 8, No 3, pp 559-568
26. The Biology of the Algae, Round FE, Chapter 6, pp 147-160, ISBN 0713124202
27. The management of hypertrophic lochs: case studies in Southwest Scotland, 1999, Naysmith FH, HYDROBIOLOGIA, Vol. 396, pp 293-307
28. Changing balance of fish production in Scotland, 1999, Coull JR, MARINE POLICY, Vol. 23, Iss. 4-5, Pp 347-358
29. Primary production and plankton stocks in the Pacific Ocean and their seasonal variation according to remote sensing and field observations, 1997, Vinogradov et al, DEEP SEA RESEARCH PART II – TOPICAL STUDIES IN OCEANOGRAPHY, Vol. 44, No. 9-10, Pg. 1979-2001
30. Determination of phytoplankton chlorophyll concentrations in Chesapeake bay with aircraft remote sensing, 1992, Harding LW, Itsweire EC, Esaias WE, REMOTE SENSING OF THE ENVIRONMENT, Vol. 40, No. 2, Pg. 79-100
31. On the colours of natural bodies, 1834, Brewster D. Sir, TRANSACTIONS OF THE ROYAL SOCIETY OF EDINBURGH, Vol. 12, pp 538-545

-
32. Notice sur la matiere verte de feuilles [chlorophylle], 1818, Pelletier J, Caventou JB, ANNAL DE CHIMIQUE PHYSIQUE, Vol. IX, pp 194-196
33. On the change of refrangibility of light, 1852, Stokes GG, PHILOSOPHICAL TRANSACTIONS OF THE ROYAL SOCIETY OF LONDON, Vol. 142, pp 463-562
34. Neue Versuche zur Kohlensaureassimilation, 1931, Kautsky H, Hirsch A, Naturwissenschaften, Vol. 19, Pg. 964
35. Multiple excitation fluorimeter for insitu oceanographic applications, 1997, Desiderio R.A, Moore C, Lantz C, Cowles T.J, APPLIED OPTICS, Vol. 36, No 6, pp 1289-1296
36. Fluorescence spectral signatures: the characterisation of phytoplankton populations by the use of excitation and emission spectra, 1979, Yentsch C.S, Yentsch C.M, JOURNAL OF MARINE RESEARCH, Vol. 37, Pp 471-483
37. Spectral fluorescence: an ataxonomical tool for studying the structure of phytoplankton populations, 1985, Yentsch C.S, Phinney D.A, JOURNAL OF PLANKTON RESEARCH, Vol. 7, Pp 617-632
38. Spectral observations of pigment fluorescence in intermediate depth waters of the North Pacific, 1985, Broenkow W.W, Lewitus A.J, Yarbrough M.A, JOURNAL OF MARINE RESEARCH, Vol. 43, Pp 875-891
39. An insitu active fluorimeter to measure coccoid cyanobacteria fluorescence, 1990, Iturriaga R, Bartz R, Zaneveld J.R.V, *OCEAN OPTICS X* – SPIE Proceedings, Vol. 1302, Pp 346-354
40. Estimation of phytoplankton photosynthesis by active fluorescence, 1993, Falkowski P.G, Kolber Z, ICES Marine Science Symposium, Vol. 197, Pp 92-103
41. Comparison of radiocarbon and fluorescence based (pump and probe) measurements of phytoplankton photosynthetic characteristics in the Northeast Atlantic Ocean, 1997, Boyd P.W, Aiken J, Kolber Z, MARINE ECOLOGY PROGRESS SERIES, Vol. 149, Pp 215-226
42. Shipboard Lidar Fluorimeter (SLF), 2000, <http://aol.wff.nasa.gov/html/slf.html>

-
43. Design and application of a lidar fluorosensor system for remote monitoring of phytoplankton, 1998, Barbini R, Colao F, Fantoni R, Micheli C, Palucci A, Ribezzo S, ICES JOURNAL OF MARINE SCIENCE, Vol. 55, Pp 793-802
44. Lidar differential absorption and scattering technique – Theory, 1983, Korb CL, Weng CY, APPLIED OPTICS, Vol.22, No. 23, Pg. 3759-3770
45. “Light Amplification Claimed By Scientists”, 1960, July 8, New York Times
46. Airborne Oceanographic Lidar, Historic Perspective, 2000, <http://aol.wff.nasa.gov/html/aoldes.html>
47. Airborne Laser Topographic Mapping Results, 1984, Krabill W et al, PHOTONICS ENGINEERING AND REMOTE SENSING, Vol. 50, No 6, Pp 685-694
48. Water Depth Measurement using an Airborne Pulsed Neon Laser System, 1980, Hoge F.E. et al, APPLIED OPTICS, Vol. 19, No 6, Pp 871-883
49. Oil Film Thickness using Airborne Laser-Induced Oil Fluorescence Backscatter, 1983, Hoge F.E, APPLIED OPTICS, Vol. 22, No 21, Pp 3316-3318
50. Active-Passive, Airborne Ocean Color Measurement. 2. Applications, 1986, Hoge F.E, Swift R.N, Yungel J.K, APPLIED OPTICS, Vol. 25, No 1, Pp 48-57
51. Detection of Phytoplankton Pigments from Ocean Colour – Improved Algorithms, 1994, Sathyendranath S, Hoge F.E, Platt T, Swift R.N, APPLIED OPTICS, Vol. 33, No 6 Pp 1081-1089
52. Measurement and analysis procedures for remote identification of oil spills using a laser fluorosensor, 1994, Quinn M.F, Al-Otaibi A.S, Sethi P.S, Al-Bahrani F, APPLIED OPTICS, Vol. 15, No 13, Pp 2637-2658.

-
53. Spectral and time resolved measurements of pollutants on water surface by a XeCl laser fluorosensor, 1991, Barbini R, Fantoni R, Palucci A, Ribezzo S, van der Steen H.J.L, SPIE EXCIMER LASERS AND APPLICATIONS III, Vol. 1503, Pp 363-374
54. Field Performance of a laser fluorosensor for the detection of oil spills, 1980, O'Neil R.A, Buja-Bijunas L, Rayner D.M, APPLIED OPTICS, Vol. 19, No 6, Pp 863-870
55. Airborne laser-induced oceanic chlorophyll fluorescence: solar-induced quenching corrections by use of concurrent down-welling irradiance measurements, 1998, Hoge F.E, Wright C.W, Swift R.N, Yungei J.K, APPLIED OPTICS, Vol. 37, No 15, Pp 3222-3226
56. Depth resolved detection of oceanographic variables in the St. Lawrence estuary using a laser fluorosensor: Instrument characteristics and first results, 1995, Nieke B et al, INTERNATIONAL JOURNAL OF REMOTE SENSING, Vol. 16, No 8, Pp 1503-1522
57. Remote sensing of water pollution by lasers, 1991, Ahmad S.R, Trans Inst MC Vol. 13, No 2, Pp 104-112
58. Shipboard LIDAR investigations of marine phytoplankton, 1993, Chekalyuk A.M, Demidov A.A, Fadeev V.V, Yu Gorbunov M, ICES MARINE SCIENCE SYMPOSIUM, No 197, Pp 266
59. Remote laser insitu measurements of phytoplankton photosynthesis efficiency, 1993, Chekalyuk A.M, Yu Gorbunov M, ICES MARINE SCIENCE SYMPOSIUM, No 197, Pp 267
60. Design and application of a lidar fluorosensor system for remote monitoring of phytoplankton, 1998, Barbini R, Colao F, Fantoni R, Micheli C, Palucci A, Ribezzo S, ICES JOURNAL OF MARINE SCIENCE, Vol. 55, Pp 793-802
61. Active-Passive, Airborne Ocean Color Measurement. 1. Instrumentation, 1986, Hoge F.E, Berry R.E, Swift R.N, APPLIED OPTICS, Vol. 25, No 1, Pp 39-47
62. Use of Water-Raman Emission to Correct Airborne Laser Fluorosensor data for Effects of Water Optical Attenuation, 1981, Bristow M.D, Nielsen D, Bundy D, Furtek F, APPLIED OPTICS, Vol. 20, Pp 2889-2906

-
63. Design and application of a lidar fluorosensor system for remote monitoring of phytoplankton, 1998, Barbini R et al, ICES JOURNAL OF MARINE SCIENCE, Vol. 55, Pp 793-802
64. Lidar Fluorosensing of mineral oil spills in the sea surface, 1990, Hengstermann T, Reuter R., APPLIED OPTICS, Vol. 29, No 22, Pp 3218-3227
65. CZCS "system calibration": A retrospective examination, 1994, Evans R.H, Gordon H.R, Journal of Geophysical Research, Vol. 99 (C4), Pg. 7293-7307
66. "Ultraviolet and Visible Absorption spectroscopy" - Biological Spectroscopy, 1984, Campbell I.D and Dwek R.A, Pp 61-88, Benjamin
67. "Fluorescence"-Theory and Interpretation of Fluorescence and Phosphorescence, Becker R.S, Ch 7, Pp 76-86, J. Wiley & Sons
68. Becker R.S, Theory and Interpretation of Fluorescence and Phosphorescence, "Fluorescence", Ch 1/2, Pp 1-18, J. Wiley & Sons
69. "Luminescence" Practical Fluorescence, 1973, Guilbaut G.G, Marcel Dekker, Pp 1-28
70. "Fluorescence" Biological Spectroscopy, Campbell I.D and Dwek R.A, 1984, Pp 91-212, Benjamin
71. Photosynthesis, 1995, Whitmarsh J, Govindjee, ENCYCLOPEDIA OF APPLIED PHYSICS, Vol. 13, Pp 513-532
72. Principles of Instrumental Analysis, 1992, D.A. Skoog, J.J. Leary, 4th Ed, Pp 46-49, Saunders College Publishing, ISBN 0030233437
73. Studies of marine planktonic diatoms. I *Cyclotella nana* Hustedt and *Detonula confervacea* Cleve, 1962, Guillard R.R.L, Rythner J.H, Canadian Journal of Microbiology, Vol. 8, Pg. 229-239

-
74. Autofluorescence and Raman Scattering in the marine underwater environment, 1990, Yentsch C.S, Phinney D.A, OCEAN OPTICS X, SPIE Vol. 1302, Pp 328-333
75. Energy transfer reaction involving carotenoids: quenching of chlorophyll fluorescence, 1996, Young A.J, Frank H.A, JOURNAL OF PHOTOCHEMISTRY AND PHOTOBIOLOGY B: BIOLOGY, Vol. 36, Pp 3-15
- 76 . Spectral fluorescence : an ataxonomic tool for studying the structure of phytoplankton populations, 1985, Yentsch CS Phinney DA, JOURNAL OF PLANKTON RESEARCH, Vol. 7, No. 5, Pg. 617-632
77. Sixty-three Year Since Kautsky: Chlorophyll-a Fluorescence, 1995, Govindjee, AUSTRALIAN JOURNAL OF PLANT PHYSIOLOGY, Vol. 22, Pp 131-160
78. The use of spectral fluorescence methods to detect changes in the phytoplankton community, 1998, Seppala J, Balode M, HYDROBIOLOGIA, Vol. 363, Pg. 207-217
79. Photosynthesis, 1995, Whitmarsh J, Govindjee, ENCYCLOPEDIA OF APPLIED PHYSICS, Vol. 13, Pp 513-532
80. Effects of enhanced solar irradiation on chlorophyll fluorescence and photosynthetic oxygen production of five species of phytoplankton, 1995, Gerber S, Hader D.P, FEMS MICROBIOLOGY ECOLOGY, Vol. 16, Pp 33-42
81. Effects of enhanced solar irradiation on chlorophyll fluorescence and photosynthetic oxygen production of five species of phytoplankton, 1995, Gerber S, Hader D.P, FEMS MICROBIOLOGY ECOLOGY, Vol. 16, Pp 33-42
82. An introduction to Time-resolved Pump/Probe spectroscopy, 1985, Lytle FE, Parrish RM, Barnes WT, APPLIED SPECTROSCOPY, Vol. 39, No. 3, Pg. 444-451

-
- 83.** Light- and heat-induced denaturation of Photosystem II core-antenna complexes CP43 and CP47, 1999, Wang et al, JOURNAL OF PHOTOCHEMISTRY AND PHOTOBIOLOGY B: BIOLOGY, Vol. 50, Pg. 189-196
- 84.** Reconstructed light-harvesting system for photosynthetic reaction centres, 1996, Goc J, Hara M, Tateishi T, Miyake J, JOURNAL OF PHOTOCHEMISTRY AND PHOTOBIOLOGY A: CHEMISTRY, Vol. 93, Pg. 137-144
- 85.** Sea trials of an Optical Fibre Marine Fluorosensor, 1995, McStay D, Milne R, Pollard P, Dunn J, MEASUREMENT SCIENCE & TECHNOLOGY, Vol.6, No.9, pp.1309- 1316
- 86.** A Single probe Fibre Optic Fluorosensor for Marine and Freshwater measurements of phytoplankton populations, 1995, McStay D, Milne R, Wright GG, Dunn J, INTERNATIONAL JOURNAL OF REMOTE SENSING, Vol.16, No.5, pp.957-965
- 87.** Sixty-three Year Since Kautsky: Chlorophyll-a Fluorescence, 1995, Govindjee, AUSTRALIAN JOURNAL OF PLANT PHYSIOLOGY, Vol. 22, Pp 131-160
- 88.** Polarized Pump-probe Spectroscopy of Excitation Transport in Bacteriochlorophyll a protein from *Prosthecochloris aestuarii*, 1988, Causgrove TP, Yang S, Struve WS, THE JOURNAL OF PHYSICAL CHEMISTRY, Vol. 92, No. 23 Pg. 6790-6795
- 89.** Excitation and Electron Transfer from Selectively Excited Primary Donor Chlorophyll (P700) in a Photosystem I Reaction Centre, 1997, Kumazaki S, Ikegami I, Yoshihara K, JOURNAL OF PHYSICAL CHEMISTRY A, Vol. 101, Pg. 597-604
- 90.** Femtosecond Transient Absorption Study of Carotenoid to Chlorophyll Energy Transfer in the Light-Harvesting Complex II of Photosystem II, 1997, Connelly JP, Muller MG, Bassi R, Croce R, Holzwarth AR, BIOCHEMISTRY, Vol. 36, No 2, Pg. 281-287

-
91. In vivo analysis of slow chlorophyll fluorescence induction kinetics in algae: Progress, problems and perspectives, 1993, Buchel C, Wilhelm C, PHOTOCHEMISTRY AND PHOTOBIOLOGY, Vol. 58, No. 1, Pg. 137-148
92. Chlorophyll a Fluorescence as a Monitor of Nanosecond Reduction of the Photo-oxidised Primary Donor P-680⁺ of Photosystem II, 1979, Sonneveld A, Rademaker H, Duysens LNM, BIOCHEMICA ET BIOPHYSICA ACTA, Vol. 548, Pg. 536-551
93. An introduction to Time-resolved Pump/Probe spectroscopy, 1985, Lytle FE, Parrish RM, Barnes WT, APPLIED SPECTROSCOPY, Vol. 39, No. 3, Pg. 444-451
94. Shipboard Lidar Fluorimeter (SLF), 2000, <http://aol.wff.nasa.gov/html/slf.html>
95. Chlorophyll a Fluorescence as a Monitor of Nanosecond Reduction of the Photo-oxidised Primary Donor P-680⁺ of Photosystem II, 1979, Sonneveld A, Rademaker H, Duysens LNM, BIOCHEMICA ET BIOPHYSICA ACTA, Vol. 548, Pg. 536-551
96. The Kautsky curve is a built-in barcode, 1999, Tyystjarvi E, Koski A, Karanen M, Nevalainen, BIOPHYSICAL JOURNAL, Vol. 77, Iss. 2, Pg. 1159-1167
97. In vivo analysis of slow chlorophyll fluorescence induction kinetics in algae: Progress, problems and perspectives, 1993, Buchel C, Wilhelm C, PHOTOCHEMISTRY AND PHOTOBIOLOGY, Vol. 58, No. 1, Pg. 137-148

Appendix

A Ship-borne system for the Detection of Surface Oil

I. Campbell and D. McStay

School of Applied Sciences, The Robert Gordon University, St Andrews Street, Aberdeen AB25 1HG, Scotland, UK, Tel : (01224) 262826 or 262809 Fax : (01224) 262828

ABSTRACT

A ship borne laser fluorescence system, designed for use in conjunction with conventional water sampling techniques, for the improved detection and quantification of surface oil is described. Oil detection is achieved by firing the amplitude modulated 488nm output beam of an Argon ion laser at the sea surface. The resultant fluorescence and scattered laser light are collected using a simple telescope arrangement and processed using a lock-in amplifier. The system is capable of detecting surface oil coatings of $20\mu\text{l}/\text{m}^2$ with an operating range of 6-20m.

Keywords: Fluorescence, Marine Surface Sensing, Oil,

2. INTRODUCTION

Oil pollution arises from a variety of sources including shore based industrial effluent, leakage from land fill sites, ship discharges and accidental spills such as those seen in the *Braer* Disaster (1991) and in the *Exxon Valdez* incident in Alaska (1989). In the North Sea, emissions from oil platforms are a major source of oil pollution.

All such pollution can have a significant impact on the local marine life. Higher profile spills such as the Braer and Exxon Valdez incidents have been studied extensively. The initial oil slick in such cases have an immediate and devastating impact on the marine environment. There is, however, limited information relating to the impact of very thin slicks that can remain on the surface of the water after the main oil slicks have dispersed and light hydrocarbons have evaporated. Traditional detection methods involve extensive water sampling and with lengthy analysis times, making the process relatively expensive for such thin oil films. In many applications where it is necessary to quantify the distribution of a given species over an area of several hundreds of meters or kilometres the use of such methods is ineffective. Further, in a wide range of marine applications such as oil spills and algae distribution, the bulk of the relevant information is to be found at or near the sea surface. This has led to the development of a variety of laser optical sensor systems for marine monitoring applications. The large optical powers and low beam divergence available from modern laser sources enable large power densities of highly monochromatic light to be delivered to locations remote from the laser. This property makes the laser an ideal tool for use in remote sensing. Additionally, they are non-contact sensors and therefore avoid the problems associated with fouling of the transducer. The presence of species in on or near the sea surface, e.g. oils or plankton, which can be recognised by characteristic fluorescence and Raman spectra are ideal candidates for such a remote sensing scheme¹.

The majority of the marine surface sensors developed over the last decade have been based on LIDAR techniques in which a pulsed laser is fired at the ocean surface and the resulting backscattered light collected and analysed. Shipborne LIDAR systems for the monitoring thick oil films (0.1-10mm) on sea water have been reported². The bulk of the research has, however, been directed towards airborne LIDAR fluorescence systems for diagnostics of the sea surface and the subsurface water (chemical and biological pollutants³⁻⁸, oil film thickness measurements⁹, natural dissolved organics and phytoplankton^{10,11} and for characterisation of the ocean laser backscatter characteristics¹². A range of fixed wavelength laser sources including: Nitrogen (337nm)⁹, Nd:YAG (frequency doubled and trebled)¹⁰ and excimer (308, 355nm)^{5,6} have been employed. More recently tuneable LIDAR systems for marine monitoring have been developed^{10,12}. However, these systems rely on excimer pumped dye laser and therefore suffer from limitations associated

with size, power requirements and toxicity and service lifetime of the laser gases. Raman scattering based LIDAR systems for oil monitoring have also been developed for the detection of oil, with some systems able to determine the film thickness³. The airborne LIDAR have limitations in that they use high power pulsed lasers which tend to be large and relatively expensive.

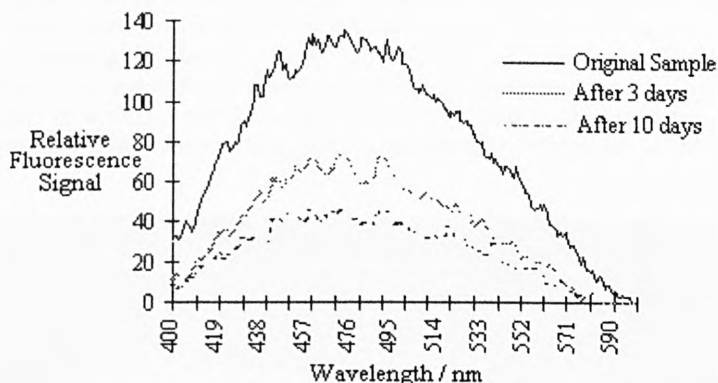


Figure 1. The change in the 380nm excited fluorescence spectra of Gulfaks oil with weathering

There is also the problem that aircraft mounted systems cannot take samples of the oil. This is important as it is well known that the Quantum yield / fluorescence intensity of the oil can change significantly with weathering as well as being strongly influenced by local water parameters such as temperature and pH. This is illustrated in figure 1 which shows the variation in the 380nm excited fluorescence spectra of Gulfaks crude oil. The change in the spectra with time when left uncovered in the laboratory at 28°C is also shown. The fluorescence yield of the oil is seen to decrease significantly due to the evolution of lighter fuel hydrocarbons with increasing time. This laboratory result is typical of reported changes in oil fluorescence with time¹³.

To enable truly quantitative measurement it is therefore necessary to take samples to obtain a fluorescence calibration. Shipborne LIDAR systems provide potential to perform integrated laser and conventional sampling measurements. There is therefore a need for a relatively low cost and compact shipborne system for detecting thin oil films on the sea surface in conjunction with a conventional sampling regime.

3. LASER MARINE SURFACE FLUOROSENSOR

The laser surface fluorosensor system developed for the monitoring of surface oil and phytoplankton plumes in conjunction with conventional water sampling is shown schematically in figure 2.

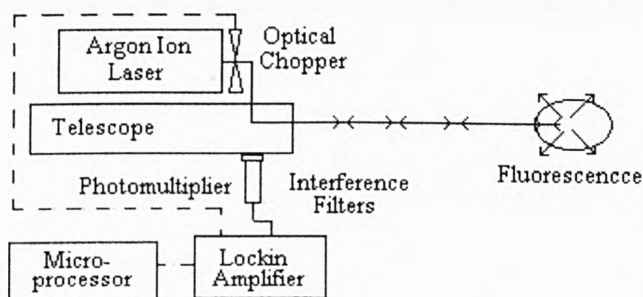


Figure 2. Schematic of the Laser Surface Fluorosensor

In the present configuration the excitation source is an argon ion laser (ILT 5500A) which produces an output of 100mW at 488nm. The laser light is amplitude modulated using an optical chopper then

expanded using a concave mirror and directed to the target area to achieve a spot size approximately 25cm in diameter at a range of 15m. The resultant backscattered fluorescence and laser light is collected using a telescope (Newtonian, 100mm Diameter mirror) and passed through a simple interference filter system to separate the laser and fluorescence components. The fluorescent component is directed onto a photomultiplier (Thorn EMI 9804B) which is in turn connected to a lock in amplifier (DIOP - ALA1010) which takes a reference from the chopper. The output from the lock-in is logged using a simple A/D converter (Picolog) allowing the real-time fluorescence data to be displayed on a microprocessor. The returning laser light is also monitored to determine the quality of the fluorescence signal. In contrast to conventional systems of a similar nature, which are generally pulsed devices and generally large, this system is both compact and provides real time data. A photograph of the system is shown below in figure 3.

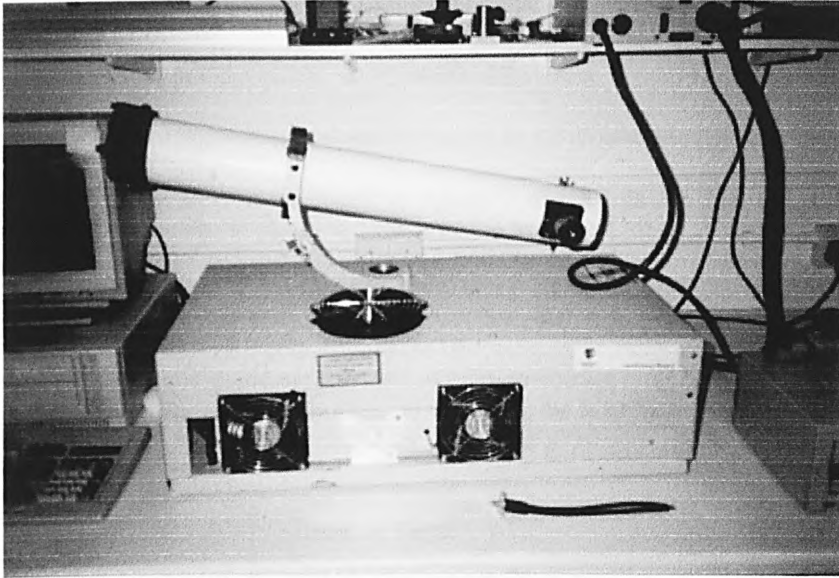


Figure 3. Photograph of the Laser Marine Surface Fluorosensor

4. RESULTS

Three main lines of the Argon ion laser are ideal sources for exciting plankton fluorescence. The effectiveness of each of these lines for oil detection using the LMSF was investigated by coupling the LMSF to a monochromator. The sample was placed at 3m from the excitation source. The drop in the signal intensities are due to the sample being moved in and out of the laser beam. It can be seen that the 476 and 488nm lines are the most efficient at exciting the oil in this case but the 488nm line was chosen as this was the most powerful line for the present laser.

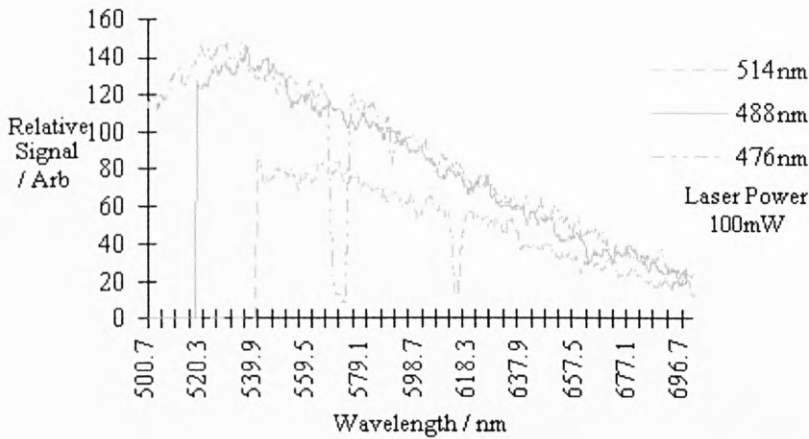


Figure 4. The induced fluorescence spectra of Gulfaks oil for three Argon-ion laser wavelengths

The performance of the system is illustrated in figures 5 and 6. In the first test, a layer of oil approximately 10cm in diameter is placed at a range of 5m from the LMSF. A typical signal when the laser spot is incident on the oil and that when removed from the oil is shown in figure 5. From the figure it can be seen that the system is capable of distinguishing oil layers from the background. In real applications the bow of the ship perturbrates the water surface. It is thus necessary for the surface fluorosensor to be able to measure a point beyond the bow wave. Obviously the area of distributed water is determined by the size and speed of the vessel and the measuring point. For the marine research vessels used in the North Sea an operating range of 6-20m for the laser marine surface fluorosensor has been found to be sufficient to ensure that the LMSF measuring point on the water surface is outwith the disturbed water of the bow wave.

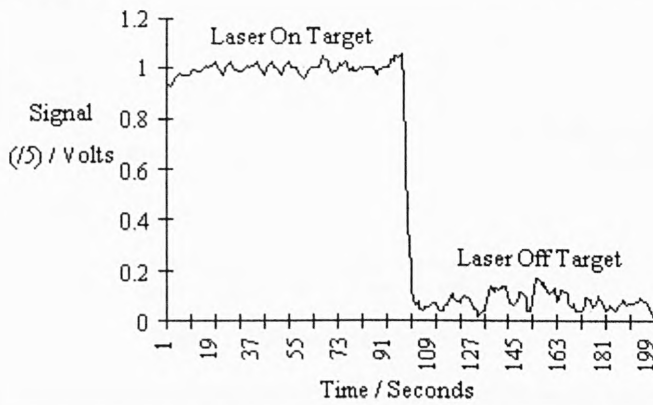


Figure 5. Typical backscattered fluorescence signal from a thin oil layer

Figure 6 shows a typical signal obtained from a sample when positioned at 6 and 15m from the LMSF for a fixed gain. As expected a reduction in the magnitude of the signal is observed. However, even at this fixed system gain it is able to detect the presence of the oil layer.

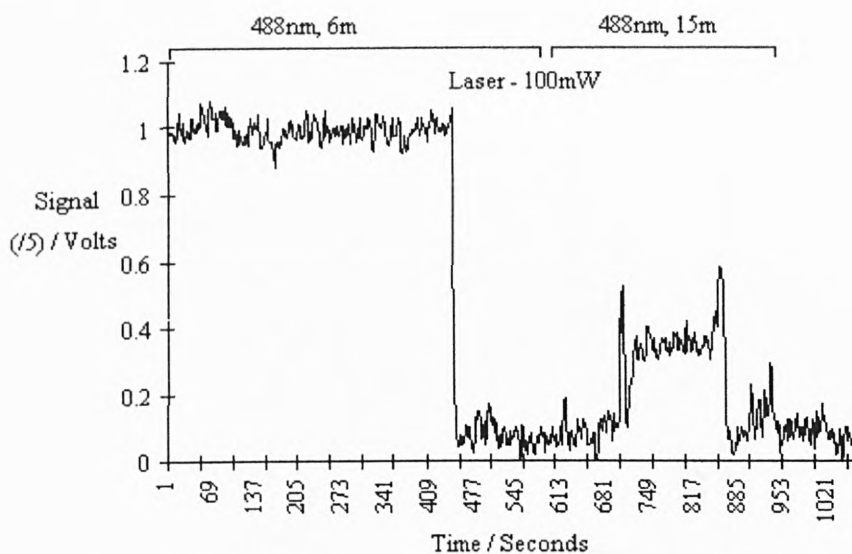


Figure 6. Typical back scattered signal for varying distances of targets

Study of the abilities of the system to distinguish between varying surface oil concentrations were also carried out. This was done using a water tank at a range of 3m from the LMSF. The amount of oil on the water surface was increased by dropping a microlitre at a time onto the surface. The LMSF signal magnitude for varying amounts of surface oil is shown in figure 7. The LMSF signal is seen to increase with the increasing amount of surface oil. At a range of 3m the system was chosen to be capable of detecting oil surface coatings of $20\mu\text{L}/\text{m}^2$

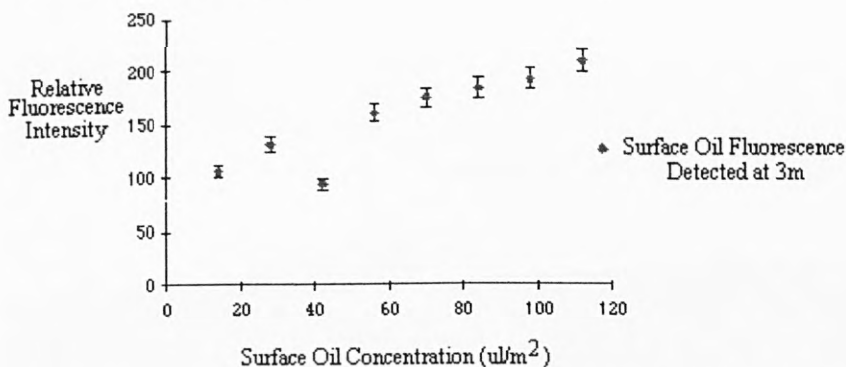


Fig 7. The variation in signal intensity with amount of oil on the water surface

5. SEA TRIALS

Practical deployment of the LMSF was investigated during a series of sea trials in the North Sea during June 1996. The route of this voyage (shown in figure 8) took the ship through several of the major North Sea oil fields. The symbols shown on the map represent the sampling stations where water samples at a depth of 20m were collected and analysed using conventional techniques for oil content. The Marine Research vessel the, MRV "Lowland Searcher" is shown in figure 9. The LMSF was housed in the top deck in an ex-radio room, as indicated in the figure. This position allowed the laser beam to be fired directly onto the sea surface at the side of the ship.

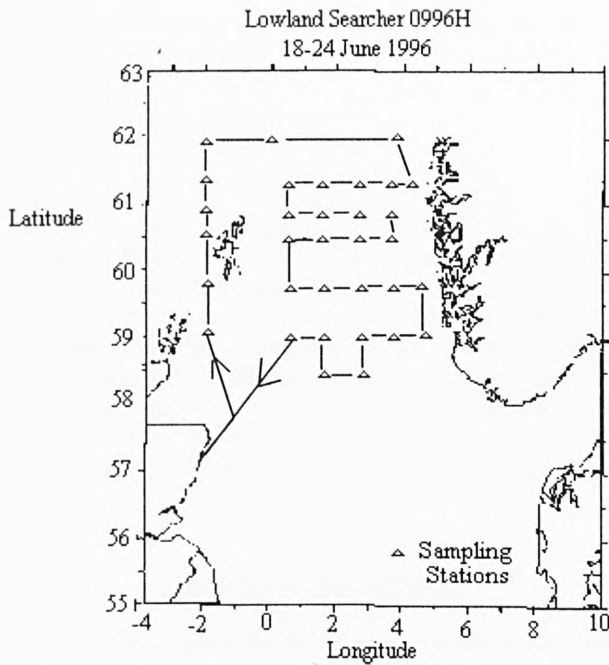


Figure 8. Map of the North Sea showing the route taken during the cruise on the MRV Lowland Searcher in June 1996. The location of sampling stations where conventional water sampling was performed are also shown.



Figure 9 . Marine Research Vessel "Lowland Searcher"

The system was located approximately 5m above the sea surface and the laser vertically directed to a location approximately 6m from the side of the ship (beyond the influence of the bow wave). The effective operating range of the system in this configuration was 8m. During the two week cruise most of the experimental work performed using the LMSF was carried out at night. This had the advantage of reducing the amount of background light. No serious practical problems relating to the deployment or operation of the system were experienced during the cruise. The system proved to be very reliable and

robust. Further tests of an upgraded version of the system are ongoing and the coupling of the system to automated water sampling techniques are currently being developed.

6. CONCLUSION

A compact shipborne surface fluorosensor system for marine monitoring application in conjunction with conventional water sampling techniques has been demonstrated. The system provides real time data for the detection of thin oil layers on the sea surface and has an operating range of 5-20m. Initial laboratory tests have shown that the system is capable of detecting surface oil coatings of $20\mu\text{l}/\text{m}^2$ at a range of 3m. The integration of the system with more traditional water sampling techniques should provide a reliable and rapid tool for the detection and analysis of surface species e.g. oil pollution. The nature of the design allows the system to be located within the superstructure of the ship, thus all electronics and optics are well protected from the harsh marine environment.

7. ACKNOWLEDGEMENTS

Thanks are due to the Scottish Office Agriculture and Fisheries Department (SOAFD) Marine Laboratory, Aberdeen for their support during the cruise and to the crew and captain of the Marine Research Vessel "Lowland Searcher" for their help and enthusiasm.

8. REFERENCES

1. M.A Blizard, SPIE Vol.925, Ocean Optics IX, 1988.
2. F.E. Hoge and R.N Swift, Applied Optics, 19 (19) 3269,1980.
3. R. Barbini et al., SPIE, V.1503, Excimer Lasers and Applications III p363, 1991.
4. R. Barbarini et al Conf Procc Vol 29-*Quantum electronics and Plasma physics*, Rigini G.C. (Ed), SIF, Bologna, 383-387, 1991
5. R.A. O'Neil et al Applied Optics 19 (6), 863-870, 1980
6. M. Bistow et al Applied Optics, 20 (17), 2889-2906, 1981
7. A. Franks et al Applied. Optics 22 (11), 1717-1721, 1983
8. J. Hobbs, Laser Focus World, November, 15, 1992.
9. S.R. Ahmad, Trans. Inst. MC, V13, No 2, 104-112, 1991
10. S.M. Babichenko and L.V. Poryvkina, SPIE Vol. 1492, 319-323. 1991
11. J.L Bufton et al Applied Optics 22 (17), 2603-2618, 1983
12. U. Gehlhaar et al Applied Optics 20 (19), 3318-3320, 1981
13. D. Gordon et al Environmental Science and Technology 10 (6), 580-585, 1976

Laser Surface Fluorosensor for Monitoring Phytoplankton

Ian Campbell, Daniel McStay, Patricia M. Pollard, Michael R. Heath², John Dunn²

School of Applied Sciences, The Robert Gordon University, Aberdeen, UK, AB25 1HG, Tel: (01224) 262826 or 262809 Fax: (01224) 262828

² Scottish Office Agriculture, Environmental and Fisheries Department, Marine Laboratory, Aberdeen, UK, AB9 8DB

ABSTRACT

A free path surface fluorosensor laser system, capable of giving a real time indication of the presence of phytoplankton at or near the sea surface, is reported. The system utilises an Argon ion laser operating at 488nm, the output beam of which is amplitude modulated, expanded and directed onto the water surface. The resulting phytoplankton fluorescence is collected via a simple telescope and filter arrangement and then passed to a phase sensitive detection system. Initial tests using a single phytoplankton species (*Thalassiosira pseudonana*) carried out in the laboratory have shown that the system is able to detect phytoplankton (500k cells/ml) at ranges up to 15m.

Keywords: Fluorescence, Phytoplankton, Marine surface sensing

2. INTRODUCTION

Phytoplankton are the staple diet of many marine species and are one of the first links in the food chain upon which fish depend. Accurate measurements of phytoplankton concentrations are thus important in marine science for the prediction of future fish stocks and the setting of fishing quotas. Phytoplankton also provide an indication as to the general health of the local marine environment. Current methods of measuring phytoplankton populations involve water sampling or net based techniques both of which are time consuming and are often not representative of the area. Satellite based measuring systems such as the National Aeronautics and Space Administration Coastal Zone Colour Scanner¹ and the soon to be commissioned Sea Wide-Field-of View Sensor (SeaWiFS) have been developed to allow large areas of the ocean colour and thus phytoplankton distribution and concentration to be monitored. Although these systems work well in areas where there is relatively predictable weather conditions, problems such as reduced sensitivity arise due to cloud cover making these type of systems less viable in areas where weather conditions and in particular cloud cover are relatively unpredictable, such as the North Sea.

Over the last 15 years the use of laser based sensing systems to monitor ocean surface parameters have been investigated. These systems have largely been based on LIDAR techniques such as NASA's Airborne Oceanographic Lidar^{2,8} (AOL) in which a pulsed laser is fired at the ocean surface and the resulting backscattered light collected and analysed. The main research in this area has been directed towards airborne LIDAR fluorescence systems for monitoring the sea surface and subsurface water. A range of fixed wavelength lasers including: Nitrogen (337nm)³, Nd:YAG (frequency doubled - 532nm and trebled - 355nm)⁴, excimer (308, 355nm)^{5,6} and tuneable dye systems^{4,8} have been used for the diagnostics of chemical and biological pollutants, natural dissolved organics, phytoplankton, and for the characterisation of the ocean laser backscatter characteristics. These systems have the limitation in that they use large pulsed lasers with the resulting system being large and relatively expensive. Furthermore, from laboratory studies⁷ it has been shown that the fluorescence yield of a phytoplankton species is dependant upon a number of variables including the nutrient supply in the local marine environment and temperature. In order to attain reliable quantification of the phytoplankton population in a given body of water at a given time using fluorescence there is thus a requirement for water samples to be taken to provide a fluorescence calibration which is something current systems cannot do without having a ship present in the test area obtaining water samples. By using an integrated approach to these measurements i.e. combining laser and conventional water monitoring measurement schemes, a more representative measurement of the phytoplankton concentration over the area under study will be achieved.

In this paper we report a low cost compact laser based system for performing such sea surface measurements, but which can readily be mounted on a ship. In this way periodic samples from the water body under investigation can be taken to provide a calibration for the fluorescence data. For

measurements of the water surface it is obviously necessary to monitor an area of the surface that is undisturbed by the ship on which the measuring instrument is based. A ship passing through a body of water, will produce some type of turbulence in the water surrounding it, thus sampling in this area would not give a true representation of the surface properties.

To overcome this, the laser is directed to a point located beyond the bow wave of the ship as shown in figure 1. This not only results in the monitoring of undisturbed water, but by measuring off the port side of the ship there is less likely to be interference from contaminants such as fuel oil from the ship itself. By considering these factors, experiments were carried out at distances of up to 18m which is sufficient for extending past the bow wave in most marine research vessels. This was demonstrated in sea trials of a prototype sensor carried out on board the Marine Research Vessel "Lowland Searcher" during June 1996.

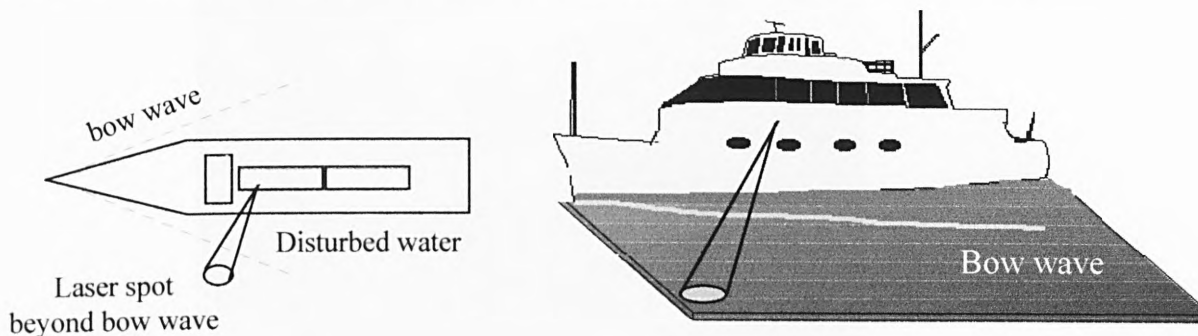


Figure 1. Schematic of the laser spot extending beyond the ships bow wave

As can be seen in figure 1, the surface sensor package itself is located within the superstructure of the ship with only a free path "window" required for delivery of the laser spot onto the sea surface, to collect the induced fluorescence and the backscatter from the sea surface.

3. LASER MARINE SURFACE FLUOROSENSOR (LMSF)

A schematic diagram of the laser surface fluorosensor system is shown in figure 2. The system comprises an air cooled Argon-ion laser (ILT 5500A) which produces 100mW at 488nm. The 488nm laser light output from this laser is amplitude modulated using an optical chopper. A confocal mirror arrangement is used to expand and direct the laser beam to the target area. Typically at a range of 15m, this produces a laser spot approximately 25cm in diameter.

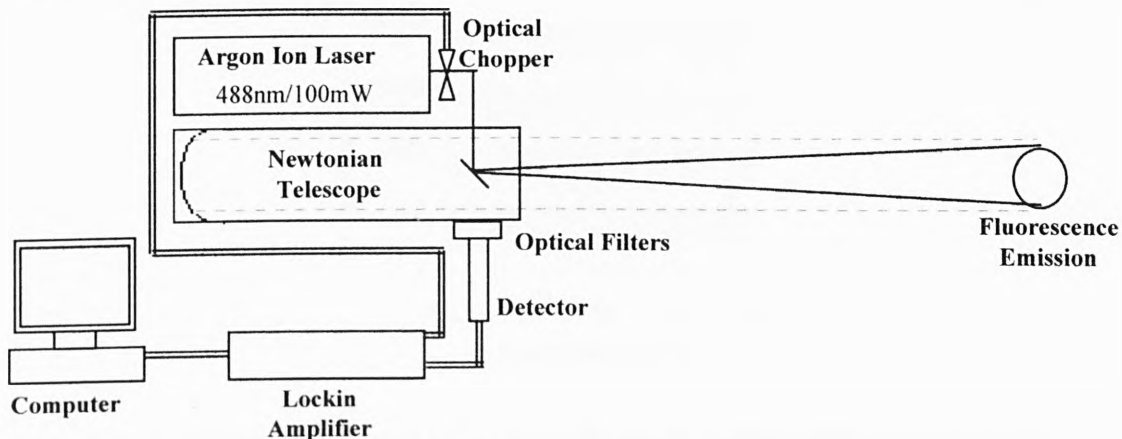


Figure 2. Schematic of the Laser Surface Fluorosensor

A telescope (Newtonian, 100mm Diameter) is used to collect the laser induced fluorescence from the sea surface and the backscattered laser light. Spectral filtering of the light is achieved using a simple interference filter system. The fluorescent component is directed onto a photomultiplier (Thorn EMI

9804B) which is in turn connected to a lock in amplifier (ALA1010) which takes its reference from the chopper. The output from the lock-in is logged using a simple A/D converter (Picolog) allowing the real-time fluorescence data to be displayed on a microprocessor.

The returning laser light is also monitored to provide a means of correcting for changes in the sea surface and ship movements. At present this data only gives an indication as to whether the fluorescence data can be accepted or rejected. A photograph of the system is shown in figure 3.

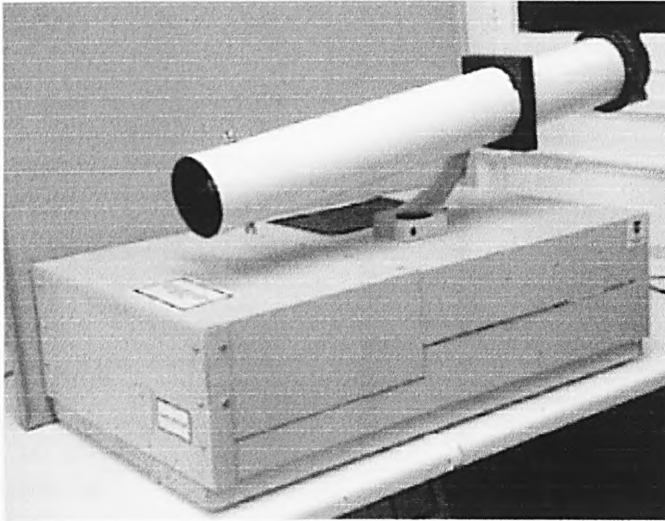


Figure 3. Photograph of the Laser Surface Fluorosensor

4. RESULTS

In order to avoid changes in the population and fluorescence yield of a live phytoplankton sample with time, fluorescein was used in the initial optimisation and testing of the system. In these tests a solution of sodium fluorescein with a concentration of $10^{-7}M$ was used as the target. The maximum emission for this is observed at 514nm and was selected using an interference filter (Ealing 35-3565). Figure 4 shows the measured variation in the detected fluorescence signal with distance from the LMSF for such a target. From the figure it can be seen that the system is able to resolve $10^{-7} M$ fluorescein solutions at ranges up to 18m.

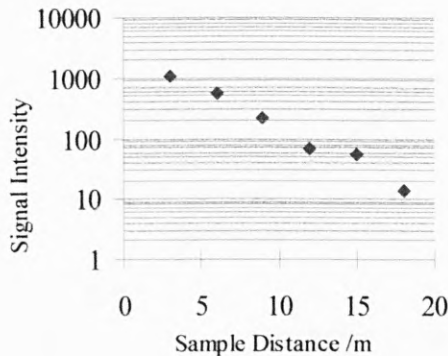


Figure 4. Back scattered fluorescence of $10^{-7}M$ Sodium fluorescein at various distances from the LMSF

In the initial tests, solutions of *Thalassiosira pseudonana* (1×10^6 cells/ml), a small, non-chain forming diatom were employed as the stock solution. The chlorophyll a fluorescence emission band at 685nm was utilised for the phytoplankton tests. A typical output from the instrument when the laser spot is incident on a sample (1×10^6 cells/ml) at a range of 6m and that when the sample removed from the beam is shown in

figure 5 (i) clearly demonstrating the ability of the system to distinguish phytoplankton containing water from the background.

Spectral selection of the 685nm light was achieved using an interference filter (Ealing 35-5669). Figure 5 (ii) shows the variation in the measured fluorescence with target range from the LMSF for the phytoplankton samples. This was done by placing a fixed volume (20cm³) of the solution containing phytoplankton in a container with a small surface area (2cm²) which was then placed at various distances from the LMSF. The system is seen to be capable of detecting 1x10⁶ cells/ml solution of phytoplankton at ranges up to 15m.

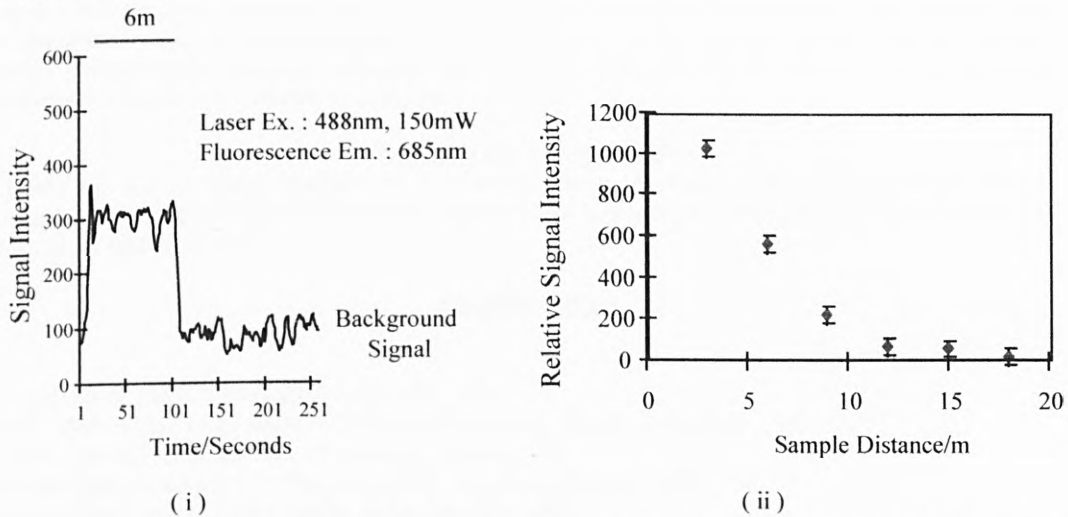


Figure 5. (i) Typical backscattered fluorescence signal from a stock phytoplankton sample
(ii) Range dependence for phytoplankton

The variation in the detected fluorescence signal with phytoplankton concentration at a fixed range of 6m is shown in figure 6. The system response is observed to be linear with phytoplankton concentration over the range investigated. From these results it can be seen that the system is capable of distinguishing different concentration of *Thalassiosira pseudonana* from 1M-90k cells/ml at a distance of 6m and that the system has a theoretical detection limit of 10875 cells/ml.

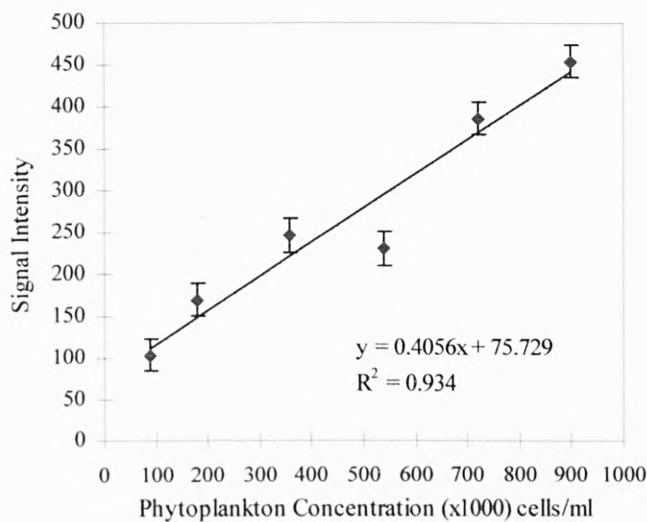


Figure 6. The variation in signal intensity with the concentration of *Thalassiosira pseudonana*.

6. CONCLUSION

A shipborne laser surface fluorescence system for monitoring phytoplankton in conjunction with conventional water sampling systems is demonstrated. Initial laboratory tests have shown the system capable of detecting sodium fluorescein solutions (10^{-7} M) up to 18m and water containing phytoplankton at about 15m. The system is capable of distinguishing phytoplankton concentrations down to 90k cells/ml at a range of 6m. By integrating the system with more conventional water sampling techniques, there exists a potential for a rapid real time detection and analysis system to be developed. The compact design of the system makes it portable/deployable on a variety of marine research vessels with the complete sensor package being contained within the superstructure of the vessel protecting the various electronics and optics from the harsh marine environment.

7. ACKNOWLEDGEMENTS

Thanks are due to Eileen Bresnane at the Scottish Office Agriculture, Environmental and Fisheries Department (SOAEFD) Marine Laboratory, Aberdeen for supplying the stock phytoplankton solutions for the various laboratory tests.

8. REFERENCES

1. C.H. Sinex, IEEE, 0-7803-2056-5, II-1-II-6, 1994
2. J.L. Bufton, F.E. Hoge and R.N Swift, Applied Optics, 22 (17) 2603-2618, 1983.
3. S.R. Ahmad, Trans. Inst. MC, V13, No 2, 104-112, 1991
4. S.M. Babichenko and L.V. Poryvkina, SPIE Vol. 1492, 319-323, 1991
5. R.A. O'Neil et al., Applied Optics, 19 (6), 863-870, 1980
6. M. Bistow et al., Applied Optics, 20 (17), 2889-2906, 1981
7. U. Gehlhaar et al., Applied Optics, 20 (19), 3318-3320, 1981
8. C. Wayne Wriget, Second International Airborne Remote Sensing Conference and exhibition, San Francisco, CA,
24-27 June 1996

A Ship-borne Laser Surface Fluorosensor for Marine Sensing Applications

I. Campbell, D. McStay, P. Pollard and M.R. Heath², John Dunn²

School of Applied Sciences, The Robert Gordon University, St Andrews Street, Aberdeen, AB25 1HG, UK, Tel : 01224 262809 Fax: 01224 262828 ² Scottish Office Agriculture, Environmental and Fisheries Department, Marine Laboratory, Aberdeen, UK, AB9 8DB

Abstract. A free path laser based surface fluorosensor for marine sensing applications is reported. The system is designed for real time monitoring of surface oil contamination and has also been used to detect phytoplankton at or near the sea surface. Laboratory trials have shown that the system is capable of real time detection of surface oil down to $20\mu\text{l}/\text{m}^2$ and phytoplankton concentrations of 90k cells/ml. The operating range of the system is 6-20m.

1. Introduction

The marine environment is an extremely complex and dynamic ecosystem [1,2]. Monitoring of such a system can be very time consuming, requiring long hours of conventional water sampling often in dangerous conditions. One of the key parameters which marine scientists need to monitor is the phytoplankton abundance. Traditionally, measurement of phytoplankton populations involve extensive water sampling or the use of towed instruments. Plankton nets are also used to collect samples, which are then preserved for subsequent laboratory analysis. These techniques provide data for only a small proportion of the water column and are not suited to measurements at or near the water surface. Similarly when investigating the impact of oil pollution, there is a requirement for measuring the very thin oil layers that exist on the sea surface long after an oil spill. Current methods of analysing such layers rely on conventional water sampling or involve a drum covered by an absorbing medium which is rolled slowly on the sea surface. The oil collected is subsequently analysed in the laboratory. Although surface specific, use of the drum is severely limited by weather and sea conditions.

Satellite based imaging systems have also been used for the monitoring of phytoplankton population and distribution [3]. An immediate disadvantage of these systems is their susceptibility to weather conditions and in particular cloud cover thus making them a non-viable option for use in the North Sea. Further, the data received is not obtained in real time, as it requires mathematical processing. Such systems are also hugely expensive with a high financial risk factor involved. As an alternative approach to satellite systems, a number of airborne LIDAR systems have been developed for marine monitoring applications [4-10]. These LIDAR systems however have limitations in that they require high power pulsed lasers which tend to have complex electronics, are bulky and expensive. As with satellite systems, aircraft mounted systems have a further disadvantage in that they are unable to obtain water samples for calibrating the instruments (Ground Truthing).

The importance of being able to perform such ground truthing measurements is illustrated by the fact that the fluorescence yield of oil changes with time and the local marine environment e.g. temperature and pH.

In order to obtain true data, it is thus necessary to take water samples to calibrate the instrument. Shipborne LIDAR systems [11,12] which allow the possibility of simultaneous water sampling have been demonstrated in the past but they have essentially been the same systems as those mounted in aircraft and therefore have the same disadvantages. There is thus a requirement for an integrated, low cost, portable, ship mounted system, capable of giving real time data and having the flexibility to be combined with conventional techniques for ground truthing. In this paper we describe such a low cost shipborne system.

2. Laser Marine Surface Fluorosensor (LMSF)

As can be seen from figure 1, the laser surface fluorosensor uses an air cooled Argon ion laser (ILT 5500A) which produces an output of 100mW at 488nm, as the excitation source. The laser light is amplitude modulated and expanded slightly to produce a spot, on the sea surface approximately 25cm in diameter at a distance of 15m. The resulting fluorescence and scattered light from the oil or phytoplankton at or near the sea surface, is collected using a telescope and the spectral components separated using an interference filter system.

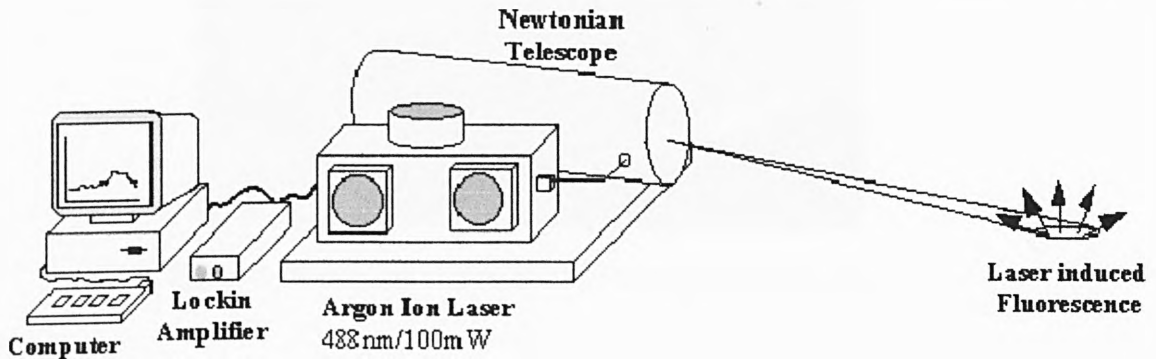


Figure 1. Schematic of the Laser Marine Surface Fluorosensor

The fluorescence component of the backscattered light is detected using a photomultiplier (Thorn EMI 9558B) which is connected to a lock-in amplifier which takes its reference signal from the optical chopper. The output from the lock-in is logged using a simple A/D converter connected to a computer and the real time fluorescence data displayed on the computer monitor. In the oil sensing mode, a bandpass filter at 550nm (40nm FWHM) is used to collect the oil fluorescence whilst for phytoplankton sensing, a bandpass filter at 700nm (40nm FWHM) is used to select the *chlorophyll-a* fluorescence. In order to obtain representative measurements of the relative concentration of a species at or near the sea surface, it is necessary to perform

measurements on undisturbed water. In practice, ships moving at any significant speed through the water produces a bow wave. For shipborne instruments it is thus necessary to perform the measurements on the water outwith the area affected by the passage of the ship. For the types of ships used in marine monitoring applications in the North Sea, this area of disturbed water is located between 6-20m from the side of the ship, depending on the speed. As the LMSF system is designed to be ship mounted, it is necessary for it to be able to detect oil or phytoplankton at ranges of up to 15m. Another important feature of the system is the angle at which the laser is incident on the water surface.

By keeping the angle relatively acute, the laser energy is effectively concentrated in the first few centimeters of the water, thus making the system relatively surface specific compared to other water sampling and LIDAR techniques. A photograph of the current version of the system is shown in figure 2.

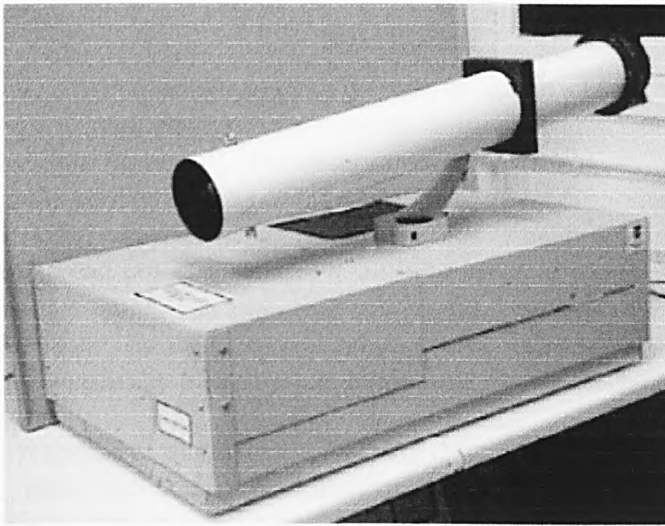


Figure 2. Photograph of the Laser Marine Surface Fluorosensor

3. Results

A typical output from the system when the laser spot is incident on a water sample with an oil layer approximately $90\mu\text{m}$ thick at a range of 6m is shown in figure 3. Also shown in this figure is the signal obtained from a clean water surface and the signal for the oil layer at a range of 15m.

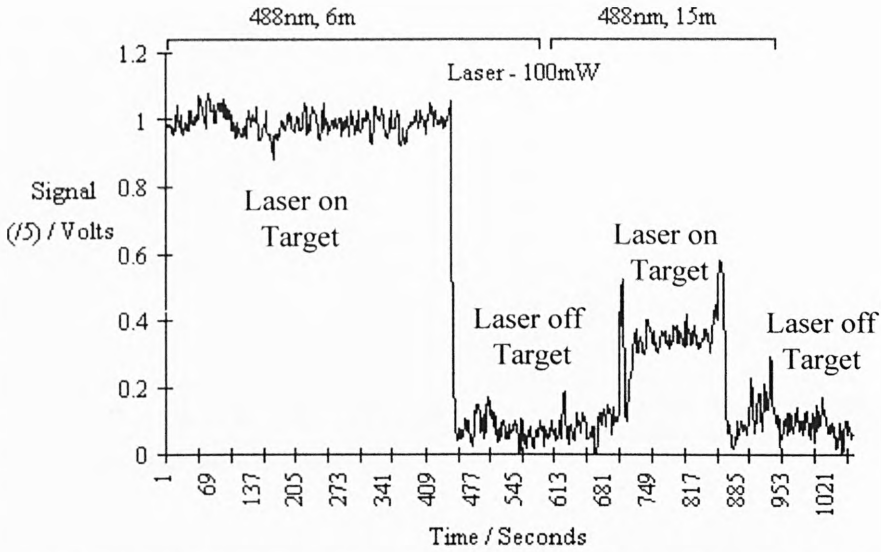


Figure 3. Typical backscattered signal for the laser on and off a $90\mu\text{m}$ thick oil layer.

The variation in the system response for varying surface oil concentrations, at a fixed range of 3m is shown in figure 4(i). For these measurements, a water tank was placed at a range of 3m and the surface coating of oil was controlled by dropping one microlitre at a time, of oil (Gulfaks) onto the surface. The surface tension properties of the water allowed the oil to spread out in a relatively uniform layer. From the results it can be seen that the system is capable of detecting oil surface coatings of $20\mu\text{l}/\text{m}^2$ using this configuration. However, by using an excitation source more suited to the absorption bands of the oil, the sensitivity of the system could easily be increased.

The response of the system to varying concentrations of phytoplankton was examined using water containing *Thalassiosira pseudonana*. Samples of various concentrations, made from a stock sample, were placed at a range of 6m and the resulting fluorescence measured. The results from these experiments can be seen in figure 4(ii). It is observed that the system is capable of detecting *Thalassiosira pseudonana* concentrations down to 90k cells/ml with a detection limit of approximately 11k cells/ml. At a range of 15m, the system is capable of detecting phytoplankton concentrations of around 1M cells/ml.

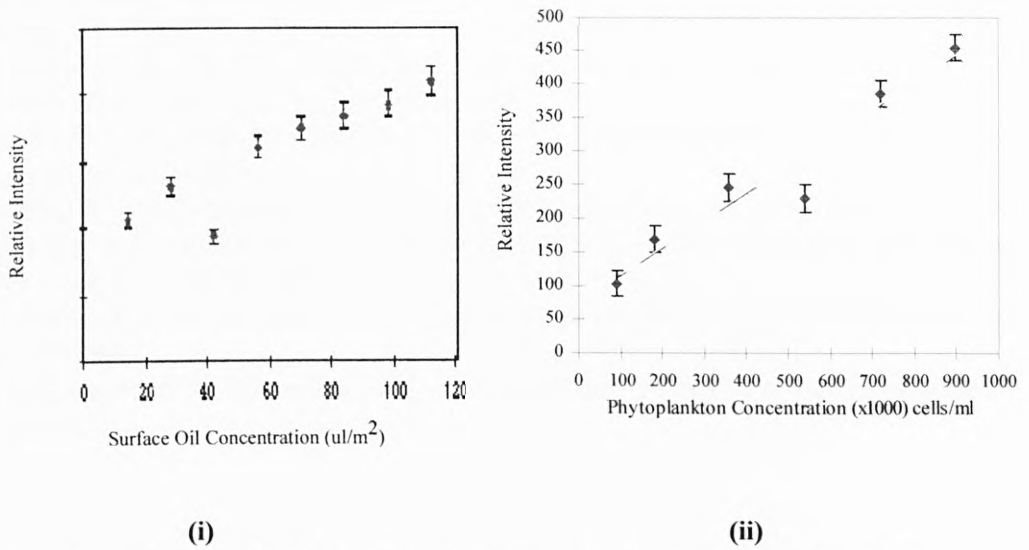


Figure 4. The variation in signal intensity with (i) oil surface layer concentration and (ii) *Thalassiosira pseudonana* cell concentration

4. Sea Trials

Initial sea trials of the LMSF were carried out during a series of voyages in the North Sea during June '96. The system was located in the top deck in an ex-radio room on board the Marine Research vessel, MRV "Lowland Searcher". This allowed the laser to be directed onto the water surface, off the port side of the ship thus minimising fluorescence signal interference from contaminants such as fuel oil from the ship itself. These sea trial allowed the investigation of the practicality of deploying the system in an area such as the North sea. Further sea trials are planned for June '97 where a revised system will be tested in both coastal waters and in the North Sea.

5. Conclusion

A low cost, shipborne laser surface fluorosensor for marine monitoring applications has been demonstrated. The system, used in conjunction with conventional water sampling, should provide a reliable and rapid integrated measurement scheme for the detection and analysis of surface species. The system is capable of detecting phytoplankton down to 90k cells/ml at a range of 6m and oil layers of down to 20 μ l/m² at a range of 3m.

6. Acknowledgements

Ian Campbell is grateful to SOAEFD for a studentship to undertake this work.

7. References

- [1] Leech M W and Walker M I 1992 Underwater Technology **Autumn** 22-28
- [2] Falowski PG and Kolber Z 1992 Aust. J Plant Physio. **22** 341-355
- [3] Sinex C H 1994 IEEE (0-7803-2056-5) II-1-6
- [4] Hoge F E and Swift R N 1980 App. Optics **19** 19 3270-3281

- [5] Hengstermann T and Reuter R 1990 *App. Optics* **29** 22 3218-3227
- [6] Bufton J L Hoge F E and Swift R N 1983 *App. Optics* **22** 17 2630-2618
- [7] Wright C W Second International Airborne Remote Sensing Conference and Exhibition, San Francisco, CA, 24-27 June 1996
- [8] Quinn M F Al-Otaibi A S Sethi P S Al-Bahrani F Alameddine O 1994 *Int. J remote Sensing* **15** 13 2637-2658
- [9] O' Neil R A Buja-Bijunas L Rayner D M 1990 *App. Optics* **19** 6 863-870
- [10] Barbini R Fantoni R Palucci A Ribezzo S 1991 *Quantum Electronics and plasma physics Conf. Proc.* **29** 383-387
- [11] Chekalyuk A M Demidov A A Fadeev V V Yu Gorbunov M 1993 *ICES Mar. Sci Symp.* **197** 266
- [12] Babichenko S M Poryvkina L V 1991 *Earth and Atmos. Remote Sensing SPIE* **1492** 319-323

A novel blue LED based hand-held fluorometer for detection of terrestrial algae on solid surfaces

E. Brechet, D. McStay, R.D. Wakefield, I.Campbell

Opto-electronics Research Group, School of Applied Sciences

Abstract. The application of an hand-held fluorometer used to monitor algal growth on stone surfaces is reported. The system is based on a modulated ultra-bright blue LED, used to induce chlorophyll-a fluorescence, as well as that of accessory pigments. With the addition of an encoding wheel and when linked to computer this system can produce real time map of the algae population on solid surface. The system has been shown to have a linear response to algal concentration, making it a viable tool for algal monitoring. The hand-held system is relatively immune to ambient light allowing it to be used on-site in various daylight conditions. Results from field and laboratory tests of the system on historically important sites and test samples are presented.

1. Introduction

The economics of stone conservation is a major concern to countries active in cultural preservation programs. An important aspect of this is the control of biological deterioration, in particular by chlorophyll containing organism such algae and lichens. The ability to map the position of biological growths on stone surfaces on-site offers many opportunities to those wishing to determine growth patterns of micro-organisms, colonisation or the efficacy of toxic biocides. The colonisation of building facades, by micro-organisms such as algae, bacteria and fungi, is a natural consequence of their exposure to the atmosphere. A range of biocidal compounds and cleaning methods can be used to control growth in order to prevent obscuring of detail and damage through biodeteriative processes. In order to assess the efficacy of these compounds and techniques, both in the laboratories and in the field, the appearance of growth at the surface of stone samples needs to be evaluated. This is currently largely monitored using visual techniques, the most common one being the human eye, and with it comes the problem of human interpretation and the need for relatively important colonies that can be seen. To shorten the length of time under which laboratory tests need to run to grow samples and remain in incubation, sensitive and quantitative on-site detection methods for measuring the initial colonising organisms are required. Colour meters have been used to assess the degree of 'greening' and 'darkening' of the surface due to microbial growth using the colour components $L^* a^* b^*$ [1], and although this technique offers a non-subjective measurement, it does not necessarily correlate to algae population. A more sensitive method, for the detection of microbial cell activity on stone samples employs fluorescence techniques. Organisms containing fluorescing pigments such as chlorophyll a, or algae, bacteria and fungi which have been suitably dyed, can be quantitatively assessed using epifluorescence or scanning epifluorescence microscopy. The latter technique is capable of mapping and quantifying organisms at the surface of solid samples [2]. However, exploitation of this analysis system is limited by the sample size that can be examined and the need to take samples from the

surface samples from the stone under investigation. Development of portable non-intrusive quantitative devices would thus be invaluable where on-site activity monitoring is required. In this paper we report a portable, low cost, hand-held device based on chlorophyll-a fluorescence measurement, for the detection of algal populations on hard surfaces.

2. Algae fluorescence

Most algae possess fluorescence emission bands centred around 320nm, 380nm, 685nm and 730nm [3]. The exact distribution of these emissions and their relative intensities depends on the specific type of algae, their nutritional state and the local environmental condition such as temperature or the water content [4]. Recent developments in LED technology allows the possibility of using a low cost, battery powered blue (centered at 450nm) excitation source instead of the red one (633nm) used in conventional chlorophyll detection systems [5]. The blue emission is capable of exciting most of the algae fluorescence bands and in particular the Soret band of Chlorophyll a (absorption 430nm). This results in the fluorescence emission at 685nm which is the most widely employed wavelength band for quantifying algal populations.

Experiment has shown that the difference in the excitation wavelengths produces very little difference in the fluorescence emission in the algae. As can be seen in figure 1, the 685nm fluorescence signal measured in a test algal sample of *Ulothrix giga*, using a Perkin Elmer Luminescence Spectrometer LS50B, has the same profile with excitation of 450nm and 633nm, the ratio of the two signal being fairly constant.

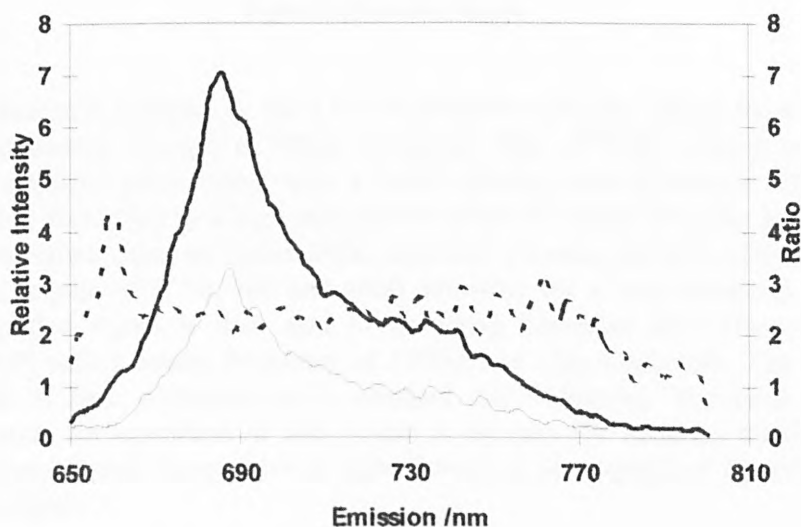


Figure 1: *Ulothrix giga* fluorescence spectrum. Measured emission spectra from 650 to 800nm for both excitations, 450nm (thick line) and 633nm (thin line). The dotted line being the ratio of both signal.

3. Instrument

3.1 Description

The instrument layout is shown in figure 2. An ultrabright blue LED (from Marl) is driven from a 555 timer which is set to modulate at a frequency of 130Hz. The light is then passed through a cut off interference filter to remove light above 600nm before being directed through a lens of focal length 20mm producing an effective spot size of 5mm on the surface. Being a hand held device, the spot had to be small enough for point measurement over a large surface, but also large enough to produce sufficient fluorescence for detection as well as being easily located by the user. A 5mm diameter excitation spot was found to be the ideal size for the type of applications foreseen for this instrument.

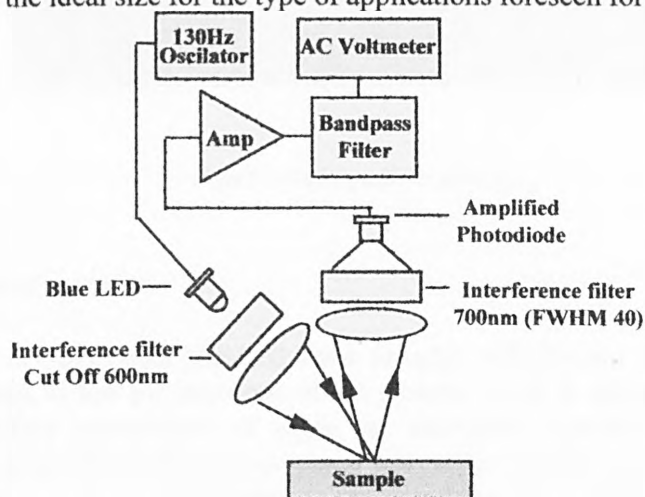


Figure 2: Instrument layout.

The fluorescence induced by the LED is collected using an 18mm focal length lens, and passed through a 700nm bandpass filter (FWHM 40nm) onto an integral amplifier photodiode, with a 5mm² sensing area (Centronic OS15K). After being decoupled by a high pass passive filter, the signal from the detector is further amplified using an instrumental amplifier (Analog devices AD524) with a selectable gain of 1, 10, 100 and 1000, allowing for a large detection range. The amplified signal is then sent to an active bandpass filter (Burr-Brown UAF42AP) with a centre frequency of 130Hz and 1Hz bandwidth. The output from this is then displayed on a standard AC voltmeter. The total power requirements for operation of the system is by two 9V batteries making the system portable and inexpensive to manufacture. A photograph of the system is shown in figure 3.

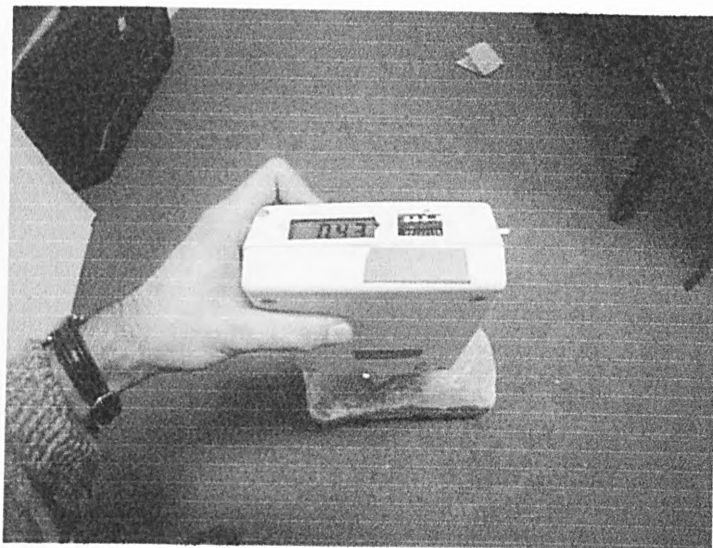


Figure 3: Photograph of system.

3.2 Instrument evaluation

Calibration of the system required stone samples with known algal populations were required to test the response of the system. As it is not possible to grow such controlled populations of algae, an alternative approach was adopted. Microtitre plates (figure 4) were prepared with mixes of fine grained acid washed sand and algal cells at concentrations ranging from 18 to 9000 cells/g of sand. The surface of each well therefore had an algal population proportional to the algae concentration used to make the mixture. The well area was 0.28cm^2 and it was 10mm deep with each well containing 0.60g of the mixture. The algal species used for the tests was *Ulothrix giga*, grown in bold basal and homogenised in a vortex prior to mixing with the sand. In order to keep the algae at a constant moisture content, a hole in the bottom of each well was drilled to allow water from beneath to wet the sand. A piece of filter paper was placed over the hole to retain the sand in the wells.

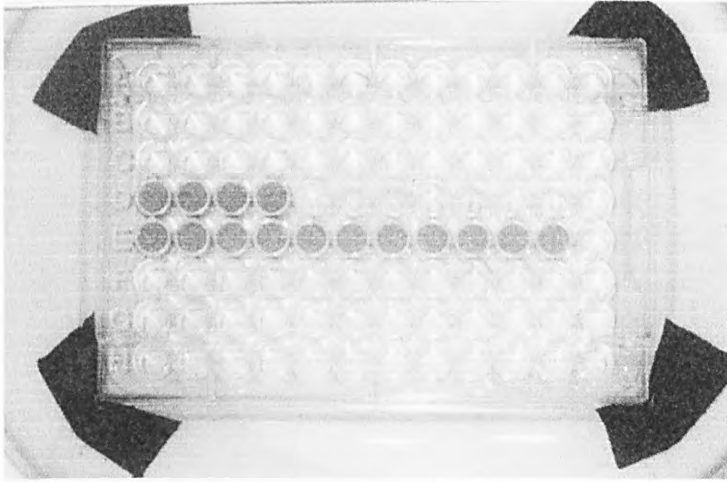


Figure 4: Microtitre plate with algae and sand mixtures. The concentration decreases from left to right on the bottom row.

The fluorescence of each well was then measured using the hand-held instrument with the amplifier set at a gain of 100. Measurements were carried out in a room with and without light to demonstrate the good immunity of the system to ambient light. Only direct, high intensity lighting caused distortion of the signal, due to the saturation of the photodiode.

4. Results

Using the hand-held fluorimeter, the fluorescence signal from the microtitre wells of increasing algal population was found to correlate well with the actual algal population, which can be seen in figure 5.

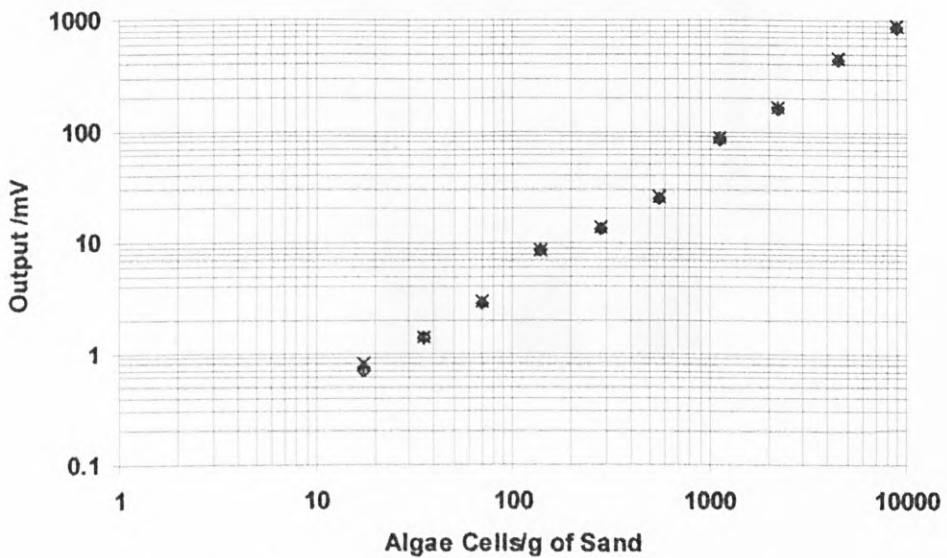
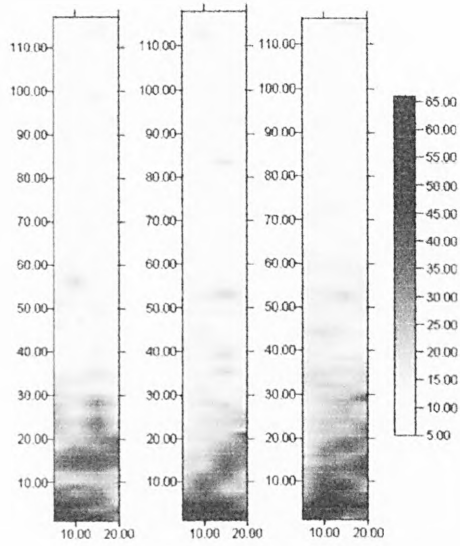
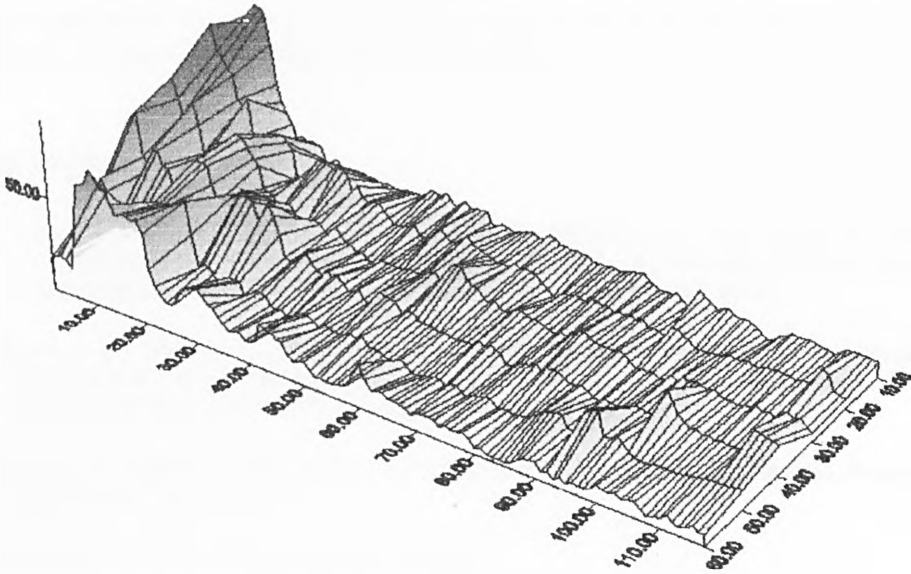


Figure 5: Fluorometer response to increasing algae concentration

The system is shown to have a linear response with algae concentration over the range 10-10000 cells/g of sand.



5. Conclusion

A hand-held system for detecting chlorophyll-a fluorescence from algae found on stone has been developed. The system is capable of detecting algal populations from 10-10000 cells/g of sand, was proven to be a sensitive instrument for the detection of algal populations on solid surfaces under ambient light. This system is suitable for detecting algal populations of less than 1000 cells/well which is invisible to the human eye, making the system much more sensitive than existing visual techniques. The suitability of this method for use on algae monitoring on a range of solid substrates in the field, and over a range of moisture contents is currently under investigation.

6. References

- [1] Young, M.E. Wakefield, R.D. Urquhart, D.C.M. Nicholson K. and Tonge, K., 1995, *Proceedings of the International Colloquium on Methods of Evaluating Products for the Conservation of Porous Building Materials in Monuments ICCROM*, 93-99.
- [2] Brechet, E., McStay, D., Wakefield, R.D., Sweet, M and Jones, M.S., 1996, *Advanced Technologies for Environmental Monitoring and Remediation, Proceedings SPIE-International Society of Optoelectronics Engineering*, **2835** 30-35.
- [3] McStay, D., Wakefield, R.D., Brechet, E. and Jones, M., 1995, ISBN 1-873394-20-4, *Processes of urban stone decay*, 78-87.
- [4] Schreiber, U., 1984, *Photosynthesis res.* **4**, 361.
- [5] Mazzinghi, P., 1996, *Rev. Sci. Instrum.* vol 67, **10**, 3737-3744